MODELLING AND SIMULATION OF FLUIDIZED-BED BOILERS AND GASIFIERS FOR CARBONACEOUS SOLIDS

A thesis presented to

the University of Sheffield

for the

Degree of Doctor of Philosophy

by

Marcio Luiz de Souza-Santos

Department of Chemical Engineering

and Fuel Technology,

University of Sheffield,

1987

Para Laura, Daniel, Nalva e meus pais.

****

To Laura, Daniel, Nalva and my parents.

SUMMARY

A comprehensive computer simulation program that can deal with a wide range of different operating conditions in fluidized bed combustion and gasification has been developed.

It includes the possibility of simulating operations with various types of coal, charcoal or wood and can predict the behaviour of a real unit by giving several important performance parameters, such as:

(a) Emulsion and bubble gas composition profiles throughout the bed height. The components included are: CO_2, CO, O_2, N_2, H_2O, H_2, CH_4, SO_2, NO, C_2H_6, H_2S, NH_3 and Tar.

(b) Gas phase composition throughout the freeboard height.

(c) Solid compositions of the coal (or any other carbonaceous material), limestone and inert in the bed and throughout the freeboard. The considered components are: C, H, O, N, S, ash, volatiles, moisture in the coal, $CaCO_3$, CaO, $CaSO_4$, moisture in the limestone, SiO_2, and moisture in the inert.

(d) Temperature profiles of all phases throughout the bed and the freeboard.

(e) Solid particle size distributions in the bed and in the freeboard sections. The considered effects are: elutriation, entrainment, attrition and recycling in all the three possible types of solid phases present;

(f) Heat transfered to water/steam inside the tubes, steam production and tube surface temperatures in the case of boiler simulation.

(g) Pressure losses in the gas phases through the distributor system and the bed, among all usual engineering design parameters.

The basic structure of the model is a system of 46 differential equations that represent the mass and energy balances in the bed and freeboard sections for all phases: carbonaceous particles, limestone, sand, gas in the emulsion and bubbles. The program can deal with two possible reaction models for the heterogeneous reactions: shrinking-core or exposed-core. The devolatilization is included as a series of heterogeneous reactions and drying as a diffusion controlled process. Simultaneous convection and radiation heat transfer between all phases and the tubes in the bed and freeboard are considered.

The program has been tested against the measured performance of industrial operating units of fluidized bed boilers consuming coal (Babcock & Wilcox, National Coal Board U.K.) and also with experimental units for coal combustion, and with gasifiers operating on biomass. Deviations between 5 and 2% for several process parameters as coal conversion, flue gas composition, entrainment rate of particles, heat transfer to tubes in the bed and freeboard, among other have been obtained in the tested cases.

ACKNOWLEDGEMENTS

To list all the persons that in some way, directly or indirectly, influenced the author in this task would take a long time. Therefore, the author would like to express his gratitude to those that made the greatest contribution.

This is so in the case of Dr. Alan B. Hedley, the supervisor of this research. His theoretical as well as practical experience on the present subject were vital during all phases of the model development and during the analysis of the generated simulation results.

To Dr. Peter Foster during sessions of discussion and who also helped with several suggestions.

To the staff of the Computing Services of the University of Sheffield that provided the assistance on the usage of the computing facilities, especially to Dr.S.Wardle and Miss C.Marsden.

To Mr.K.Alexander and Dr.E.Garbett for their friendship and help in the day by day aspects of the work and life.

On the other side of the Atlantic, the team of researchers of the Agrupamento de Engenharia Têrmica-IPT, specially the friends and colleagues Eng.Francisco D.A. de Souza, Eng.Nelson S. Yokaichiya, Eng.Saburo Ikeda and Eng.Lin Chau Jen. Their technical, moral and even financial help permitted the continuation of the work at crucial stages.

It is difficult to find the right words to

express my gratitude to Mrs. Noreen Cowell and to Mr. Eric Cowell whose kindness and hospitality I will never forget.

We would like to acknowledge the financial support from:

IPT-Instituto de Pesquisas Tecnologicas do Estado de São Paulo,S.A., Brazil;

CNPq-Conselho Nacional de Desenvolvimento Cientifico e Tecnológico, Brazil;

The British Council, and to

The Committee of Vice-Chancellors and Principals of the Universities of the United Kingdom - for the "Overseas Research Student Award".

CONTENTS

LIST OF FIGURES

LIST OF TABLES

NOMENCLATURE

a : stoichiometry parameter

a_e : solid friction coefficient used in the calculations of the rate of elutriation

a_{orif} : open area ratio of the distributor

a_Y : characteristic length for the decay of particles entrainment flux (m^{-1})

a'_{uxmf} , a''_{uxmf} , a'''_{uxmf} : auxiliary parameters for the calculations of minimum fluidizing conditions

A : area (m^2)

b ,b',b'' : stoichiometry parameters

c : molar concentration (kmol m^{-3})

C : specific heat (J kg^{-1} K^{-1})

d : diameter or equivalent hydraulic diameter (m)

d_{maxB} : maximum bubble diameter (m)

d_{orif} : diameter of the orifices in the distributor (m)

D : diffusivity coefficient (m^2 s^{-1})

E : rate of energy produced $^+$,consumed (-) or transferred per unit of length of the vertical direction (W m^{-1})

$\tilde{E}$: activation energy (J $kmol^{-1}$)

f : mass fraction of particles. Example: f_1 = mass fraction of carbonaceous material particles among all the solids

f' : fraction based on the number of particles in the bed

f'' : fraction based on the area of particles in the bed

f''' : fraction based on the volume of particles in the bed

$\dot{f}$: mass fraction of the entrained particles at the top of the bed that return as forced recycle to the bed

$\overline{f}_m$: correction factor ($m_G^3\ m_{S,m}^{-3}$)

f_{bexp} : factor of bed expansion from the minimum fluidizing to the operating fluidizing condition

f_r : fuel ratio (fixed carbon d.b /volatile matter d.b)

f_V : auxiliary parameters used in devolatilization calculations

F : mass flow (kg s^{-1})

G : mass flux in the vertical direction (kg m^{-2} s^{-1})

H : enthalpy (J $kmol^{-1}$)

i_T : tube inclination relative to the horizontal (rad)

k_i : Arrhenius constant for reaction "i" (dimension depends on the reaction)

$k_{o,i}$: pre-exponential Arrhenius constant for reaction "i" (same dimension as k)

K_i : equilibrium constant for reaction "i" (dimension depends on the reaction)

$K_{o,i}$: pre-exponential equilibrium constant for reaction "i" (same dimension as K)

L : length (m)

m' : solids mixing parameter

m'' : fraction of wake solids thrown into the freeboard

M_j : molecular mass of component "j" (kg $kmol^{-1}$)

n_{orif} : number of orifices in the distributor

N : molar flow (kmol s^{-1})

N_{Pr} : Prandtl number

N_{Nu} : Nusselt number

N_{Re} : Reynolds number

N_{Sh} : Sherwood number

p : partial pressure (Pa)

P : pressure (Pa)

q : heat flux (W m^{-2})

r_i : rate of chemical reaction "i" (for the gas-solid reactions: kmol m^{-2} (of particle surface) s^{-1}); for the gas-gas reactions : kmol m^{-3} (volume of gas phase) s^{-1})

R : universal constant of gases (J $kmol^{-1}$ K^{-1})

R_S : rate of production of chemical component due to the solid-gas reactions (base=area of solid phase referred in the inferior index) (kg m^{-2} s^{-1})

R_{VE} : rate of production of chemical component due to the gas-gas reactions occuring in the gas phase of the emulsion (base =volume of gas phase in the emulsion) (kg m^{-3} s^{-1})

R_{VB} : rate of production of chemical component due to the gas-gas reactions occuring in the bubble phase (base=volume of bubble phase) (kg m^{-3} s^{-1}) .

s : mass fraction in particle size distribution

$\dot{s}$: mass fraction in particle size distribution referred to the individual species. It is important to distinguish between the mass fraction distribution within each species "m" given by " $\dot{s}_{m,l}$ " and the mass fraction in the mixture " $s_{m,l}$ ". They are related by: $s_{m,l} = \dot{s}_{m,l} f_m$.

$\bar{s}$: specific surface area of limestone particles (m^2 kg^{-1})

$\tilde{s}_{m,l}$: mass fraction of particles in the bed smaller than size $d_{P,m,l}$

S : bed sectional area (m^2)

S' : surface area (m^2)

T : temperature (K)

T^* : reference temperature (298.15 K)

u_1 , u_2 : auxiliary parameters to the heat transfer calculations

u' , u'' : parameters in the devolatilization calculations

U : superficial gas velocity (m s^{-1})

v : volume of pores per mass of solid (m^3 kg^{-1})

V : volume (m^3)

w : mass fraction in solid or gas phases

x_{dist} : thickness of the distributor plate (m)

X : elutriation flow of a particle for a bed consisted only of the referred size in the subscript (kg s^{-1})

y_j : molar fraction of component "j"

z : vertical coordinate (m)

Greek Symbols

α : coefficient of heat transfer (W m^{-2} K^{-1})

β : stoichiometry coefficient

γ_i stoichiometric coefficient for the solid reactant in the gas-solid reaction "i"

Γ : rate of fines production due to particle attrition (kg s^{-1})

δ_{film} : film thickness (m)

Δ : indicates variation related to the accompanying variable

ε : void fraction in the bed

ε_F : estimated void fraction in the freeboard

ε_T : parameter used in the calculations for the heat transfer coefficient for the internal wall of the tubes (Appendix D)

ε' : surface emissivity

ζ , ζ' : resistances factors to chemical reactions (Pa m^3 s $kmol^{-1}$)

η : effectiveness factor for a reaction in the core

θ : void fraction inside a solid

ι : limestone reactivity

λ : thermal conductivity (W m^{-1} K^{-1})

Λ : fraction of conversion of chemical component in the system

μ : dynamic viscosity (kg m^{-1} s^{-1})

ν : coefficient of stoichiometry

Ξ : fraction of the space occupied by the unreacted part of the particle

ρ : density (kg m^{-3})

T : particle terminal velocity (m s^{-1})

τ : fraction of the particle radius occupied by the unreacted core

ϕ : sphericity of a particle

Φ : Thiele modulus

ψ : material friability constant (m^{-1})

Ψ_D : total mass in the bed (kg)

ω_{BE} : coefficient of mass transfer between bubble and emulsion (s^{-1})

ω_{SG} : coefficient of mass transfer between solid and gas (kmol m^{-2} s^{-1})

Subscripts

In this work a system of combined subscripts is used. For instance : $d_{PI,m}$ means particle diameter of specie m as entering the system. Here, as no other information is given, it is assumed that the diameter is an average within the specie "m". If indicated just d_p it would mean the average diameter in the bed.

amb : relative to the external ambient to the reactor

ash : relative to the ash content in the proximate analysis of carbonaceous material (wet basis)

A : relative to the average condition at a point "z" of the bed or the freeboard

bed : relative to the bed (normally to define a property as an average at a point in the bed)

B : relative to the bubble phase

core : relative to the unreacted or not still affected internal core of a solid particle

C : relative to heat transfer by convection

d : dry or calculated at dry basis

daf : dried and ash free basis

dist : relative to the distributor or distributor surface in contact with the bed

D : relative to the bed or at the top of the bed as in z_D.

E : relative to the emulsion phase

fix : relative to fixed carbon in the proximate analysis (wet basis)

F : relative to the freeboard section or at the top of the

freeboard as in z_F.

G : relative to gas phase

GE : relative to gas in the emulsion

GB : relative to the gas in the bubble

i : relative to the reaction "R-i"

ins : relative to the reactor external insulation

I : entering the system or section

j : relative to the component "j" : Gas components: 1=CO_2, 2=CO, 3=O_2, 4=N_2, 5=H_2O, 6=H_2, 7=CH_4, 8=SO_2, 9=NO, 10=C_2H_6, 11=H_2S, 12=NH_3, 13=Tar; Solid components in the carbonaceous particles: 14=C, 15=H, 16=O, 17=N, 18=O, 19=Ash, 20=Volatiles, 21=Moisture; Solid components in the limestone particles: 22=$CaCO_3$, 23=CaO, 24=$CaSO_4$, 25=Moisture; Solid components in the inert particles: 26=SiO_2, 27=Moisture

J : relative to the internal surface

K : relative to recycling of particles to the bed

l : relative to the level in the particle size classification

(l increases with the particle size)

lm : maximum number of levels in the size particle classification of the solid kind "m"

L : leaving the system or the indicated section

m : relative to the solid kind "m" (1=carbonaceous material, 2=limestone, 3=inert)

mf : at the minimum fluidizing condition

mst : relative to the moisture in the solid particle

M : relative to mass transfer between phases

N : due to the solid turnover in the bed

orif : relative to the orifices in the distributor

O : relative to the outside (for instance: OTD = to the outside of the tubes in the bed) or to external wall (as in OW = external wall of the reactor)

P : relative to the solid particles

Q : relative to chemical reaction

R : relative to radiative heat transfer

shell : relative to the reacted or processed external shell that covers the core of a solid particle

S : relative to solid phase in the emulsion

T : relative to the tubes

U : relative to the real or skeletal density

vol : relative to the volatiles content in the proximate analysis of carbonaceous material (wet basis)

V : relative to the devolatilization processes

W : relative to the wall (for instance: WOTD = relative to the outside wall of the tubes in the bed)

X : relative to particle elutriation from the bed

Y : relative to particle entrainment

Z : solid material that covers the unreacted core. Its nature depends on the kind of solid particle and on the reaction that has been treated. For instance, in the combustion and gasification reactions of the carbonaceous material Z means ash, in the devolatilization reactions Z means devolatilized solid and in the drying processes Z means dry material.

Superscripts

o : relative to the "as fed condition"

* : relative to the equilibrium condition

CHAPTER I

1. INTRODUCTION

The present work is intended to be a contribution to the state of mathematical modelling and simulation of fluidized bed boilers and gasifiers. The computer program was developed having in mind its possible use as a tool for engineering design and operation optimization by predicting the behaviour of a real unit during its steady-state operation.

This work started in 1980 and has been developed in parallel to the experimental research carried out in biomass fluidized bed gasification in the IPT (Instituto de Pesquisas Tecnológicas do Estado de São Paulo, Brazil) and also with the fluidized bed combustion research programme in the Department of Chemical Engineering and Fuel Technology of the University of Sheffield.

For the sake of clarity, and also to establish some basic nomenclature before presenting a more detailed discussion on the motivation and justification of the present model, a brief discussion about the concept of a bed of fluidised particles is presented below.

1.1. Bed of particles

The various possible conditions of a bed of particles can be seen as progressive behaviour of the system if an increasing flux of fluid (liquid or gas) is injected from the vessel base. The intensity of the fluid flow can be described by the superficial velocity (U) of the fluid through the bed that corresponds to the average fluid velocity measured if the bed was empty of solid particles.

Another characteristic parameter that shows the different behaviour of the possible conditions is the pressure loss in the bed. If it is plotted against the increasing superficial velocity, a typical graph is obtained, as shown in Fig.1.1 (figures are located at the end of each respective chapter).

From U=0, the increase in the superficial velocity causes a steady increase in the pressure drop through the bed until a condition called "minimum fluidization" is reached. This corresponds to a situation where any further increase in the injected mass flow of fluid leads to the appearance of bubbles. These bubbles which pass through the bed are almost free of solid particles and carry the "excess" of injected gas flow, according to the "two-phase theory" originally idealized by Toomey and Johnstone (1952).

It should be stressed that this description is valid for an isothermal bed. In most common situations, for example in fluidized bed combustion or gasification, as the

fluid is normally injected at a lower temperature than the bed average, the superficial velocity tends to quickly increase due to the gas expansion throughout the bed height. Therefore, even if at the bed bottom the regime is at the condition of "minimum fluidization" it is impossible to maintain this and a bubbling regime will follow a few millimetres above the bed base.

Due to the short circuit of bubbles an almost constant pressure drop in the gas through the bed is observed in the bubbling regime despite increasing superficial velocities, as shown in the region (b) of Fig.1.1. In this region the bed behaves as a fluid.

Also in the bubbling regime, as the bubbles burst at the bed surface, solid particles are thrown into the region above, called the freeboard. The lighter ones are carried out with the gas flow while the the heavier ones tend to return to the bed if enough space is provided. This space is usually called TDH (transport disengaging height) although an exact definition for this parameter is a matter for some discussion - as it will be detailed below - the common idea is that it corresponds to the height above which no appreciable decrease in the amount of carried particles can be achieved with an increase in the freeboard height. The parameter that describes the decrease of the flow of solids in the freeboard with the height is the entrainment while the elutriation can be understood to be the value of entrainment at an infinite height of the freeboard.

The next quality change in the behaviour of the bed is reached by increasing the superficial velocity above the average terminal velocity of particles in the bed. This leads to a situation where no bubbles or bed surface can be clearly observed and a pneumatic transport condition is set. The pressure loss decreases with further increases in the superficial velocity.

Due to its special characteristics, the fluidized bed condition brings several advantages with respect to particle combustion and gasification if compared with the other possible regimes. These are described below.

1.2. Motivation

As a result of combinations of several advantages over the conventional processes of solid fuel combustion and gasification, the technology of the fluidized bed has been studied with increasing interest.

Some of these advantages are:

a) Greater flexibility in coping with the quality of the fuel consumed, for example: high ash coal, wood or biomass;

b) Higher heat transfer coefficients to tubes when compared with conventional boilers;

c) Lower pollutant emissions due to the possibility of using limestone as an absorbent material added to the bed;

d) Lower tar emission, mainly important in wood gasification;

e) Higher possible variation on the rate of fuel feeding or turn-over;

f) Higher degree of automation attainable.

Although some medium size and large units have been operated, there are restrictions for a more widespread commercial acceptance. Among the usual problems found the more important are:

a) Bed collapsing due to particle agglomeration caused by localized regions of high temperature, i.e. above the ash softening point;

b) Areas of high corrosion on tubes immersed in the bed;

c) High sensitivity of the operation with respect to variations of fuel physical characteristics such as particle density and size distribution.

Countries such as, for instance, Brazil with immense resources of wood and poor quality coal and other nations where the high rank coal resources are in decline or due to the increasing demand for lower pollutant emissions, have been forced to investigate this technique.

On the other hand, to better face possible problems in the application of this technology, a deeper understanding of the various phenomena occuring inside the fluidized bed reactor - which includes combustors, boilers and gasifiers - is essential. This can be achieved only by a combination of experimental and theoretical research in which a comprehensive simulation program can play an important role.

1.3. Objectives

The objectives of a mathematical model and simulation are to use it for:

a) Optimization. A mathematical simulation program is a very important and powerful tool for the study of the influences of various parameters on the process. Contrasting with experimental and pilot plant research, which has to rely on corrections to predict the effects of scale changes and demands a considerable amount of material and human resources, a mathematical model, that uses such practical knowledge which has already been accumulated, can be used to verify or predict the many influences regardless either to differences in scale or to the particular kind of operation. This is possible if most of the basic phenomena that affect the process have been taken into account by the model equations. Besides, the cost of model development and computer processing time is usually negligible when compared with the former empirical alternatives to investigate the same range of variables.

b) A design tool. Depending on the comprehensiveness of the mathematical model, it can be used to verify the response of a complex system for possible changes in load, fuel characteristics and quality, inert and limestone qualities, equipment geometry, system of heat exchangers in the bed and freeboard, distributor design, insulation characteristics, among several other factors.

c) Operation control. As a simulation program it can be processed in a very short time, it is compatible

with the time scales for decision making due to changes in any external factor such as, for instance, characteristics and qualities of fed materials. It can eventually be used as a tool to diagnose problems and faults in the operation of the plant.

d) Prediction or control of pollutants emission. With the increasing restrictions on SO_x and NO_x emissions, a simulation program can be used to find, during the design phase or even in operation time, a feasible range of operational conditions that meet the required standards.

It is important, also, to stress that a mathematical model is a tool that can be improved continuously to include better or more recently published correlations for the involved phenomena leading to more precise predictions and/or to enlarge the range of the program applicability.

1.4. Validity of the model

The validity of a model is evaluated by comparisons between the generated results and the real data at various operational conditions.

The development of a mathematical model can be carried out at different levels of sophistication, which depend on the characteristics, quantity and quality of the required information about the process. For instance, a very simple model could be satisfactory for improving the control system during the operation of a particular unit but could not be enough if predictions about the operation

at different conditions, strategies or equipment geometries are considered.

As all relationships and equations are approximate representations of nature, some factors that could be considered, at first glance to be negligible can actually play a very important role in the stabilization of the entire calculation. The instabilities are normally reflected in impossible mathematical operations, non-convergence for loops or systems of differential equations and excessive computer processing time. Therefore a compromise between these factors should be found for the success of the task. On the other hand, as the ever increasing power and processing speed of computers has brought a proportional increase on the amount of details and phenomena that can be included in mathematical models, the compromise between sophistication and processing time is continuously changing.

1.5. The model development

As might be expected, this work passed through several stages.

The first version of the mathematical model was completed within a period of six months. It considered seven chemical reactions, thirteen gas and six solid components but the solution of the mass balance equations was accomplished by dividing the bed into small compartments where complete mixing was assumed. This approach proved to lead to a very unstable calculation with results that depended too much on the assumed size of the compartment. The temperature was still assumed constant throughout the bed leading to unsatisfactory results.

A second version was initiated by writing differential mass balances having the bed height as the independent variable. Although the temperature was assumed constant, that version showed a distinct quality change with respect to the method of computation, and the mentioned instabilities of the first version were eliminated. At this point the program considered:

a) Twenty five chemical reactions (all in the present version). In addition to the combustion and gasification of solid and gases, the devolatilization of the carbonaceous material and the drying of all solids in the bed were included;

b) Complete dynamics of fluidization, including the variation of the bubble size with the bed height;

c) Possibility to choose between the unreacted

core (shrinking core) model or the exposed core model for the heterogeneous reactions;

d) Elutriation, entrainment and attrition of solid particles. This allowed the determination of both the particle size distribution in the bed and throughout the freeboard.

On the other hand, as the average temperature in the bed was calculated by an iterative overall energy balance, the results showed some difference from the experimental data.

This analysis pointed to the necessity of the development of a third version of the model which could include not only the differential mass balances but, also, the differential energy balances throughout the bed height for each phase, i.e., solid carbonaceous material, solid inert, limestone, gas in the emulsion and gas in the bubbles.

After some problems with instabilities during the solution of the set of coupled non linear differential equations, this version showed much more realism and good agreement between the simulation and published experimental data. The most interesting point is the immense importance of the first few millimetres of the bed height where almost all the processes in the emulsion phase are defined. Gradients of temperature (10^6 K m^{-1}) much higher than the rest of the bed height (10^2 K m^{-1}) were determined. Similar differences in the gas concentration gradients were observed. After the first layers from the bed base all the

combustion reactions are mainly controlled by the relatively slow mass transfer between the emulsion and bubble phases explaining the almost constant temperature observed throughout the bed during real operations. These aspects are discussed in more detail later in the text.

The points found to be the more time consuming during the development of this mathematical model and simulation were:

a) The constant reviewing of appropriate mathematical descriptions for the chemical reaction kinetics. The published reaction rate relationships are normally developed to reproduce experimental observations in narrow ranges of temperature, pressure and concentration. Moreover the kinetics for solid-gas reactions are developed for a specific solid material. A special procedure to account for the reactivity of carbonaceous materials had to be developed and is described later in the text;

b) The combination of several phenomena in order to built a coherent system of calculations is a cumbersome and sometimes misleading work. The various published correlations, which describe individual behaviour of these phenomena, are frequently in contradiction not to mention mistakes found in the reproduction of the referred equations from different authors. On the other hand, several phenomena are not properly understood at the present moment therefore contributing to mathematical contradictions in the model. In these cases careful

investigation and comparisons among the available formulae are necessary to in order to choose the best description for the individual process;

c) The program uses several calculation strategies that include convergence calculations which are supposed to lead to real values but during the computation could pass through values which though mathematical plausible, are physically impossible. Most of these flaws can be found only by exhaustive running of the program and special mechanisms must be set to avoid singularities and to speed up the computation.

The model is believed to be at least as comprehensive, if not more so than any previously published works on fluidized bed modelling. Of course it is always possible to improve any model indefinitely due the very fact that all correlations are approximations of the natural behaviour. A fair compromise must be achieved between precision and computer processing time. This correlation changes continuously with the increasing computation capacity available.

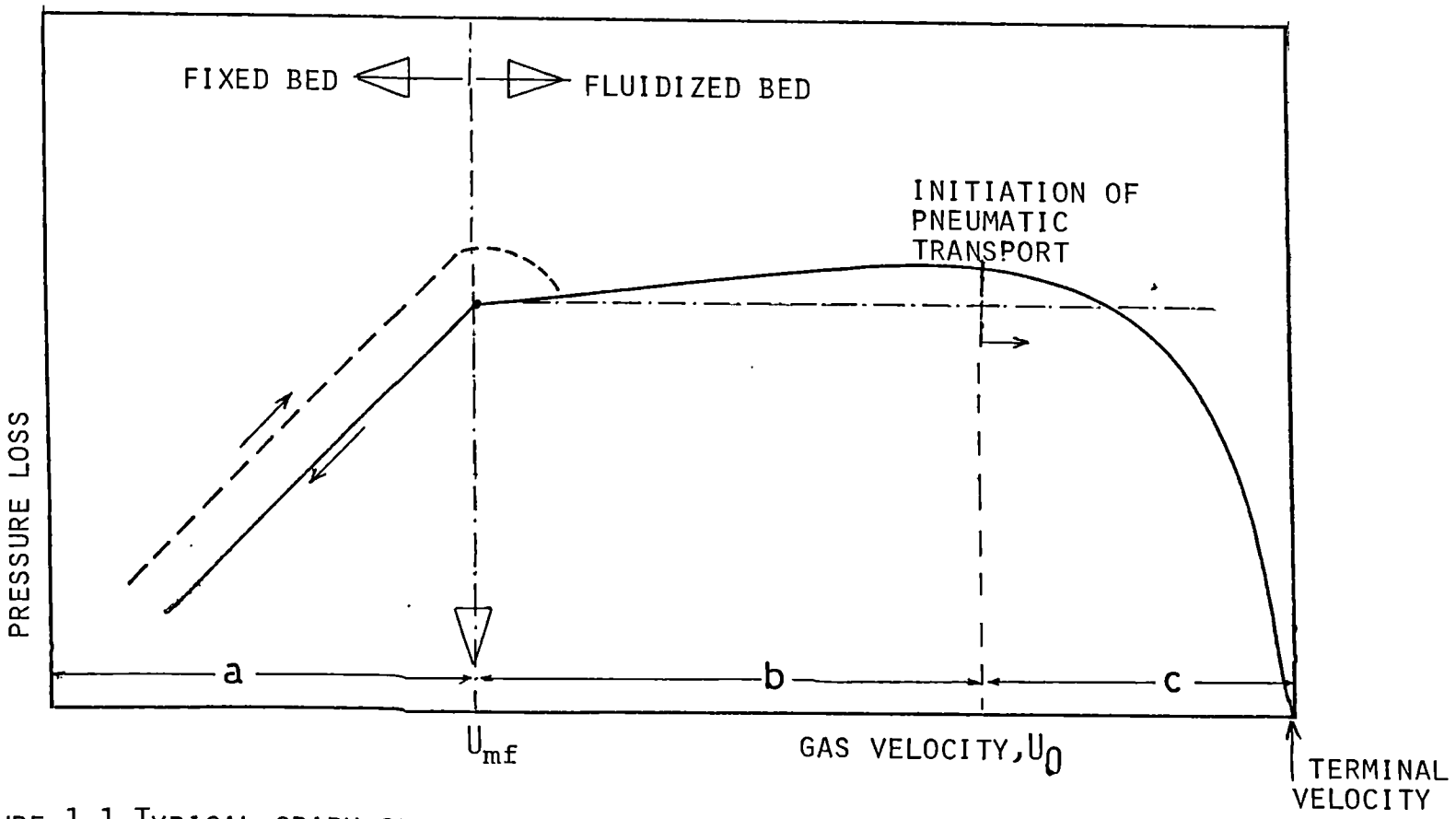

FIGURE 1.1. TYPICAL GRAPH OF PRESSURE LOSS IN THE BED AGAINST THE SUPERFICIAL VELOCITY.

CHAPTER II

2. HISTORICAL BACKGROUND

Due to its importance, several works on mathematical modelling of fluidized bed combustion and gasification have been published. The present historical review is intended to provide an overall description of these models.

As in any other scientific and technical progress, the development of mathematical model is not a clear path in which one step represents, necessarily, an improvement on every aspect of a previous one. The main reason for this is that the simulation programs, most of the time, are built to predict a particular phenomenon or group of phenomena of the process with some accuracy and allowing some rough hypothesis or severe simplifications to other aspects of less interest. Therefore an historical review must be done by dividing the subject into several sections concerned with each basic aspect of the process and with the modelling itself. The chosen sections are:

1) The bed fluid dynamics;
2) The bed flow regimes;
3) The chemical reactions involved;
4) The chemical kinetics;
5) The heat transfer to immersed surfaces;
6) The particle size distribution;
7) The basic structure of the model.

In the present historical review a classification

of the various mathematical models as a function of the involved details on each aspect is proposed. To accomplish this, a table for each of the above items is included which contains a list of the previous published mathematical models in chronological order.

2.1. Models involving fluid dynamics

The total flow rate in the emulsion and bubble phases are determined by a suitable model of the fluid dynamics for the process. The basic models found in the published literature so far are:

1) The two-phase model;

2) The three-phase model.

Fig.2.1 illustrates some main aspects of these models.

2.1.1. Two-phase model

The two-phase model assumes:

a) The existence of two phases in the bed: a particulate or emulsion phase that contains all the solid particles suspended in the gas and a bubble phase that contains no solid particle;

b) The emulsion phase remains in the state of minimum fluidization, i.e., the mass flow of gases through this phase is equal to the flow rate of a minimum fluidization condition, already described. Also, all other dynamic parameters of this phase, as for instance the voidage fraction, are maintained at the minimum fluidization condition;

c) Through the bubble phase passes all flow in excess of the flow rate equal to the minimum fluidization condition.

This model was first postulated by Toomey and Johnstone (1952) and later used by Davidson and Harrison (1963) who added the following assumptions:

d) The particulate phase is an incompressible fluid and has a bulk density of $\rho_P (1 - \epsilon_{mf})$;

e) The gas bubbles are free of solids and have spherical shape;

f) The gas flow in the particulate phase is an incompressible viscous fluid. The relative velocity between gas and solids satisfies in any direction x the so called D'Arcy's Law for the percolation through fixed beds:

$$U_G - U_S = - \text{const.} \frac{\partial P}{\partial x} \qquad (2.1)$$

g) The pressure in the bubble is constant;

h) The undisturbed pressure gradient in the vertical direction exists far from the bubble.

These detailed hypothesis were used to deduce the various parameters of fluidization as, for example:

1) Solid rate circulation and

2) Mass transfer between bubble and emulsion phases.

In addition, Davidson and Harrison extended the two-phase theory to two distinct possibilities concerning the bubble rise velocity:

a) A slow-bubble regime, where the bubble rise

velocity is lower than the interstitial velocity of the percolating gas through the emulsion or

$U_B < U_f = U_{mf}/\varepsilon_{mf}$

where the bubbles can act as a short-cut to the gas in the emulsion and there is a free gas transfer between the phases. This model is called here: "E+(B+C)" or Emulsion + (Bubble+Cloud);

b) A fast-bubble regime, where:

$U_B > U_f = U_{mf}/\varepsilon_{mf}$

and the bubbles are surrounded by a cloud layer which remains with the bubbles and constitutes a barrier to the mass transfer between the emulsion and the bubbles. This model is called here: "(E+C)+B".

It is interesting to note that some fluidized bed, particularly a FBC unit, can operate in both regimes simultaneously. Near the distributor, due to the lower average temperature and small bubbles, it is possible to have a slow-bubble regime while for the rest of the bed a fast-bubble regime could predominate. As it will be seen, the present work does not assume one or another model but the local regime is dictated by the mass and energy balances throughout the bed.

A detailed analysis of Davidson's theory is not included here as some of the equations derived from this theory are discussed in the text ahead. On the other hand, it must be mentioned that the work of Davidson and Harrison was a breakthrough in the understanding of bubbling fluidization phenomena and brought to light a series of

physical aspects as for instance:

1) The explanation of bubble stability;

2) How the bubble retains its identity leading to relatively small interaction with the emulsion phase.

2.1.2. Three-phase model

This model was first set by Kunii and Levenspiel (1968) and came as an extension of the Davidson and Harrison's theory due to the failure of the previous one in explaining the following facts:

a) The observed form of the bubbles are not spherical but present a concavity at the bottom. This is due to a pressure gradient between the lower part of the bubble and the gas in the emulsion leading to a turbulent mixing zone behind the bubble. This, as suggested by Rowe and Patridge (1962), is the main mechanism for the solid mixing in a bed;

b) The presence of a wake behind the bubble which has a great influence on the mass transfer between the bubble and emulsion phase;

c) The experimental verification of the departure of the minimum fluidization condition in the emulsion phase from the bottom to the top of the bed during fluidized combustion.

In order to explain these contradictions, the three-phase model assumes that (quoted from Kunii and Levenspiel, 1969):

1) "Every rising bubble drags behind it a wake of material. Let the ratio of wake to the bubble volume be

α_{kn}, estimate $\alpha_{kn} = V_{wake}/V_B$ from the experiments, and take the void fraction of the wake to that of the emulsion phase";

2) "Just above the distributor, solid is entrained by the rising bubbles to form the bubble wake. This solid is carried up the bed at velocity U_B and is continually exchanged with fresh emulsion solid as it rises. At the top of the bed this wake solid rejoins the emulsion to move down the bed at velocity U_S";

3) "The relative velocity between upward percolating emulsion gas U_E and downward flowing solid U_S is given by the minimum fluidizing conditions:

$$U_E = U_f - U_S = \frac{U_{mf}}{\varepsilon_{mf}} - U_S \qquad (2.2)$$

This expression shows that if the downward velocity of solids is sufficiently high, as may be the case in vigorously bubbling beds, then the emulsion gas will reverse its direction of flow. This result may seem surprising to some; nevertheless, tracer studies in vigorously beds support this finding (Kunii et al. 1967)";

4) "We consider only beds having fast moving bubbles accompanied by thin clouds (or $U_B/U_f > 5$)".

By the use of this model, Kunii and Levenspiel managed to deduce equations for the bed dynamics as for example:

a) The upward velocity of gas in the emulsion phase as:

$$U_{GE} = \frac{U_{mf}}{\varepsilon_{mf}} - \frac{\alpha_{kn}\, U_o}{1 - \delta_{kn} - \alpha_{kn}\, \delta_{kn}} - \alpha_{kn}\, U_{mf} \qquad (2.3)$$

where the volume fraction of the bubble phase in the bed is estimated by:

$$\delta_{kn} = \frac{U_o - U_{mf}}{U_B} \qquad (2.4)$$

b) The downward velocity of solid particles in the emulsion as:

$$U_S = \frac{\alpha_{kn}\, \delta_{kn}\, U_B}{1 - \delta_{kn} - \alpha_{kn}\, \delta_{kn}} \qquad (2.5)$$

Thus the important derivations from this theory, some of which are discussed in the specific sections of the present work, are:

1) The "Turnover rate of solids" that represents the flux of solids across any horizontal plane is given by:

$$G_S = \alpha_{kn}\, \delta_{kn}\, U_B\, \rho_S\, (1 - \varepsilon_{mf}) \qquad (2.6)$$

2) The mass transfer coefficient between bubble and emulsion phases with the help of the penetration model of diffusion from Higbie (1935). This equation is discussed in the section for mass transfer coefficients.

2.1.3. Variations on the basic models

Since these two basic models have been developed some variations have been proposed in order to improve descriptions of particular phenomena.

For instance, the assumption of spherical bubbles in the Davidson and Harrison (1963) theory was reviewed by Murray (1966) who worked out a modification of the Davidson's model to accommodate the fact that the bubble is concave at its bottom due to a depression in this region. This led to a cumbersome treatment which is out of the scope of this review.

Another important example is the work of Mori and Wen (1975), which is usually known as "Modified Bubble Assemblage Model". It is an improvement on the two-phase theory that, in contrast with the previous models, takes into consideration the growth of bubbles along the bed height. The correlations to account for the bubble growth are both semi-empirical and empirical and are presented in the "Bubble phase parameter" of the present work.

The model of Mori and Wen (1975) also includes various aspects concerning the continuous changing in the conditions along the bed height. They assumed the existence of compartments or cells in series, inside which the mixing of solids and gases was perfect. This contrasts with previous works that assumed a perfectly mixed bed as a whole. The aspects of models of flow regimes is discussed in Sec.2.2.

More recently, Glicksman et al.(1981) presented a

model to describe the fluid mechanics in a fluidized bed. They deduced some relationships between the gas flows through the emulsion and bubble phases which do not distinguish between fast and slow bubble regimes. It seems that the application of this theory could lead to some improvement over the previous models if an overall balance model is to be used as an approximation.

The present work assumes the two-phase theory only to define the boundary conditions at the base of the bed. The condition of mass flows throughout the emulsion and bubble phase are determined by mass balances that are set for each chemical species. Also the voidage fraction in the emulsion phase is not necessarily the same as at the minimum fluidization condition. This is described in the next chapter.

2.1.4. Classification according the fluid dynamics

As has been commented before, a classification for the available models in each phenomenon of the fluidized bed process is suggested in the present work. The idea is to present each aspect in tables which contain the progressive level of detail and a list of the works that used that particular line of reasoning.

In this section a classification for the models in fluid dynamics is presented along with a similar one according to the bubble characteristics assumed by each author. They are shown in the two tables below.

It must be said that although attempts have been made to cover most of the available literature, it is

possible that some work could be missing in the lists presented.

Basic aspect of the model	First level of assumption	Second level of assumption	Examples of modelling
Fluid dynamics	No distinction between bubble and emulsion		Park et al.(1981)
	Two-phase model	(Emulsion+ Cloud) & Bubble or (E+C)-B	Shen & Johnstone(1955) May(1959) van Deemter(1961) Orcutt et al.(1962) Davidson(1963) Mamuro & Muchi(1965) Mori & Muchi(1972) Avedesian(1973) Gibbs(1975) Gordon et al.(1976,78) MIT(1978) Raman et al.(1981) Tojo et al.(1981) Weimer(1981) Overturf(1983a,b) Chang et al.(1984) Present work *
		E-(C+B) (3)	Johnstone et al.(1955) Davidson(1963) Kobayashi & Arai(1965) Muchi(1965) Partridge & Rowe(1966) Toor(1967) Kobayachi et al.(1969) Kato & Wen(1969) Mori & Wen(1975) Horio et al.(1977a,b) MIT(1978) Rajan et al.(1979) Rajan and Wen(1980)
	Three-phase or E-C-B		Kunii (1968) Chen(1977,78) Saxena et al.(1978)

TABLE 2.1.Classification of models according to the fluid dynamics in the bed. (*)= Two-phase theory is assumed only at the base of the bed.

In this table and throughout this Chapter the following abbreviations have been used to save space:

Avedesian = Avedesian and Davidson

Chen = Chen and Saxena

Davidson = Davidson and Harrison

Kunii = Kunii and Levenspiel

Overturf = Overturf and Reklaitis

Toor = Toor and Calderbank

Weimer = Weimer and Clough

The second table below, presents a classification according to the bubble characteristics. It can be seen that the great majority of the mathematical models use the idea of spherical and growing bubbles.

Basic aspect of the model	First level of assumption	Second level of assumption	Examples of modelling
Bubble characteristics	Spherical	Constant size	Orcutt et al.(1962) Davidson(1963) Kunii (1968) Avedesian(1973) Gibbs(1975) Gordon(1976,78) Tojo et al.(1981)
		Variable size	Mamuro & Muchi(1965) Partidge & Rowe(1966) Toor(1967) Kobayashi et al.(1969) Kato & Wen(1969) Mori & Muchi(1969) Mori & Wen(1975) Horio et al.(1977) Chen(1977,78) Saxena et al.(1978) MIT(1978) Rajan et al.(1979) Rajan and Wen(1980) Raman et al.(1981) Weimer(1981) Overturf(1983a,b) Chang et al.(1984) Present work
	Non-spherical	Constant size	Murray(1966)
		Variable size	No work found

TABLE 2.2.Classification of models according to the bubble characteristics.

2.2.Models involving bed flow regimes

As for any other packed bed, a fluidized bed is basically a system where the fluid percolates through the particles. The additional complications arise from the fact that part of the fluid by-passes contact with particles via the bubble phase and the particles themselves have a strong

circulation in the bed.

Several models for the flow regimes for each different phase (gas in the emulsion, gas in the bubbles and solids) in the bed have been tried over the years and can be summarised as:

1) Complete mixing in the bed;

2) Complete mixing in finite compartments in the bed;

3) Plug flow or one-space dimensional variation;

4) Two-space dimensional variation.

These possibilities can be applied for each different phase. For instance a complete mixing for the gas in the emulsion will assume that in this phase no variation in any property (composition, temperature or pressure) is observed throughout the bed height. The complete mixing within each finite compartment would need a definition of the size or length of the compartment. The plug flow model will need the calculation of every property at each point of the bed height and will assume that these variations occur only in the vertical (axial) direction of the bed.

Some recent works have attempted to approach the two-space variations by considering the axial and radial variations in the bed. This level of sophistication seems to fall in the category of an over complicated model that leads to some false results. As it is commented ahead, this is due to the very few experimental works available in the current literature to support the correlations used in these models. This forces the adoption of an increasing

number of assumptions that normally jeopardize the reliability of the simulation.

2.2.1. Classification according the flow regimes

The table below shows a proposed classification of the mathematical models published so far according to the adopted flow regimes for the various phases in the bed.

Basic aspect of the model	First level of assumption	Second level of assumption	Examples of modelling
Flow regimes	Complete mixing	In the bubble	Davidson(1963) Kunii (1968)
		For the emulsion gas	Davidson(1963) Kunii (1968) Avedesian(1975) Gibbs(1975) Gordon et al.(1976,78) Weimer(1981) Overturf(1983a,b) *
		For the solids	Davidson(1963) Kunii (1968) Avedesian(1975) Gibbs(1975) Gordon et al.(1976,78) Chen(1977,78) Saxena et al.(1978) Park et al.(1981) Raman et al.(1981) Weimer(1981) Overturf(1983a,b) Present work
	Complete mixing within each compartment	In the bubble	Mori & Wen(1975) Horio et a.(1977) Rajan et al.(1979) Rajan and Wen(1980)
		For the emulsion gas	Mori & Wen(1975) Horio et al.(1977) Rajan et al.(1979) Rajan and Wen(1980)
		For the solids	Mori & Wen(1975) Horio et al.(1977) Rajan et al.(1979) Rajan and Wen(1980)

CONT...

CONT...

Basic aspect of the model	First level of assumption	Second level of assumption	Examples of modelling
Flow regimes	Plug-flow	For the bubble	Avedesian(1975) Gibbs(1975) Gordon et al.(1976,78) Chen(1977,78) Saxena et al.(1978) Raman et al.(1981) Tojo et al.(1981) Weimer(1981) Overturf(1983a,b) Chang et al.(1984) Present work
		For the emulsion gas	Chen(1977,78) Saxena et al.(1978) Raman et al.(1981) Overturf(1983a,b)** Chang et al.(1984) Present work
	Radial or horizontal dispersion	For the bubble	Park et al.(1981)***
		For the emulsion gas	Park et al.(1981)*** Tojo et al.(1981)
		For the solids	Tojo et al.(1981)

TABLE 2.3.Classification of models according to the flow regimes. (*)=above the "jet" region of the bed;(**)=only in the "jet" region; (***)=no distinction between phases is made.

2.3.Models involving chemical reactions

The process of combustion and/or gasification inside a fluidized bed reactor involves an innumerable number of different chemical reactions.

On the other hand, a combustion process can be

seen as a particular case of gasification of carbonaceous material because all reactions that take part in the latter also occur in the former process and vice-versa.

Several models for the combustion process tend to neglect the so called, gasification reactions (mainly $C-H_2O$, $C-CO_2$, $CO-H_2O$) due to their relative slow rate if compared with the combustion reactions (mainly $C-O_2$ and $CO-O_2$). This could be true for regions near the distributor where the oxygen concentration is high but could lead to severe error in the predictions of composition and temperature profiles at points distant from the distributor or in the emulsion phase.

Another aspect that is frequently neglected in FBC modelling is the devolatilization process and reactions. As will be shown in the model classification table prepared for this aspect, several mathematical models do not take into account these reactions and others tend to use strong simplifications. For instance to consider them as instantaneous or evenly distributed production or controlled by factors completely independent of the kinetics such as the mixing rate of solids in the bed. If a simple choice between instantaneous and continuous devolatilization is to be made, the work of Borghi et al.(1977) leads to the second one. As in the present work the devolatilization reactions are treated by considering their kinetics associated with the resistances for diffusion of the products from the carbonaceous solid, there is no need to assume either one or another extreme

situation.

Although drying is not a chemical reaction, its inclusion as a source for water plays an important part as a reactant in the process is very important. Surprisingly, almost all models and simulation programs found in the literature do not take into account the drying process, not only of the carbonaceous solid but also for the inert (sand for instance) and the limestone.

2.3.1. Models of the chemical kinetics

The results generated by the simulation are strongly influenced not only by the kind of chemical reactions considered in the mathematical model but also by how their reaction rates are computed.

Basically there are two main categories of reactions involved in the processes of combustion and gasification:

a) Homogeneous or gas-gas reactions;

b) Heterogeneous or gas-solid reactions.

During the past decades, the reactions involved in the combustion and gasification processes have had their kinetics studied in some detail and these are discussed during the description of the mathematical model ahead. For the moment it is enough to know that the simulation models of FBC or FBG published so far have sharp differences concerning the calculation of the gas-solid reaction rates. This is due to two basic reasons:

1) The first concerns the fact that a reacting solid particle can behave in two basic limiting situations

during its consumption by combustion or gasification:

a) Unreacted-core or shrinking-core model;

b) Exposed-core or segregated-ash model.

The unreacted-core model assumes the solid particle to be covered by a layer of solid material already reacted and therefore chemically inert which is known as ash, in the case of carbonaceous material. This layer constitutes a resistance to the advance of the gas-solid reaction due the necessary diffusion process for the gas through this layer to reach the internal core of unreacted solid. The process of diffusion is normally slower than the basic chemical reaction rate, which is normally determined using very small particles to minimize diffusion resistances, leading to a behaviour called: diffusion-controlled reaction. The other possibility, i.e. the exposed-core model, the formed ash does not remain attached to the unreacted core and the layer resistance ceases to exist. This ash or inert material will increase the inert concentration within the process and must be computed during the calculations. The physical characteristics of the solid and the ash and the conditions of temperature and attrition, among other influences, can determine the main behaviour of the particle. In a fluidized bed reactor both possibilities can be found and certainly an intermediate model is more likely to happen. On the other hand, the degree of combination of the two extremes is almost impossible to predict without a previous experimental test and the existing mathematical models for FBC or FBG usually

must assume one or another behaviour. The present program was developed to allow the user to choose either solid-gas model.

2) The second source for differences in the published chemical rates is due to the variable reactivity of the carbonaceous solid. As no published work takes into account this factor, they can be used only for a certain specific kind of carbonaceous solid for which the introduced correlations were originally developed.

2.3.2. Classification according the chemical reactions

The table below presents a classification of the mathematical models for FBC and FBG according to the chemical reactions considered by the various authors. Also a classification for the treatment given for the devolatilization process is included.

Basic aspect of the model	First level of detail	Second level of detail	Third level of detail	Examples of modelling
Chemical reactions considered	Carbonaceous solid combustion and CO combustion	In the bed	In the emulsion phase	Avedesian(1973) Gibbs(1975) Gordon et al.(1976,78) Horio et al.(1977) Chen(1977,78) Saxena et al.(1978) MIT(1978) Rajan et al.(1979) Rajan and Wen(1980) Park et al.(1981) Tojo et al.(1981) Weimer(1981) Overturf(1983a,b) Present work
			In the bubble phase	Gordon et al.(1976,78) Chen(1977,78) Saxena et al.(1978) Rajan et al.(1979) Rajan & Wen(1980) Park et al.(1981) Weimer(1981) Overturf(1983a,b) Present model
		In the freeboard		Rajan et al.(1979) Rajan and Wen(1980) Park et al.(1981) Overturf(1983a,b) Present work

CONT...

CONT...

Basic aspect of the model	First level of detail	Second level of detail	Third level of detail	Examples of modelling
Chemical reactions considered	Devolatilization or pyrolysis	Instantaneous		Gibbs(1975) Horio et a.(1977) Park et al.(1981) Raman et al.(1981) Overturf(1983a,b)
		Homogeneous release		Weimer(1981) Chang et al.(1984)
		Proportional to the mixing rate or to the feeding rate		Baron et al.(1977) Rajan et al.(1979) Rajan & Wen(1980) Chang et al.(1984)
		Diffusion & kinetic control		Present work
	Gasification reactions	In the bed	In the emulsion phase	Horio et al.(1977)* Rajan et al.(1979)* Rajan & Wen(1980)* Raman et al.(1981)@ Weimer(1981)+ Chang et al.(1984)@ Present work @
			In the bubble	Rajan et al.(1979) Rajan & Wen(1980) Raman et al.(1981) Weimer(1981) Chang et al.(1984) Present work
		In the free-board		Present work

CONT...

CONT...

Basic aspect of the model	First level of detail	Second level of detail	Third level of detail	Examples of modelling
Chemical reactions considered	SO_2 generation and absorption	In the bed		Horio et al.(1977) Chen(1977) MIT(1978) Rajan et al.(1979) Rajan & Wen(1980) Present work
		In the freeboard		Rajan et al.(1979) Rajan & Wen(1980) Present work
	NO_x generation and absorption	In the bed		Horio et al.(1977) MIT(1978) Rajan et al.(1979) Rajan & Wen(1980) Present work
		In the freeboard		Rajan et al.(1979) Rajan & Wen(1980) Present work
	Diffusion controlled drying	In the bed		Present work
		In the freeboard		Present work

TABLE 2.4.Classification of models according to the involved chemical reactions.(*)=Char+CO_2 reaction; (+)=Char+H_2O, Char+CO_2, CO+H_2O reactions; [2](@)=Char+H_2O, Char+CO_2, CO+H_2O, Char+H_2 reactions.

2.4. Models involving heat transfer

Among the several phenomena occuring in a boiler or gasifier that operates with a fluidized bed, the heat transfer processes have a very important influence. These processes can occur between:

a) Emulsion gas and bubbles in the bed;

b) Solids and gases in the bed and in the freeboard;

c) Solids and solids in the bed and in the freeboard;

d) Gases and immersed surfaces - walls, tubes and distributor - in the bed and in the freeboard;

e) Solids and immersed surfaces in the bed and in the freeboard;

Only by the computation of these effects can the prediction of temperature profiles in the bed and freeboard become possible. The knowledge of such profiles can improve the simulation because:

1) Chemical reaction rates vary dramatically with temperature;

2) Mass transfer between phases, physical properties, fluid dynamic parameters, among other various phenomena, depend on local temperature and on concentrations;

3) Heat transfer between bed or freeboard and immersed surfaces are determined by temperature differences;

4) Spots of high temperature can initiate ash softening and provoke bed collapse due to the increasing

the possibility of particles sticking together, or can increase tube and wall corrosion.

Several simplifications more or less critical have been found in the published works. Most of the works do not consider any heat transfer at all because no energy balance is performed and therefore a constant uniform temperature must be chosen in each case. Others include only an overall heat balance in the bed and therefore cannot compute the differences of temperature between the various phases. Even some models that include a differential energy balance in the bed do not take into account differences of temperature between gas in the emulsion, particles and bubbles and therefore cannot compute the different temperature profiles of these phases and particles.

2.4.1. Classification according the heat transfer

A table where the developed models are listed in chronological order and classified according the considered heat transfer influences is shown next in Table 2.5.

Basic aspect of the model	First level of detail	Second level of detail	Examples of modelling
Heat transfer	Considered to immersed tubes or surfaces	In the bed	Gordon et al.(1976,78) Horio et al.(1977) MIT(1978) Rajan et al.(1979) Rajan & Wen(1980) Present work
		In the freeboard	Rajan et al.(1979) Rajan & Wen(1980) Present work
	Considered between gases and solids	In the bed	Overturf(1983a,b) Present work
		In the freeboard	Present work
	Considered between solids and solids	In the bed	Present work
		In the freeboard	Present work

TABLE 2.5.Classification of models according to the heat transfer.

2.5.Models involving particle size distributions

As the solid particles are fed to the fluidized bed they suffer a series of simultaneous processes that will determine the particle size distribution in the bed. These factors are:

a) Reduction of the particle size due to the chemical reactions between gases and solids. This reduction is verified if the particles lose their already reacted outer layer due to a weak mechanical structure;

b) Reduction due to the attrition among the various particles or between particles and internal surfaces;

c) Variations due to the withdrawal of particles from the bed due to entrainment and elutriation to the freeboard.

As can be imagined, the computation of these effects is of paramount importance in the determination of almost all processes in a fluidized bed combustor or gasifier because they depend on the particle sizes as a parameter. Their importance depends as well on each kind of solid particle in the bed.

2.5.1. Classification according the particle size distribution

The existing mathematical models of FBC and FBG take into account one or more of the mentioned effects and they are listed below accordingly in Table 2.6.

Basic aspect of the model	First level of detail	Second level of detail	Examples of modelling
Particle size distribution	Considers variations in the bed	Due to chemical reactions	Gibbs(1975) Chen(1977,78) Saxena et al.(1978) Rajan et al.(1979) Rajan & Wen(1980) Park et al.(1981) Weimer(1981) Overturf(1983a,b) Present work
		Due to attrition	Rajan et al.(1979) Rajan & Wen(1980) Overturf(1983a,b) Present work
		Elutriation & entrainment	Chen(1977,78) Saxena et al.(1978) Rajan et al.(1979) Rajan & Wen(1980) Park et al.(1981) Overturf(1983a,b) Present work
	Considers variations in the freeboard	Due to chemical reactions	Rajan et al.(1979) Rajan & Wen(1980) Present work
		Elutriation & entrainment	Rajan et al.(1979) Rajan & Wen(1980) Overturf(1983a,b) Present work

TABLE 2.6. Classification of models according to the considered effects on the particle size distribution.

2.6. Basic structures of fluidized-bed models

The mathematical modelling of any chemical process usually requires the solution of basic mass and energy balances that describe the combination of phenomena in the studied system. Fluidized bed combustion and gasification are typical examples of chemical reactors and

therefore follow the necessity of the above mentioned solutions.

Normally a mathematical simulation is described by:

a) The number of phenomena and effects included in the basic mass and energy balances;

b) The way in which these equations are solved.

It is common to verify that a relationship exists between the chronological order of a model development and its complexity. At the end, the complexity more or less dictates the model structure. For example, the models that do not take into consideration the local variations inside the system but only the global effects are solved by overall mass and energy balances.

The other aspect when analysing a mathematical simulation is that the item (b) is, usually, the more evident aspect. Therefore the model structure can be chosen to classify the various simulation programs in different generations.

2.6.1. Classification according the model structures

As justified above, the handling of mass and energy balances have been chosen as a parameter to be used in the classification of a model structure and are presented in the two following tables 2.7 and 2.8.

Basic aspect of the model	First level of assump.	Second level of assump.	Third level of assump.	Examples of modelling
Mass balances	None or assumed composition	In the bed		Davidson(1963) Kunii (1968)
		In the free-board		Davidson(1963) Kunii (1968) Avedesian(1973) Gibbs(1975) Gordon et al.(1976,78) Horio et al.(1977) Saxena et al.(1978) MIT(1978) Raman et al.(1981) Tojo et al.(1981) Weimer(1981) Chang et al.(1984)
	Overall	In the bed		Avedesian(1973) Gibbs(1975) Gordon et al.(1976,78) MIT(1978) Weimer(1981)+ Overturf(1983a,b)*
		In the free-board		Park et al.(1981)
	Overall in each compart-ment	In the bed		Mori & Wen(1975) Horio et al.(1977) Rajan et al.(1979) Rajan & Wen(1980)
		In the free-board		Rajan et al.(1979) Rajan & Wen(1980)

CONT...

CONT...

Basic aspect of the model	First level of assump.	Second level of assump.	Third level of assump.	Examples of modelling
Mass balances	Differential in the vertical direction	In the bed	Neglects axial dispersion	Chen(1977,78) Saxena et al.(1978) Tojo et al.(1981)++ Weimer(1981)++ Overturf (1983a,b)** Present work
			Considers axial dispersion	Raman et al.(1981) Chang et al.(1984)
		In the free-board		Overturf (1983a,b)*** Present work
	Differential in two directions	In the bed		Park et al.(1981)+++
		In the free-board		None

TABLE 2.7.Classification of models according to their structure based on the handling of mass balance equations. (*)=above the "jet" region of the bed; (**)=only in the "jet" region; (***)=only for the gas phase;(+)=only for the emulsion phase; (++)=only for the bubble phase;(+++)=no distinction between phases.

Basic aspect of the model	First level of assump.	Second level of assump.	Examples of modelling
Energy balances	None or assumed average temperature	In the bed	Avedesian(1973) Gibbs(1975) Chen(1977,78) Saxena et al.(1978) Park et al.(1981) Raman et al.(1981) Tojo et al.(1981) Chang et al.(1984)
		In the free-board	Avedesian(1973) Gibbs(1975) Gordon et al.(1976,78) Horio et al.(1977) Saxena et al.(1978) Raman et al.(1981) Weimer(1981) Chang et al.(1984)
	Overall	In the bed	Gordon et al.(1976,78) Weimer(1981)+ Overturf(1983a,b)* Park et al.(1981)+++
	Overall in each compart-ment	In the bed	Mori & Wen(1975) Horio et al.(1977) Rajan et al.(1979) Rajan & Wen(1980)
		In the free-board	Rajan et al.(1979) Rajan & Wen(1980)
	Differen-tial throughout vertical direction	In the bed	Weimer(1981)++ Overturf(1983a,b)** Present work
		In the free-board	Overturf(1983a,b)*** Present work

TABLE 2.8.Classification of models according to their structure based on the handling of energy balance equations.(*)=above the "jet" region of the bed;(**)=only in the "jet" region; (***)=only for the gas phase;(+)=only for the emulsion phase; (++)=only for the bubble phase;(+++)=only for the solids.

2.7. Comments on the more recent mathematical models

Besides the various classification tables presented above, this section is intended to analyse some more recent mathematical models in FBC and FBG from the point of view of the results achieved by them when simulation and real operations were compared. The presented sequence of works obeys a chronological order and it will discuss only the models claimed to be comprehensive, i.e., not intended to study few specific aspects of the operation of a FBC boiler or a FBG.

2.7.1. Rajan and Wen (1980)

This work was chosen because it is, from our point of view, the first of what can be called "Comprehensive Mathematical Model". This is due to the amount of detail covered by the model that embraces several important aspects of a FBC process. The complete report of this work with the original simulation program can be found in Rajan et al.(1979).

The model is intended to simulate a FBC and claimed to be capable of predicting:

a) Combustion efficiency;

b) Char and Limestone elutriation;

c) Particle size distribution in the bed and in the entrained materials;

d) Solids withdrawal rate from the bed;

e) Bed temperature profile;

f) SO_2 retention;

g) SO_2 and NO_x emissions;

h) Concentration profiles along the bed height for: CO_2, CO, O_2, SO_2, NO_x and Volatiles.

The importance of this work is due to the inclusion of several aspects which have been partially or not considered in former works, among them:

1) Devolatilization of coal;

2) SO_2 capture by limestone;

3) NO_x release and reduction by char;

4) Attrition and elutriation of char and limestone;

5) Bubble hydrodynamics;

6) Solids mixing;

7) Heat transfer between gas and solid and solids and heat exchange surfaces;

8) Freeboard reactions.

2.7.1.1.Model assumptions

Although the model assumptions have been already described by the tables 2.1 to 2.8 a few comments on some points are necessary.

One important aspect of this program is the one concerning the devolatilization process. Rajan and Wen assumed that the devolatilization rate of coal is neither instantaneous nor uniform in the bed but proportional to the solids mixing rate. This seems to originate from the observation that most of the volatiles are released near the feeding point of the coal in the bed. On the other hand it is known that the devolatilization process is a problem of kinetics and diffusion of volatiles from the interior of

the coal particle. Therefore there is no real correlation between solids mixing rate and volatiles release.

The Bubble Assemblage Model, originally idealized by Kato and Wen (1969) and modified by Mori and Wen (1975) is used. This means that the bed is represented by a series of compartments or cells in which there is perfect mixing and the size of each compartment must be chosen. The normal procedure was to set the compartment height as the bubble diameter. As the bubble diameters vary from a minimum value, which is normally about few centimetres,to the size of several centimetres and as most of the oxygen present in the emulsion phase is consumed in the first few millimetres of the bed, the model cannot determine the influence of the carbon combustion in the emulsion as a fast process which determines the temperature profile near the base of the bed. Therefore the model could represent only the sections where the oxygen comes from the bubble phase due to a slow diffusion process. Besides, the dependence on the choice for the heights of the compartments would serve as a strong parameter to be adjusted in order to fit results.

A similar technique of finite layers was tried in the first version of the present work which led to various problems of instability during the solution of the mass and energy balances throughout the bed and freeboard height. The instabilities were reduced by the reduction of the layer size which lead us to realize the necessity for a continuum formulation to the problem.

In order to illustrate the strategy used by the

authors, a diagram showing the model basic structure is shown in Fig.2.2.

2.7.1.2.Model evaluation

It is possible to list the positive points of this model as:

a) The aspect of comprehensiveness by including and trying to verify the combined effects of devolatilization, combustion, NO_x and SO_2 release and capture, particle size distribution, heat transfer to immersed surfaces among other in the bed and in the freeboard;

b) The possibility to predict the average temperature profile in the bed and freeboard. The results seem to agree very well at least with the presented experimental result;

c) The possibility to predict the concentration profiles in the bed and in the freeboard for CO_2, CO, O_2, Volatiles, NO_x and SO_2. Results have been compared with experiments only in the case of NO_x and showed a reasonable agreement;

d) It shows the importance of taking into account the variations of bubble size in the bed;

e) It shows the influence of the heat transfer between tubes and bed on the temperature profile;

f) It shows the effect of fluidising dynamics in the SO_2 retention by the limestone.

As weak points it is possible to list:

a) Although the good agreement between the

simulation prediction for the size distribution in the bed and one operation of a NASA experimental plant result, it should be pointed that the use of the correlations from Merrick and Highley (1974) to calculate the particle elutriation rates could lead to false results. This has been shown by Wen and Chen (1982) because elutriation rates cannot depend on the bed hydrodynamics as implied in the mentioned work. It seems that the excellent results were obtained due to the use of two adjustable parameters:

1) A solid mixing parameter that could vary from 0.075 to 0.3;

2) A parameter that represents the fraction of wake solids thrown into the freeboard which could vary from 0.1 to 0.5. The equations from Merrick and Highley (1974) are discussed in some detail in the section for particle size distribution calculations in the present thesis;

b) Several other simulation parameters are chosen and maintained fixed as such:

1) Bed to tube heat transfer coefficient as 320.3 W m^{-2} K^{-1};

2) Freeboard heat transfer coefficient as a third of the previous value;

3) Bed to wall heat transfer coefficient as 87.9 W m^{-2} K^{-1};

4) Wall heat transfer coefficient in the freeboard as 10.47 W m^{-2} K^{-1};

5) Cooling water temperature as 300K;

6) Heat capacity of solids as 900.1 J kg^{-1} K^{-1};

7) Heat capacity of gases as function of temperature only;

8) Density of limestone as 2400 kg m^{-3};

9) Density of coal as 1400 kg m^{-3}.

c) No comparisons between simulation and experimental results were made for:

1) The gas compositions throughout the bed or the freeboard and not even for the stack gas;

2) The combustion efficiency or carbon conversion in the process;

d) Important reactions as CO-H_2O, C-H_2O and CO-C have not been considered;

e) Apart from the carbon, no details or indication of how the various other components of the char have been considered in the stoichiometry of the heterogeneous reactions;

f) The solution by using finite compartments the size of which must be chosen, as already discussed.

2.7.2.Weimer and Clough (1981)

The second model that claims comprehensiveness is the modelling of a low pressure steam-oxygen fluidized bed coal gasification reactor.

The model included several innovations at that time, which will be described below.

2.7.2.1.Model assumptions

Assumptions have been stated already in the tables of the present chapter but the most interesting one is the idea of a space near the distributor that is denoted by the authors as a "jet region" and consists of gas jets instead of bubbles. These jets are assumed to have a

cylindrical shape that do not change inside the "jet region". The idea behind this concept is to divide the bed in two sections for the solution of the mass and energy balances. These sections have different behaviour mostly related to the rate of heat and mass transfer between the dilute phase (jets or bubbles) and the emulsion phase. The authors introduce a factor that is adjusted to correct the classical Kunii and Levenspiel (1969) transfer coefficients that, as is known today, underestimate these coefficients. The dilute phase is solved by a system of differential mass and energy balances throughout the bed height, and the emulsion phase, including the interstitial gas, is solved as a perfect mixed reactor. This avoids the arbitrary choice of compartment sizes, as in Rajan and Wen (1980), and speeds the calculations by overall mass and energy balances because the most stiff differential equation problem is related to the emulsion phase. On the other hand this approach brought some problems, as described below.

The simplified diagram showing the basic strategy used by the authors is presented in Fig.2.3.

2.7.2.2.Model evaluation

As positive points in this model it is possible to list:

a) Mass and energy balances in differential form, at least for the dilute phase, which avoids the arbitrary choice of compartments sizes;

b) Indicates the influence of various phenomena, such as:

1) Homogeneous and heterogeneous reactions as: $C-O_2$, $C-CO_2$, $C-H_2O$, $CO-H_2O$, $CO-O_2$, and H_2-O_2;

2) Heat and mass transfer between dilute and emulsion phases and gas and solids;

3) Elutriation of particles;

4) Effect of the gas superficial velocity on the carbon conversion, on the average bed temperature and on the H_2/CO ratio in the product gas;

5) Effect of O_2 concentration in the inlet gas on the carbon conversion, average bed temperature and H_2/CO ratio in the product gas;

6) Temperature and concentration profiles in the jet phase.

As weak points it is possible to list:

a) The method applies the differential mass and energy balances only for the dilute ("jets" and bubbles) phase. This does not allow the determination of temperature and concentration profiles for the system throughout the bed; Furthermore, as the local (i.e. at any height of the bed) conditions of concentration and temperature for the emulsion phase are not determined the whole meaning for calculations of local mass and heat transfer processes between bubble and emulsion is spoiled because of the intrinsic dependence between these respective parameters;

b) No treatment for the freeboard is given. The reactions in the freeboard region have great influence on the process as a whole, especially in the product gas composition and in the case of gasifiers;

c) The use of the Merrick and Highley (1974)

treatment to evaluate the elutriation, as already commented;

d) The concept of "jet region" was used, in a certain way, to correct the Kunii and Levenspiel (1969) coefficients for heat and mass transfer between bubble and emulsion. The authors applied a correction factor to multiply the coefficients. This factor was allowed to vary between 5 and 90. No conclusion about a definite value was reported;

e) Several parameters were fixed as, for instance:

1) Physical properties for the solids and gases;

2) Minimum fluidization voidage;

3) Flow rate of solids by entrainment at the top of the bed;

4) Cyclone efficiency;

f) No comparisons between experimental and simulation results are shown. The authors claim that the experimental results from a Winkler gasifier reported in the literature are not sufficiently well documented to permit a rigorous evaluation of the theoretical model.

2.7.3. Raman et al.(1981)

The next model to be analysed was developed by Raman, Walawender, Fan and Chang for the biomass gasification in fluidized bed. It was chosen for a more detailed analysis due to its approach for the solution of the mass balances, that was accomplished by differential equations applied to both emulsion and bubble phases.

Actually the model is a dynamic simulation of the process but, as will be seen, only results for steady-state condition were compared against experimental data.

Later Chang, Fan and Walawender (Chang et al.,1984) tried to improve the model by assuming the devolatilization as proportional to the feeding rate of the carbonaceous solid and by using a different numerical method for the integration of the partial differential equation system. They obtained some results for the transient operation of the gasifier but no comparison against experimental result was published and the results for the steady-state condition have the same level of deviations as the former work.

2.7.3.1.Model assumptions

Apart from the assumptions already described in the previous sections, it is important to stress that although this model represents progress over the Weimer and Clough (1981) model from the point of view of mass balances it is also a setback due to the assumption of uniform temperature for the entire bed.

The simplified diagram showing the basic strategy used by the authors is presented in Fig.2.4.

2.7.3.2.Model evaluation

As positive points of this model it is possible to list:

a) Differential mass balances for the bubble and emulsion phases. This allows a more realistic computation of the mass transfer between the phases and the determination of the composition profiles for the gases throughout the bed.

b) Axial dispersion in the mass balances are included;

c) Inclusion of several important chemical reactions; among them the methane production by the C-H_2O reaction added to all included in the work of Weimer and Clough (1981);

d) Comparisons between experimental steady-state condition and simulation results are presented;

e) A guide for future improvements in the model is presented.

As weak points it is possible to list:

a) Neither the differential nor global energy balance are set. The bed is assumed isothermal and an average temperature in the bed is chosen as a parameter during the computations;

b) The devolatilization is assumed instantaneous. This can be very critical mainly in the case of biomass where the volatiles content is around 80% of the inflow solid;

c) No cracking and reforming of the tar is

included;

d) Although the model is intended to simulate gasification using air as a gasification agent (verified by the N_2 concentration in the reported results) neither homogeneous nor heterogeneous combustion reactions are considered;

e) No elutriation is considered and no particle size computation is accomplished;

f) Several parameters are assumed as fixed values and taken from experimental data, such as:

1) Minimum fluidization velocity and voidage;

2) Axial dispersion coefficients.

It seems, also, that the physical properties for gases and solids have been chosen as constants because no indication of their calculation is given;

g) Poor results are generated by the simulation when compared with experimental data. For instance, they show average deviations in the range of 27 to 30% for the gas molar fractions of the product gas, 13 to 30% for the gas yield and 24 to 30% for the char remaining concentration in the bed.

2.7.4. Overturf and Reklaitis (1983a,b)

This work was published in two papers. The first showing the general formulation and and the method applied to obtain the solution (i.e., the mathematical model and simulation program) and in the second an application for coal combustion.

This work is particularly interesting due to

various conclusions about the FBC process and about the mathematical modelling itself. Some of these conclusions even come to justify certain assumptions made in the model presented in this thesis.

2.7.4.1.Model assumptions

From the assumptions already shown in the tables 2.1 to 2.8, it is important to note that this was the first work where the freeboard section was treated in a more realistic way, i.e., assuming a plug flow and with a consideration of the chemical processes in this region. On the other hand it sets almost the same structure used by Weimer and Clough (1981) for the bed section which assumes a "CSTR" model for the emulsion phase.

The simplified diagram showing the basic strategy used by the authors is presented in Fig.2.5.

2.7.4.2.Model evaluation

As positive points of the Overturf and Reklaitis model it is possible to list:

a) Mass and energy balances in differential form for the "grid region" (or region near the distributor that Weimer called "jet region") and for the dilute phase;

b) Includes the effect of various phenomena, such as:

1) Homogeneous and heterogeneous reactions in a general form although in the application presented for coal combustion, only the following were considered: $C-O_2$, $C-CO_2$ and $CO-O_2$;

2) Single particle gas-solid reaction-diffusion or

shrinking core model for the heterogeneous reactions;

3) Heat and mass transfer between dilute and emulsion phases and gas and solids;

4) Detailed balance to allow the calculation for the particle distribution in the bed, in the overflow from the bed and in the elutriated stream. This balance considers the influences of the various currents of inflow and outflow of particles, elutriation and chemical reactions.

c) Comparisons between simulation and industrial unit operation from Babcock and Wilcox;

d) Influencing factors on the generated results are studied, among them:

1) Bubble size;

2) Emulsion phase temperature;

3) Elutriation rate;

4) Particle size;

5) Particle temperature;

6) Char emissivity.

e) Some conclusions are interesting and could help with future work such as:

1) "Representation of reactive solids by an average size and density is adequate for the prediction of combustor performance". They reached to this after verifying that disparities from the use of a monosized average particle on the calculations of heterogeneous reaction rates are caused mainly by the differences in fluidization properties.

2) "Satisfactory modelling of combustors requires a more reliable prediction of single-particle elutriation rates

and a more detailed description of single-particle combustion than is offered by the conventional single-film shrinking core model".

As weak or negative points it is possible to list:

a) The model structure suffers the same problems as the one developed by Weimer and Clough (1981), i.e., the assumption of a CSTR behaviour for the emulsion phase, which includes all solid particles and interstitial gas, that contrasts with the plug flow model for the dilute phase or jet/bubble phase. As the conditions within the emulsion phase must be taken as average constants for the entire bed, the local mass and energy transfer processes to the dilute phase are bound to bring deviations. These deviations, probably, forced to account for a correction factor that multiplies the heat and mass transfer coefficients in the model. Such deviations are more critical at points near the distributor due to the greater differences in concentrations and temperatures in this region, which the authors called "grid region" and the multiplication factor was called "Grid Enhancement Factor". In fact this factor was made to vary from 10 to 150 in order to adjust simulated results against experimental ones. It is interesting to note that the first conclusion achieved by the authors was: "Proper representation of the grid region is essential in combustor modelling. If, as is likely the case, most dilute to emulsion-phase transfer occurs in the grid region, bubbling-bed models may be of

limited value in the predicting reactor performance";

b) The above problem led, in our point of view, to some false conclusions as, for instance, that "the reactor performance is insensitive to the average bubble size".

c) No secondary reactions were taken into account in the simulation of the FBC reactor therefore no prediction of several gas concentrations were possible as for instance: H_2, CH_4, pollutants, etc;

d) The reaction of SO_2 with CaO was neglected;

e) The use of Merrick and Highley (1974) correlations to calculate elutriation rates, as already commented. The authors found inconsistencies or "anomalous behaviour" that they could not;

f) The authors failed to comment on the unusual temperature profile predicted by their model for the bubble phase. By that result, the bubble temperature was almost always higher than the emulsion phase temperature throughout the bed, although all important exothermic reactions occur in the emulsion phase;

g) Sherwood and Nusselt numbers were assumed as constants (equal to 2.0) in the calculations of mass and heat transfer between particles and gases;

h) To account for the effect of char reactivity, the authors assumed another arbitrary multiplying factor that took on values as big as 100.0;

i) Unfortunately, due to the amount of adjusting factors that tranformed the model into an overdetermined

system, no definite conclusions could be made about the performance of the model against experimental results. Indeed the authors suggest this by saying that "flue gas compositions as well as carbon and oxygen conversions of an experimental fluidized-bed combustor can be predicted by suitable tuning of model parameters".

2.8. Conclusions from the historical review and justification for the approach adopted in the present work

From the analysis of previously published mathematical models and simulations of fluidized bed boilers and gasifiers it is possible to merge the conclusions and the points that justify the development of the present model. They are:

a) The opportunity to combine in a single model the chemical reactions and phenomena common to combustion and gasification because the former can be seen as a particular case of the latter. Indeed, it is impossible to separate these aspects if a comprehensive approach to simulation of boilers or gasifiers is aimed for;

b) The published works, so far, do not include important aspects and phenomena of the process, such as:
1) The devolatilization reactions. Several works, as shown, do not consider these reactions or take them as an instantaneous process. Others assume that the rate of volatiles release is homogeneously distributed throughout the bed and finally some assume their rates to be proportional to the feeding rate or to the mixing rate of

solids. As it will be shown, there are several effects affecting the rate of such reactions and they interfere strongly in the process, mainly in the gasification of high volatiles content materials such as wood;

2) The dynamics of drying processes for the various solids added to the reactor, again, are not considered in the almost all existing works;

3) The chemical reactions other than carbon and CO combustion are not considered in almost all previous works and none have been found that take these reactions into account in the freeboard;

4) Although its importance on various aspects of the process, no published simulation model of FBC boiler has included the kinetics of limestone calcination;

5) The possibility to deal with different carbonaceous solid due to its physical structure or its reactivity;

6) Energy transfer between gas in the emulsion, gas in the bubble phase, coal (or other carbonaceous solid content), limestone (if added) and inert, and gas and particles in the freeboard. Again not considered by several authors. Others do not take into account the heat transfer between the different kind of particles.

7) Heat transfer between immersed surfaces (tubes and walls) and all solids and gases inside the bed and the freeboard. These processes are accomplished by all possible ways, including radiative transfer. Few works take into account these phenomena and none has been found that considers the effects of temperature differences among the

various solid particles and gaseous phases in these processes. Another unprecedented aspect of the present work is the ability to determine the heat losses to the environment and to include these effects during the solution of the differential energy balances throughout the bed and the freeboard.

c) A continuous differential mathematical treatment of the mass and energy balances for the bed and freeboard sections that contrasts with the overall or compartmented balances or even differential balances for imagined separated sections of the bed in the previously published works, as was seen in the historical review. This continuous approach leads to a real increase in the amount of information that can obtained by simulation. The main framework of the model includes a system of 46 differential equations that represent the mass and energy balances throughout the bed and in the freeboard. Considering the five phases in the bed, already mentioned, 13 gas components (CO_2, CO, O_2, N_2, H_2O, H_2, CH_4, SO_2, NO, C_2H_6, H_2S, NH_3 and tar), 14 solid components (C, H, O, N, S, ash, volatiles and moisture in the carbonaceous material, $CaCO_3$, CaO, $CaSO_4$, moisture in the limestone, SiO_2 and moisture in the inert) and 24 reaction kinetics, the mass and energy balances can provide a complete picture of almost all important processes in the bed. A similar approach is taken for the freeboard section. Therefore an important feature of the present program is concerned with the possibility of obtaining the concentration and temperature profiles in the

bed and in the freeboard for all gas and solid phases. Also the tube interior and surface temperature are calculated at each point. This information is vital for a safe and optimum design, allowing the identification of high temperature regions in the solid phases or on the tubes. The former, in some conditions, can lead to a bed collapse due to temperatures higher than the ash softening point and the latter to high erosion of tube surfaces;

d) Finally, during the development of the present computer simulation its possible use as a tool for engineering design has been kept in mind. This means that several aspects, not found in published programs, are produced by the computation, such as:

1) Composition, flow rate and temperature profiles for all gaseous phases (bubbles and emulsion interstitial gas) throughout the bed and for the gas current in the freeboard;

2) Temperature profiles for all solids throughout the bed and the freeboard;

3) Composition and flow rate (entrainment) profiles for all solids throughout the entire freeboard;

4) Average composition for each solid in the bed;

5) Particle size distributions for all solids in the bed and throughout the freeboard;

6) Average particle diameters in the bed and at any point of the freeboard;

7) Overflow of solids from the bed;

8) Average mass, volume, area, and number fractions among

the various solids in the bed and at any point of the freeboard;

9) Fluidization parameters as: superficial velocity, minimum superficial velocity, emulsion voidage, bubble voidage, total bed voidage, minimum fluidization voidage, bubble diameter at any point of the bed;

10) Carbon and any other solid component conversion in the bed and at any point of the freeboard;

11) Average residence time for any solid in the bed;

12) Calcium to sulphur molar ratio in the bed (in the case of using limestone to sulphur retension);

13) Static bed depth;

14) In the case of gasifiers, the energy output (flow rate of produced gas times its heat value) or efficiency (rate of energy output over rate of energy input) in the case of any fluidized bed boiler or gasifier;

15) Heat losses to the external ambience and temperature of the external insulation surface at any point of the bed and the freeboard;

16) Total heat transfered to the water/steam inside the tubes in the bed and in the freeboard (in the case of boilers);

17) Total mass flow of steam produced inside the tubes;

18) Heat transfer coefficients (internal, external and total) for the heat transfer to tubes in the bed and in the freeboard;

19) Heat transfer coefficients for the heat transfer to the external ambience;

20) Oxygen excess;

21) Pressure drop across the distributor and pressure loss in the bed;

22) Any property of gases or solids at any point of the system. This include: density, specific heat, viscosity (for gases), thermal conductivity, etc.

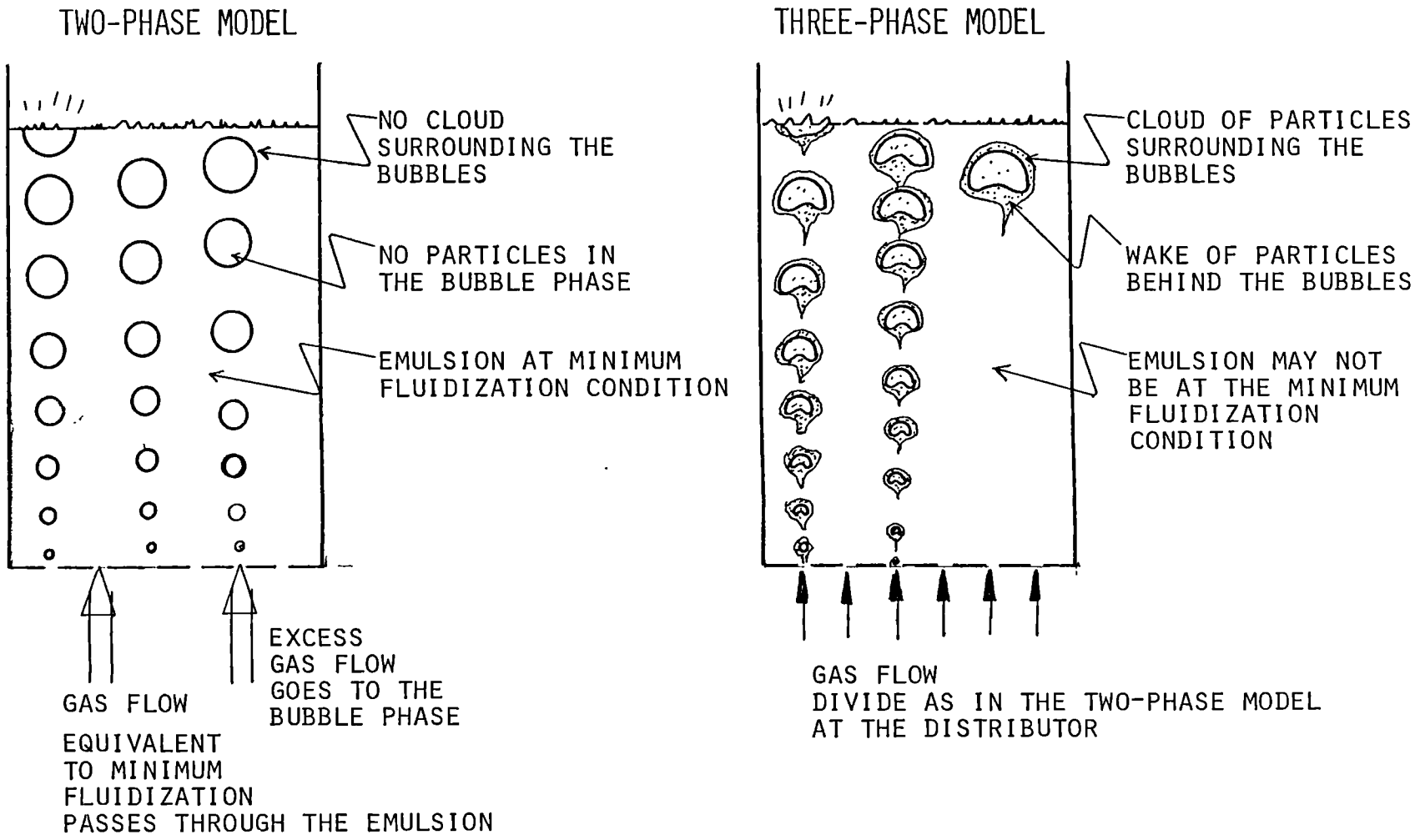

FIGURE 2.1. THE TWO BASIC MODELS FOR THE BED FLUID DYNAMICS.

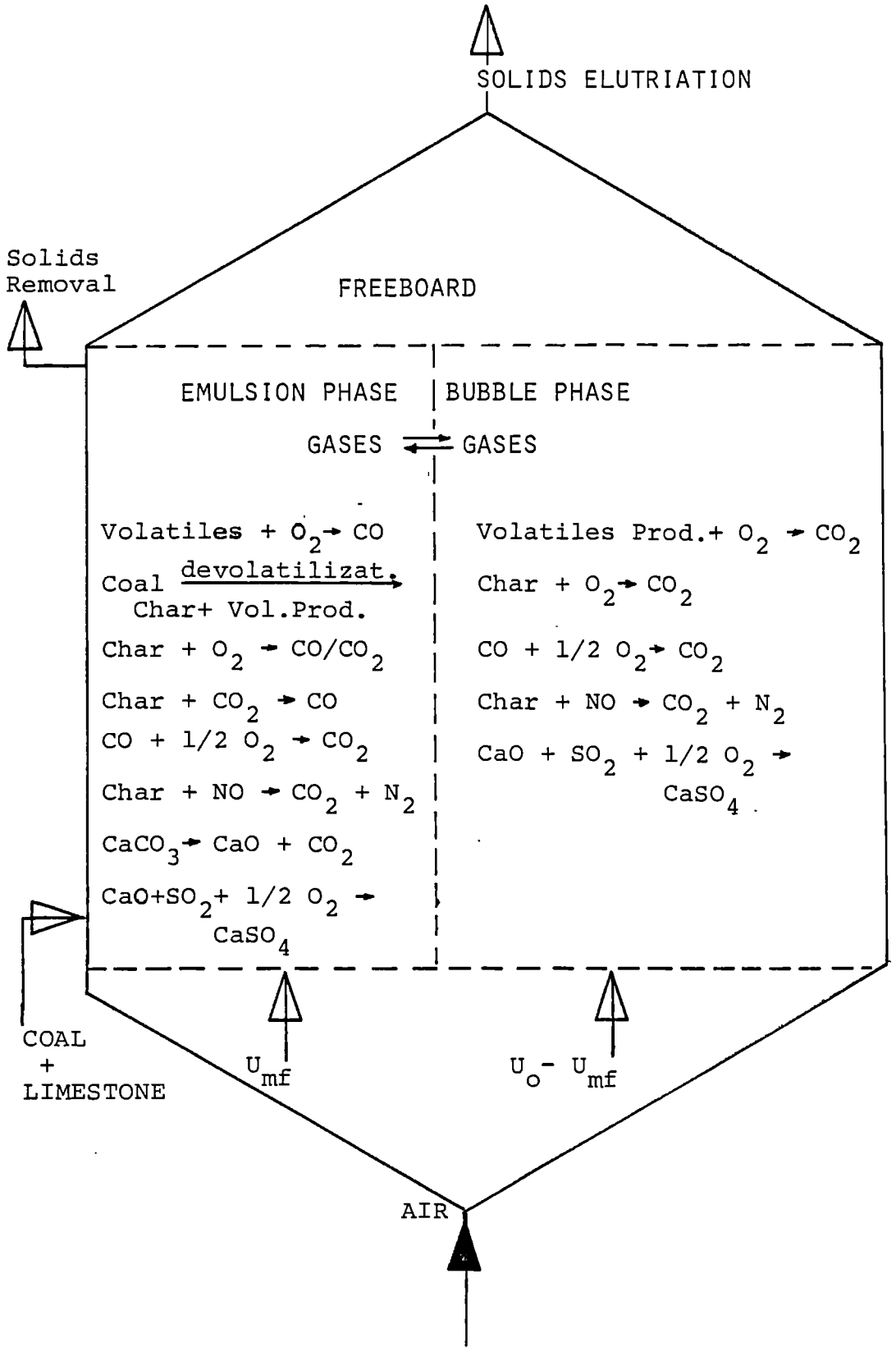

FIGURE 2.2. BASIC STRUCTURE OF THE RAJAN AND WEN (1980) MODEL.

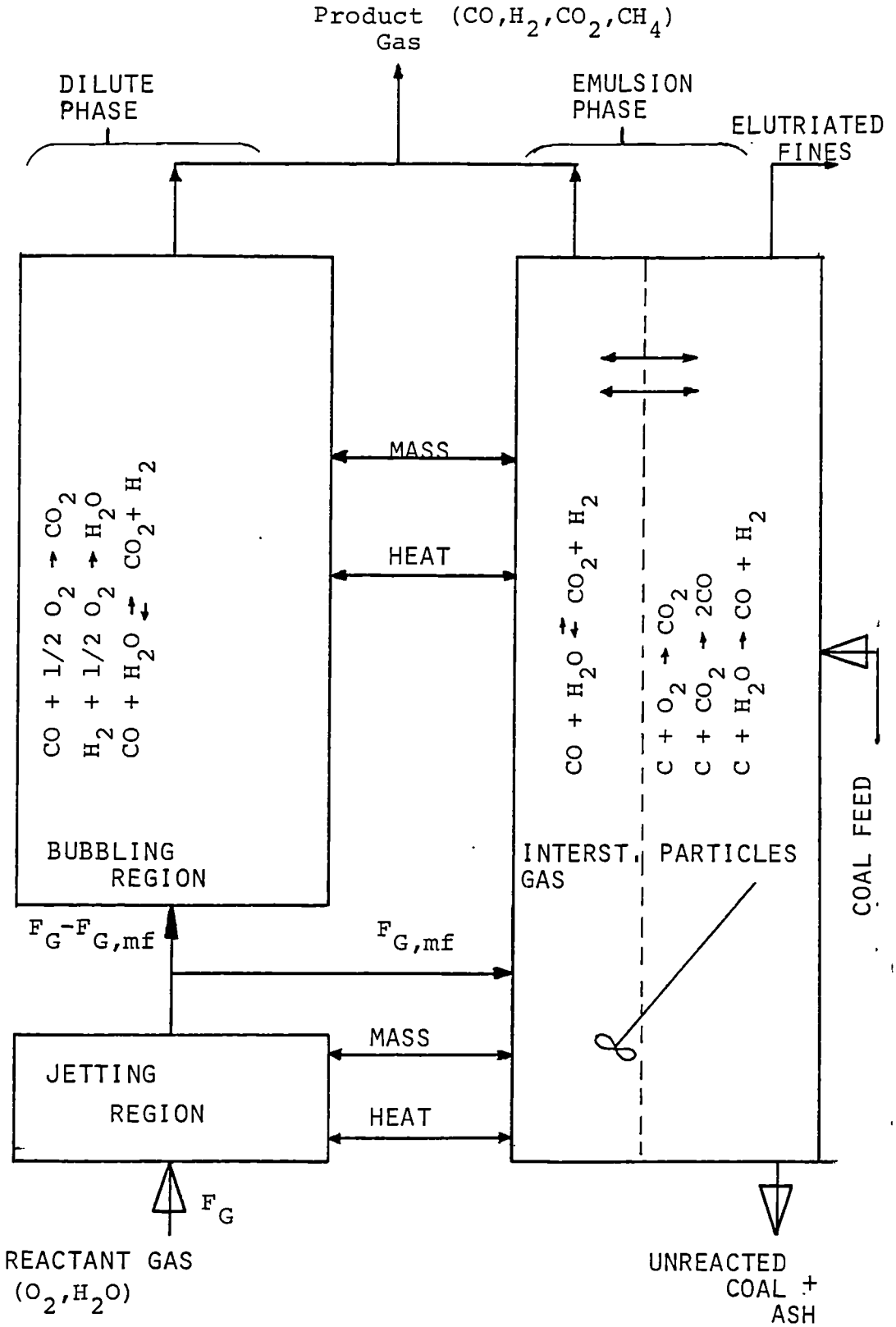

FIGURE 2.3. BASIC STRUCTURE OF THE WEIMER AND CLOUGH (1981) MODEL.

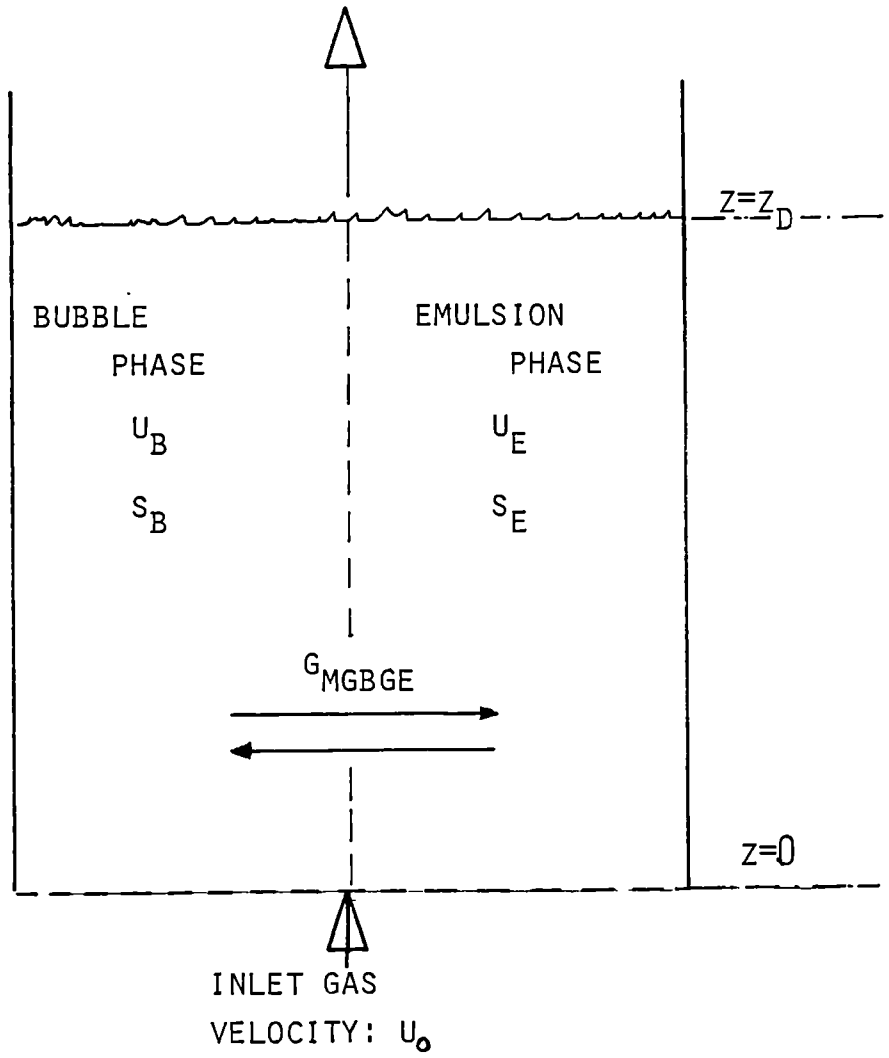

FIGURE 2.4. BASIC STRUCTURE OF THE RAMAN ET AL. (1981) MODEL.

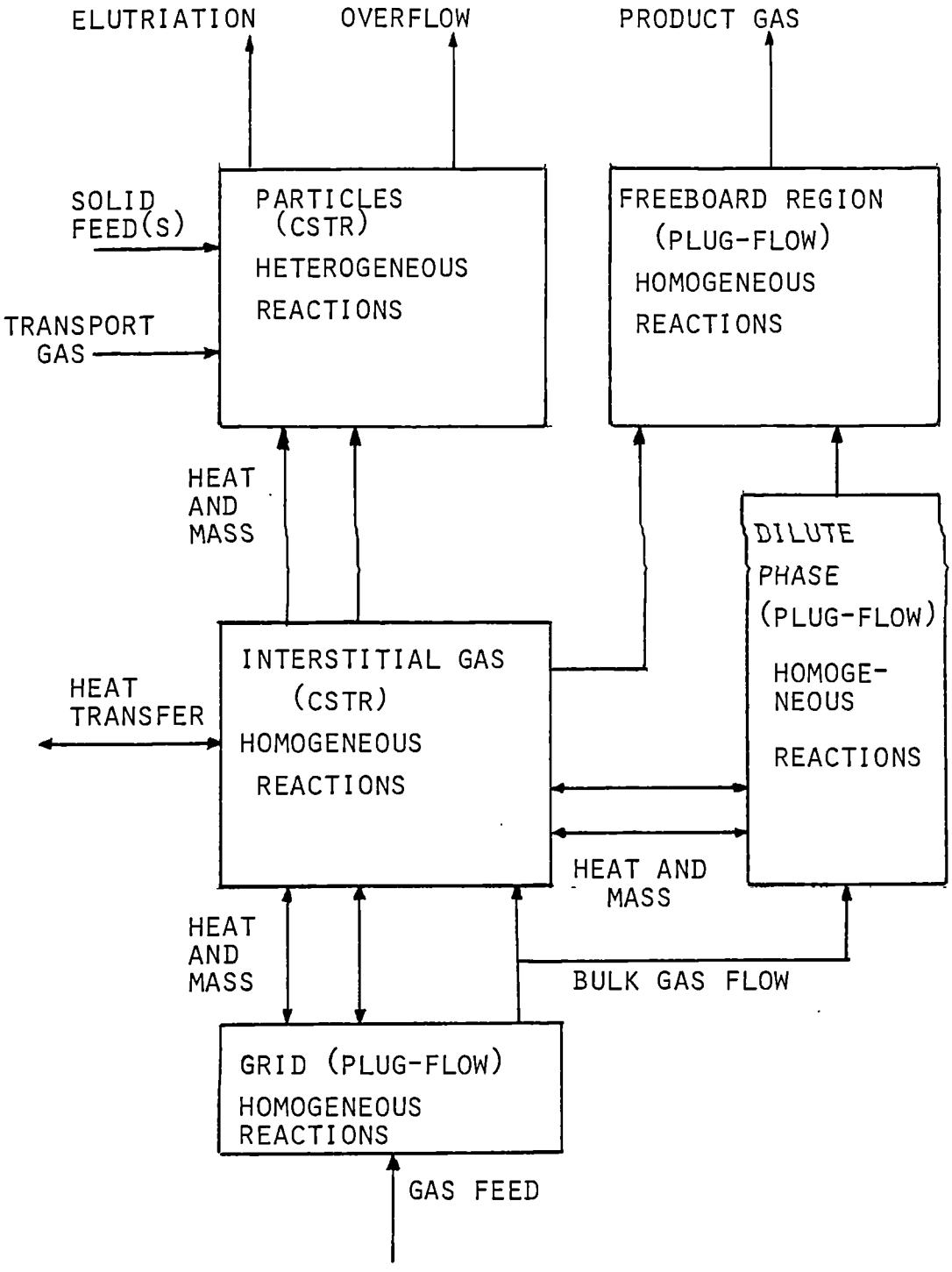

FIGURE 2.5. BASIC STRUCTURE OF THE OVERTURF AND REKLAITIS (1983) MODEL.

CHAPTER III

3. MATHEMATICAL MODEL

Here the mathematical details of the present model are shown.

It is important to stress that wherever it was necessary to use published empirical or semi-empirical correlations, the choice between the various possibilities was dictated by the following criteria:

a) To select the one that is supported by more experimental data and that which produced the smallest average deviation within the range of applicability;

b) To select the most recent work;

c) To select the one that has the greatest range of applicability.

These criteria were weighted as equally as possible.

3.1. Basic hypotheses and model strategy

The program is intended to simulate the steady-state regime operation, of a fluidized bed combustor boiler or a fluidized bed gasifier where the carbonaceous material, inert bed material and/or limestone are fed in continously. It also assumes that the material in the bed is withdrawn continuously to maintain the bed level.

In this situation the basic hypotheses are:

a) Any variation in conditions are assumed to occur only in the vertical or axial "z" direction.

b) At the base of the bed (z=0), the two-phase model, originally proposed by Toomey and Johnstone (1952) and later improved by Davidson and Harrison (1963), has been assumed. Therefore two main phases are considered to be present:

1) A particulate (or emulsion) phase in which the gas flow rate is equal to the flow of the minimum fluidization condition and;

2) A bubble phase where all excess gas flow, above that of the the minimum fluidization condition, passes through.

One implication is that the voidage fraction in the emulsion phase is equal to the voidage fraction at minimum fluidization at z=0. This model can be criticized (Horio and Wen(1977), Rowe(1978), Catipovic(1978)) for beds with average particle diameters below 50 μm or above 2 mm and the use of the present program for the cases outside of the above size interval must be analyzed carefully. Also, it should be noticed that in the original two-phase theory the minimum fluidization parameters were taken as constants throughout the bed height. In the present work, those parameters are allowed to change due to changes in the temperature and compositions in the emulsion and bubble phases. These changes are computed simultaneously with the solution of the differential system that describes the mass and energy balances throughout the bed height.

c) The emulsion phase is composed of four possible different species: interstitial gas, carbonaceous solid, inert and limestone - these last two are optional

but one of them, at least, is present.

d) The bubble phase is free of solid particles and the clouds are incorporated to the emulsion phase.

e) Plug-flow regimes for the gas in the bubble and for the interstitial gas of the emulsion phase. The gas flow in the freeboard is also treated as in a plug-flow regime.

f) Limestone and or inert (normally sand and free ash from the carbonaceous material) are assumed to have a homogeneous composition throughout the bed but their temperatures could change along the bed height. The same is assumed for the carbonaceous solid with respect to its fixed carbon composition which is calculated by a reiteration procedure. On the other hand, in order to verify the influence of the feed point position, the drying process and the devolatilization reactions are allowed to progress only in regions near the feeding point in the bed. The temperatures and compositions of the gas phases change throughout the bed height as a consequence of the physical and chemical processes. Within the freeboard, any solids are treated as flowing in the vertical direction with a decreasing flow rate due to the return of particles to the bed, i.e., due to entrainment phenomena and to chemical reactions. Therefore the consumption of particles in the freeboard is computed.

g) Bubble size is a function of the bed height. For the beds with immersed tubes, the maximum bubble size is limited by the minimum horizontal distance between

neighbour tubes in the region of the tube bundle. This treatment was suggested by Rajan and Wen (1980) and gave better results when compared with experimental data than the other alternative of not considering the influence of the tube pitch as suggested by the work of Asai et al.(1984).

h) The heterogeneous reactions between gases and carbonaceous solid can be described by two possible mechanisms:

1) The unreacted-core or shrinking-core model, where the active centre of the particle is kept covered with an ash shell, formed by the already reacted solid material;

2) The exposed-core or segregated-ash model, where the ash layer decomposes into very small particles at the same velocity as it is formed.

The behaviour of a carbonaceous particle would depend on the mechanical strength of the formed ash layer which can be verified by a simple experimental test. The simulation program accepts either possibility but in a fluidized bed, due to the intense attrition, the second mechanism has been found to be the more appropriate for reactions other than those related to devolatilization.

i) The drying of solids and the devolatilization of carbonaceous material are assumed to be complete within the bed, but no special assumption is taken related to the velocity of these process as they are treated taking their proper kinetics into account. The model of unreacted core is taken for these process, regardless the model adopted

for the other reactions.

To illustrate the assumptions described, the Figure 3.1 shows a scheme of the fluidized bed reactor with the adopted coordinate system and the Fig.3.2 shows a simplified diagram of the model structure.

3.2. Basic equations

Due to the inherent complexity of the process, which involves several chemical reactions, chemical components and different physical phases, a brief description of the system of indexing to be used is now given.

There are basically three indices: "i","j","m". The index "i" indicates a particular chemical reaction "R-i" (the various reactions are described in the section 3.5). The index "j" stands for a particular chemical component among the following:

a) Gas components: 1=CO_2, 2=CO, 3=O_2, 4=N_2, 5=H_2O, 6=H_2, 7=CH_4, 8=SO_2, 9=NO, 10=C_2H_6, 11=H_2S, 12=NH_3, 13=Tar;

b) Solid components in the carbonaceous particles: 14=C, 15=H, 16=O, 17=N, 18=O, 19=Ash, 20=Volatiles, 21=Moisture;

c) Solid components in the limestone particles: 22=$CaCO_3$, 23=CaO, 24=$CaSO_4$, 25=Moisture;

d) Solid components in the inert particles: 26=SiO_2, 27=Moisture.

The index "m" stands for the type of solid

material as: 1=Carbonaceous, 2=Limestone, 3=Inert.

Added to this, the two basic phases, i.e. emulsion and bubbles, are indicated by indexes "E" and "B", respectively. The emulsion is composed of gases ("G") and solids ("S"). Therefore a composite system of subscripts is necessary, and needs to be indicated as clearly as possible. As an example: "GE" for gas in the emulsion, "SE" for solid in the emulsion and "GB" for gas in the bubble phase. A complete description of all symbols is given in the nomenclature.

3.2.1. Bed section

The following equations describe the derivative of the mass flow of each gas component in the emulsion with the coordinate of the bed height "z".

$$\frac{dF_{GE,j}}{dz} = \sum_{m=1}^{3} R_{SE,m,j} \frac{dA_{PE,m}}{dz} + R_{GE,j} \frac{dV_{GE}}{dz} +$$

$$G_{MGBGE,j} \frac{dA_B}{dz} \quad , \; 1 \leq j \leq 13 \qquad (3.1)$$

The involved parameters are:

a) The rate of production of component "j" due to gas-gas or volume reactions is given by:

$$R_{GE,j} = \sum_{i=21}^{30} \nu_{j,i} \, M_j \, r_i \Big|_{T_{GE}} \quad , \; 1 \leq j \leq 13 \qquad (3.2)$$

b) The rate of production of component "j" due to surface gas-solid-"m" reactions are given by:

$$R_{SE,m,j} = \sum_{i=i_0}^{i_1} \nu_{j,i}\, M_j\, r_i\Big|_{T_{SE,m}} \quad , \; j_0 \leq j \leq j_1 \qquad (3.3)$$

As each set of gas-solid reactions "i" can occur on the surface of a solid "m" the table below shows the relationships for the limits "i" and "j" in the summations.

m	i_0	i_1	j_0	j_1
1	1	10	14	21
2	11	13	22	25
3	14	14	26	27

TABLE 3.1.Relation between solid "m" where the reaction "i" ($i_0 \leq i \leq i_1$) takes place involving the components "j" ($j_0 \leq j \leq j_1$).

c) The flux of mass transfer between the bubble and emulsion for each component "j" is given by:

$$G_{MGBGE,j} = d_B\, \omega_{BE}\, c_G\, M_j\, \frac{(y_{GB,j} - y_{GE,j})}{6} \qquad (3.4)$$

where the mass transfer coefficient "ω_{BE}" is described in the section (3.7.1) and the the bubble diameter in the section (3.3.3).

d) The variation of solid particle surfaces among other similar parameters are described in section (3.10).

For the gas in the bubble phase:

$$\frac{dF_{GB,j}}{dz} = R_{GB,j} \frac{dV_B}{dz} - G_{MGBGE,j} \frac{dA_B}{dz} \quad , 1 \leq j \leq 13 \quad (3.5)$$

Where the rate of production of component "j" due to gas-gas or volume reactions is given by:

$$R_{GB,j} = \sum_{i=21}^{30} \nu_{j,i} M_j r_i|_{T_{GB}} \quad , 1 \leq j \leq 13 \quad (3.6)$$

At any position "z" in the bed, the total mass flow of gases is given by:

$$F_G = F_{GE} + F_{GB} \quad (3.7)$$

and the average mass fraction of each component "j" by:

$$w_{GA,j} = \frac{F_{GE,j} + F_{GB,j}}{F_G} \quad , 1 \leq j \leq 13 \quad (3.8)$$

The fractional consumption of each solid component in the bed is computed as:

$$\Lambda_{D,j} = 1 - \frac{F_{LD,j}}{F_{ID,j}} \quad , 14 \leq j \leq 27 \quad (3.9)$$

where

$$F_{LD,j} = F_{ID,j} - \sum_{m=1}^{3} \int_{z=0}^{z_D} R_{SE,m,j} \frac{dA_{PE,m}}{dz} dz \qquad (3.10)$$

The energy balances are given below.

For the gas in the emulsion :

$$F_{GE}\ C_{GE} \frac{dT_{GE}}{dz} = - E_{QGE} + \sum_{m=1}^{3} (E_{CSEGE_m} + E_{MSEGE_m}) +$$

$$E_{CGBGE} + E_{MGBGE} - E_{CGETD} + E_{GEWD} \qquad (3.11)$$

Where the energy released due to chemical reactions is given by:

$$E_{QGE} = \sum_{j=1}^{13} R_{GE,j}\ H_{TGE,j} \frac{dV_{GE}}{dz} \qquad (3.12)$$

The terms that account for the heat transfer by:

a) Convection between solids and gas in the emulsion (E_{CSEGE});

b) Convection between gas in the bubbles and in the emulsion (E_{CGBGE});

c) Convection between gas in the emulsion and tubes (E_{CGETD});

d) Convection and radiation between gas in the emulsion and the internal wall of the reactor (E_{GEWD}) (normally a negative value).

These terms will be detailed in the sections concerning to the heat transfer parameters.

The term relative to the energy transfer between the gas in the emulsion and solids due to mass transfer is given by:

$$E_{MSEGE,m} = \sum_{j=1}^{13} R_{SE,m,j} \left(H_j|_{T_{SE,m}} - H_j|_{T_{GE}} \right) \frac{dA_{PE,m}}{dz} \quad (3.13)$$

where $1 \leq m \leq 3$, and the term relative to the energy transfer between the gas in the emulsion and the bubbles due to the mass transfer is given by:

$$E_{MGBGE} = \sum_{j=1}^{13} G_{MGBGE,j} \left(H_j|_{T_{GB}} - H_j|_{T_{GE}} \right) \frac{dA_B}{dz} \quad (3.14)$$

For the gas in the bubbles :

$$F_{GB}\, C_{GB} \frac{dT_{GB}}{dz} = -E_{QGB} - E_{CGBGE} + E_{MGBGE} - E_{CGBTD} \quad (3.15)$$

Here the term relative to the energy release due to chemical reactions in the bubble phase is given by:

$$E_{QGB} = \sum_{j=1}^{13} R_{GB,j}\, H_j|_{T_{GB}} \frac{dV_B}{dz} \quad (3.16)$$

and the terms representing the heat transfer between bubbles and tubes immersed in the bed (E_{CGBTD}) will be detailed in the section concerning the heat transfer

coefficients.

For the solids in the emulsion :

$$F_{N,m}\ C_{SE,m}\ \frac{dT_{PE,m}}{dz} = -\ E_{QSE,m} - E_{CSEGE,m} - E_{MSEGE,m} -$$

$$E_{RSETD,m} - \sum_{n=1}^{3}(E_{RSESE,m,n} + E_{CSESE,m,n}) \qquad (3.17)$$

where $1 \leq m \leq 3$.

The expression for the rate of solid turnover ($F_{N,m}$) is described in the section (3.9).

The term relative to the energy released due to solid surface reactions is given by:

$$E_{QSE,m} = \sum_{j=1}^{27} R_{SE,m,j}\ H_j|^{T_{SE,m}}\ \frac{dA_{PE,m}}{dz} \qquad (3.18)$$

where $1 \leq m \leq 3$.

The radiative heat transfer between solids (E_{RSESE}) and convection (E_{CSESE}) as well as the total heat transfer between solids will be detailed ahead.

At any position "z" in the bed, an average gas temperature is defined by the "enthalpy" average or:

$$T_{GA} = T^{*} + \frac{(T_{GE} - T^{*})\ F_{GE}C_{GE} + (T_{GB} - T^{*})\ F_{GB}C_{GB}}{F_{GE}\ C_{GE} + F_{GB}\ C_{GB}} \qquad (3.19)$$

Other complementary parameters are described in the section 3.13.

In this way, the system of differential mass and energy balances is now complete and includes 46 coupled equations that must be solved by the simulation strategy. Once solved, this system provides all the concentration, flow and temperature profiles throughout the bed height.

3.2.2. Freeboard section

The differential balances in the freeboard section are described below.

Mass balance:

$$\frac{dF_{F,j}}{dz} = \sum_{m=1}^{3} R_{SF,m,j} \frac{dA_{PF,m}}{dz} + R_{GF,j} \frac{dV_{GF}}{dz} \qquad (3.20)$$

where $1 \leq j \leq 27$.

It should be noticed that, contrasting with the equation (3.1), this mass balance applies for the solid components ($j > 13$) - of course $R_{GF} = 0.0$ for $j > 13$. Therefore, in the freeboard section each solid composition and flux are functions of z.

The energy balance for the gas phase is given by:

$$F_{GF}C_{GF} \frac{dT_{GF}}{dz} = - E_{QGF} + \sum_{m=1}^{3} (E_{CSFGF,m} + E_{MSFGF}) -$$

$$E_{CGFTF} + E_{GFWF} \qquad (3.21)$$

For the solid phase:

$$F_{PF,m}\, C_{SF,m}\, \frac{dT_{PF,m}}{dz} = - E_{QSF,m} - E_{CSFGF,m} - E_{MSFGF,m} -$$

$$E_{RSFTF,m} - \sum_{n=1}^{3} E_{RSFSF,m,n} \quad , \quad 1 \leq m \leq 3 \qquad (3.22)$$

The flow of solid particles of kind "m" is given by:

$$F_{PF,m} = \sum_{j=j_0}^{j_1} F_{F,j} \quad , \quad 1 \leq m \leq 3 \qquad (3.23)$$

The limits j_1 and j_0 depend on "m" and as shown in the Table 3.1.

The various parameters concerning the heat transfer in the freeboard section are in some cases similar to those in the bed section. The similarities and differences are discussed in the section for heat transfer coefficients.

3.3. Fluidization dynamics

Before defining the proper boundary conditions of the differential system problem, it is necessary to describe the equations of the fluid dynamics of the system due to the intrinsic connection between them.

3.3.1. Two-phase theory balance

As has been said, the two-phase theory assumes that the emulsion phase is at the "minimum fluidization condition". In the present model this is assumed at the

distributor, or at z=0. Therefore all the excess flow of gases above the condition of minimum fluidization passes through the bubble phase.

From the following balance that holds at any point of the bed:

$$U_E = \frac{F_{GE}}{\rho_{GE} S_E} \tag{3.24}$$

and

$$F_G = F_{GE} + F_{GB} \tag{3.25}$$

as

$$S = S_E + S_B \tag{3.26}$$

the "two-phase" theory is applied at the base of the bed which leads to the implication that the superficial velocity of the interstitial emulsion "U_E" must be equal to the minimum fluidization velocity or:

$$U_E = U_{mf} \quad \text{at} \quad z=0 \tag{3.27}$$

as well the emulsion phase voidage as:

$$\varepsilon_E = \varepsilon_{mf} \quad \text{at} \quad z=0 \tag{3.28}$$

These minimum fluidization parameters are determined by suitable correlations which are defined in the next section.

The fractions "S_E" and "S_B" of the cross-section area "S" at a height "z" of the bed section, which is

occupied by the emulsion and bubble phases respectively, are deduced as follows:

As the volume occupied by the bubble phase is due to the bed expansion from the static condition, it is possible to write:

$$S_B \, z_D = S \, (z_D - z_{D_{st}}) \tag{3.29}$$

therefore

$$S_E = S \, \frac{z_{D_{st}}}{z_D} = \frac{S}{f_{bexp}} \tag{3.30}$$

leading immediately to the determination of the void fraction in the bed at a height "z" by the well known relationship:

$$\varepsilon = 1 - \frac{(1 - \varepsilon_E)}{f_{bexp}} \tag{3.31}$$

The factor of bed expansion from minimum fluidization to bubbling fluidization is given by IGT (1976) or Babu et al.(1978) as:

$$f_{bexp} = 1 + \frac{1.032 \, (U - U_{mf})^{0.57} \, \rho_{GA}^{0.083}}{\rho_P^{0.166} \, U_{mf}^{0.063} \, D_d^{0.445}} \tag{3.32}$$

for $d_D < 0.0635$ and

$$f_{bexp} = 1 + \frac{14.314 \, (U - U_{mf})^{0.738} \, d_P^{1.006} \, \rho_P^{0.376}}{U_{mf}^{0.937} \, \rho_{GA}^{0.126}} \tag{3.33}$$

for $d_D \geq 0.0635$.

It is important to note that as the superficial velocity "U", among the other variables, changes with the height "z" mainly due to the temperature and composition variation, the factor "f_{bexp}" is a strong function of the vertical coordinate and therefore the fractions "S_E" and "S_B". The normal tendency in combustors is an increase in the ratio (S_B / S_E) due to the basic increase in the difference ($U - U_{mf}$).

It must be stressed that:

a) Due to the continuum model of the present model, all the parameters involved in the present model, unless specifically stated, are functions of the height "z";

b) It has been shown how the mass and energy balances determine the variations for the mass flow of each gas component throughout the bed height and freeboard and for the solid in the freeboard. Therefore the total flow for each phase, emulsion and bubbles, at any coordinate point "z" are given by:

$$F_{GE} = \sum_{j=1}^{13} F_{GE,j} \quad ,\text{for: } 0 \leq z \leq z_D \tag{3.34}$$

and

$$F_{GB} = \sum_{j=1}^{13} F_{GB,j} \quad ,\text{for: } 0 \leq z \leq z_D \tag{3.35}$$

while the total mass flow of gases and solids in the freeboard by:

$$F_{GF} = \sum_{j=1}^{13} F_{GF,j} \quad \text{,for:} \quad z_D < z \leq z_F \tag{3.36}$$

and

$$F_{SF} = \sum_{j=14}^{27} F_{SF,j} \quad \text{,for:} \quad z_D < z \leq z_F \tag{3.37}$$

These equations allow the determination of compositions throughout the system, i.e., bed and freeboard;

c) Most of the published works assume the approximation:

$$\varepsilon_E = \varepsilon_{mf} \tag{3.38}$$

but as the mass flow "F_{GE}" is given by the differential mass balance in the bed and the area fraction "S_E" is determined by the above correlations, the void fraction in the emulsion "ε_E" is likely to differ from the value of "ε_{mf}". This has been interpreted, physically, by the presence of the cloud phase that in this model has been included as part of the emulsion. The computation of the void fraction in the emulsion at any height "z" of the bed is given by the correlation taken from Delvosalle and Vanderschuren (1985) as:

$$\varepsilon_E = \varepsilon_{mf} \left(\frac{U_E}{U_{mf}}\right)^{1/6.7} \tag{3.39}$$

The minimum fluidizing conditions are described below.

3.3.2. Minimum fluidizing conditions

The minimum fluidization parameters are among the basic variables of every model of FBC or FBG.

The first to be described is the minimum fluidization superficial velocity. Several correlations can be found in the literature (listed for instance in Babu et al.,1978). Besides this, as observed by Kunii and Levenspiel (1969) and also by Babu et al.(1978), the simplest and more reliable form is given by Wen and Yu (1966) as:

$$U_{mf} = \frac{N_{Re_{mf}} \mu_{GA}}{d_P \rho_{GA}} \tag{3.40}$$

where

$$N_{Re_{mf}} = \left[a^2_{uxmf} + a'_{uxmf} \frac{d_P^3 \rho_{GA} (\rho_P - \rho_{GA})}{\mu^2_{GA}} \right]^{1/2} - a^2_{uxmf} \tag{3.41}$$

As can be seen, this correlation does not include parameters like the average particle sphericity, which very seldom is given as data and even if known for the fed particles is likely to suffer a great modification after some time in the bed with no reasonable method for estimation. At the same time, Wen and Yu (1966) define the minimum fluidization voidage ε_{mf} by suggesting that for a wide variety of systems:

$$\frac{1}{\phi_A \varepsilon^3_{mf}} = a''_{uxmf} \tag{3.42}$$

and

$$\frac{1 - \varepsilon_{mf}}{\phi_A^2 \ \varepsilon_{mf}^3} = a'''_{uxmf} \qquad (3.42a)$$

Here the auxiliary parameters take the values: $a_{uxmf} = 33.7$, $a'_{uxmf} = 0.0408$, $a''_{uxmf} = 14$ and $a'''_{uxmf} = 11$. In the report from IGT(1976) and later by Babu et al.(1978) a more specific study showed that for the case of coal these parameters should be replaced by: 25.25, 0.0651, 8.81 and 5.19 respectively. Therefore from eq.(3.42) and (3.42a) comes that Wen and Yu (1966) fixed the value of ε_{mf} at approximately 0.48 while IGT(1976) at 0.52. As the voidage in the emulsion phase (ε_E) is calculated at each point of the bed by the equation (3.39), the value of ε_{mf} is taken as a constant. The value described by IGT(1976) was chosen because it is better fitted to specific cases of fluidized beds of coal related materials.

3.3.3. Bubble phase parameters

The parameters related with the bubble phase are presented below:

$$\varepsilon_B = 1 - \frac{1 - \varepsilon}{1 - \varepsilon_{mf}} \qquad (3.43)$$

From Mori and Wen(1975),

$$d_B = d_{maxB} - (d_{maxB} - d'_B) \exp(- 0.3 \frac{z}{d_D}) \qquad (3.44)$$

where

$$d_{maxB} = 1.638 \left[S\ (U - U_{mf})\right]^{0.4} \qquad (3.45)$$

and, for perforated plates:

$$d_B' = 0.872 \left[\frac{S\ (U - U_{mf})}{n_{orif}}\right]^{0.4} \qquad (3.46)$$

or, for porous plates:

$$d_B' = 0.376\ (U - U_{mf})^2 \qquad (3.46a)$$

A new correlation for the bubble diameter has been published by Stubington et al.(1984):

$$d_B = 0.430\ (U - U_{mf})^{0.4}\ (z + 0.1272)^{0.8}\ g^{-0.2} \qquad (3.46a)$$

This equation gives the same results as the one already used in the present model. As the above one does not consider the maximum size of the bubble nor the number of orifices in the distributor, it was preferable to use the model from Mori and Wen (1975).

From Davidson and Harrison(1963) it is possible to calculate the velocity of bubble rise by:

$$U_B = U - U_{mf} + 0.711\ (g\ d_B)^{1/2} \qquad (3.47)$$

It is important to note that as the gas temperature and composition changes throughout the bed height so do the physical properties and, therefore, all the fluidization parameters. As the differential system is solved throughout the bed, these parameters are also calculated at each height "z" of the bed.

3.4. Boundary Conditions

The differential mass and energy balances represented by the system of equations (3.1), (3.5), (3.11), (3.17), (3.20), (3.21) and (3.22) are the very core of the present work. They represent an unprecedented aspect in FBC and FBG modelling, because the prediction of individual profiles for the compositions and temperatures in each phase is attempted.

Some of the boundary conditions are immediately set as for the gas in the emulsion and bubble composition and temperature at the bottom of the bed or distributor because the conditions of the injected gas stream are known. On the other hand, as this model includes the various particle temperature profiles, the determination of the corresponding boundary conditions at z=0 can be considered as one of the most difficult aspects faced during the development of the simulation program.

3.4.1. Boundary conditions for the gases

As the conditions of the gas stream injected through the distributor (z=0) are known, the total gas flow rate F_G and its composition $w_{G,j}$ and temperature T_G are determined. Therefore it is possible to write:

$$w_{GE,j,z=0} = w_{GB,j,z=0} = w_{G,j,z=0} \tag{3.48}$$

and

$$T_{GE,z=0} = T_{GB,z=0} = T_{G,z=0} \tag{3.49}$$

The determination of the individual mass flow

rates that go into the emulsion and bubble phases, $F_{GE,j}$ and $F_{GB,j}$ for $1 \leq j \leq 13$, at z=0 are immediately given by:

$$F_{GE,j,z=0} = w_{G,j,z=0} \, F_{GE,z=0} \quad , \; 1 \leq j \leq 13 \qquad (3.50)$$

and

$$F_{GB,j,z=0} = F_{G,j,z=0} - F_{GE,j,z=0} \quad , \; 1 \leq j \leq 13 \qquad (3.51)$$

where the gas flow through the emulsion phase "F_{GE}" at z=0 is given by the two-phase theory as already described in the section (3.3.1).

Naturally, for the freeboard equations the boundary conditions are taken as the conditions at the top of the bed ($z=z_D$) and therefore set after the solution of the equations for that section. For instance:

$$F_{GF,j,z=z_D} = F_{GE,j,z=z_D} + F_{GB,j,z=z_D} \qquad (3.52)$$

3.4.2. Boundary conditions for the solids

Due to the simplification of homogeneous composition for each type of solid in the bed, it is only necessary to set the mass flow rate of solids at the top of the bed or at the base of the freeboard. They are given by:

$$F_{F,j,z=z_D} = \sum_{l=1}^{lm} F_{Y,m,l,z=z_D} \, w_{PLD,j} \qquad (3.53)$$

where $1 \leq m \leq 3$ and $14 \leq j \leq 27$. The relation between "m" and "j" indexes are:

for m=1 $14 \leq j \leq 21$;

for m=2 $22 \leq j \leq 25$;

for m=3 $26 \leq j \leq 27$.

The more difficult set of boundary conditions are those for the temperature of the various solids at the base of the bed. This is due to the fact that no apparent behaviour seemed to describe these conditions and during the development of this model several hypotheses were tried as, for instance, assuming no heat transfer between the bed and the distributor which would imply an average temperature derivative at z=0 equal to zero. This led to great instabilities during the computations and big deviations between the simulation and the available experimental results.

The difficulty arises because the solution of the mass and energy balances are strongly coupled and therefore very sensitive to the set boundary conditions especially those for the temperatures. Added to this, the presence of at least two different kind of solid particles (carbonaceous and limestone or sand) that have different temperatures to be set, brought about the problem of how to balance the average temperature and its derivative at z=0. It must be said that this problem was temporarily put aside and during a long period of the development of this work and the temperatures of particles at z=0 were calculated using a overall energy balance in the bed. This was very inconvenient because the energy flux out of the bed as losses and enthalpy carried by gases and solids leaving the bed could not be estimated before the complete solution of the set of differential equations in the bed. An iteration

procedure would be incredibly time consuming and very unstable because it would be superimposed on the carbon consumption convergence procedure. The energy losses were estimated as a fraction of the input energy to the system (carbonaceous mass flow into the system times its heat value) and therefore an adjusting factor needed to be set. This was done by comparisons between simulation results and one experimental result for a given industrial or pilot unit.

Finally the problem was solved, due to the possibility of a more precise computation of the heat transfer between bed and distributor with the publication of the work of Zhang and Ouyang (1985). This allowed the definition of a coherent boundary condition by equating the heat flux transfered by convection and the heat transfered by conduction at the bed base or:

$$\lambda_{bed,z=0} \frac{dT_{A,z=0}}{dz} = \alpha_{bed-dist} (T_{A,z=0} - T_{dist}) \qquad (3.54)$$

The various involved parameters are described below:

a) The representative thermal conductivity for the bed is taken from Xavier and Davidson (1978) (referred to as λ_{mf}) and shown in the Appendix B;

b) The average temperature at any point "z" of the bed height (T_A and its derivative (dT_A/dz) are given in the Appendix C;

c) As was said the heat transfer coefficient between bed and distributor $\alpha_{bed-dist}$ is given from Zhang

and Ouyang (1985) as:

$$\frac{\alpha_{bed\text{-}dist}\ d_{PA}}{k_{GA}} = 0.09 \left[\frac{\rho_{SA}\ C_{SA}}{\rho_{GA}\ C_{GA}}\right]^{0.4} \left[\frac{d_{PA}\ \rho_{GA}\ U_o}{\mu_{GA}}\right]^{0.15} \quad (3.55)$$

and valid for

$$3 < \frac{\left[d_{PA}\ \rho_{GA}\ U_o\right]}{\mu_{GA}} < 40$$

d) The temperature at the distributor surface T_{dist} is given by equating the heat flux through the distributor base with the the transference to the bed or:

$$\frac{k_{dist}}{x_{dist}} (T_{dist} - T_{G,z=0}) = \alpha_{dist} (T_{A,z=0} - T_{dist}) \quad (3.56)$$

Once the average temperature as well its derivative are defined as functions of the various individual temperatures and derivatives, the determination of the particle temperatures at z=0, ($T_{P,m,z=0}$) is achieved by a convergence routine based on the equation (3.54). This is done by assuming, in a first computation, the various temperatures for the solid particles and computing the derivatives at z=0 using the differential energy and mass balances in the bed. The iterations do not take too much computing time because a very small step is used to compute derivatives at z=0. After this, all the necessary boundary conditions are set and the solution proceeds to the top of the bed.

The basic strategy used to accomplish the calculations is described in section (4.1).

3.5. Chemical reactions

The model includes a set of 23 possible chemical reactions listed below:

$$CH_{a_{15}}O_{a_{16}}N_{a_{17}}S_{a_{18}} + \left(\beta + \frac{a_{15}}{4} - \frac{a_{16}}{2} + \frac{a_{17}}{2} + a_{18}\right) O_2 \rightarrow$$

$$(2\beta - 1)\, CO_2 + (2 - 2\beta)\, CO + \frac{a_{15}}{2} H_2O + a_{17}\, NO +$$

$$a_{18}\, SO_2 \qquad \text{(R-1)}$$

$$CH_{a_{15}}O_{a_{16}}N_{a_{17}}S_{a_{18}} + (1 - a_{16})\, H_2O \rightarrow$$

$$\left(1 + \frac{a_{15}}{2} - a_{16} - a_{18}\right) H_2 + CO + \frac{a_{17}}{2} N_2 + a_{18}\, H_2S \qquad \text{(R-2)}$$

$$CH_{a_{15}}O_{a_{16}}N_{a_{17}}S_{a_{18}} + CO_2 \leftrightarrow 2\, CO + a_{16}\, H_2O + a_{17}\, NH_3 +$$

$$a_{18}\, H_2S + \left(\frac{a_{15}}{2} - a_{16} - \frac{3}{2} a_{17} - a_{18}\right) H_2 \qquad \text{(R-3)}$$

$$CH_{a_{15}}O_{a_{16}}N_{a_{17}}S_{a_{18}} + \left(2 - \frac{a_{15}}{2} + a_{16} + \frac{3}{2} a_{17} + a_{18}\right) H_2 \leftrightarrow$$

$$CH_4 + a_{16}\, H_2O + a_{17}\, NH_3 + a_{18}\, H_2S \qquad \text{(R-4)}$$

$$CH_{a_{15}}O_{a_{16}}N_{a_{17}}S_{a_{18}} + (2 - a_{16})\ NO \leftrightarrow$$

$$CO_2 + (1 - \frac{a_{17}}{2})\ N_2 + a_{18}\ H_2S + (\frac{a_{15}}{2} - a_{18})\ H_2 \qquad (R\text{-}5)$$

Reaction R-6 was left as a space for future developments.

$$\text{Volatiles} \rightarrow \text{Tar} \qquad (R\text{-}7)$$

Here the Volatiles and therefore Tar is represented by : $C_{\dot{b}_{14}}H_{\dot{b}_{15}}O_{\dot{b}_{16}}N_{\dot{b}_{17}}S_{\dot{b}_{18}}$.

$$\text{Volatiles} \rightarrow \ddot{b}_1CO_2 + \ddot{b}_2CO + \ddot{b}_3O_2 + \ddot{b}_4N_2 + \ddot{b}_5H_2O +$$

$$\ddot{b}_6H_2 + \ddot{b}_7CH_4 + \ddot{b}_8SO_2 + \ddot{b}_9NO + \ddot{b}_{10}C_2H_6 +$$

$$\ddot{b}_{11}H_2S + \ddot{b}_{12}NH_3 \qquad (R\text{-}8)$$

$$\text{Volatiles} + (\dot{b}_{14}\ \beta + \frac{\dot{b}_{15}}{4} - \frac{\dot{b}_{16}}{2} + \frac{\dot{b}_{17}}{2} + \dot{b}_{18})\ O_2 \rightarrow$$

$$(2\ \dot{b}_{14}\ \beta - 1)\ CO_2 + (2 - 2\ \dot{b}_{14}\ \beta)\ CO + \frac{\dot{b}_{15}}{2}\ H_2O + \dot{b}_{17}\ NO +$$

$$\dot{b}_{18}\ SO_2 \qquad (R\text{-}9)$$

$$\text{Moist Carbonaceous Solid} \rightarrow \text{Dry Solid} + H_2O \qquad (R\text{-}10)$$

$$CaCO_3 \rightarrow CaO + CO_2 \qquad (R\text{-}11)$$

$$2CaO + 2SO_2 + O_2 \rightarrow 2CaSO_4 \qquad \text{(R-12)}$$

$$\text{Moist Limestone} \rightarrow \text{Dry Limestone} + H_2O \qquad \text{(R-13)}$$

$$\text{Moist Inert} \rightarrow \text{Dry Inert} + H_2O \qquad \text{(R-14)}$$

Numbers R-15 to R-19 are left free to include more solid-gas reactions to the model, if proved to be necessary in future work.

$$CO + H_2O \leftrightarrow CO_2 + H_2 \qquad \text{(R-20)}$$

$$2CO + O_2 \leftrightarrow 2CO_2 \qquad \text{(R-21)}$$

$$2H_2 + O_2 \rightarrow 2H_2O \qquad \text{(R-22)}$$

$$CH_4 + 2O_2 \rightarrow CO_2 + 2H_2O \qquad \text{(R-23)}$$

$$2C_2H_6 + 7O_2 \rightarrow 4CO_2 + 6H_2O \qquad \text{(R-24)}$$

$$4NH_3 + 5O_2 \rightarrow 4NO + 6H_2O \qquad \text{(R-25)}$$

$$2H_2S + 3O_2 \rightarrow 2SO_2 + 2H_2O \qquad \text{(R-26)}$$

$$N_2 + O_2 \leftrightarrow 2\ NO \qquad \text{(R-27)}$$

$$\text{Tar} + \left(\dot{b}_{14} + \frac{\dot{b}_{15}}{4} - \frac{\dot{b}_{16}}{2} + \frac{\dot{b}_{17}}{2} + \dot{b}_{18}\right) O_2 \rightarrow \dot{b}_{14}CO_2 +$$

$$\frac{\dot{b}_{15}}{2} H_2O + \dot{b}_{17}NO + \dot{b}_{18}SO_2 \qquad \text{(R-28)}$$

$$\text{Tar} \rightarrow \ddot{b}_1CO_2 + \ddot{b}_2CO + \ddot{b}_3O_2 + \ddot{b}_4N_2 + \ddot{b}_5H_2O +$$

$$\ddot{b}_6H_2 + \ddot{b}_7CH_4 + \ddot{b}_8SO_2 + \ddot{b}_9NO + \ddot{b}_{10}C_2H_6 +$$

$$\ddot{b}_{11}H_2S + \ddot{b}_{12}NH_3 \qquad \text{(R-29)}$$

$$\text{Tar} \rightarrow \text{Coke} \qquad \text{(R-30)}$$

The forms presented in the reactions R-1 to R-2 have been taken from DeSai and Wen (1978) and forms from R-3 to R-5 adapted from the work of Kim and Joseph (1983). The stoichiometry coefficient "β" will depend on the particle temperature, as detailed ahead in the text.

The calculations of the stoichiometry coefficients in reactions R-7 to R-9 and R-29 to R-30 should be accomplished by convergence calculations that involve the routine to estimate the devolatilization products. This point is described ahead.

3.6. Reaction kinetics

The parameters $R_{MVE,j}$, $R_{MVB,j}$, $R_{MS,j}$, E_{QGE}, E_{QGB}, $E_{QSE,m}$ and $E_{MSEGE,m}$ are calculated with the help of the rate of chemical reactions that are described next.

3.6.1. Reactivity of the carbonaceous material

Before discussing the reaction rates, it is important to stress that the kinetics, mainly with regard to the case of gas-carbonaceous solid reactions, depend to a considerable extent on the kind of the carbonaceous material that has been processed. This is known as fuel reactivity and recent publications have tried to relate this to the solid fuel properties and/or processing methods used. A good review of the subject can be found in van Heek and Muhlen (1985), and the factors influencing reactivity, apart from the basic composition of the solid, are:

a) The minerals, which seem to have a catalytic effect, although no proper correlation has been published so far;

b) The pyrolysis conditions (rate and temperature) that could be responsible for the development or blockage of internal surfaces;

c) The pre-treatment of the solid fuel which has also been found to have an important influence by Maloney and Jenkins(1985).

More recently, Kasaoka et al.(1985) found a reasonable correlation between the reactivity and the basic composition of the carbonaceous solid, more specifically, the volatiles/fixed-carbon ratio. As in the present process

of fluidized combustion/gasification the rates of pyrolysis are expected to be of the same order for all carbonaceous materials, and as a first attempt to include the reactivity, the present work uses the findings of these authors in order to estimate the fuel reactivity, that is based on the so called fuel-ratio which is discussed later.

3.6.2. Models for the gas-solid reactions

Added to the reactivity, the influence of the characteristic physical structure of the solid has been taken into account using two possible models for the gas-solid reactions: the unreacted core or the exposed core model, which have been described in Yoon et al.(1978) for the carbonaceous gas-solid reaction. These models have been generalized here to deal also with the devolatilization reactions, drying of solids, calcination of limestone and sulphur absorption.

The present simulation program allows the user to choose between the two models. The decision should be based on the processed solid characteristics. On the other hand, it should be stressed that inside a fluidized bed the severe attrition seldom allows the carbonaceous solid particle to retain the formed ash layer as the surface reactions proceed. Therefore, with few exceptions, the model of exposed-core should be chosen. In any case, a simple experimental test is enough to indicate the best decision.

This picture is different for the cases of the drying of solids, devolatilization of carbonaceous solids,

calcination of limestone or sulphur absorption by CaO. This is because no fragile shell is formed during these processes but just the formation of dried, devolatilized or reacted external layers of the particles. Therefore in all these cases the program calculates the "reaction rates" for these process using an adaptation of the model of unreacted core, as it is shown below.

It is, also, important to note that the present model does not impose any restriction to the possibility of simultaneous gas-solid reactions. This means that it allows, for instance, a carbonaceous solid to have a external layer reacting with oxygen (combustion) and an internal core still not completely devolatilized and therefore all processes occuring at the same time.

The general expression for the gas-solid reactions in the case of unreacted core model is given by:

$$r_i = \frac{d_{P,m}}{6} \frac{p_j - p_j^*}{\sum_{k=1}^{3} \zeta_{k,i}} \qquad (3.57)$$

where

$$1 \leq i \leq 14 \quad , \quad 1 \leq j \leq 26 \quad \text{and} \quad 1 \leq m \leq 3$$

The connection between the three indexes "i", "j" and "k", which describe the choice of the representative component "j" in the solid phase "m" to the reaction "i", used in the present work, is shown in Table 3.2. This table also indicates the component chosen to represent the solid

material of the unreacted core for each reaction. This is necessary for the calculation of parameters: "τ_i","$D_{shell,i}$",and"$c_{SI,i}$", as described in the Appendix A.

Gas-solid reaction "i"	Representative component "j"	solid phase "m"	Representative unreacted solid component
1	3	1	14
2	5	1	14
3	1	1	14
4	6	1	14
5	9	1	14
7	20	1	20
8	20	1	20
9	20	1	20
10	5	1	21
11	1	2	22
12	8	2	23
13	5	2	25
14	5	3	26

TABLE 3.2.Correspondence between the heterogeneous reaction "i" and its respective representative component "j" and solid phase "m".

The parameters "ζ_k" are given by:

$$\zeta_{1,i} = \frac{P\ d_{PI,m}}{6\ \omega_{SEGE,m}} \tag{3.58}$$

$$\zeta_{2,i} = \frac{(d_{PI,m})^2\ (1-\tau_i)\ R\ T_{PE,m}}{12\ \tau_i\ D_{shell,i}} \tag{3.59}$$

$$\zeta_{3,i} = \frac{1}{n_i\ \tau_i^3\ k_i\ c_{SI,i}} \tag{3.60}$$

These three terms represents the resistances to the mass transfer of gases from and to the porous solid particle due to:

1) The diffusion through the gas boundary layer surrounding the particle;

2) The diffusion through the formed non-active shell surrounding the unreacted core;

3) The diffusion through the core combined with the kinetics.

For the gas-carbonaceous solid reactions (R-1 to R-6) the non-active layer is the formed shell of ash around the unburned core. For the devolatilization reactions (R-7 to R-9) the non-active layer is formed by the already devolatilized material. For the drying processes (R-10, 13 and 14) the dried material is the resistance solid layer and the factor $\zeta_{3,i}$ is taken as equal to nil as there is no chemical reaction in these cases. In the case of limestone calcination (R-11) the resistance material is the CaO solid and the nucleus formed by $CaCO_3$ while for the sulphur capture reaction (R-12) the outer shell layer is formed by the converted calcium or $CaSO_4$. The representative unreacted solid component for each reaction is shown in the last column of Tab.3.2.

The calculation for the mass transfer coefficient between gas and solid particle ($\omega_{SEGE,m}$) is shown in the section (3.7.2) relative to mass transfer coefficients while the other parameters can be found in the Appendix A.

In the exposed core model the gas-solid reaction rates are given by:

$$r_i = \frac{d_{P,m}}{6} \frac{(p_j - p_j^*)\ \Xi}{\sum_{k=1}^{3} \zeta'_{k,i}} \qquad (3.61)$$

where: $1 \leq i \leq 6$, $1 \leq j \leq 21$, $m=1$. Here hold the same relationships given in Table 3.2 among "i", "j" and "m". As has been said, the model considers that reactions R-7 to R-14 always follow the unreacted core model even when the reactions R-1 to R-5 are represented by the exposed core model.

The parameters are given below:

$$\Xi = \frac{1 - \Lambda_{24}}{1 - \Lambda_{24} + \frac{\Lambda_{24}\ \rho_{PI,m=1}\ W_{PI,ash}}{\rho_{j=19}}} \qquad (3.62)$$

Here the index "m" could be set to equal "1" because this model is applied only to the gas-carbonaceous material,

$$\zeta'_{1,i} = \frac{P\ d_{PI,1}\ (1 - \tau_i)}{6\ \omega_{SEGE,m=1}} \qquad (3.63)$$

$$\zeta'_{2,i} = 0 \qquad (3.64)$$

$$\zeta'_{3,i} = \frac{1}{\eta_i k_i c_{SI,i}} \qquad (3.65)$$

3.6.3. Individual kinetic coefficients

The kinetic coefficients and the equilibrium parameters for the reactions are described ahead. Here it has been decided to substitute the common name of "equilibrium constants" by equilibrium coefficients because of their dependence on the temperature.

It is important to remember that during the calculations of the reaction rates and equilibrium coefficients the temperature "$T_{PE,m}$" is used for the gas-solid-"m" heterogeneous reactions while temperature "T_{GE}" is used for the homogeneous reactions in the emulsion phase and "T_{GB}" for the reactions in the bubble phase.

3.6.3.1. Reactions C-O_2

They are represented by reactions (R-1) for the char and by reaction (R-9) for the volatiles combustion.

The distribution of the oxygen in the formation of CO_2 or CO is described by the stoichiometry coefficient "β" that depends on the temperature, as given by Arthur(1951) and Rossberg(1956):

$$\beta = \frac{2 + \beta'}{2 + 2\beta'} \qquad (3.66)$$

where

$$\beta' = 2500 \exp(-\frac{6240}{T_{P,1}}) \qquad (3.67)$$

The stoichiometry coefficients "a_j" ($14 \leq j \leq 18$) are calculated from the average carbonaceous solid composition in the bed. As in all gas-solid carbonaceous

reactions (R-1 to R-5), the active components of the fixed carbon (H, O, N, and S) are considered and the ratio between their concentration in the solid is assumed, for the first iteration, to be the same as the fed material. After each iteration, the consumption of these components are calculated by the eq.(3.10) and therefore the average composition in the bed can be computed again.

The Arrhenius coefficients for these and several other considered reactions are given in the Table 3.3.

Reaction	$k_{o,i}$	Unit	$\tilde{E}_i/R$ (K)	Source
R-1 & R-9	17.67	$Pa^{-1}\ s^{-1}$	13597	Sergeant & Smith(1973)
R-20	2.78×10^3	$kmol^{-1}\ m^3\ s^{-1}$	1510	Biba(1978)
R-21	1.0×10^{15}	$kmol^{-0.75}\ m^{2.25}\ K^{1.5}\ s^{-1}$	16000	Vilienskii & Hezmalian(1978)
R-22	5.159×10^{13}	$kmol^{1.5}\ m^{4.5}\ K^{1.5}\ s^{-1}$	3430	Vilienskii & Hezmalian(1978)
R-23 and R-24	3.552×10^{14}	$kmol^{-1}\ m^3\ s^{-1}\ K$	15700	Vilienskii & Hezmalian(1978)

CONT...

CONT...

Reaction	$k_{o,i}$	Unit	$\tilde{E}_i/R$ (K)	Source
R-25	9.78×10^{11}	$kmol^{-0.9}\ m^{2.7}\ s^{-1}$	19655	Branch & Sawyer(1972)
R-27	1.815×10^{13}	$kmol^{-0.5}\ m^{1.5}\ s^{-1}$	67338	Quan et al.(1972)
R-28	59.8	$kmol^{-0.5}\ m^{1.5}\ Pa^{-0.3}\ s^{-1}\ K^{-1}$	12200	Siminski et al.(1972)

TABLE 3.3.Kinetic coefficients for some of the considered reactions.

The reactions R-1 and R-9 are considered irreversible, as the concentration of oxygen in the equilibrium state is negligible. Haslam and Russel(1926) showed, for instance, that the ratio of molar fractions of CO_2 and O_2, in equilibrium at 1170 K, is 3.5×10^{17}.

3.6.3.2. Reactions $C-H_2O$, $C-CO_2$, $C-H_2$

The reactions R-2, R-3 and R-4 have been extensively studied and various descriptions for its rate have been reported - for instance: Blackwood(1959), Ergun(1962), Frederrsdorff and Elliot(1963), Gibson and Euker(1975), Johnson(1979), Muhlen et al.(1985), among others and are described below.

3.6.3.2.1. Correction for the reactivity

As has been said before, the rates of the above reactions are strongly affected by the specific characteristics of the reacting carbonaceous material and this effect is known as solid-fuel reactivity. These effects are not very easily correlated to the physical properties of the particular carbonaceous solid but recently a correction factor derived from Kasaoka et al.(1985) based on the fuel-ratio (fixed carbon/volatile matter) proved to be useful in improving the calculations.

Basically, the method determines a correction coefficient that is multiplied by the kinetic coefficients of the reactions R-i (i=2,3 or 4) which have been evaluated for a reference coal. This allows the determination of the kinetic coefficients for the respective reactions with the given carbonaceous material, as follows:

$$k_i = k_{i_{ref.}} \frac{\bar{k}_i}{\bar{k}_{ref.}} \qquad (3.68)$$

The parameters $\bar{k}$ are given by:

$$\bar{k}_i = \bar{a}_i \, f_r^{\bar{b}} \tag{3.69}$$

$$f_r = \frac{\text{FIXED CARBON mass fraction}}{\text{VOLATILE MATTER mass fraction}} \tag{3.70}$$

with coefficients described in the table below.

Reaction	$\bar{a}$	$\bar{b}$	reference coal	$f_{r,ref.}$
R-2 & R-4(*)			Illinois	1.32
$f_r < 3$	4.49×10^{-4}	-1.736		
$f_r \geq 3$	3.97×10^{-5}	0.491		
R-3			Lignite	1.93
$f_r \leq 3$	1.33×10^{-3}	-4.454		
$f_r > 3$	7.67×10^{-7}	2.152		

TABLE 3.4. Auxiliary parameters used for solid-fuel reactivity estimation. (*)=for the reaction R-4 the same correction as R-2 was assumed; the composition of the Illinois coal is reproduced from Yoon et al.(1978) and the Spanish Lignite from Adánez et al.(1985).

The kinetic coefficients for reactions R-3 and R-4 are given by:

$$k_3 = \frac{k_{3,1}}{1 + k_{3,2} \, p_1 + k_{3,3} \, p_2} \tag{3.71}$$

and

$$k_4 = \frac{k_{42}\, p_6}{1 + k_{42}\, p_6} \qquad (3.72)$$

The coefficients are shown in Table 3.5.

Coeff. index	k_o	Unit	$\tilde{E}/R$ (K)	Referred coal	Reference
2	6.05×10^{-3}	$Pa^{-1}\ s^{-1}$	21150	Illinois	Gibson & Euker(1975)
31	1.91×10^{-3}	$Pa^{-1}\ s^{-1}$	16840	Spanish Lignite	Adánez et al.(1985)
32	1.33×10^{-8}	Pa^{-1}	-7220	Spanish	Adánez et
33	3.13×10^{-8}	Pa^{-1}	-5050	Lignite	al.(1985)
41	2.345×10^{-11}	$Pa^{-2}\ s^{-1}$	13670	Illinois	Johnson (1979)
42	4.742×10^{-12}	Pa^{-1}	-11096	" "	" "

TABLE 3.5.Arrhenius coefficients related to the reactions R-2, R-3 and R-4.

The equilibrium coefficients for these and some other reactions are presented below.

Reaction	$K_{o,i}$	Unit	$\Delta H_i/R$ (K)	Relationship with partial pressures	Source
R-2	3.139×10^{12}	Pa	16344	$p_2\ p_6\ p_5^{-1}$	Hottel and Howard(1971)
R-3	1.238×10^{14}	Pa	20294	$p_2^{2}\ p_1^{-1}$	Parent and Katz(1948)
R-4	1.453×10^{-11}	Pa^{-1}	-11005	$p_7\ p_6^{-2}$	Hottel and Howard(1971)
R-20	0.0265	- -	-3958	$p_1\ p_6\ p_2^{-1}\ p_5^{-1}$	Parent Katz(1948)
R-21	8.264×10^{-15}	Pa^{-1}	-68080	$p_1^{2}\ p_2^{-2}\ p_3^{-1}$	Kanury(1975)

CONT...

CONT...

Reaction	$K_{o,i}$	Unit	$\Delta H_i/R$ (K)	Relationship with partial pressures	Source
R-22	8.109×10^{-13}	Pa^{-1}	-60230	$p_5^{2}\, p_6^{-2}\, p_3^{-1}$	Kanury(1975)
R-27	19.254	-	21570	$p_9^{2}\, p_4^{-1}\, p_3^{-1}$	Kanury(1975)

TABLE 3.6.Equilibrium constants for some reactions.

$$[K_i = K_{o,i} \exp(-\frac{\Delta H_i}{RT})].$$

3.6.3.3.Reaction C-NO

The kinetic equation is given by Oguma et al.(1977) and Horio et al.(1977a,b) and written here as:

$$k_s = 5.24 \times 10^5 \exp(-\frac{17127}{T_{P,1}}) \frac{6}{d_{P,1}\, P} \quad , (Pa^{-1}\, s^{-1}) \quad (3.73)$$

3.6.3.4.Devolatilization reactions

Due to the comprehensive approach used in the present work, the devolatilization or pyrolysis reactions cannot be completely separated from the other reactions and processes in the system. To illustrate this the scheme in Fig 3.3 shows the reactions and process considered in the system for the carbonaceous solid material. It shows also,

the strategy used to account for the various possible routes.

The kinetics of the devolatilization reactions (R-7, R-8, R-29 and R-30) have been taken from Wen and Lee (1979) and Wen and Chen (1983) for the case of coal and by Thurner and Mann(1981) for the case of wood. The coefficients are reported in Table 3.7.

It is assumed that the devolatilization reactions follow a model similar to the unreacted core in which the already devolatilized material acts as the reacted shell. Therefore the pre-exponential coefficients have been related with the pressure in order to adapt to the form of unreacted core model equation. This led to the definition of a pseudo partial pressure for the volatiles in the solid as:

$$p_{z0} = P\, w_{PI,vol} \qquad (3.74)$$

Reaction	Kind of material	k_o ($Pa^{-1}\ s^{-1}$)	$\tilde{E}/R$ (K)	Ref.
R-7 (a)	bitum.coal	$w_{tar}\ 1.1x10^5/P$	-10669	Wen and Chen(1983)
	sub-bitum.	$w_{tar}\ 7.5x10^4/P$	-9406	
	lignite	$w_{tar}\ 5.1x10^4/P$	-8155	
	wood	$4.125x10^6/P$	-13555	Thurner*
R-8 (a)	bitum.	$w_{gas}\ 1.1x10^5/P$	-10669	Wen and Chen(1983)
	sub-bitum.	$w_{gas}\ 7.5x10^4/P$	-9406	
	lignite	$w_{gas}\ 5.1x10^4/P$	-8155	
	wood	$1.435x10^4/P$	-10657	Thurner*
R-29 (b)	bitum.	$9.7x10^9$	-14590	Wen and Chen(1983)
	sub-bitum.	$3.5x10^{10}$	-13964	
	lignite	$8.0x10^{10}$	-13339	
	wood	$9.7x10^9$	-14590	Thurner*
R-30 (b)	bitum.	$5.3x10^4$	-3524	Wen and Chen(1983)
	sub-bitum.	$2.5x10^4$	-2766	
	lignite	$1.1x10^3$	-2009	
	wood	$5.3x10^4$	-3524	Thurner*

TABLE 3.7.Arrehenius coefficients for devolatilization reactions. (a): $T_{P,1}$ must be used in calculations; (b): T_{GE} must be used and k_o units are s^{-1};(*): Thurner and Mann (1981).

In this table the indicated mass fractions are

defined by:

$$w_{tar} = \frac{F_{V,13}}{\sum_{j=1}^{13} F_{V,j}} \qquad (3.75)$$

$$w_{gas} = 1 - w_{tar} \qquad (3.76)$$

It should be noticed that, in contrast with the work of Wen and Chen (1983), the present model does not include the transformation of carbonaceous solid into volatiles because the char and volatiles have been treated as independent species, whose fractions are taken into account by the stoichiometry, as shown below.

3.6.3.4.1.Devolatilization stoichiometry

The production rate of gas compounds due to the devolatilization reactions depends on the distribution of stoichiometric coefficients as shown by reaction R-8. Its stoichiometry depends also on an approximate formula for the tar.

In order to resolve this point, the model uses the mass flow , "$F_{V,j}$", that represents the flow of each volatile compound as if in a batch devolatilization. Obviously these are not the actual flows but just used to calculate the relative production of volatiles compounds. For the case of coal (bituminous or sub-bituminous), from Loison and Chauvin (1964), the relative flow for each gas component is given by:

$$F_{V,j} = u'_j \, (F_V - F_{V,j=11} - F_{V,j=12}) \quad , 1 \leq j \leq 13 \tag{3.77}$$

where

$$u'_1 = 0.135 - 0.900 \, w_{PI,vol,daf} + 1.906 \, w^2_{PI,vol,daf} \tag{3.78}$$

$$u'_2 = 0.423 - 2.653 \, w_{PI,vol,daf} + 4.845 \, w^2_{PI,vol,daf} \tag{3.79}$$

$$u'_5 = 0.409 - 2.389 \, w_{PI,vol,daf} + 4.554 \, w^2_{PI,vol,daf} \tag{3.80}$$

$$u'_6 = 0.157 - 0.869 \, w_{PI,vol,daf} + 1.338 \, w^2_{PI,vol,daf} \tag{3.81}$$

$$u'_7 = 0.201 - 0.469 \, w_{PI,vol,daf} + 0.241 \, w^2_{PI,vol,daf} \tag{3.82}$$

$$u'_{13} = - 0.325 + 7.279 \, w_{PI,vol,daf} -$$

$$12.884 \, w^2_{PI,vol,daf} \tag{3.83}$$

From Gregory and Littlejohn (1965), the total flow of volatiles released is given by:

$$F_V = F_{PI,m=1,daf} \, (w_{PI,vol,daf} - u' - u'') \tag{3.84}$$

where

$$u' = 10^{-2} \exp(26.41 - 3.961 \ln(T_{P,1} - 273.15) +$$

$$1.15 \, w_{PI,vol,daf}) \tag{3.85}$$

and

$$u'' = 20\ (w_{PI,vol,daf} - 0.109) \tag{3.86}$$

The mass flow of H_2S and NH_3 can be found as:

$$F_{V,j=11} = F_{PI,m=1,d}\ w_{PI,m=1,18}\ f_{V,18} \tag{3.87}$$

and

$$F_{V,j=12} = F_{PI,m=1,d}\ w_{PI,m=1,17}\ f_{V,17} \tag{3.88}$$

where, from Fine et al.(1974) :

$$f_{V,18} = (0.001\ T_{P,1} - 0.6)\ \frac{M_{11}\ M_{18}}{M_{11}\ M_{18} + M_{12}\ M_{17}} \tag{3.89}$$

and

$$f_{V,17} = (0.001\ T_{P,1} - 0.6)\ \frac{M_{12}\ M_{17}}{M_{11}\ M_{18} + M_{12}\ M_{17}} \tag{3.90}$$

These flows can be used now to calculate the composition of the gas released during the devolatilization and therefore to compute the stoichiometry coefficients $\ddot{b}_j$. This must be done as a function of the coefficients $\dot{b}_j$. Although not a critical parameter concerning the final simulation results, the molecular mass of the Tar has been assumed equal to the glucose (180.16 kg $kmol^{-1}$), during this computation. This is based on some evidence (IPT, 1979) that this product is an important fraction of that Tar residual, mainly for the case of wood (see also sec.3.11). A simple convergence routine allows the determination of these coefficients.

For the case of wood,the production of each gas species during the pyrolysis has been deduced from Nunn et al.(1985) as:

$$F_{V,j} = F_{PI,m=1,d}\ {}^{w}_{PI,vol}\ \frac{f_{V,j}}{93.0} \tag{3.91}$$

for $1 \leq j \leq 13$, where

$$f_{V,1} = 0.0610 \tag{3.92}$$

$$f_{V,2} = 0.1700 \tag{3.93}$$

$$f_{V,5} = 0.0510 \tag{3.94}$$

$$f_{V,6} = 0.0020 \tag{3.95}$$

$$f_{V,7} = 0.0230 \tag{3.96}$$

$$f_{V,10} = 0.0020 \tag{3.97}$$

$$f_{V,13} = 0.6210 \tag{3.98}$$

All the compounds that have not been considered in this model, but described by Nunn et al.(1985), have been summed to the tar fraction. Also, as these authors did not analyze the hydrogen production during the pyrolysis but other papers showed its existence, the hydrogen fraction has been taken as 10% of the methane fraction as suggested in IPT(1979).

3.6.3.5.Drying processes

As for the devolatilization reactions R-7, 8 and 9, the drying processes are treated by the unreacted core model. It is obvious, in this case the term "reaction rate" is meaningless and therefore the coefficients $\varsigma_{3,i}$ (for i=10,13,14) are equal to zero.

For the drying of the carbonaceous material (R-10) as well as for the limestone (R-13) and for the inert solid (R-14), the difference used between the pressures is given by:

$$p_s - p_s^* = (p_s - p_{5,i}^*)\ (1 - \Lambda_j) \qquad (3.99)$$

where: j=21 for i=10 , j=25 for i=13 and j=26 for i=14. The equilibrium pressures $p_{5,i}^*$ are the saturation pressure of water at the temperatures of the corresponding solid phases.

3.6.3.6.Calcium carbonate decomposition

The calcination of limestone represented by reaction (R-11) provides the carbon oxide that is the active solid in the absorption of SO_2, as indicated by the reaction (R-12).

Usually the calcination does not constitute a limiting step for the sulphur dioxide absorption. This is due to the relatively high reaction rate of the calcination if compared with the rate of sulphur capture and because the sulphur dioxide can be also absorbed by the $CaCO_3$ directly as:

$$CaCO_3 + SO_2 + 1/2\ O_2 \rightarrow CaSO_4 + CO_2 \qquad (3.100)$$

On the other hand, as pointed out in Babcock and Wilcox (1976), this later reaction is much slower than (R-11) and therefore a constant supply of CaO must be guaranteed for a efficient absorption of SO_2.

The thermodynamics of the calcination shows that at high partial pressures of carbon dioxide the equilibrium can be attained which would stop the calcination. As indicated in Babcock and Wilcox (1976) the calcination is difficult at pressures above 300 kPa (~3 atm.) at the usual fluidized bed operation conditions.

From Kubashewski et al.(1967), among other works, the CO_2 equilibrium partial pressure for this reaction can be written as:

$$p_1^* = 3.336 \times 10^7\ P \exp\left(-\frac{20269}{T_{S,m=2}}\right) \qquad (3.101)$$

The unreacted-core model the eq.(3.57) can be used taking the driving differences of partial pressures given by: $p_1^* - p_1$.

The kinetics for the limestone calcination is described in several papers. For instance, Ingraham and Marier (1963) and more recently Borgwardt (1985). The paper from Asaki et al.(1974) show how to apply the standard form of kinetic coefficient to the case of unreacted core model. Therefore using this combined with the determinations from Borgwardt (1985) it is possible to write:

$$k_{11} = \frac{3.07x10_{11}}{p^*_1} \exp\left(-\frac{24670}{T_{P,2}}\right) \quad (Pa^{-1}\ s^{-1}) \qquad (3.102)$$

From these equations some points deserve to be stressed:

(a) As the SO_2 does not react significantly with $CaCO_3$, (Babcock and Wilcox, 1976), the absorption of SO_2 is accomplished mainly by the CaO by reaction R-12. Therefore the limestone calcination can be seen as a limiting step for the sulphur absorption in a fluidized bed;

(b) The calcination is very sensitive on respect to the CO_2 partial pressure and stops as soon it reaches values equal or above the equilibrium given by eq.(3.101). It is shown later in this work that CO_2 partial pressures of 14kPa are common in FBC process. This would stop all calcination at temperatures of limestone below, approximately, 840K.

3.6.3.7.Sulphur absorption

As described before, in the present work the approach of unreacted core has been taken by the use of eq.(3.57) to compute the rate of this reaction.

The kinetics of this reaction has been studied by Borgwardt (1970,1971) who verified a strong influence of the kind of stone on the rate of reaction. The formation of $CaSO_4$ tends to block the pores of the limestone particle and reduce the reactivity of limestone. Therefore it is is a function of the temperature, limestone conversion and the particle size. Rajan et al.(1978,1979) using the grain model developed by Ishida and Wen (1973), present a simple

method to calculate the correction factor for the reactivity (ι in the equation below) as function of the calcium fractional conversion and the limestone particle diameter by interpolation among various curves relating these three parameters. The same method is used in the present work and the kinetic coefficient is written as:

$$k_{12} = \frac{2.0}{P} \exp\left(-\frac{4080}{T_{P,m=2}}\right) \iota \qquad (Pa^{-1}\ s^{-1}) \qquad (3.103)$$

It must be said that no correlation has been found to account for the effect of temperature on the reactivity. Also, it is suspected that the presence of chemical compounds, apart from the calcium based ones, have an important role on this reactivity. Again no work has been found which includes this aspect.

The thickness of $CaSO_4$ layer is determined by the calcium conversion in the bed and given by:

$$\Lambda_{j=23} = \frac{N_{L,j=24}}{N_{L,j=22} + N_{L,j=23} + N_{L,j=24}} \qquad (3.104)$$

The calculation of Λ_{23} is repeated each time the program solves the system of differential equations throughout the bed and the convergence is usually achieved before the convergence for the carbon conversion Λ_{14} .

3.6.3.8. Shift reaction

The water-gas shift reaction rate is given by Franks(1967) as:

$$r_{20} = k_{20} \left[y_2 \, y_5 - \frac{y_1 \, y_6}{K^*_{20}} \right] c_G^2 \qquad (3.105)$$

Here the equilibrium constant is calculated with the values given in Table 3.6.

3.6.3.9. Combustion of gases

The kinetics of carbon monoxide combustion is the first to be described. It has been extensively studied and presented in Batchelder et al.(1953), Hottel et al.(1965), Dryer and Glassman(1972) and Howard et al.(1975). The range of applicability and situation varies considerably and all the correlations taken from these works have been tried in the present simulation. The best results have been obtained by the usage of a more recent review that considers the conjugate effect of this reaction along with other simultaneous gas combustion reactions and accomplished by Vilienskii and Hezmalian (1978) which gives:

$$r_{21} = \frac{k_{21}}{T_G^{1.5}} \, y_2 \, y_3^{0.25} \, y_5^{0.5} \, c_G^{1.75} \qquad (3.106)$$

For the hydrogen combustion a global equation is taken also from Vilienskii and Hezmalian (1978) as:

$$r_{22} = \frac{k_{22}}{T_G^{1.5}} \, y_6^{1.5} \, y_3 \, c_G^{2.5} \qquad (3.107)$$

as well as for the methane combustion:

$$r_{23} = \frac{k_{23}}{T_G} y_7 y_3 c_G^2 \qquad (3.108)$$

For the ethane combustion due to some uncertainty found in the literature (for instance Edelman and Fortune, 1969) and also because it normally does not represent a sensitive point in the process, it has been decided to take a similar correlation used in the methane combustion to write:

$$r_{24} = \frac{k_{24}}{T_G} y_{10} y_3 c_G^2 \qquad (3.109)$$

Several works have been published on the reaction rate of the ammonia oxidation - Thompson et al.(1972), De Soete(1973), among others - but the more appropriate range for the present application has been found in Branch and Sawyer (1972) as:

$$r_{25} = k_{25} y_{12}^{0.86} y_3^{1.04} c_G^{1.90} \qquad (3.110)$$

The reaction R-26 has been assumed to have the same behaviour as the reaction R-25 and its kinetics is computed by the equation above only substituting y_{12} by y_{11}.

Because of the relatively low temperatures it must be expected that most of the nitrogen monoxide comes from the consumption of the nitrogen in the fuel, however the oxidation of nitrogen from the injected gas (air or

other mixture of gases) has been included for completeness of the present model. The kinetics has been taken from Quan et al.(1972) as:

$$r_{27} = k_{27}\, y_4\, y_3^{0.5}\, c_G^{1.5} \qquad (3.111)$$

The kinetic of tar combustion has been modelled as the combustion of long organic molecules and taken from Siminski et al.(1972) as:

$$r_{28} = k_{28}\, P^{0.3}\, c_G^{1.5}\, y_{13}^{0.5}\, y_3\, T_G \qquad (3.112)$$

3.7. Mass transfer

The performance of a mathematical model of a fluidized bed combustor or gasifier is very sensitive to the mass transfer between the various phases in the system. Several works, for instance Weimer and Clough (1981) and Overturf and Reklaitis (1983), have demonstrated this fact.

These transfer processes take place between:

a) Bubbles and gas in the emulsion;

b) Solids and gas in the emulsion.

As can be noticed, due to the hypotheses of a bubble phase free of solids, no direct mass transfer were considered to occur between solids and this phase. This transference is computed indirectly through the interstitial gas in the emulsion.

In the two following sections the mass transfer coefficients, necessary in the description of the present model, are discussed.

3.7.1. Bubbles and gas in the emulsion

Probably one of the most studied phenomena in the fluidization process is the mass transfer between these phases.

Among the correlations available that have been used in modelling of fluidized bed combustion and gasification are:

a) Kobayashi and Arai (1967) that describes the referred mass transfer coefficient by:

$$\omega_{BE} = \frac{0.11}{d_B} \tag{3.113}$$

This correlation was applied, for instance, by Rajan et al.(1980), Raman et al.(1981) and Chang et al.(1984);

b) Kunii and Levenspiel (1969) improved this correlation to account for the effects of the bed dynamics and mass transfer properties. Their correlation is described by:

$$\omega_{BE} = \frac{1}{\frac{1}{\omega_{BC}} + \frac{1}{\omega_{CE}}} \tag{3.114}$$

which is based on the three-phase model and the mass transfer between Bubble and Emulsion (BE) is given by a mechanism of resistances of the transfer between Bubble and Clouds (BC) and Clouds and Emulsion (CE). These individual mass transfer coefficients are given by:

$$\omega_{BC} = 4.5 \frac{U_{mf}}{d_B} + 5.85 \frac{D_G^{0.5} \, g^{0.25}}{d_B^{1.25}} \tag{3.115}$$

and

$$\omega_{CE} = 6.78 \left[\frac{\varepsilon_{mf} \, D_G \, U_B}{d_B^3} \right]^{0.5} \qquad (3.116)$$

This formulation is used in several mathematical models as, for instance: Fan et al.(1979), Tojo et al.(1981), Weimer and Clough (1981) and Overturf and Reklaitis (1983a,b);

c) Later, Sit and Grace (1981) verified that the above correlations underestimated the mass transfer in the regions of intense bubble interaction or coalescence, which occur with greater intensity near the distributor. Strong evidence for this comes from the conclusions from Behie and Kehoe (1973) and later by Overturf and Reklaitis (1983), who had to apply "Grid Enhancement Factors" (from 10 to 150) to correct the Kunii and Levenspiel (1969) mass transfer coefficients in order to match simulation and experimental results. The same order of corrections were applied in the model of Weimer and Clough (1981). On the other hand, the Sit and Grace correlation deals with only two phases and includes the cloud as part of the emulsion, as it is assumed in the present work. Due to this and also because Sit and Grace explain the verified contradictions their correlation is used in the equation (3.4) of the model and is described by:

$$\omega_{BE} = 2 \frac{U_{mf}}{d_B} + \frac{12}{d_B^{3/2}} \left[\frac{D_G \, \varepsilon_{mf} \, U_B}{\pi} \right]^{1/2} \qquad (3.117)$$

The gas-gas diffusivity (D_G) is described in the Appendix

A, and the parameters referred to the bubble phase are defined in the section (3.3.3).

3.7.2. Solids and gas in the emulsion

The mass transfer between a solid phase and the emulsion gas is given by:

$$\omega_{SEGE,m} = N_{Sh,m}\, D_G \frac{c_{GE}}{d_{PE,m}} \quad , \; 1 \leq m \leq 3 \qquad (3.118)$$

Therefore the determination of Sherwood number for each particle is the critical point in this calculation. In spite of its importance (measured by the influence on the rate of heterogeneous reactions), several mathematical models make strong simplifications in the determination of this parameter. For instance, Overturf and Reklaitis (1983) assumed N_{Sh} as a constant equal to 2. Other works do not even mention the adopted value or correlation.

After the literature survey, the work of La Nauze et al.(1984) appeared to be the most appropriate for the present application because it can predict the mass transfer coefficient for a wide range of particle sizes and it fits the conditions of temperature and fluidization normally found in operation. Their correlations are expressed by:

$$N_{Sh,m} = 2\,\varepsilon_{mf} + \left[\frac{4\, d_{PE,m}\, \varepsilon_{mf}\, U_B}{\pi\, D_G}\right]^{1/2} \qquad (3.119)$$

valid for relatively small particles or $d_{P,m}/d_{PA} \leq 1$, and

$$N_{Sh,m} = 2\,\epsilon_{mf} + \left[\frac{4\,d_{PE,m}\,(U_{mf} + U_B\,\epsilon_{mf})}{\pi\,D_G}\right]^{1/2} \qquad (3.120)$$

for relatively large particles or $d_{P,m}/d_{PA} \geq 3$. For the intermediate region, the following formula has been adopted here :

$$N_{Sh,m} = N_{Sh,m,eq.119}\,\tilde{u} + N_{Sh,m,eq.120}\,(1 - \tilde{u}) \qquad (3.121)$$

where

$$\tilde{u} = \frac{3 - (d_{P,m}/d_{PA})}{2} \qquad (3.122)$$

3.8. Heat transfer

As shown before, inside a fluidized bed boiler or gasifier several possible modes of heat transfer occur.

In order to determine the individual solid and gas phase profiles, the present work considers the following heat transfer between:

a) Gas in the bubble and gas in the emulsion;

b) Solids and gas in the emulsion and gas in the freeboard;

c) Solids and solids in the bed and in the freeboard;

d) Gas in the bubble and immersed tubes in the bed;

e) Gas in the emulsion and tubes in the bed;

f) Gas and tubes in the freeboard;

g) Solids and tubes in the bed and in the freeboard;

i) Bed and distributor;

j) Bed and internal reactor wall;

k) Gas in the freeboard and internal wall;

l) External reactor wall and environment;

m) Internal wall of tubes in the bed or in the freeboard and steam or liquid water inside the tubes.

Those that have not been detailed already are presented below.

3.8.1. Bubbles and gas in the emulsion

A specific method to calculate the heat transfer by convection between gas in a bubble and gas in the emulsion has not been found. Therefore as suggested in Kunii and Levenspiel(1969) and by other previous works on modelling of fluidized combustion, an analogy with the equivalent mass transfer equation (3.117) was assumed to give:

$$\alpha_{CGBGE} = \frac{U_{mf}\ \rho_{GA}\ C_{GA}}{3} + 2\left[\frac{\lambda_{GA}\ \varepsilon_{mf}\ U_B\ \rho_{GA}\ C_{GA}}{d_B}\right]^{1/2} \quad (3.123)$$

which is used to calculate the parameter for the convection heat transfer between these gaseous phases as:

$$E_{CGBGE} = \alpha_{CGBGE}\ (T_{GB} - T_{GE})\ \frac{dA_B}{dz} \quad (3.124)$$

3.8.2. Solids and gas in the emulsion

The heat transfer by convection between the solids and the gas in the emulsion has a coefficient described as :

$$E_{CSEGE,m} = \alpha_{CSEGE,m} \, (T_{PE,m} - T_{GE}) \, \frac{dA_{PE,m}}{dz} \qquad (3.125)$$

where

$$\alpha_{CSEGE,m} = \frac{N_{Nu,m} \, C_{GA}}{d_{PE,m}} \qquad (3.126)$$

The Nusselt number for this situation is defined by Kothari (1967) as:

$$N_{Nu,m} = 0.3 \, N_{Re,m}^{1.3} \quad \text{for} \quad N_{Re,m} < 100 \qquad (3.127)$$

here

$$N_{Re,m} = \frac{F_G \, d_{PE,m}}{S \, \mu_G} \qquad (3.128)$$

For $N_{Re,m} \geq 100$,the Nusselt number has been taken from Gelperin et al.(1967), as :

$$N_{Nu,m} = 0.4 \left[\frac{N_{Re,m}}{\varepsilon} \right]^{2/3} N_{Pr,G}^{1/3} \qquad (3.129)$$

3.8.3. Solids and solids

The radiative heat transfer between the various solids in the bed are calculated as:

$$E_{RSESE,m,n} = \sigma \, \epsilon_S' \, f_n'' \, (T_{PE,m}^{*} - T_{PE,n}^{*}) \, \frac{dA_{PE,m}}{dz} \qquad (3.130)$$

where $1 \leq m \leq 3$ and $1 \leq n \leq 3$.

Here it has been assumed that a particle of type "m" is surrounded by all kind of particles and therefore "sees" the other type of particles "n" by an area fraction given by " f_n'' ". Also that the gas layer between the particles is assumed to be transparent.

The heat transfer processes by convection and conduction, due to the contact between the various solids particles are calculated as:

$$E_{CSESE,m,n} = \alpha_{SESE,m,n} \, f_n'' \, (T_{PE,m} - T_{PE,n}) \, \frac{dA_{PE,m}}{dz} \qquad (3.131)$$

where $1 \leq m \leq 3$ and $1 \leq n \leq 3$. The heat transfer coefficients are given by:

$$\alpha_{SESE,m,n} = 4.51 \times 10^{-2} \, d_{PE,m,n}^{-1.22} \, \left(\frac{U}{U_{mf}}\right)^{-0.56} \qquad (3.132)$$

which has been found in the recent work of Delvosalle and Vanderschuren (1985) and adapted to allow the calculation of the heat transfer coefficient between particles of different diameters. Therefore the definition of an "average" diameter $d_{PE,m,n}$ is necessary and it is adopted

here as:

$$d_{PE,m,n} = \frac{1}{\frac{f_m}{d_{PE,m}} + \frac{f_n}{d_{PE,n}}} \qquad (3.133)$$

3.8.4. Tubes and the bed

The heat transfer between tubes and bed is accounted for by three terms:

1) Convection with the gas in the emulsion (E_{CGETD});

2) Convection with the gas in the bubble (E_{CGBTD});

3) Radiative with the particles in the emulsion (E_{RSETD}).

The convection between particles and tubes is indirectly computed with the convection between emulsion and tubes because the empirical correlations do not separate these phenomena.

Due to the small thickness of interstitial gas layers, all radiative transfer from or to gases have been neglected in the present model.

3.8.4.1. Convection between tubes and the bed

The convection between emulsion interstitial gas and tubes, referred in the equation (3.11) is described by:

$$E_{CGETD} = \alpha_{EOTD} (T_{GE} - T_{WOTD}) \frac{dA_{OTD}}{dz} \qquad (3.134)$$

and the equivalent for the gas in the bubbles, for the equation (3.15), by:

$$E_{CGBTD} = \alpha_{BOTD} (T_{GB} - T_{WOTD}) \frac{dA_{OTD}}{dz} \qquad (3.135)$$

The heat transfer coefficients have been taken from Xavier and Davidson(1978) who managed to separate the heat transfered from the tubes to the bed in the parts exchanged with the particulate and the gas phases. Here these expressions have been adapted to match the hypotheses that the heat transfer by convection between tubes and emulsion is accomplished by the gas in the emulsion and in the bubbles. These correlations are presented as:

$$\alpha_{EOTD} =$$

$$\alpha' \left[\frac{(\pi u_1)^{1/2}}{u_2 (1 + u_1)} (\text{erfc } u_2 \exp u_2^2 - 1) + \frac{2 u_1^{1/2}}{1 + u_1} \right] \qquad (3.136)$$

where

$$\alpha' = 2 \left[\frac{\lambda_{mf} \rho_{mf} C_{mf} (U - U_{mf})}{\pi d_{OTD}} \right]^{1/2} \frac{U_B}{U - U_{mf} + U_B} \qquad (3.137)$$

$$u_1 = \frac{U - U_{mf}}{0.35 (g d_D)^{1/2}} \qquad (3.138)$$

$$u_2 = \frac{\alpha''}{\alpha' (\pi u_1)^{1/2}} \qquad (3.139)$$

$$\alpha'' = \frac{\lambda_{GA}}{\delta_{film}} \qquad (3.140)$$

Here the film thickness for inclined tubes has been taken as an average between the relative to the horizontal and the vertical values as:

$$\delta_{film} = d_P \left[\frac{\cos(i_{TD})}{4} + \frac{1 - \cos(i_{TD})}{10} \right] \qquad (3.141)$$

The calculations of the indicated physical properties with the index "mf", have been done as recommended by the author and are described in the Appendix B.

The average gas temperature and composition in each differential section,that has been used to evaluate some physical properties, are also described in the Appendix.

For the bubble phase:

$$\alpha_{BOTD} = \left[\frac{4 \lambda_{mf} \rho_{GA} C_{GA} U_{mf}}{\pi d_{OTD}} \right]^{1/2} \qquad (3.142)$$

Again the physical properties mentioned with the subscript "mf" are related in the Appendix B.

The external tube overall heat transfer coefficient can be calculated from these, as shown by Gallo et al.(1981),as:

$$\alpha_{OTD} = \alpha_{EOTD} (1 - 0.7125 \varepsilon_B) + \alpha_{BOTD} 0.7125 \varepsilon_B \qquad (3.143)$$

The external wall temperature of the tubes in the bed at each height "z" is calculated by an iterative convergence with the aid of the calculation of the tube internal and external heat transfer coefficient The basic convergence equation is :

$$T_{WOTD} = \frac{\alpha_{OTD}\, T_{GA} + \alpha_{JTD}\, T_{HJTD}}{\alpha_{OTD} + \alpha_{JTD}} \qquad (3.144)$$

The internal tube heat transfer coefficient calculation must take into account the various possibilities of the thermodynamic state of the flowing water inside the tubes. Although in boilers almost all the tube is used for nucleate boiling, this need not be the case of a unit operating with a cooling coil, for instance. Therefore a special subroutine has been introduced into the program in order to determine the internal fluid condition and temperature at each point of the tubes. This is accomplished by a convergence strategy described as follows:

1) The feed water temperature is known as data of the equipment operation. If not, it is assumed, by the program, that it is a common boiler operation and the temperature will be taken as the saturation temperature at the tube internal pressure;

2) Then, the temperature in the tubes, at the lowest point of the tube bundle, is compared with the saturation temperature of the water at the operating internal pressure," T^{*}_{HJTD} ", and the heat transfer regime

is determined for that point;

3) This allows the calculation (see Appendix D) of the heat transfered to the fluid inside the tubes and the temperature or quality of the steam can be determined for the next differential section;

4) The procedure is repeated for the entire section of the bed occupied by the tube bundle.

The heat transfer coefficients for each possible situation (liquid convection, nucleate boiling, film boiling, vapour convection and even vapour condensation) are described in any classical text on heat transfer. Isachenko et al.(1977) was used as source for the present work and the heat transfer coefficients between the internal surface of the tubes and the watersteam are listed in the Appendix D.

3.8.4.2. Radiation between tubes and solids

The radiative heat transfer between solids and tubes in the bed are calculated as follows:

$$E_{RSETD,m} = f''_m \, \sigma \, \epsilon'_{DTD} \, (T^{*}_{PE,m} - T^{*}_{WOTD}) \, \frac{dA_{OTD}}{dz} \qquad (3.145)$$

for $1 \leq m \leq 3$. The equivalent bed-tubes emissivity has been taken from Botteril (1983) as:

$$\epsilon'_{DTD} = \frac{1}{\frac{1}{\epsilon'_S} + \frac{1}{\epsilon'_{TD}} - 1} \qquad (3.146)$$

3.8.5. Tubes and the freeboard

These calculations assume the classical correlations from the literature and are presented in the Appendix E.

3.8.6. Reactor and external ambience

In a well designed boiler or gasifier the heat losses to the ambience are negligible when compared to the heat generation inside the equipment. These losses are, on average, around 1 to 2% of the energy involved in the process. Some few exceptions can occur for gasification operations where only steam or other hot gasification agent is used in the absence of oxygen. In these cases, the heat losses could reach to around 10% of the energy involved in the process.

The present work includes the calculation of these losses mainly to maintain the completeness and generality of the model.

The calculations for the referred heat transfer, assume the existence of an insulation that covers the entire external wall of the reactor and constitutes the main resistance for this heat exchange. Therefore the simulation assumes the internal wall of the reactor at a given height "z" to be at the temperature of the phase in contact with this point of the wall at the same height.

The total heat transfer coefficient between the external wall (OW) and ambience is estimated by a relatively simple routine based of the paper from Hughes and Deumaga (1974) and given by:

$$\alpha_{OW} = 1.9468\ (T_{OW} - T_{amb})^{1/4}\ (2.8633\ U_{amb} + 1)^{1/2} +$$

$$5.75\ \varepsilon'_{ins}\ \frac{\left[\left(\frac{T_{OW}}{100}\right) - \left(\frac{T_{amb}}{100}\right)\right]}{(T_{OW} - T_{amb})} \qquad (3.147)$$

Here the velocity U_{amb} refers to the average wind velocity of the air (normally taken as 2 m/s, if no information is provided).

This coefficient must be calculated at each point of the reactor height to be used in the differential energy balance equations. To accomplish this, a computational routine is provided to calculate the external temperature (T_{OW}) at any given point "z" and based on the following relationship that relates the heat flux through the insulation wall and to the ambience:

$$q_{OW} = \alpha_{OW}\ (T_{OW} - T_{amb}) = \lambda_{ins}\ \varepsilon'_{ins}\ (T_{JW} - T_{OW}) \qquad (3.148)$$

The surface internal temperature (T_{JW}) is defined properly for each section of the reactor.

3.8.6.1. Bed section

In the bed section the calculation of the heat transfer between the reactor and the environment has been simplified by the assumption that this transfer is basically accomplished between the internal wall and the emulsion gas. This means that the other phases (solids and bubbles) will be affected indirectly. This would not bring any substantial effects on the results due to the magnitude

of this transference when compared to the other effects. Therefore the term E_{GEWD} is given by:

$$E_{GEWD} = q_{OWD} \frac{S'_{OWD}}{z_D} \qquad (3.149)$$

where S_{OWD} is the external area of the bed section of the reactor and q_{OWD} is heat flux to the external ambience and given by the equation shown in the last section. Due to the simplification adopted, the surface temperature of the internal wall (T_{JW}) is assumed to be equal to that of the gas in the emulsion (T_{GE}) at any point "z" of the bed section.

3.8.6.2. Freeboard section

An analogous hypothesis to that for the bed section, is made for the freeboard, i.e., the heat transfer between the reactor and the environment is accomplished between the internal wall and the gas phase or:

$$E_{GFWF} = q_{OWF} \frac{S'_{OWF}}{z_F - z_D} \qquad (3.150)$$

with the analogous definitions for the respective parameters as in the case of the bed section. Here, it has been assumed that $T_{JW}=T_{GF}$.

3.9. Solid circulation

The total rate of solid circulation in the bed is described by Talmor and Benenati (1963) as:

$$\frac{F_N}{2} = 785\ (U - U_{mf})\ \exp(-\ 6630\ d_{PA}) \qquad (3.151)$$

This expression cannot describe the rate of individual solid circulation, as needed for the energy balances. On the other hand, no publication have been found to describe these individual circulation.

An adaptation is tried and by following the comments in Kunii and Levenspiel (1969), these circulation have been modelled, in the present work, as:

$$\frac{F_{N,m}}{2} = \rho_{P,m}\ (1 - \varepsilon_{mf})\ (U - U_{mf})$$

$$\exp(-\ 6630\ d_{PE,m})\ f_m'''\ S \quad , \quad 1 \leq m \leq 3 \qquad (3.151a)$$

This equation worked well for the range of conditions tested, as shown ahead. However, this must be seen as a first approximation, and more research in this field is necessary, as also pointed by Kunni and Levenspiel (1969).

3.10. Particle size distribution

A very important part of the model is the determination of the particle size distribution in the bed at every set of operational conditions. This determination must take into account the various physical and chemical

processes that occur during the equipment operation. The effects are:

a) The already explained reduction of the particle size due to the chemical reactions, mainly in the case of the carbonaceous material the exposed-core model has been chosen as the more appropriate;

b) The reduction of the particle size due to the attrition among the various particles;

c) The variation due to the entrainment and elutriation of particles from the bed.

In order to compute the combined effects of these factors, a mass balance for the size level "l" of particles of kind "m" is done and an iterative routine must be set. The balance is given by:

$$\dot{s}_{m,l} =$$

$$\left[\dot{s}_{I,m,l} F_{L,m} + F_{K,m,l} + \Gamma_{m,l+1} + F_{Y,m,l,z=z_D} - F_{Y,m,l,z=z_F}\right] /$$

$$\left[F_{LD,m} + \psi_m \Psi_D (U - U_{mf}) f_m \tilde{s}_{m,l}\right] \qquad (3.152)$$

where the mass flow of particles leaving the bed is related to the mass flow of particles leaving the system by:

$$F_{LD,m} = F_{L,m} + F_{K,m} + F_{Y,m,z=z_D} - F_{Y,m,z=z_F} \qquad (3.153)$$

and

$$F_{K,m,l} = F_{Y,m,z=z_F} \eta_{cy,m,l} \qquad (3.154)$$

The mass fraction of particles recycled to the bed is related with the cyclone efficiency of the cyclone system η_{cy} for each particular kind "m,l" of particle. The correlations used to calculated these parameters are described ahead in the section (3.10.3).

The rate of production of fines was taken from Merrick and Highley(1974) and used as in Rajan et al.(1980):

$$r_{m,l} = \psi_m \Psi_D (U - U_{mf}) \dot{s}_{m,l} f_m \tilde{s}_{m,l} \qquad (3.155)$$

where

$$\tilde{s}_{m,l} = 1 - \sum_{k=l+1}^{lm} \dot{s}_{m,k} \qquad (3.156)$$

It is interesting to observe that the parameter $\tilde{s}_{m,l}$, which represents the mass fraction of particles in the bed smaller that the respective diameter $d_{P,m,l}$, accounts for the greater rate of abrasion of the coarser particles than the finer ones. This is because, although the coarser particles are continuously in contact with other particles, the finer ones will spend part of the time in voids between larger particles. Curiously, this effect is stressed in the work of Merrick and Highley (1974) but not included by Rajan and Wen (1980) when they used the correlations of those authors.

For the sake of simplicity, the solid friability coefficients have been taken as constants, despite the fact that some recent works - for instance Chirone et al.(1984),

Salatino and Massimilla(1985) and Vaux and Schruben(1983) - have shown that they are not truly constants. These values have been taken from Merrick and Highley(1974) as: $\psi_1 = 9.11 \times 10^{-6}\ m^{-1}$, $\psi_2 = 2.73 \times 10^{-6}\ m^{-1}$. The friability factor for the inert (sand) was assumed to be $7.30 \times 10^{-6}\ m^{-1}$. This value was calculated from the information found in Perry and Chilton(1973) for the abrasion coefficients.

Some attention should be given to the work of Vaux and Schruben(1983) because it provides a relationship between the rate of production of fines and the time. It is known that the rate decreases asymptotically with time to a constant value at the steady-state condition. This leads to the conclusion that the coefficients ψ_m are functions of time but also tend to constant values that should converge to those reported by Merrick and Highley(1974).

The routine starts from the highest size level" $l = lm$", for which there is no increase due the generation of fines by attrition because "$r_{m,lm+1} = 0$". As the next size is "$l = lm-1$",the new value of "$\dot{s}_{m,lm}$" can be used to calculate "$r_{m,lm}$" and the process can be repeated till $l = 1$.

3.10.1.Entrainment and Elutriation

As stated before, the rate of entrainment is a function of the position in the freeboard. Some uncertainty has been pointed out with regard to the correlations found in the literature. For instance, Rajan et al.(1979) modelled this flow rate as:

$$F_{Y,m,l} = F_{Y,m,z=z_D} \; s_{D,m,l} \; \exp\left(\frac{z - z_D}{2.75}\right)$$

$$\ln\left(\frac{F_{X,m,l}}{F_{Y,m,z=z_D} \; s_{D,m,l}}\right) \qquad (3.157)$$

for $1 \leq m \leq 3$ and $1 \leq l \leq lm$. where, for the rate of solids thrown into the freeboard they used the correlation from Yates and Rowe(1977):

$$F_{Y,m,z=z_D} = S \; (U - U_{mf})^{m'} \; (1 - \varepsilon_{mf})^{m''} \; \rho_{PE,m} \qquad (3.158)$$

For the elutriation rate of particle of kind "m" and size level "l" they used:

$$F_{X,m,l} = X_{m,l} \; s_{D,m,l} \quad , \; 1 \leq m \leq 3 \; , \; 1 \leq l \leq lm \qquad (3.159)$$

where the elutriation rate parameter was taken from the work of Merrick and Highley (1974) as:

$$X_{m,l} = F_{GIF} \exp\left[- 10.4 \left(\frac{\tau_{m,l}}{U}\right)^{1/2} \left(\frac{U_{mf}}{U - U_{mf}}\right)^{0.25} \right] \qquad (3.160)$$

The basic criticisms of this treatment are:

1) The value of 2.75 in eq.(3.157), which is supposed to be the height of the freeboard, was taken from a particular case of experimental conditions published by Merrick and Higley(1974). Therefore that equation has no generality at all;

2) The values of elutriation rate depend on the bed dynamics which is in contradiction with the nature of the elutriation phenomena. This flaw is pointed by Wen and

Chen (1982);

3) The values of the solid mixing parameter "m'" and the fraction of wake solids thrown into the freeboard "m''", have been taken within a range from 0.075 to 0.3 and 0.1 to 0.5, respectively. This increases considerably the uncertainty of the referred model.

Recently some more careful studies on the subject have been published. The work of Wen and Chen (1982) is an example and due to its agreement with experimental results has been chosen to be used in the present model. The authors showed some conceptual flaws in the work of Merrick and Highley (1974), one of them, is related to the rate of elutriation $F_{X,m,l}$. Merrick and Highley had found some elutriated particles whose terminal velocities were above the superficial velocities in the freeboard. Due to this, the correlations used by them to calculate the entrainment rate depended on the minimum fluidization velocity in the bed. Wen and Chen, after a careful examination of the experimental data, published by the former workers, concluded that the freeboard height used by them was smaller than the Transport Disengaging Height (TDH). Based on new experimental work, they stated that the rate of elutriation should be independent of the dynamics of the bed and proposed the following equation to compute this parameter:

$$F_{X,m,l} = X_{m,l}\, s_{D,m,l} \qquad (3.161)$$

where,

$$X_{m,1} = \rho_{P,m} (1 - \epsilon_{F,m,1}) (U_o - T_{m,1}) S \qquad (3.162)$$

The void fraction in the freeboard is estimated by:

$$\epsilon_{F,m,1} = \left[1 + \frac{a_{e,m,1} (U_o - T_{m,1})^2}{2 g d_D} \right]^{-1/4.7} \qquad (3.163)$$

The coefficients a_e are given by the following relationships:

$$\frac{a_{e,m,1} \rho_{P,m,1}}{d^2_{P,m,1}} \left[\frac{\mu_G}{\rho_G} \right]^{2.5} = 5.17 (N_{Re_{m,1}})^{-1.5} d_D^2 \qquad (3.164)$$

valid for $N_{Re_{m,1}} \leq N_{Re_c}$, and

$$\frac{a_{e,m,1} \rho_{P,m,1}}{d^2_{P,m,1}} \left[\frac{\mu_G}{\rho_G} \right]^{2.5} = 12.3 (N_{Re_{m,1}})^{-1.5} d_D \qquad (3.165)$$

valid for $N_{Re_{m,1}} > N_{Re_c}$. Here

$$N_{Re_c} = 2.38/d_D \qquad (3.166)$$

and

$$N_{Re_{m,1}} = \rho_G (U_o - T_{m,1}) d_{P,m,1} / \mu_G \qquad (3.167)$$

The usual relationships given in the literature (see for instance Perry and Chilton(1973)) are used for the calculations of particle terminal velocities.

For the rate of entrainment at a height "z" they followed the equation of Kunii and Levenspiel (1969):

$$F_{Y,m,l} = F_{X,m,l} +$$

$$(F_{Y,m,l,z=z_D} - F_{X,m,l}) \exp[-a_Y (z - z_D)] \qquad (3.168)$$

where the rate at the bed surface is given by:

$$F_{Y,m,l,z=z_D} =$$

$$3.07\times10^{-9} S^2 d_B \rho_G^{3.5} g^{0.5} \frac{(U_o - U_{mf})^{2.5}}{\mu_G^{2.5}} \dot{S}_{m,l} \qquad (3.169)$$

Several discrepancies have been observed on the reported correlations and values for the parameter a_Y. Wen and Chen (1982) could not find a correlation to determine this parameter. Their experimental work, as well as the published ones, showed that its value varies from 3.5 to 6.4 m^{-1}. They maintain that: "Since the value is not very sensitive in the estimation of the entrainment rate, it is recommended that a value of 4.0 m^{-1} be used for a system in which no information on entrainment rate is available". On the other hand, Lewis et al.(1962) reported values from 0.4 to 0.8 s^{-1} for the product: $a_Y U_o$. More recently, Walsh et al.(1984) found the same product to be between 2.7 and 3.7 s^{-1} which contradicts a graph presented by Wen and Chen where the scattering of the characteristic length for the decay of particles flux (a_Y) against U_o cannot ensure the validity of the above correlation. In view of that and based on the values given by the simulation of several examples, it was decided to follow the suggestion from Wen

and Chen (1982), or to fix the value of 4.0 for the parameter a_Y. It is obvious that only further experimental investigation could clarify this point.

In addition, Walsh et al.(1984) suggested a different correlation to calculate the rate of entrainment at the surface of the bed given by:

$$F_{Y,m,1,z=z_D} = F_{X,m,1} + S\ (U_o - U_{mf})^{2.1} \qquad (3.170)$$

This equation for $F_{Y,z=z_D}$ seems to agree with some previous works but give differences of 10 to 100 times smaller than the flows obtained by Wen and Chen (1982). Walsh et al. suggest that these differences could be caused by the presence of a heat exchanger at the surface of the bed on their experimental equipment.

Finally, it was decided to employ the correlations of Wen and Chen (1982), instead any other mentioned above, because:

a) The amount of experimental data used to establish the correlations;

b) The coherence of the theoretical model with the factors that influence the phenomena of entrainment and elutriation;

c) The much smaller deviations between predicted and measured values, obtained during simulations, using the Wen and Chen correlations against the other published methods.

3.10.2. Transport Disengaging Height, TDH

The concept of TDH is an auxiliary tool for didactic explanation of the phenomena of entrainment and elutriation rather than a precise physical parameter. This is due to the very nature of particle flow in the freeboard.

As the bubbles blast at the bed surface and the gaseous current leaves the bed entering the freeboard, particles are carried to this region. Usually, the main part of the solid flow, immediately above the bed surface, consists of particles whose terminal velocities are greater than the average gas velocity in this section of the freeboard, and therefore they tend to return to the bed after a short distance on their way up. The number of particles that return decreases exponentially with height, as indicated by the correlations shown above. In practical terms, there is a height where no appreciable further decrease in the solid flow is observed and this height is called Transport Disengaging Height.

On the other hand, as the gas velocity in the freeboard decreases near regions close to the chamber walls, the flow of returning particles can never cease completely but decreases asymptotically. This imposes a difficulty or even a theoretical impossibility to define a height in which the flow of particles would remain constant. Therefore only an approximation criteria can be used to define the Transport Disengaging Height.

Some correlations found in the literature seem to

ignore this intrinsic nature of the phenomena and, for instance, to define TDH as a function solely of the average gas velocity and do not take into account the particles characteristics at different heights in the freeboard. As for example, the work of Amitin et al.(1968) that was used in the mathematical model of Rajan et al.(1979) which describes TDH by:

$$z_{TDH} = z_D + 0.369\ U^{1.2}\ (16.87 - 1.2\ \ln U) \qquad (3.171)$$

In the present work however, due to the use of the exponential law to describe the entrainment flow of particles, the use of a correlation for TDH is completely unnecessary. On the other hand, for the sake of completeness in the print out of the equipment operation parameters, it has been decided to adopt the suggestion of Wen and Chen (1982) and define the TDH as the height at which the entrainment rate is within one percent of the elutriation rate and therefore is given by:

$$z_{TDH} = z_D + (1/a)\ \ln\left(\frac{F_{Y,z=z_D}}{0.01\ F_X}\right) \qquad (3.172)$$

3.10.3. Recycling of particles

Several commercial units operate with recycling to the bed of a fraction of the entrained material from the top of the freeboard. This is accomplished by using a cyclone or a system of cyclones.

As it has been described in the previous sections, the program calculates the particle size

distribution inside the bed, and after that at each height in the freeboard, a coherent method to evaluate the flow and the particle size distribution of the recycled material is therefore necessary. On the other hand, it is out of the scope of the present work to derive a detailed simulation of the behaviour of a cyclone system due to the already complex nature of the present simulation. Therefore it was decided to use a simpler correlation for the cyclone efficiency based on the average operation of commercial cyclones.

A paper from Leith and Mehta (1973) was found quite useful for this purpose because it provides clear information on commercial cyclone operations. For instance, the cyclone efficiency is correlated as:

$$\eta_{cy,m,l} = 1 - \exp\left[-2 \left(c_{cy}\ \psi_{cy,m,l}\right)^{\frac{1}{2n_{cy}+2}} \right] \qquad (3.173)$$

where the parameter c_{cy} is a function of the cyclone geometry that for a wide range of standard designs (see Table 1 in the referred paper) fluctuates around the value 50. The coefficient "n_{cy}" is given by:

$$n_{cy} = 1 - \left[1 - \frac{(39.4\ d_{cy})^{0.14}}{2.5} \right] \left(\frac{T}{283}\right)^{0.3} \qquad (3.174)$$

here, "d_{cy}" is the cyclone diameter in m and T is the absolute temperature (K) of the cyclone operation.

The parameter "$\psi_{cy,m,l}$" can be related to the particle terminal velocity by:

$$\psi_{cy,m,l} = \frac{\tau_{m,l}\, U_{cy,G}}{g\, d_{cy}} (n_{cy} + 1) \qquad (3.175)$$

The gas inlet velocity $U_{cy,G}$ is calculated using the fact that for standard cyclones the cyclone entrance has a square cross section measuring:

$$S_{cy,entry} = 0.125\, d_{cy}^2 \qquad (3.176)$$

3.11. Physical properties

All the gas and solid and mixture physical properties have been taken from Reid et al.(1977), Karapetyants(1978), Yaws et al.(1976a,b,c) and Williamson(1972).

The expressions to determine the average thermal conductivity and viscosity for a gas mixture have been taken from Perry and Chilton(1973).

A special note must be taken of the fact that the physical properties of the tar have been modelled as being the same as those of glucose. This can be partly justified because:

a) The glucose molecule is the basic unit of cellulose;

b) Has been verified that glucose is formed in appreciable quantities during the pyrolysis of wood;

c) The similarity of the physical characteristics between glucose and tar.

3.12. Pressure losses in the system

The gas current suffers, basically, two main pressure losses in the system. The first is due to the distributor in the bed base and the other in the bed itself. The pressure loss in the freeboard is, normally, negligible when compared to the former ones.

Due to the negligible variation of the pressure in the bed, which is normally below 1% of the absolute pressure of the entering gas current, the present program takes as a datum the average pressure inside the bed and uses it as a constant parameter in the calculations. On the other hand the pressure loss in the distributor is important as a design variable.

The program calculates these pressure losses which are clearly indicated in the print out of the simulation results but they do not interfere in the main body of the simulation.

3.12.1. Pressure drop across the distributor

For this calculation, the correlations described in Ho et al.(1984) are used:

$$\Delta P_{dist} = 0.73\ U_{orif}^{2}\ a_{orif}^{-0.06}\ \left(\frac{x_{dist}}{d_{orif}}\right)^{-0.2} \qquad (3.177)$$

Here the open area ratio of the distributor "a_{orif}" is given by:

$$a_{orif} = \frac{n_{orif}\ d_{orif}^{2}}{d_{D}^{2}} \qquad (3.178)$$

and the gas velocity through the distributor holes by:

$$U_{orif} = \frac{U_{z=0}}{a_{orif}} \qquad (3.179)$$

In the case of porous plate the value 0.02 is assumed for a_{orif}.

3.12.2. Pressure loss in the bed

The simple equation is taken from Kunii and Levenspiel (1969):

$$\Delta P_{bed} = z_D (1 - \varepsilon) (\rho_{PA} - \rho_{GA}) \qquad (3.180)$$

3.13. Auxiliary equations

This section contains some of the equations and relationships that have been used throughout this work and included in the simulation program.

3.13.1. Average particle parameters

In the system, various kinds of solid particles are present as carbonaceous material, limestone and inert, that could include free-ash from the carbonaceous solid. In addition each solid has its particle size distribution and therefore a system to represent the various average characteristics is necessary.

The fraction of particles in the bed has four possible definitions and they are used in different conditions:

a) Mass fraction:

$$f_m = \sum_{l=1}^{l=lm} s_{m,l} \qquad (3.181)$$

b) Number fraction:

$$f'_m = \frac{\frac{f'''_m}{V_{PE,m}}}{\sum_{n=1}^{3} \frac{f'''_n}{V_{PE,n}}} \quad , \; 1 \leq m \leq 3 \qquad (3.182)$$

c) Area fraction:

$$f''_m = \frac{f'_m \, A_{PE,m}}{\sum_{n=1}^{3} f'_n \, A_{PE,n}} \quad , \; 1 \leq m \leq 3 \qquad (3.183)$$

d) Volume fraction:

$$f'''_m = \frac{\frac{f_m}{\rho_{PE,m}}}{\sum_{n=1}^{3} \frac{f_n}{\rho_{PE,n}}} \quad , \; 1 \leq m \leq 3 \qquad (3.184)$$

The relations below can illustrate the difference between the various possible definitions for mass fraction of particles:

$$\sum_{m=1}^{3} f_m = 1 \qquad (3.185)$$

$$\sum_{l=1}^{lm} \dot{s}_{m,l} = 1 \quad , \; 1 \leq m \leq 3 \tag{3.186}$$

and

$$\sum_{m=1}^{3} \sum_{l=1}^{lm} s_{m,l} = 1 \tag{3.187}$$

As can be noticed, each kind "m" of particle has "lm" levels of particle size each with its " $\dot{s}_{E,m,l}$ " mass fraction. This mass fraction is calculated after the computation of the effects of attrition, chemical reactions, entrainment and elutriation.

With the help of the former definitions it is possible to establish some useful averages for the particle characteristics:

1) Average density:

$$\rho_P = \sum_{m=1}^{3} f_m \; \rho_{P,m} \tag{3.188}$$

Except for the carbonaceous solid material, the density "$\rho_{P,m}$" of each particle in the bed (steady state condition) is the same as in the feeding condition if the exposed core model is assumed. On the other hand, if the case of the unreacted core model is assumed, the density of the carbonaceous particles is given by:

$$\rho_{P,1} = \rho_{PI,m=1} \; (1 - \Lambda_{1,4}) + \Lambda_{1,4} \; \rho_Z \tag{3.189}$$

where the ash layer density is given by

$$\rho_Z = \rho_{PI,1}\, w_{PI,ash} \qquad (3.190)$$

If the exposed core model is assumed, the density of the carbonaceous material is the same as in the feeding condition and the generated ash goes to the inert phase therefore modifying the density of this phase. It has been assumed that the generated ash increases the mass fraction of the lowest particle size level of the inert phase and the average density of that phase ($\rho_{P,3}$) is recalculated.

2) The average sphericity has been calculated by:

$$\phi_P = \sum_{m=1}^{3} f''_m \, \phi_{PE,m} \qquad (3.191)$$

3) The average diameter is calculated as suggested by Kunii and Levenspiel (1969) as:

$$d_P = \frac{1}{\sum_{m=1}^{3} \frac{f_m}{d_{P,m}}} \qquad (3.192)$$

and

$$d_{P,m} = \frac{1}{\sum_{l=1}^{lm} \frac{\dot{s}_{m,l}}{d_{P,m,l}}} \quad , \; 1 \leq m \leq 3 \qquad (3.193)$$

3.13.2. Derivatives of areas and volumes with "z"

Several derivatives must be computed during the calculations and some of them are described below:

1) The variation of the total particle surface areas, in the bed section, are given by:

$$\frac{dA_{PE,m}}{dz} = S_E(1 - \varepsilon_E)\, f_m''' \frac{A_{PE,m}}{V_{PE,m}} \quad , \; 1 \leq m \leq 3 \qquad (3.194)$$

2) In the freeboard section by:

$$\frac{dA_{PF,m}}{dz} = S_F(1 - \varepsilon_F)\, f_m''' \frac{A_{PF,m}}{V_{PF,m}} \quad , \; 1 \leq m \leq 3 \qquad (3.194a)$$

3) The variation of total bubble surface area is given by:

$$\frac{dA_B}{dz} = S_B \frac{A_B}{V_B} \qquad (3.195)$$

4) The variation of the volume occupied by the gas in the emulsion phase is given by:

$$\frac{dV_{GE}}{dz} = S_E\, \varepsilon_{mf} \qquad (3.196)$$

5) The variation of the volume occupied by the gas in the bubble phase is given by:

$$\frac{dV_B}{dz} = S_B \qquad (3.197)$$

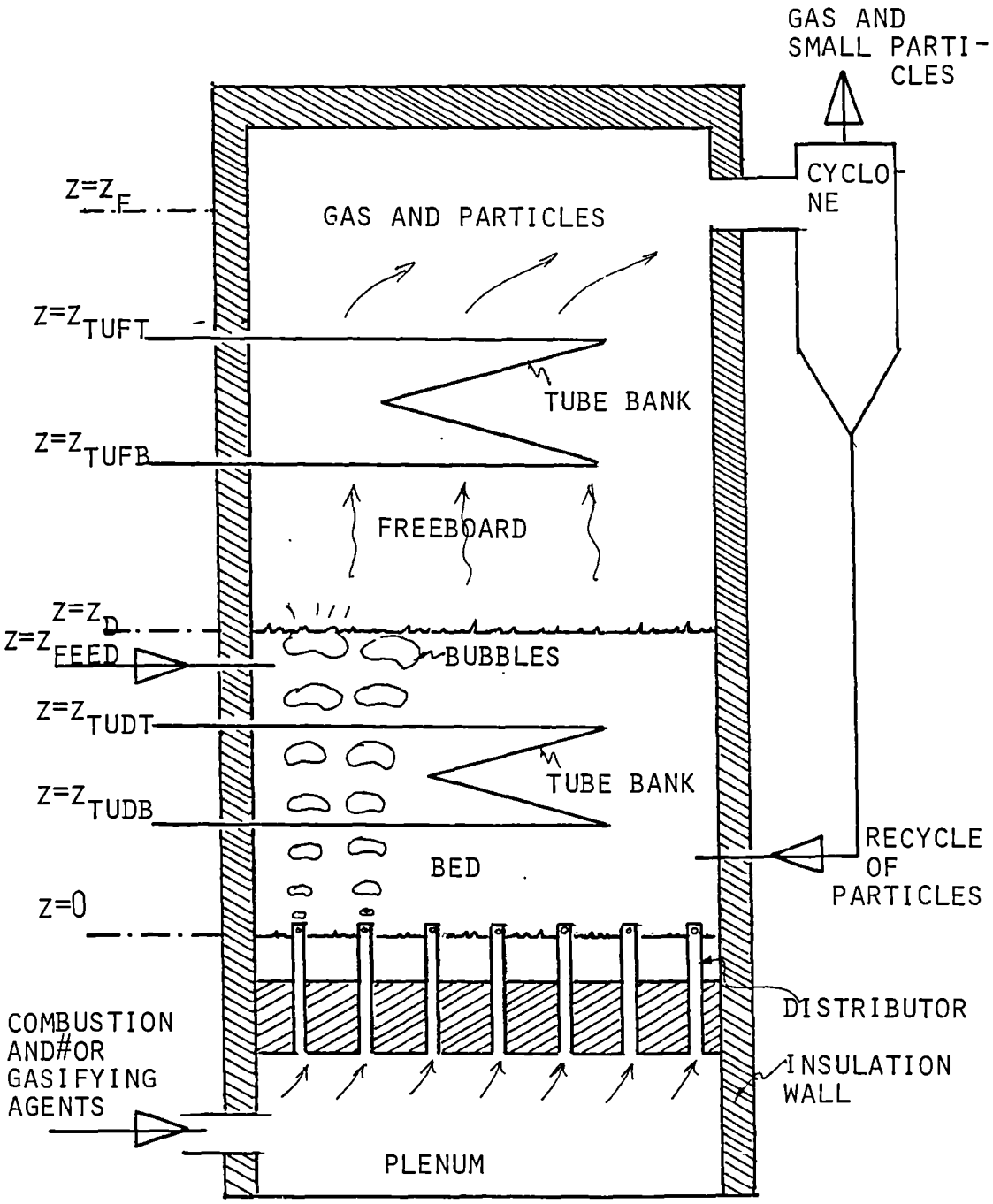

FIGURE 3.1. SCHEME OF A FLUIDIZED BED REACTOR.

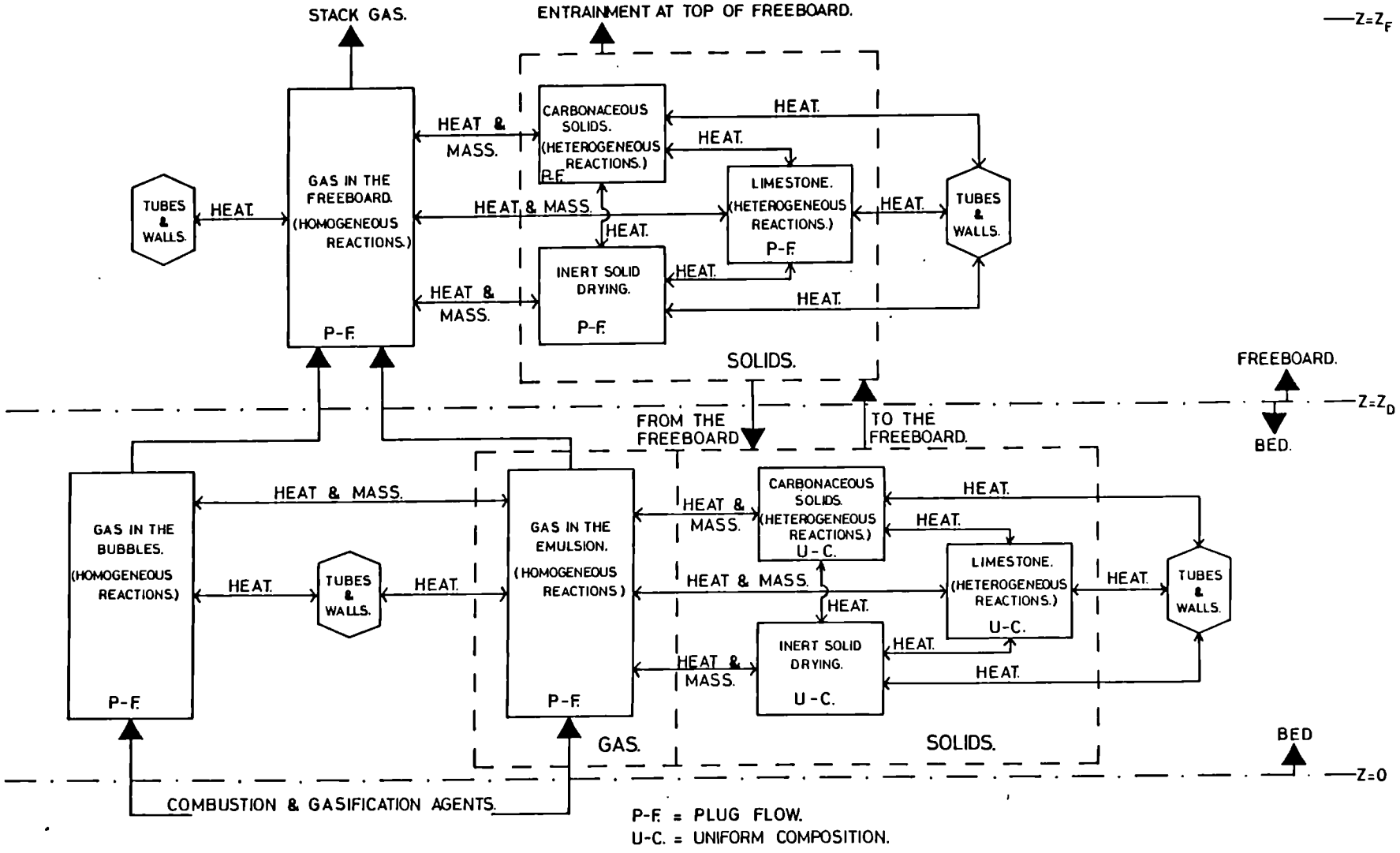

FIGURE 3.2. SIMPLIFIED DIAGRAM OF THE MODEL BASIC STRUCTURE.

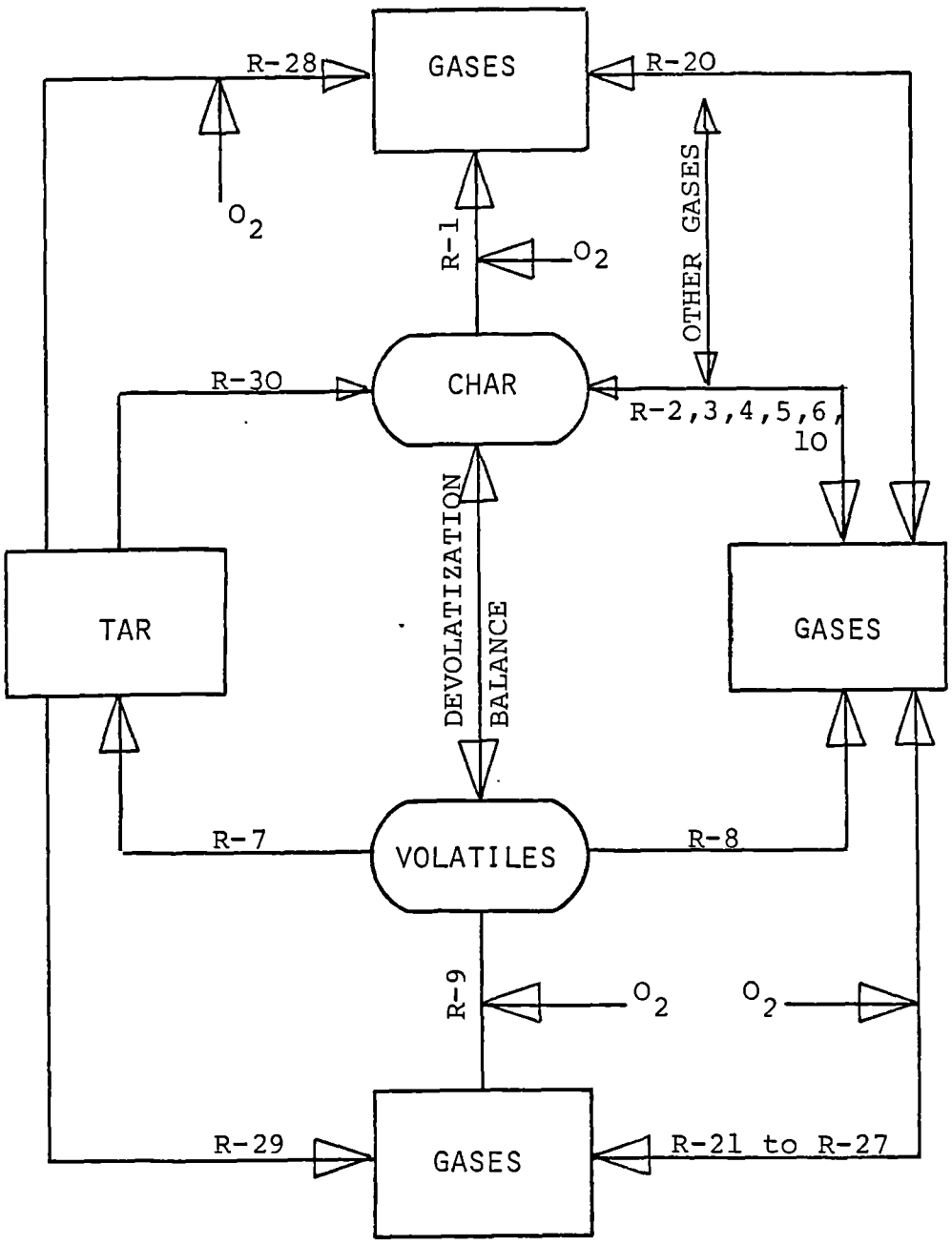

FIGURE 3.3. SCHEME REPRESENTING THE REACTIONS INVOLVING THE CARBONACEOUS SOLID.

CHAPTER IV

4.DESCRIPTION OF THE SIMULATION PROGRAM

The simplified block diagram of the computer simulation program that was built based on the present mathematical model is presented in the next section. A detailed description and listing of the FORTRAN program in this thesis has been considered to be out of the scope of this text. However, a version of the program with an operation manual can be obtained from the author.

The program input data is fed in S.I. units and all the calculations as well the results are also accomplished and produced in S.I. units.

As an illustration, the data necessary to run the simulation and the data generated by it are included in this chapter.

4.1.Basic calculation strategy

The overall logic diagram for the program is presented in Fig.4.1.

4.2.Data to be fed into the program

The following list is included to illustrate the data necessary to be fed into the program for a general case. Depending on the equipment operation or design, some of these data may have no meanings and should be set to zero.

Data are fed to the program in S.I. units and the

symbology used during the computation is indicated:

Observations:

1) Material here refers to the Carbonaceous Solid fed to the system;

2) All the data relating the solid characteristics must be given in the condition "AS FED TO THE BED";

3) If the data is unknown or not relevant just set it to zero.

PROXIMATE ANALYSIS OF THE CARBONACEOUS MATERIAL:

AMTPES(1) = Material moisture content, wet basis (%)

VOLAT = Material volatile content, wet basis (%)

CARFIX = Material fixed carbon content, wet basis (%)

ASHES = Material ash content, wet basis (%)

ENTCBC = Material combustion enthalpy (high heat value of the dry material) (J/kg)

MTKIND = Indicates the kind of material fed to the bed (1=bituminous coal; 2=semibituminous coal; 3=lignite; 4=charcoal; 5=wood or any other biomass)

ULTIMATE ANALYSIS OF THE CARBONACEOUS MATERIAL:

WPDB(14) = Material carbon mass fraction, dry basis (kg/kg)

WPDB(15) = Material hydrogen mass fraction, dry basis (kg/kg)

WPDB(16) = Material oxygen mass fraction, dry basis (kg/kg)

WPDB(17) = Material nitrogen mass fraction, dry basis (kg/kg)

WPDB(18) = Material sulphur mass fraction, dry basis

(kg/kg)

WPDB(19) = Material ash mass fraction, dry basis (kg/kg)

ROGCES = Material global density (or density of a fixed bed of this material) (kg/m^3)

ROPES(1) = Material apparent particle density (kg/m^3)

RORES(1) = Material real (or true) density (kg/m^3)

MODLR = Reaction model:

(MODLR=0 indicates that the exposed core model is to be adopted during the calculations (ash does not cover the unreacted core of the carbonaceous material during the process);

MODLR=1: indicates that the shrinking core model or unreacted core model is to be adopted during the calculations (ash covers the unreacted core of the carbonaceous material during the process)

FISP(1) = Material particle sphericity (dimensionless) (if unknown, the program assumes 0.7)

AMTPES(2) = Limestone moisture content, mass percentage (%)

AMTPES(3) = Inert moisture content, mass percentage (%)

LIMESTONE ANALYSIS:

WPDB(22) = Limestone $CaCO_3$ content, mass fraction, dry basis (kg/kg)

WPDB(23) = Limestone CaO content, mass fraction, dry basis (kg/kg)

WPDB(24) = Limestone $CaSO_4$ content, mass fraction, dry basis (kg/kg)

FMPES(2) = Limestone mass flow fed to the bed (kg/s)

ROPES(2) = Limestone apparent particle density (kg/m^3)

RORES(2) = Limestone real (or true) density (kg/m^3)

FISP(2) = Limestone particle sphericity (dimensionless) (if unknown, the program assumes 0.7)

FMPES(3) = Mass flow of inert fed to the bed (kg/s)

ROPES(3) = Inert apparent particle density (kg/m^3)

RORES(3) = Inert real (or true) density (kg/m^3)

FISP(3) = Inert particle sphericity (dimensionless) (if unknown, the program assumes 0.7)

FMPES(1) = Mass flow of Material fed to the bed (kg/s)

FMCAG = Mass flow of gas (combustion agent) blown through the distributor into the bed (this flow does not include steam if used as agent for gasification) (kg/s)

WCAG(1 to 13) = Array that specifies the composition (mass fractions) of the gas (combustion agent) blown through the distributor (the indexes 1 to 13 are referred to: 1=CO_2, 2=CO, 3=O_2, 4=N_2, 5=H_2O, 6=H_2, 7=CH_4, 8=SO_2, 9=NO, 10=C_2H_6, 11=H_2S, 12=NH_3, 13=Tar) (for instance, in the case of dry air WCAG(3)=0.233 and

WCAG(4)=0.767 the others are nil)

FMSFG = Mass flow of steam if added to the combustion agent through the distributor (kg/s) (this steam flow must not be confused with the steam that eventually could be used in the boiler system and flows inside the tubes)

TPES(1) = Temperature of the material entering the bed (K)

TECAG = Temperature of the combustion agent blown into the bed (K)

TESFG = Temperature of the steam blown through the distributor (K)

POPER = Bed operation absolute pressure (average pressure in the bed) (Pa)

PECAG = Absolute pressure of the combustion agent before the distributor system (Pa)

PESFG = Absolute pressure of the steam for gasification before the distributor (Pa)

TPES(2) = Temperature of the limestone entering the bed (K)

TPES(3) = Temperature of the inert entering the bed (K)

DATA RELATING TO THE EQUIPMENT GEOMETRY:

DD = Internal diameter (or equivalent hydraulic diameter) of the bed section (m)

ZD = Dynamic height of the bed (taken from the base of the bed) (m)

DF = Internal diameter (or equivalent hydraulic diameter)

of the freeboard section (m)

ZF = Height of the top of the freeboard (from the base of the bed) (m)

ZBTUD = Height of the bottom of the tube bundle in the bed (taken from the base of the bed and in the centre line) (m)

ZTTUD = Height of the top of the tube bundle in the bed (taken from the base of the bed and in the centre line) (m)

ZBTUF = Height of the bottom of the tube bundle in the freeboard (Taken from the base of the bed and in the centre line) (m)

ZTTUF = Height of the top of the tube bundle in the freeboard (taken from the base of the bed and in the centre line) (m)

ZFEEDS(M) = height of the feeding point of each solid (taken from the base of the bed) (array: 1=Material; 2=Limestone; 3=Inert) (m)

DATA CONCERNING THE INSULATION OF THE SYSTEM:

XISD = Thickness of the insulation wall in the bed section (m)

AKISD = Average thermal conductivity of the insulation wall in the bed section (W m^{-1} K^{-1})

EPSD = Average emissivity of the external surface of the insulation wall in the bed section (dimensionless)

XISF = Thickness of the insulation wall in the freeboard section (m)

AKISF = Average thermal conductivity of the insulation wall in the freeboard section (W m^{-1} K^{-1})

EPSF = Average emissivity of the external surface of the

insulation wall in the freeboard section (dimensionless)

TAMB = External ambient temperature (K)

VV = Average velocity of the wind (m/s) (if unknown, the program assumes 2m/s)

DATA CONCERNING THE HEAT TRANSFER TO TUBES IN THE SYSTEM:

TULD = Length of each tube immersed in the bed (m) (if a continuous tube, as for instance in a serpentine, TULD can be informed either as the length of one entire serpentine or the length of one pass but all in accordance with NTUD below)

NTUD = Number of tubes in the bed (if serpentine and TULD was given as the length of one serpentine therefore NTUD is the number of serpentine but if TULD was given as the length of one pass NTUD will be the number of serpentine times the number of passes of each serpentine)

DITUD = Internal diameter of the tubes in the bed (m)

DOTUD = External diameter of the tubes in the bed (m)

AGTUD = Inclination (relative to the horizontal position) of the tubes inside the bed (degrees)

EMTUD = Average emissivity of the tubes in the bed (if unknown, the program assumes as 0.9) (dimensionless)

TULF = Length of each tube in the freeboard (m) (see observation in TULD)

NTUF = Number of tubes in the freeboard (see observation in NUTD)

DITUF = Internal diameter of the tubes in the freeboard (m)

DOTUF = External diameter of the tubes in the freeboard (m)

AGTUF = Inclination (relative to the horizontal position) of the tubes in the freeboard (degrees)

PITU = Absolute pressure of the boiler or cooling system (pressure inside the tubes of the steam generation or inside the refrigeration system) (Pa)

EMSD = Average emissivity of the bed (if unknown, the program assumes 0.9)

IREF = Index that indicates whether the tubes in the system work as cooling coil (forced flow) (IREF=1) or as standard boiler (natural recirculation) (IREF=0)

FMHETU = Total water mass flow entering the tubes in the system (must be informed if IREF=1; if IREF=0 this parameter could be set as zero) (kg/s)

THETUD = Temperature of the water entering the tubes in the bed (if IREF=0, the program assumes THETUD as the saturation temperature at the pressure PITU)

IATUD = Index that indicates the tube arrangement in the bed compartment (if in-line: IATUD=0 OR 1; if staggered: IATUD=2)

PITCHD = Horizontal pitch of tube bank in the bed compartment (m)

NSERPD = Number of serpentine in the bed (if zero, the program assumes NSERPD=NTUD)

IATUF = Index that indicates the tube arrangement in the freeboard compartment (if in-line: IATUF=0 OR 1; if staggered: IATUF=2)

PITCHF = Horizontal pitch of the tube bank in the freeboard compartment (m)

NSERPF = Number of serpentine in the freeboard (if zero, the program assumes NSERPF=NTUF)

AHTBED = Total heat transfer area to tubes or cooling jacket wall in the bed section. Can be set as zero if there is only tubes in this section and the details of the tube bank were given.

AHTFRB = Total heat transfer area to tubes or cooling jacket wall in the freeboard section. Can be set as zero if there is only tubes in this section and the details of the tube bank were given.

DATA CONCERNING THE DISTRIBUTOR CHARACTERISTICS:

XISDI= Thickness of the distributor base (plate + insulation)(m)

AKISDI= Average thermal conductivity of the distributor base (W m^{-1} K^{-1})

DOD = Diameter of the distributor holes (m) (if DOD=0.0 and NOD not zero the program assumes DOD=0.003 m; if DOD=0.0 and NOD=0 the program assumes the distributor as a porous plate)

NOD = Number of orifices in the distributor (see observation in DOD)

DATA CONCERNING THE RECYCLING OF PARTICLES TO THE BED:

IRCY = Index that indicates whether (IRCY=1) or not (IRCY=0) there is a recycling of particles from the top of the freeboard to the bed

NCY = number of cyclones used to separate particles for the recycling (if unknown, must be set as zero and the program

will assume an inlet gas velocity into any cyclone as 3 m/s, which is a typical value for commercial systems)

DCY = Diameter of the cyclone used on the recycling system (m) (if IRCY=1 and DCY=0.0 the program will perform calculations based on the common data for commercial cyclone systems)

TPRCY = Temperature of the recycled solid flow to the bed (K) (if IRCY=1 and TPRCY=0.0 the program assumes TPRCY=424 K)

PARTICLE SIZE DISTRIBUTIONS OF THE SOLIDS FED TO THE BED:

CARBONACEOUS SOLID (described by two arrays of data: the first with the increasing value of the average diameter (m) at each range of particle size and the second with the respective mass fraction of that range of particle size)

LIMESTONE (described in the same way as explained above)

INERT (described in the same way as explained above)

4.3. Results generated by the program

The following lists the data generated by the simulation:

a) Concentration profiles in the emulsion and bubble gas phases for the following gases throughout the bed height: CO_2, CO, O_2, N_2, H_2O, H_2, CH_4, SO_2, NO, C_2H_6, H_2S, NH_3, Tar. An average concentration between the emulsion and the bubble gases throughout the bed height is also provided.

b) Concentration profiles throughout the

freeboard height for the mentioned gases.

c) Temperature profiles for the following phases throughout the bed and the freeboard height:

1) Gas in the emulsion phase (in the bed region);

2) Gas in the bubble phase (in the bed region);

3) Carbonaceous solid material (for the entire system);

4) Limestone (if any, for the entire system);

5) Inert (if any, for the entire system)

d) Average compositions for each individual solid phase (already mentioned) in the bed section. Composition profiles are provided in the freeboard section.

e) Particle size distributions for each individual solid phase in the bed and throughout the freeboard height. Overall particle size distribution is also provided in the bed and freeboard.

f) Elutriation flow for each particle size and specie.

g) Entrainment flow throughout the freeboard height and total carryover for each particle size and specie.

h) Parameters that allow the analysis of the equipment performance:

1) Total carbon conversion;

2) Mass and molar fractions of gases entering and leaving the freeboard;

3) Mass and molar flow rates of gases entering and leaving the freeboard;

4) Total flow and composition of the solids leaving the

bed;

5) Minimum fluidization velocity at the bottom and at various points of the bed;

6) Gas superficial velocity at the bottom and at various points of the bed;

7) Total mass in the bed;

8) Average residence time for the particles in the bed;

9) Transport disengaging height;

10) Calcium to sulphur molar ratio (if limestone is added) in the bed;

11) Oxygen excess.

12) Total heat transfered between the reactor and the external ambience;

13) Temperature of the external wall at any point of the bed section and the freeboard section;

14) Heat transfer coefficient between the external surface of the reactor and the ambience at any point of that surface.

i) If working as a boiler the following parameters are presented:

1) Total heat transfered between bed and tubes immersed in it;

2) Total heat transfered between freeboard and tubes in this section;

3) Overall heat transfer coefficient between tubes and bed;

4) Overall heat transfer coefficient between tubes and freeboard;

5) Steam (or hot water) flow rate produced by the boiler

and all the its physical conditions (quality or fraction of condensed water, temperature and pressure);

6) Tubes wall temperature in the bed and in the freeboard;

7) Boiler efficiency.

j) If simulating a gasifier the following information is, also, printed ("Cold" condition refers to the produced gas at 298K, atmospheric pressure, clean and dry while "Hot" condition refers to the gas as produced or as leaving the freeboard condition):

1) "Cold" and "hot" combustion enthalpy (heat value) of the produced gas;

2) "Cold" and "hot" rate of energy output (heat value x mass flow) of the gasifier;

3) "Cold" and "hot" efficiency of the gasifier.

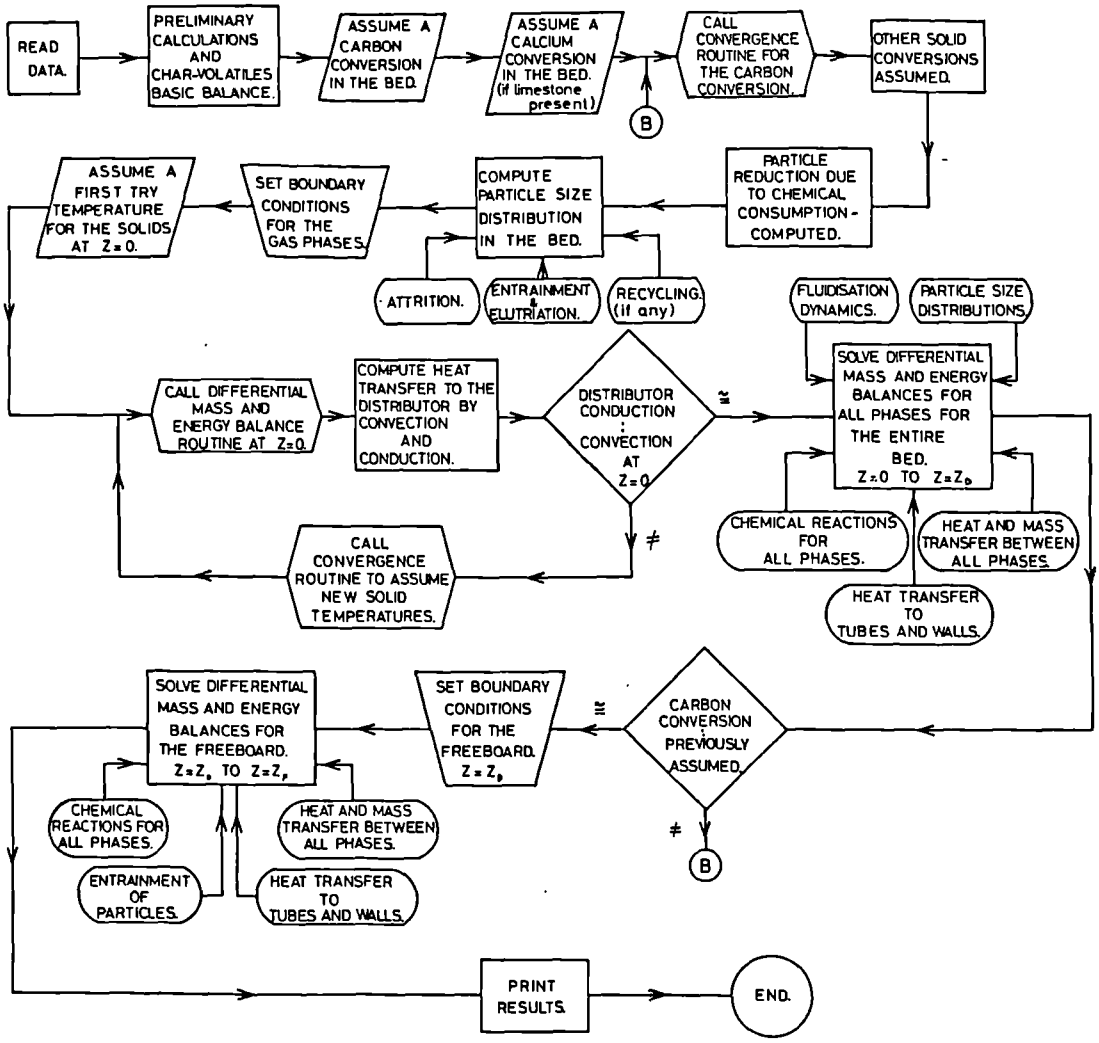

FIGURE 4.1. BASIC LOGIC DIAGRAM OF THE SIMULATION PROGRAM.

CHAPTER V

5. OPERATIONAL DATA AND COMPARISON AGAINST SIMULATION.

In this chapter data concerning the operation of some pilot and industrial scale boilers and gasifiers are presented in parallel with the data generated by the present simulation program.

It must be stressed that the task of obtaining operational data is a difficult one due to several reasons, such as:

a) Confidentiality. Due to the current state of development, most of the pilot and industrial units are under some sort of commercial contract which does not allow any kind of free publication of such data;

b) Unreliability. Several experimental data reveal flaws when analysed thoroughly and are mainly due to careless measurements or even mistakes and misinterpretations of the operation;

c) Inaccuracy. Data must state the conditions in which they have been measured and there a frequent lack of such information;

d) Incomplete information. Even published reports do not mention several fundamental facts which are required to fulfil the data to run the simulation program.

In spite of these problems, some data were collected to use as references for comparisons between real operation and simulation results. They are believed to be enough to validate the present mathematical model. These

data are from:

a) Babcock & Wilcox Co.(USA), Fluidized Bed Unit (Babcock and Wilcox, 1978);

b) National Coal Board (UK), Fluidized Combustion Test Rig.

For the case of gasifier no reliable data have been found in the literature. Some details about the fluidized bed gasification unit installed in the "Agrupamento de Engenharia Têrmica" of IPT (Instituto de Pesquisas Tecnológicas do Estado de São Paulo, Brazil) are given.

5.1.Combustors

In this section the data obtained for some Fluidized Bed Combustors are presented along with the results obtained by simulation using the present model.

5.1.1.Babcock and Wilcox Unit, USA

A series of monitored tests were carried out by Babcock and Wilcox on a 0.9x0.9 m^2 fluidized bed unit over several years. The final report of such tests (Babcock and Wilcox, 1978) describes the experiments and this information has been one of the more important sources used to verify the present simulation.

A great number of tests were described, but for only one (Test 26) was the complete mass balance compiled and only this one therefore is of great value for the present comparison between the real operation and the present simulation. This same test was used by Overturf and

Reklaitis (1983b) for their comparisons.

5.1.1.1. Plant description

As the details of this unit are fully described in the report, it has been decided only to stress some more important features of the unit.

A schematic view of the unit is shown in the Fig.5.1.

- Combustor:

Basically it consists of a vertical furnace with an insulation wall of 114mm of Babcock and Wilcox 80 firebrick and an atmospheric water jacket that surrounds the entire enclosure. During the simulation tests, it had been assumed that the main resistance to the heat transfer from the interior to the external ambience is represented by the insulation wall.

Below the combustor there is a wind box made of 6.4mm carbon steel plate and protected with a refractory lining.

- Air distribution system:

It is made of 38mm carbon steel plate. Air flows through 188 (25mm diameter) stainless steel pipes, which are 3m long. Each pipe contains eight 4mm radial holes. The base is protected by a total of 280mm of a refractory layer.

- Coal and Limestone feed system:

Crushed coal and limestone are transfered from feeder belts into a rotatory seal valve. The valve is of the high pressure air-swept design and operates at 22 to 33

rpm. The coal-limestone mixture is conveyed to the furnace by a stream of transport air. The transport line is 45.7m long and is made of 51mm (2" schedule 40 standard) pipe which terminates inside the furnace below the tube bank.

- Cooling system:

The unit is not a boiler and the cooling system works to control the temperature in the bed. It consists of six serpentine of 38mm (1-1/2" schedule 40) pipes and each pipe makes 10 passes through the furnace. The tubes are on a staggered 114mm square pitch and cooled by recirculating sub-cooled water at 11.73 bar approximately. The water flow is maintained at a minimum of 11.4 m^3/h to ensure that no boiling occurs and enters the tube bank normally at 100°C and exits between 127 and 138°C.

5.1.1.2.Plant operational data

The tables below show the data obtained for the operation conditions in three tests and used to run the the simulation program.

The symbols and the units used in the data tables are described in section (4.2).

Data	Value	Data	Value
AMTPES(1)	5.0	TPES(1)	290
VOLAT	40.0	TECAG	305
CARFIX	50.1	POPER	101.3×10^3
ASHES	9.9	PECAG	102.1×10^3
ENTCBC	30.84×10^6	TPES(2)	290
MTKIND	2	DD	1.118
WPDB(14)	0.7320	ZD	0.700
WPDB(15)	0.0510	DF	1.118
WPDB(16)	0.0790	ZF	3.442
WPDB(17)	0.0090	ZBTUD	0.330
WPDB(18)	0.0300	ZTTUD	0.700
WPDB(19)	0.0990	ZBTUF	0.701
ROGCES	700 (*)	ZTTUF	3.442(c)
ROPES(1)	1400 (*)	ZFEEDS(1)	0.305
RORES(1)	2100 (*)	ZFEEDS(2)	0.305
MODLR	0	XISD	0.114
FISP(1)	0.7 (*)	AKISD	0.22
AMTPES(2)	0.400	EPSD	0.9 (*)
WPDB(22)	0.9385	XISF	0.114
WPDB(24)	0.0615 (+)	AKISF	0.22
FMPES(2)	0.01215	EPSF	0.9 (*)
ROPES(2)	2300 (*)	TULD	0.991
RORES(2)	3000 (*)	NTUD	30
FISP(2)	0.7 (*)	DITUD	0.0409
FMPES(1)	0.0585	DOTUD	0.483
FMCAG	0.6952	AGTUD	0.0
WCAG(3)	0.22785	EMTUD	0.60 (*)
WCAG(4)	0.75428	TULF	0.991
WCAG(5)	0.01210	NTUF	49(c)
WCAG(7)	0.00432	DITUF	0.0409
WCAG(10)	0.00154	DOTUF	0.0483
AGTUF	0.0	PITU	1273×10^3
EMSD	0.60 (*)	IREF	1
FMHETU	7.0	THETUD	373
IATUD	2	PITCHD	0.114
NSERPD	6(b)	IATUF	2
PITCHF	0.114	NSERPF	6(b)
XISDI	0.279	AKISDI	0.22
DOD	0.004	NOD	1504

TABLE 5.1.Real operation data fed to simulate the Babcock and Wilcox unit, test No.26. (*)=most probable value due to the lack of information;(a)=assumed to allow an approximate average velocity of 1m/s in each tube);(b)=the tube bank was partially immersed in the bed, therefore the 6 serpentine belonged to same system;(c)=the effect of heat transfer to the water jacket in the freeboard was simulated by summing 19 tubes(equivalent area) to the existing 30 tubes in the freeboard;(+)=inert in the limestone assumed here as $CaSO_4$.

Carbonaceous		Limestone	
Diameter (μm)(*)	Mass percen.	Diameter (μm)(*)	Mass percen.
59	6.40	112	4.45
107	2.85	223	1.05
219	4.95	444	7.35
444	8.80	890	43.00
890	20.40	1845	43.15
1175	36.55	2900	1.00
2845	9.85		
4825	10.20		

TABLE 5.2.Particle size distribution of solids fed during the operation of the Babcock and Wilcox unit, test No.26.(*)=average inside the slice to which the respective mass fraction is indicated.

5.1.1.3.Test results and comparisons

The simulation program was put to process the above data and the results were generated after a few iterations for the bed section and the solution for the freeboard section. The complete computation used approximately 1000 seconds of central unit computer time on a IBM 3083 machine.

A complete report is printed and the more important results are reproduced in the tables below that contain, also, the real operation data whenever possible. A series of graphs to illustrate the results were plotted and are included at the end of the present chapter.

Component	% molar, dry basis	
	Real operation	Simulation
CO_2	13.8	13.00962
CO	0 to 0.9	0.00002
O_2	3.9	3.83248
N_2	81.2	83.07219
NO	0.03	0.03823
SO_2	0.08	0.04737
H_2	-	0.00009
CH_4	-	8.5×10^{-15}
C_2H_6	-	$<1.0 \times 10^{-50}$
H_2S	0 to 2.4×10^{-4}	5.8×10^{-7}
NH_3	-	2.2×10^{-12}
Tar	-	$<1.0 \times 10^{-50}$

TABLE 5.3. Composition of the gas leaving the freeboard (stack gas) during the operation of the Babcock and Wilcox unit, test No.26. (-)=not determined.

Condition	Temperatures (K)	
	Real operation	Simulation
Gas entering the bed	305	305.00
Gas leaving the bed	987	1093.4
Gas leaving the freeboard	923	960.2
Carbonaceous particles(*)	-	1166.0
Limestone particles(*)	-	1168.1
Inert particles(*)	-	1163.7
Emulsion gas(*)	-	1167.2
Bubble gas(*)	-	799.0
Average at the distributor	1097	1008.5
Average at the middle of the bed	1108	1145.1
Average at the top of the bed	987	1101.0
Average at the top of the freeb.	923	959.6

TABLE 5.4.Various temperatures achieved in the process during the operation of the Babcock and Wilcox unit, test No.26. (*)= at the middle of the bed;
(-)= not measured.

Component	Mass percentage (wet basis)		
	Fed	Average in the bed	Top of freeboard
C	40.260	10.932	14.806
H	2.805	0.76165	1.0315
O	4.345	1.1798	1.5979
N	0.495	0.13441	0.18204
S	1.650	0.44803	0.60679
Ash	5.445	86.544	81.776
Volat.	40.000	0.0000	0.0000
Moist.	5.000	0.0000	0.0000

TABLE 5.5.Carbonaceous solid compositions during the operation of the Babcock and Wilcox unit, test No.26 (simulation results).

Component	Mass percentages (w.b.)			
	Feed	Average in the bed		Top of freeboard
		Exp.	Simul.	Simul.
$CaCO_3$	93.475	1.00	0.0000	0.0000
CaO	0.000	51.44	50.625	50.229
$CaSO_4$	6.125	47.56	49.375	49.771
Moist.	0.40	nil	0.0000	0.0000

TABLE 5.6.Limestone solid compositions during the operation of the Babcock and Wilcox unit, test No.26.

Component	Average in the bed (mass,%)	
	Exper.	Simul.
C (*)	0.21	0.110
$CaCO_3$	0.91	0.000
CaO	46.34	50.529
$CaSO_4$	42.84	49.281
Moist.	0.00	0.0000
Inert	9.70(+)	0.080

TABLE 5.7.Total solid composition in the bed during the operation of the Babcock and Wilcox unit, test No.26. (*)=includes all components in the carbonaceous solid.

Diameter µm (*)	Mass percentages	
	Bed average	Top of freeboard
15	3.111	8.016
28	1.027	3.537
56	1.274	6.121
114	2.386	10.88
229	8.089	25.38
303	20.52	46.03
732	31.28	0.016
1243	32.31	0.016

TABLE 5.8.Particle size distribution of the carbonaceous solids during the operation of the Babcock and Wilcox unit, test No.26 (results by simulation). (*)=average inside the slice to which the respective mass fraction is indicated and the extremes are taken as the minimum and maximum reported values.

Diameter μm (*)	Mass percentages	
	Bed average	Top of freeboard
112	0.009	20.08
223	0.050	51.34
444	7.777	2.225
890	45.50	13.01
1845	45.61	13.05
2900	1.056	0.302

TABLE 5.9.Particle size distribution of the limestone during the operation of the Babcock and Wilcox unit, test No.26 (results by simulation). (*)=average inside the slice to which the respective mass fraction is indicated and the extremes are taken as the minimum and maximum reported values.

Diameter(*) μm	Mass percentage			
	Mixture in the bed		Mixture at the top of freeboard(**)	
	Exper.	Simul.	Exper.	Simul.
59(44-74)	0.0	0.086	10.30	46.152
111(74-149)	0.0	0.012	42.05	9.557
223(149-297)	0.0	0.059	13.75	23.894
443(297-590)	17.40	7.785	26.65	11.017
890(590-1190)	47.70	45.446	5.60	4.631
1775(1190-2360)	32.90	45.558	1.65	4.643
2860(2360-3360)	1.45	1.054	0.0	0.108
4855(3360-6350)	0.45	0.000	0.0	0.000

TABLE 5.10.Particle size distribution of the solids during the operation of the Babcock and Wilcox unit, test No.26.(*)=average inside the indicated slice and the extremes are taken as the minimum and maximum reported values; (**)=collected in the ash hopper after the freeboard exit.

Solid	Flow (g/s)	
	Operation	Simulation
Carbonaceous	4.46	2.9985
Limestone	3.46	4.8000
Free-ash	4.78	5.6997
Carbonaceous plus free-ash	9.25	8.6983
Total	12.70	13.498

TABLE 5.11.Entrainment flows of particles at the top of the freeboard during the test of the Babcock and Wilcox unit, test No.26.

Solid	Diameters (μm)				
	Fed	Bed		Top of freeboard	
		Exp.	Sim.	Exp.	Sim.
Carbonaceous	422	-	247	-	89
Limestone	752	-	1061	-	229
Free-ash	*	-	15	-	15
Total aver.	456	893	1002	143	314

TABLE 5.12.Average diameters of particles at various positions during the operation of the Babcock and Wilcox unit, test No.26. Results obtained by simulation. (-)=not determined;(*)=not relevant.

Process parameter	Real operation	Simulation
Mass flow of flue gas (kg/s)	0.790	0.7525
Total flow solids leaving the bed (kg/s)(includes entrainment at the top of the bed)	-	79.772
Minimum fluidization voidage at the middle of the bed	-	0.520
Overall voidage at the middle of the bed	-	0.8080
Minimum fluidization velocity at the middle of the bed (m/s)	-	0.635
Superficial velocity at the middle of the bed (m/s)	2.5(a)	2.691
Bed transversal area (m^2)	0.9817	0.9817
Carbon conversion (fraction of the fed carbon) (%)	95.8	98.158
Mass of the bed (kg)	-	444.8
TDH = Transport Disengaging Height (from the bed surface) (m)	-	4.049
Freeboard space (m)	2.742	2.742

CONT...

CONT...

Process parameter	Real operation	Simulation
Ca/S = Calcium to Sulphur ratio in the bed	2.2	2.287
Calcium conversion (%)	28.09	28.9864
Sulfur retention (%) (based on the fed sulphur)	58.7	57.449
Static bed depth (m)	-	0.411
Rate of energy input to the system(kW)	1713.9	1713.9
Percentage of the energy input lost to the external environment through the walls	-	1.048
Pressure loss across the distributor (Pa)	-	412
Pressure loss across the bed (Pa)	-	3029

TABLE 5.13.Various process parameters for the operation of the Babcock and Wilcox unit, test No.26. (-)= not determined; (a)=probably calculated at the bed base; (+)= includes H,O,S and N in the carbonaceous solid.

Parameter	Real operation	Simulation
Total heat transfer to the tubes in the system (kW)	788.4(*)	655.11
Heat transfer to tubes inside the bed (kW)	-	397.31
Heat transfer to tubes in the freeboard (kW)	-	257.80
Total mass flow of steam generated by the system (kg/s)	0.0	0.0
Total heat loss to the external ambience (kW)	113.1(a)	17.97(b)

CONT...

CONT...

Process parameter	Real operation	Simulation
Heat loss in the bed section (kW)	-	4.25
Heat loss in the freeboard section (kW)	-	13.72
Overall heat transfer coefficient between tubes and bed at the middle of the bundle($W\ m^{-2}\ K^{-1}$)	-	69.28
Overall heat transfer coefficient between tubes and freeboard at the middle of the bundle ($W\ m^{-2}\ K^{-1}$)	-	5.35
Wall temperature of tubes in the bed (middle of the bundle)(K)	-	702.5
Wall temperature of tubes in the freeboard(middle of the bundle)(K)	-	455.3
Percentage of heat loss to the ambience in relation to the heat transfer to the tubes	-	2.699
Temperature of the water leaving the tubes (K)	400	395.3
Temperature of the external wall at the top of the bed section (K)	-	356.7
Temperature of the external wall at the top of the freeboard section(K)	-	347.2
Heat transfer coefficient between external wall and ambience(top of the bed section)($W\ m^{-2}\ K^{-1}$)	-	21.56
Heat transfer coefficient between external wall and ambience(top of the freeboard)($W\ m^{-2}\ K^{-1}$)	-	20.68

TABLE 5.14.Some parameters related to heat transfer during the operation of the Babcock and Wilcox unit, test No.26. (-)=not determined; (*)=the Babcock and Wilcox report gives only the total value for the heat transfer to tubes which includes the tubes in the stack gas cooling system; (a)=losses to the water jacket; (b)=losses to the external ambience.

5.1.1.4.Parameter profiles and other graphs

Below a series of graphs are presented. They describe several important features of the operation of the Babcock and Wilcox unit as, for example,

- Various temperature profiles in the bed and freeboard;
- Various concentration profiles in the bed (emulsion and bubbles) and in the freeboard;
- Particle distributions of various solid materials in several different situations;
- Gas and solid flows in the freeboard;
- Bubble diameter and superficial velocities in the bed.

The discussion of these results are presented in the following chapter.

5.1.2.National Coal Board Test Rig

Operational data presented here have been made kindly available due to the cooperation of the National Coal Board, Coal Research Establishment (U.K.)

5.1.2.1.Plant description

- Combustor:

The combustor consisted of a mild steel shell lined with 0.1m insulating blocks over which a 0.08m lining of hard face refractory had been cast. The internal dimensions of the combustor were 0.3m square by 2.4m high. The test rig is shown schematically in Figure 5.17.

- Coal and limestone feeds:

Coal, nominally less than 3.2mm in size, was pneumatically fed into the combustor from a pressurized hopper system. Limestone, again nominally less than 3.2mm in size, was

also fed pneumatically into the combustor from a separate hopper system. Both the coal and limestone feeds were individually monitored and entered the combustor through a common feed probe. The exit of this probe was positioned at the centre of the combustor, 0.1m above the holes of the air distributor.

- Air distributor:

The air distributor consisted of nine vertical tubes spaced on a 0.11m square pitch. Each tube, which had six 3mm holes drilled below its closed end, was connected to a manifold which supplied the fluidising air.

- Cooling System:

Within the fluidised bed, there were four rows of 50mm O.D. tubes on a 0.15m triangular pitch. Heat generated by the combustion of the coal was removed by these tubes, which could be cooled in two ways. During this test programme, eight tubes were air cooled and two tubes were water cooled (unfortunately, no data were presented on the heat balances).

5.1.2.2.Plant operational data

The tables below show the data obtained for the operation conditions in three tests and fed to run the simulation program. The tests No.3, No.5 and No.6 were chosen due to the greater differences in the operational conditions among them. Recycling of particles were used in all tests except No.6.

The symbols used in the data tables is described in section (4.2).

Data	Test No.3	Test No.5	Test No.6
AMTPES(1)	6.2	5.9	6.1
VOLAT	31.3	32.2	32.0
CARFIX	47.5	46.0	46.0
ASHES	15.0	15.9	15.9
ENTCBC	26.67×10^{6}	26.67×10^{6}(*)	26.67×10^{6}(*)
MTKIND	1	1	1
WPDB(14)	0.637	0.657	0.682
WPDB(15)	0.041	0.043	0.044
WPDB(16)	0.101	0.095	0.094
WPDB(17)	0.015	0.0165(*)	0.0165
WPDB(18)	0.0435	0.044	0.038
WPDB(19)	0.1625	0.1445	0.1255
ROGCES	700(*)	same	same
ROPES(1)	1400(*)	same	same
RORES(1)	2100(*)	same	same
MODLR	0	0	0
FISP(1)	0.7(*)	same	same
AMTPES(2)	0.0	4.0	0.0
WPDB(22)	1.0	same	same
WPDB(23)	0.0	same	same
WPDB(24)	0.0	same	same
FMPES(2)	1.750×10^{-3}	2.250×10^{-3}	3.000×10^{-3}
ROPES(2)	2300(*)	same	same
RORES(2)	3000(*)	same	same
FISP(2)	0.7(*)	same	same
FMPES(1)	5.000×10^{-3}	6.556×10^{-3}	6.417×10^{-3}
FMCAG	44.780×10^{-3}	66.778×10^{-3}	63.111×10^{-3}
WCAG(3)	0.2329	same	same
WCAG(4)	0.7669	same	same
WCAG(5)	0.0002(*)	same	same

TABLE 5.15.First part of the real operation data fed to simulate the NCB test rig. (*)=not determined, assumed most probable value.

Data	Test No.3	Test No.5	Test No.6
TPES(1)	288	288	288
TECAG	283	284	290
POPER	109.5×10^3	113.4×10^3(*)	117.5×10^3(*)
PECAG	122.0×10^3	132.3×10^3	130.3×10^3
TPES(2)	288	288	288
DD	0.339	same	same
ZD	0.500	0.700	0.600
DF	0.339	same	same
ZF	2.400	same	same
ZBTUD	0.100	same	same
ZTTUD	0.450	same	same
ZFEEDS(1)	0.100	same	same
ZFEEDS(2)	0.100	same	same
XISD	0.100	same	same
AKISD	0.30	same	same
EPSD	0.9(*)	same	same
XISF	0.100	same	same
AKISF	0.30	same	same
EPSF	0.9(*)	same	same
TAMB	288(*)	same	same
VV	2.0(*)	same	same
TULD	0.300	same	same
NTUD	10	same	same
DITUD	0.0410	same	same
DOTUD	0.0500	same	same
AGTUD	0.0	same	same
EMTUD	0.57(*)	same	same
PITU	120×10^3(*)	same	same
EMSD	0.8(*)	same	same
IREF	1	same	same
FMHETU	2.64(a)	same	same
THETUD	288(*)	same	same
IATUD	2	same	same
PITCHD	0.150	same	same
NSERPD	2	same	same

TABLE 5.16.Second part of the real operation data fed to the simulate the NCB test rig. (*)=most probable value due to the lack of information; (a)=water flow rate of two tubes assumed distributed among the ten tubes (see description of the cooling system)(velocity in the water tubes=1m/s).

Data	Test No.3	Test No.5	Test No.6
XISDI	0.100(*)	same	same
AKISDI	0.30(*)	same	same
DOD	0.003	same	same
NOD	54	same	same
IRCY	1	1	0
NCY	1	1	0
DCY	0.300	0.300	-
TPRCY	709	944	-

TABLE 5.17.Third part of the real operation data fed to the simulate the NCB test rig. (*)=most probable value due to the lack of information.

Diameter μm (*)	Mass percentage					
	Test number					
	3		5		6	
	Coal	Lime-stone	Coal	Lime-stone	Coal	Limes-stone
45(-45) 54	6.5	0.06	2.3	0.2	3.6	0.10
(45-63) 69	1.2	0.06	7.8	0.15	1.7	0.05
(63-75) 100	1.4	0.06	2.0	0.15	1.0	0.05
(75-125) 188	4.8	0.07	9.9	0.1	3.8	0.10
(125-250) 375	11.3	0.07	10.0	0.1	11.8	0.10
(250-500) 1100	34.4	0.07	34.3	0.3	48.6	0.2
(500-1700) 2440	36.2	0.07	30.6	11.4	28.3	7.9
(1700-3180) 3180	3.9	91.7	2.8	86.8	1.0	90.6
(+3180)	0.3	0.2	0.3	0.8	0.2	0.9

TABLE 5.18.Particle size distributions of the solids fed during the operations of the NCB test rig. (*)=average inside the indicated slice and the extremes are taken as the minimum and maximum reported values.

5.1.2.3. Test results and comparisons

As in the the previous case of Babcock and Wilcox, the results are presented in the tables below. Plotted graphs are included at the end of the present chapter.

Compon.	Molar percentage (dry basis)					
	Test No.3		Test No.5		Test No.6	
	Exper.	Simul.	Exper.	Simul.	Exper.	Simul.
CO_2	16.6	14.43330	14.6	12.57132	15.4	14.12303
CO^2	nil	0.00124	nil	0.00461	nil	0.00009
O_2	2.3-2.7	3.96583	4.6-5.0	6.09769	4.3-5.1	4.57106
N_2	-	81.35509	-	81.06452	-	81.21124
H_2	-	0.00023	-	0.00032	-	0.00011
CH_4	nil	1.2×10^{-13}	nil	4.2×10^{-13}	nil	1.9×10^{-14}
SO_2	0.0477(*)	0.24324	0.0305(*)	0.26033	0.0408(*)	0.07837
NO^2	-	0.00107	-	0.00120	-	0.01610
C_2H_6	-	$<10^{-50}$	-	$<10^{-50}$	-	$<10^{-50}$
H_2S	-	2.9×10^{-7}	-	1.3×10^{-6}	-	6.7×10^{-7}
NH_3	0.0001	1.5×10^{-10}	0.0002	5.0×10^{-9}	0.0010	1.3×10^{-11}
Tar	-	$<10^{-50}$	-	$<10^{-50}$	-	$<10^{-50}$

TABLE 5.19.Compositions of the gas leaving the freeboard (stack gas) during the operations of the NCB test rig (% molar or volume d.b.). (-)=not determined;(*)=average between different methods of analysis.

Point or condition	Temperatures (K)					
	Test No.3		Test No.5		Test No.6	
	Real oper.	Sim.	Real oper.	Sim.	Real oper.	Sim.
Gas entering the bed	283	283	284	284	290	290
Gas leaving the bed	-	976	-	770	1120	1063
Gas leaving freeb.	-	1066		984		1002
Emulsion gas(*)	-	982		930		1051
Bubble gas(*)	-	700		610		926
Carbonaceous part.(*)	-	991		934		1052
Limest. part.(*)	-	942		910		1051
Inert part.(*)	-	987		932		1051
Average z=0.1m	1115	972	1119	926	1118	1039
Average z=0.3m	1125	971	1122	924	1122	1045
Average z=0.6m	1123	1041	1123	925	1120	1057
Average z=1.1m	1138	1083	1109	970	1130	1049
Average z=1.5m	1160	1087	1153	985	1144	1035

TABLE 5.20.Various temperatures achieved during the operations of the NCB test rig. (*)=at the middle of the bed; (-)= not measured.

Component	Mass percentages (wet basis)								
	Test No.3			Test No.5			Test No.6		
	Feed	Bed	Top freeb.	Feed	Bed	Top freeb.	Feed	Bed	Top freeb.
C	39.81	24.59	5.89	40.67	31.15	11.40	42.22	9.58	10.96
H	2.56	1.58	0.37	2.66	2.04	0.75	2.72	0.62	0.71
O	6.31	3.90	0.93	5.88	4.50	1.65	5.82	1.32	1.51
N	0.94	0.58	0.14	1.02	0.78	0.29	1.02	0.23	0.27
S	2.72	1.68	0.40	2.72	2.09	0.76	2.35	0.53	0.61
Ash	10.16	67.66	92.26	8.95	59.44	85.15	7.77	87.71	85.95
Volat.	31.300	0.00	0.00	32.20	0.00	0.00	32.00	0.00	0.00
Moist.	6.200	0.00	0.00	5.900	0.00	0.00	6.100	0.00	0.00

TABLE 5.21. Carbonaceous solid compositions during the operations of NCB test rig. Results by simulation (no experimental value is reported for independent solid species).

Component	Mass percentages (wet basis)								
	Test No.3			Test No.5			Test No.6		
	Feed	Bed	Top freeb.	Feed	Bed	Top freeb.	Feed	Bed	Top freeb.
$CaCO_3$	100.0	0.00	0.00	95.33	0.00	0.00	99.60	0.00	0.00
CaO	0.0	80.79	80.73	0.0	89.66	89.57	0.0	71.26	71.25
$CaSO_4$	0.0	19.21	19.27	0.67	10.34	10.43	0.04	28.74	28.75
Moist.	0.0	0.000	0.000	4.0	0.000	0.00	0.0	0.000	0.000

TABLE 5.22.Limestone solid compositions during the operations of the NCB test rig. Results by simulation (no experimental values have been reported for independent species).

Diameter µm (*)	Mass percentage			
	Mixture in the bed		Top of freeboard(**)	
	Exper.	Simul.	Exper.	Simul.
16(-16)	-	0.00	3.5	0.0
24(16-32)	-	3.84	6.2	29.22
54(32-75)	0.2	0.51	9.7	4.54
100(75-125)	0.1	3.61	16.5	28.63
188(125-250)	1.1	11.09	35.3	37.13
375(250-500)	12.2	11.64	24.9	0.07
1100(500-1700)	44.9	6.73	3.9	0.04
2440(1700-3180)	41.4	62.45	-	0.37
3180(+3180)	0.1	0.13	-	0.00

TABLE 5.23.Particle size distributions of the solids during the operation with the NCB test rig, test No.3. (*)= average inside the indicated slice and the extremes are taken as the minimum and maximum reported values; (**)=or loading of primary cyclone; (-)=not determined.

Diameter µm (*)	Mass percentage			
	Mixture in the bed		Top of freeboard(**)	
	Exper.	Simul.	Exper.	Simul.
16(-16)	-	0.00	4.1	0.00
24(16-32)	-	3.45	7.8	23.18
54(32-75)	0.1	1.37	8.2	9.57
100(75-125)	0.1	3.18	16.9	23.40
188(125-250)	0.1	10.85	31.6	41.19
375(250-500)	5.2	0.23	25.2	0.01
1100(500-1700)	49.7	18.80	6.2	0.62
2440(1700-3180)	44.4	61.56	-	2.02
3180(+3180)	0.4	0.56	-	0.01

TABLE 5.24.Particle size distributions of the solids during the operation of the NCB test rig, test No.5. (*)=average inside the indicated slice and the extremes are taken as the minimum and maximum reported values; (**)=or loading of primary cyclone; (-)=not determined.

Diameter µm (*)	Mass percentage			
	Mixture in the bed		Top of freeboard(**)	
	Exper.	Simul.	Exper.	Simul.
20(-20)	-	0.54	25.1	48.87
26(20-32)	-	0.01	14.9	1.71
54(32-75)	0.10	0.14	12.7	7.29
100(75-125)	0.10	0.26	13.4	26.02
188(125-250)	0.20	0.10	15.8	0.01
375(250-500)	8.5	0.67	17.1	8.76
1100(500-1700)	48.8	7.94	1.1	0.59
2440(1700-3180)	42.0	89.46	0.0	6.69
3180(+3180)	0.3	0.88	0.0	0.06

TABLE 5.25.Particle size distributions of the solids during the operation of the NCB test rig, test No.6. (*)=average inside the indicated slice and the extremes are taken as the minimum and maximum reported values; (**)=or loading of primary cyclone; (-)=not determined.

Solid	Mass flow (g/s)					
	Test No.3		Test No.5		Test No.6	
	Exp.	Sim.	Exp.	Sim.	Exp.	Sim.
Carbona-ceous	-	12.07	-	26.98	-	0.75
Limest.	-	0.10	-	0.82	-	0.13
Free-ash	-	4.44	-	7.39	-	0.80
Total	16.0	16.61	23.6	35.19	2.08	1.68

TABLE 5.26.Entrainment flows of particles at the top of the freeboard during the tests of the NCB test rig. (-)=not determined.

Solid	Mass flow (g/s)			
	Test No.3		Test No.5	
	Exper.	Simul.	Exper.	Simul.
Carbonaceous	-	11.96	-	26.73
Limestone	-	0.099	-	0.82
Free-ash	-	3.83	-	6.54
Total	14.61	15.88	23.61	34.09

TABLE 5.27.Recycled flows of particles during the tests of the NCB test rig. (during the test No.6 the recycling was not used). (-)=not determined.

Solid	Diameters (m)								
	Test No.3			Test No.5			Test No.6		
	Fed	Bed aver.	Top freeb.	Fed	Bed aver.	Top freeb.	Fed	Bed aver.	Top freeb
Carbona-ceous	237	181	96	201	143	99	261	159	71
Limest.	2019	2013	133	1727	1723	1721	1980	2064	970
Free ash	0	20	20	0	22	22	0	12	12
Total	308	260	48	260	254	58	361	1040	22

TABLE 5.28.Average diameters of particles at various positions for the operations of the NCB test rig. Results obtained by simulation.

Process parameter	Real operation	Simulation
Mass flow of flue gas (g/s)	48.89	49.685
Total flow of solids leaving the bed (g/s) (includes entrainment at the top of the bed)	-	198.99
Total flow of solids at the top of the freeboard (g/s)	16.0	16.61
Average mass fraction of inert in the bed (including free-ash)	-	0.0389
Average mass fraction of limestone in the bed	-	0.6722
Average mass fraction of carbonaceous solid in the bed (does not include free-ash)	-	0.2889
Minimum fluidization voidage at the middle of the bed	-	0.52
Overall voidage at the middle of the bed	-	0.84720
Minimum fluidization velocity at the middle of the bed (m/s)	-	0.05234
Superficial velocity at the middle of the bed (m/s)	1.5(a)	1.0854
Bed transversal area (m^2)	0.0903	0.0903
Carbon conversion (fraction of the fed carbon) (%)	96.8	98.704
Average residence time of particles in the system (s)	-	7344
TDH = Transport Disengaging Height (m)(height from the bed surface)	-	2.225
Freeboard space (m)	1.900	1.900

CONT...

CONT...

Process parameter	Real operation	Simulation
Ca/S = Calcium to Sulphur ratio in the bed	2.9	2.74791
Calcium conversion (%)	-	8.951
Sulphur retention efficiency based on the fed sulphur) (%)	-	24.609
Sulphur retention efficiency based on the burned sulphur) (%)	-	24.878
Static bed depth (m)	-	0.194
Rate of energy input to the system(kW)	125	125.08
Percentage of the energy input lost to external environment through the walls	-	6.532
Pressure loss across the distributor (kPa)	9.7	3.837
Pressure loss across the bed (kPa)	5.6	1.528

TABLE 5.29.Various process parameters for the operation of the NCB test rig, test No.3. (-)= not determined; (a)=data do not indicate the condition.

Parameter	Real operation	Simulation
Total heat transfer to the tubes in the system (kW)	-	9.626
Heat transfer to tubes inside the bed (kW)	-	9.626
Total mass flow of steam generated by the system (kg/s)	-	0.000
Total heat loss to the external ambience (kW)	-	8.170
Heat loss in the bed section (kW)	-	1.537
Heat loss in the freeboard section (kW)	-	6.633
Overall heat transfer coefficient between tubes and bed at the middle of the bundle ($W\ m^{-2}\ K^{-1}$)	-	181.9
Wall temperature of the tubes the bed (middle of the bundle)(K)	-	432.8
Percentage of heat loss to the ambience in relation to the heat transfer to the tubes	-	84.87
Temperature of the water leaving the tubes (K)	-	288.9
Temperature of the external wall at the top of the bed section (K)	-	370.0
Temperature of the external wall at the top of freeboard section(K)	-	378.2
Heat transfer coefficient between external wall and ambience at the top of the bed section ($W\ m^{-2}\ K^{-1}$)	-	22.7
Heat transfer coefficient between external wall and ambience at the top of the freeboard section ($W\ m^{-2}\ K^{-1}$)	-	23.4

TABLE 5.30.Some parameters related to heat transfer during the operation of the NCB test rig, test No.3. (-)=not determined.

Process parameter	Real operation	Simula-tion
Mass flow of flue gas (g/s)	71.92	73.237
Total flow of solids leaving the bed (g/s)(includes entrainment at the top of the bed)	-	1036.71
Total flow of solids at the top of the freeboard (g/s)	23.61	34.197
Average mass percentage of inert in the bed (including free-ash)	-	3.337
Average mass percentage of limestone in the bed	-	68.259
Average mass percentage of carbonaceous solid in the bed (does not include free-ash)	-	28.367
Minimum fluidization voidage at the middle of the bed	-	0.52
Overall voidage at the middle of the bed	-	0.8604
Minimum fluidization velocity at the middle of the bed (m/s)	-	0.5510
Superficial velocity at the middle of the bed (m/s)	2.2(a)	1.3597
Bed transversal area (m^2)	0.0903	0.0903
Carbon conversion (fraction of the fed carbon) (%)	97.3	97.658
Average residence time of particles in the system (s)	-	9256
TDH = Transport Disengaging Height (from the bed surface) (m)	-	2.545
Freeboard space (m)	1.700	1.700

CONT...

CONT...

Process parameter	Real operation	Simulation
Ca/S = Calcium to Sulphur ratio in the bed	2.8	2.544
Calcium conversion (%)	-	4.575
Sulphur retention efficiency based on the fed sulphur) (%)	-	10.332
Sulphur retention efficiency based on the burned sulphur) (%)	-	10.536
Static bed depth (m)	-	0.303
Rate of energy input to the system(kW)	164	164.53
Percentage of the energy input lost to the environment through the walls	-	4.439
Pressure loss across the distributor (kPa)	15.9	8.01
Pressure loss across the bed(kPa)	6.0	1.96

TABLE 5.31.Various process parameters for the operation of the NCB test rig, test No.5. (-)= not determined; (a)=data do not indicate the condition.

Parameter	Real operation	Simulation
Total heat transfer to the tubes in the system (kW)	-	5.985
Heat transfer to tubes inside the the bed (kW)	-	5.985
Total heat loss to the external ambience (kW)	-	7.304
Heat loss in the bed section (kW)	-	2.000
Heat loss in the freeboard section (kW)	-	5.304
Overall heat transfer coefficient between tubes and bed at the middle of the bundle ($W\ m^{-2}\ K^{-1}$)	-	164.5
Wall temperature of the tubes in the bed (middle of the bundle)(K)	-	379.0
Percentage of heat loss to the ambience relation to the heat transfer to the tubes	-	122.0
Temperature of the generated steam or temperature of the water (K)	-	288.5
Temperature of the external wall at the top of the bed section (K)	-	364.0
Temperature of the external wall at the top of the freeboard (K)	-	369.3
Heat transfer coefficient between external wall and ambience at the top of the bed($W\ m^{-2}\ K^{-1}$)	-	22.20
Heat transfer coefficient between external wall and ambience at the top of the freeboard ($W\ m^{-2}\ K^{-1}$)	-	22.66

TABLE 5.32.Some parameters related to heat transfer during the operation of the NCB test rig, test No.5. (-)=not determined.

Process parameter	Real operation	Simulation
Mass flow of flue gas (g/s)	68.42	69.743
Total flow of solids leaving the bed (g/s)(includes entrainment at the top of the bed)	-	170.37
Total flow of solids at the top of the freeboard (g/s)	2.08	1.680
Average mass percentage of inert in the bed (including free-ash)	-	0.508
Average mass percentage of limestone in the bed	-	98.360
Average mass percentage of carbonaceous solid in the bed (does not include free-ash)	-	1.132
Minimum fluidization voidage at the middle of the bed	-	0.52
Overall voidage at the middle of the bed	-	0.7149
Minimum fluidization velocity at the middle of the bed (m/s)	-	0.6761
Superficial velocity at the middle of the bed (m/s)	2.2(a)	1.917
Bed transversal area (m^2)	0.9026	0.9026
Carbon conversion (fraction of the fed carbon) (%)	92.0	98.120
Average mass percentage of carbon in the bed	0.05	0.074
Average residence time of particles in the system (s)	-	11267
TDH = Transport Disengaging Height (m)(from the bed surface)	-	2.921
Freeboard space	1.800	1.800

CONT...

CONT...

Process parameter	Real operation	Simulation
Ca/S = Calcium to Sulphur ratio in the bed	4.4	4.1928
Calcium conversion (%)	-	14.251
Sulphur retention efficiency based on the fed sulphur) (%)	-	58.573
Sulphur retention efficiency based on the burned sulphur) (%)	-	59.493
Static bed depth (m)	-	0.390
Rate of energy input to the system(kW)	161	160.7
Percentage of the energy input lost to external environment through the walls	-	4.880
Pressure loss across the distributor (kPa)	-	6.952
Pressure loss across the bed(kPa)	5.5	3.841

TABLE 5.33.Various process parameters for the operation of the NCB test rig, test No.6. (-)= not determined; (a)=data do not indicate the condition.

Parameter	Real operation	Simulation
Total heat transfer to the tubes in the system (kW)	-	8.801
Heat transfer to tubes inside the the bed (kW)	-	8.801
Total mass flow of steam generated by the system (kg/s)	-	0.000
Total heat loss to the external ambience (kW)	-	7.843
Heat loss in the bed section (kW)	-	2.075
Heat loss in the freeboard section (kW)	-	5.768
Overall heat transfer coefficient between tubes and bed at the middle of the bundle ($W\ m^{-2}\ K^{-1}$)	-	101.85
Wall temperature of the tubes in the bed (middle of the bundle) (K)	-	406.4
Percentage of heat loss to the ambience in relation to the heat transfer to the tubes	-	89.111
Temperature of the water leaving the tubes (K)	-	288.8
Temperature of the external wall at the top of the bed section (K)	-	376.0
Temperature of the external wall at the top of freeboard section(K)	-	371.0
Heat transfer coefficient between external wall and ambience at the top of the bed ($W\ m^{-2}\ K^{-1}$)	-	23.212
Heat transfer coefficient between external wall and ambience at the top of the freeboard ($W\ m^{-2}\ K^{-1}$)	-	22.797

TABLE 5.34.Some parameters related to heat transfer during the operation of the NCB test rig, test No.6. (-)=not determined.

5.1.2.4. Parameter profiles and other graphs

As in the case of the Babcock and Wilcox unit, this section contains several graphics that describe important features of the operation of the NCB unit. As the various operations are in several aspects similar, it has been decided to present the complete set of graphics for just two of the cases simulated.

The discussion of these profiles are presented in the following chapter.

5.2. Gasifiers

Although the present mathematical model was devised to allow the simulation of fluidized bed boilers and gasifiers no industrial scale operation data has been published for the case of gasifiers. The only data available refer to the operation of a pilot scale unit installed in the IPT/São Paulo/Brazil.

Unfortunately the tests could not be used to compare with the simulations because:

a) The operation was not in steady-state regime. Inert (sand) was not added continuously and the present model does not applies to such operations;

b) Pellets of sugar cane bagasse had dimensions and physical characteristics completely out of the range of correlations found in the literature.

Therefore, although tried, the present simulation program could not reproduce the experimental data. It has been decided to leave the extension of the mathematical

model to include these cases as future developments of the present work.

For the sake of completeness, the description of the equipment and operational data are given below.

5.2.1.IPT Pilot Gasifier

The gasification of coal,wood and biomass residuals is an important line of research in this institute.

During several years research projects have been carried out in moving bed gasification of various materials. Special emphasis was put in the case of wood and biomass residuals but the problems with tar generation could not be solved completely.

In 1981 it was decided to start the research with a fluidized bed that could solve the problem of tar concentration in the product gas. A semi-industrial pilot was built and several experiments have been carried out since then.

5.2.1.1.Plant description

A simplified scheme of the unit is presented in the Fig.5.48.

- Reactor:

It is basically a vertical cylindrical 0.48m internal diameter reactor with 0.145m thick insulating walls of refractory bricks. The total height of the chamber is 2.8m and during the operations the bed height was maintained at around 0.5m.

- Air distributor:

Below the reactor there is a wind box with 60 stand pipes for the air injection and 12 for LPG - that is used during the start-up.

The pipes are 80mm above the distributor base and each one has 53mm diameter orifices. The orifices are 66mm above the distributor plate and the space is filled with sand for the plate protection.

Steam can be injected eventually with the air. This could be used in the case of coal gasification but no steam was fed otherwise and was used only for shut-down procedure.

- Biomass feeding:

The feeding system consists of a hopper that is fed by pneumatic transport from the floor. From this hopper a sealed screw feeds a pneumatic ejector that blows the carbonaceous material above the bed height. Part of the product gas is recycled to serve as transport gas in this process.

The feeding of carbonaceous material is continuous but no sand is fed during the operation.

- Cleaning system:

To separate the gas from particulate material and some eventual tar a system composed of a cyclone, wet and dry scrubber and a packed column is installed.

5.2.1.2. Plant operational data

The tables below show the data obtained for the operation conditions in a typical test (Test No.GLF-12,21/03/86)

The symbols used in the data tables is described in section (4.2).

Data	Value	Data	Value
AMTPES(1)	9.2	TPES(1)	303
VOLAT	78.1	TECAG	333
CARFIX	11.8	POPER	102.3×10^3
ASHES	0.9	PECAG	105.6×10^3
ENTCBC	10×10^6	DD	0.48
MTKIND	5	ZD	0.45
WPDB(14)	0.4670	DF	0.48
WPDB(15)	0.0580	ZF	2.49
WPDB(16)	0.4660	ZFEEDS(1)	1.2
WPDB(17)	0.0000	XISD	0.145
WPDB(18)	0.0000	AKISD	0.93
WPDB(19)	0.0090	EPSD	0.9(*)
ROGCES	420	XISF	0.145
ROPES(1)	1140	AKISF	0.93
RORES(1)	1400	EPSF	0.9(*)
MODLR	1	TAMB	288
FISP(1)	0.8	VV	0.0
FMPES(1)	5.034×10^{-02}	XISDI	0.066
FMPES(3)	0.0(**)	AKISDI	0.30(*)
ROPES(3)	2300	DOD	0.003
RORES(3)	2660	NOD	300
FMCAG	6.892×10^{-2}		
WCAG(3)	0.232		
WCAG(4)	0.766		
WCAG(5)	0.002		

TABLE 5.35.Operation data of the IPT unit.(*)=most probable assumed value due to to the lack of information;(**)=it was a batch operation in respect to the inert(sand) added at the beginning of the test.

Pellets		Sand	
Diameter µm	Mass %	Diameter µm	Mass %
53	0.03	250	8.40
570	0.24	750	23.30
1620	0.39	1500	46.40
4600	3.97	2420	18.30
6800(*)	23.48	3420	3.00
7700(*)	23.48	6800	0.60
8600(*)	23.48		
9500(*)	23.47		
13500	1.34		

TABLE 5.36.Particle size distributions of the solids fed during the operations of the IPT unit. (*)=minimum and maximum pellets size has been divided in four equally distributed slices.

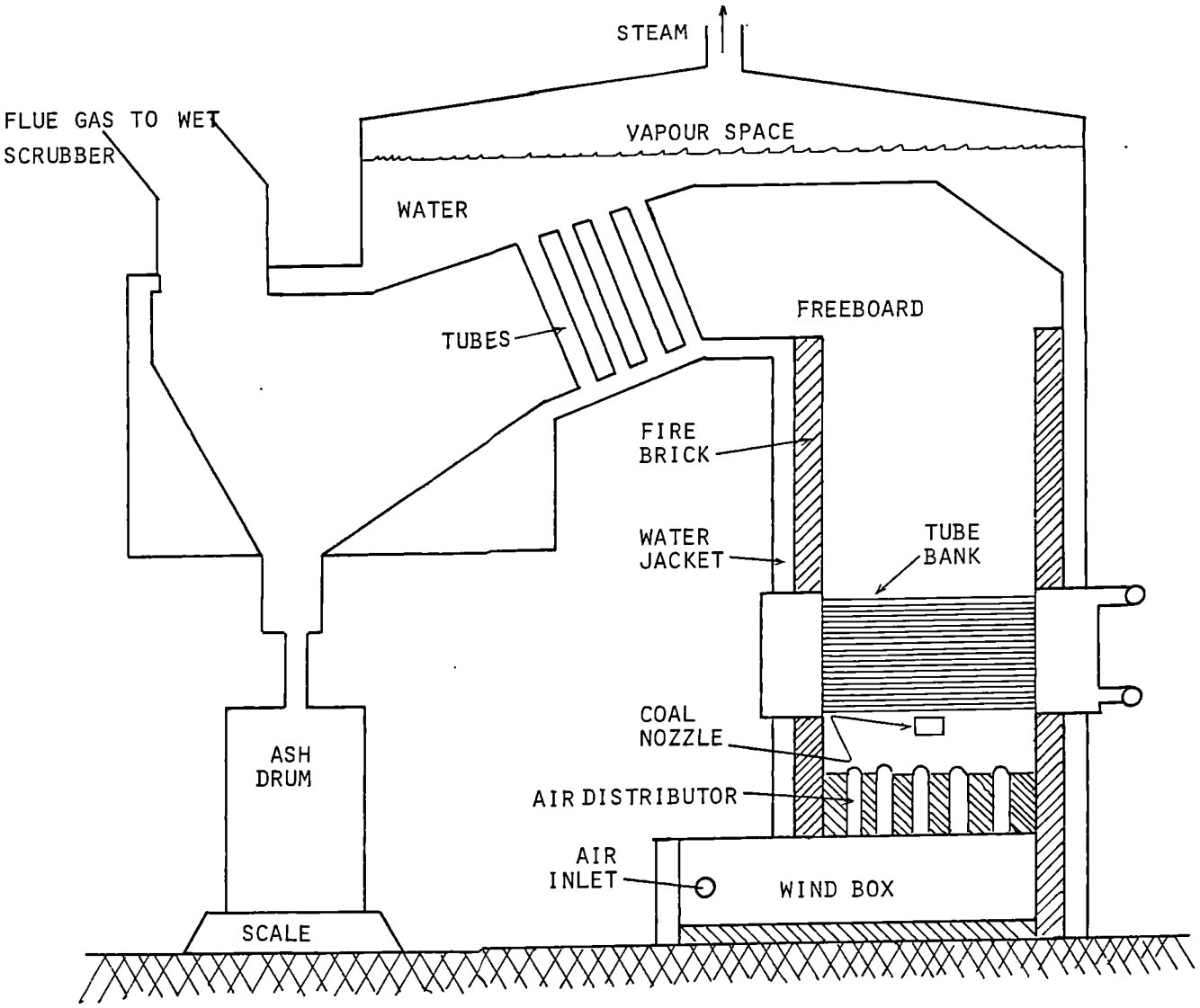

FIGURE 5.1. SCHEMATIC VIEW OF THE BABCOCK AND WILCOX TEST UNIT.

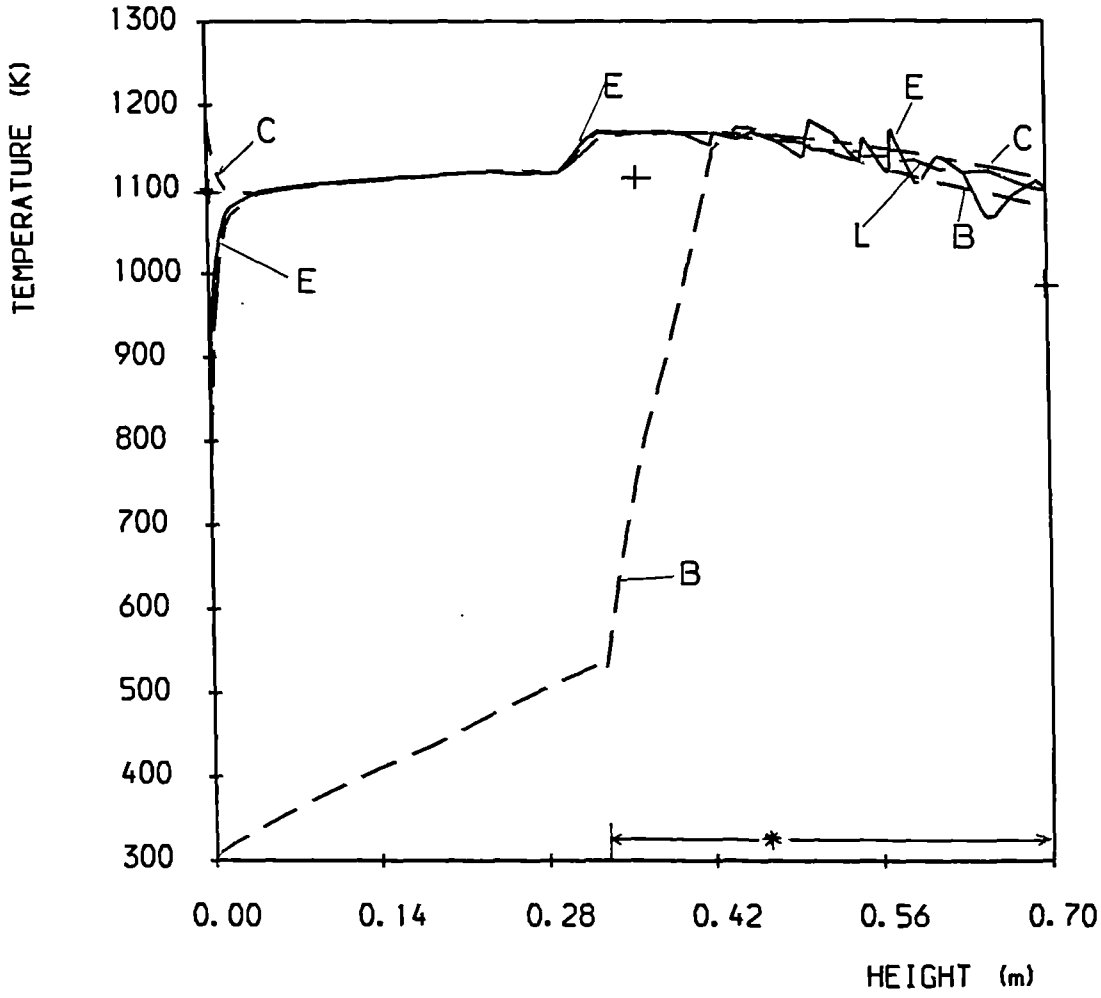

FIGURE 5.2. BED TEMPERATURE PROFILES-B&W, TEST 26
(E=EMULSION GAS, B=BUBBLE GAS, C=COAL, L=LIMESTONE,
+ =MEASURED AVERAGE, * =TUBE BANK REGION)

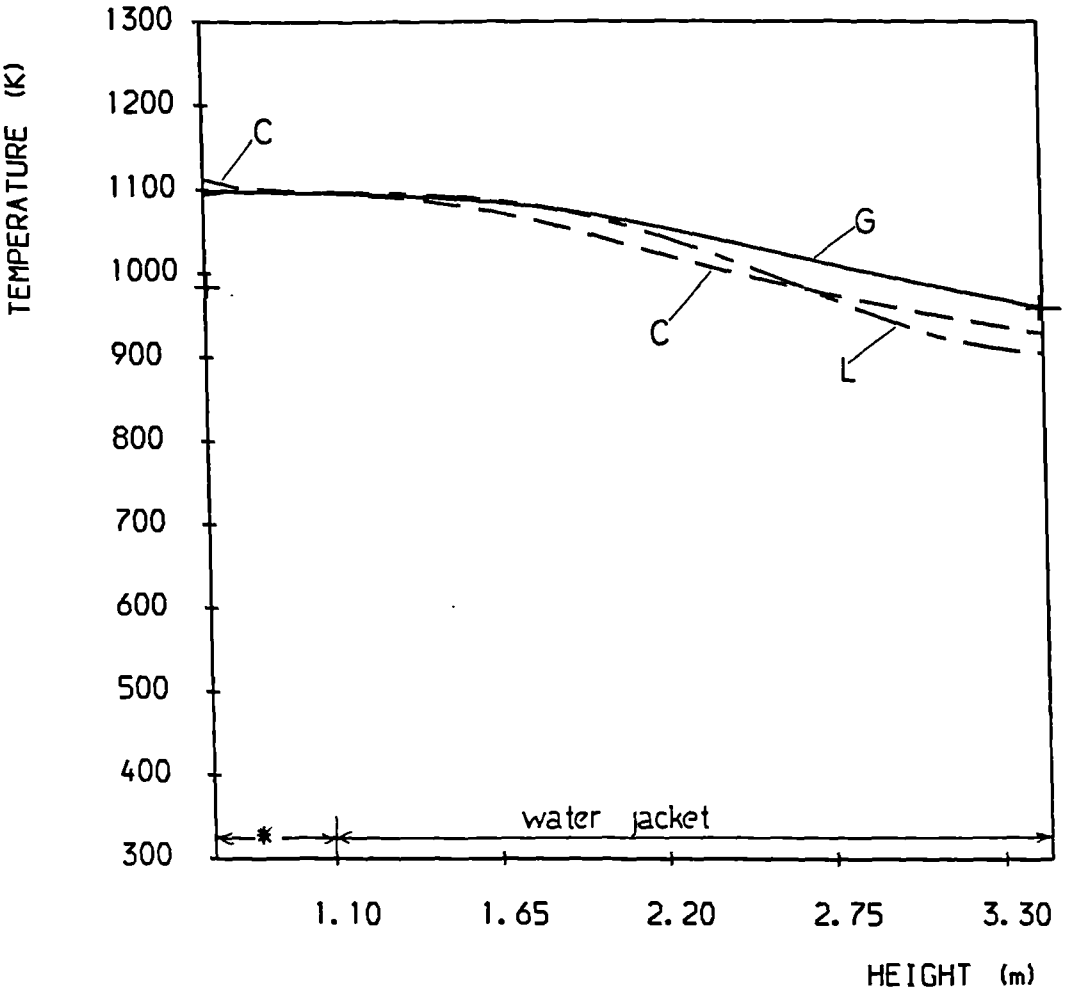

FIGURE 5.3. FREEBOARD TEMPERATURE PROFILES-B&W, TEST 26 (G=GAS, C=COAL, L=LIMESTONE, + =MEASURED AVERAGE, * =TUBE BANK REGION).

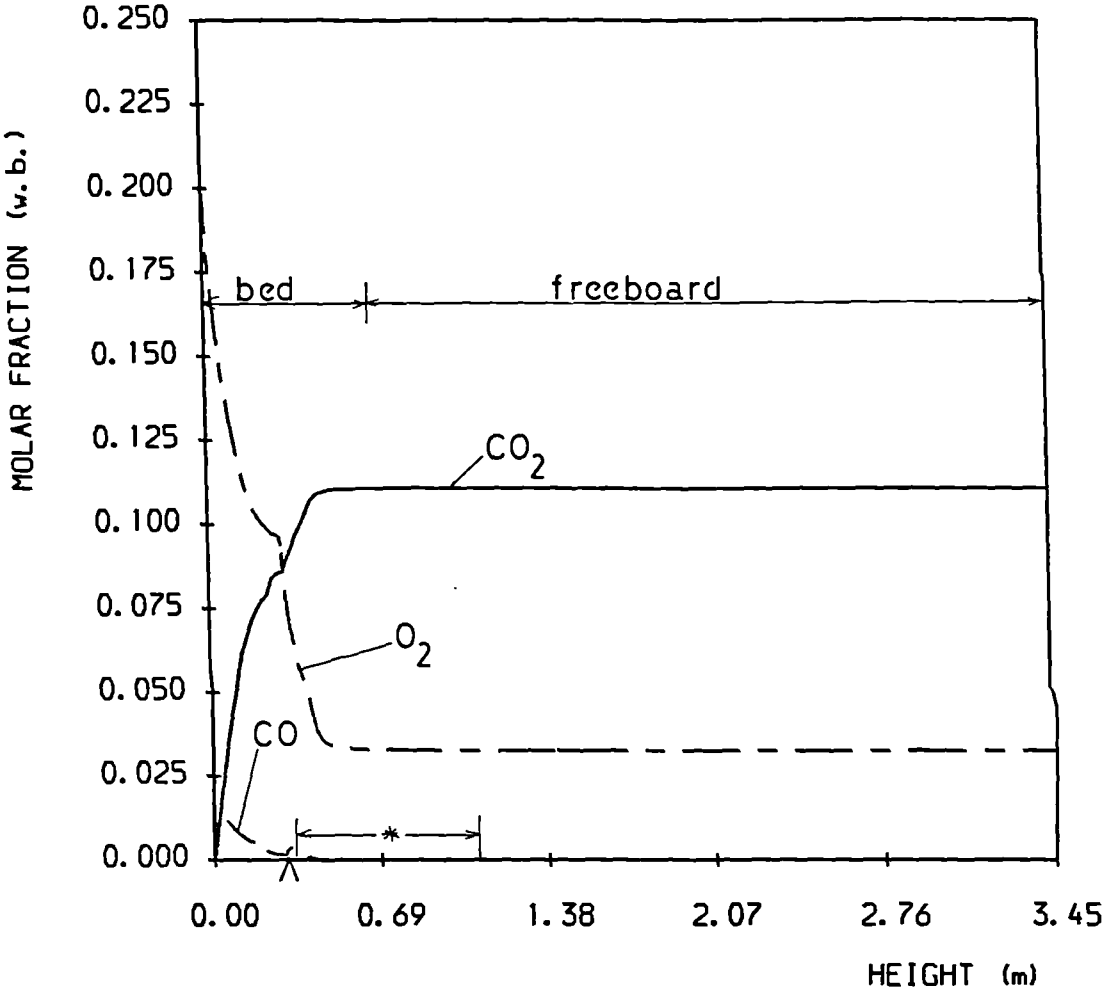

FIGURE 5.4. CONCENTRATION PROFILES IN THE SYSTEM-B&W, TEST 26 (CO2, CO, O2, ^ =COAL FEEDING POINT, * =TUBE BANK REGION).

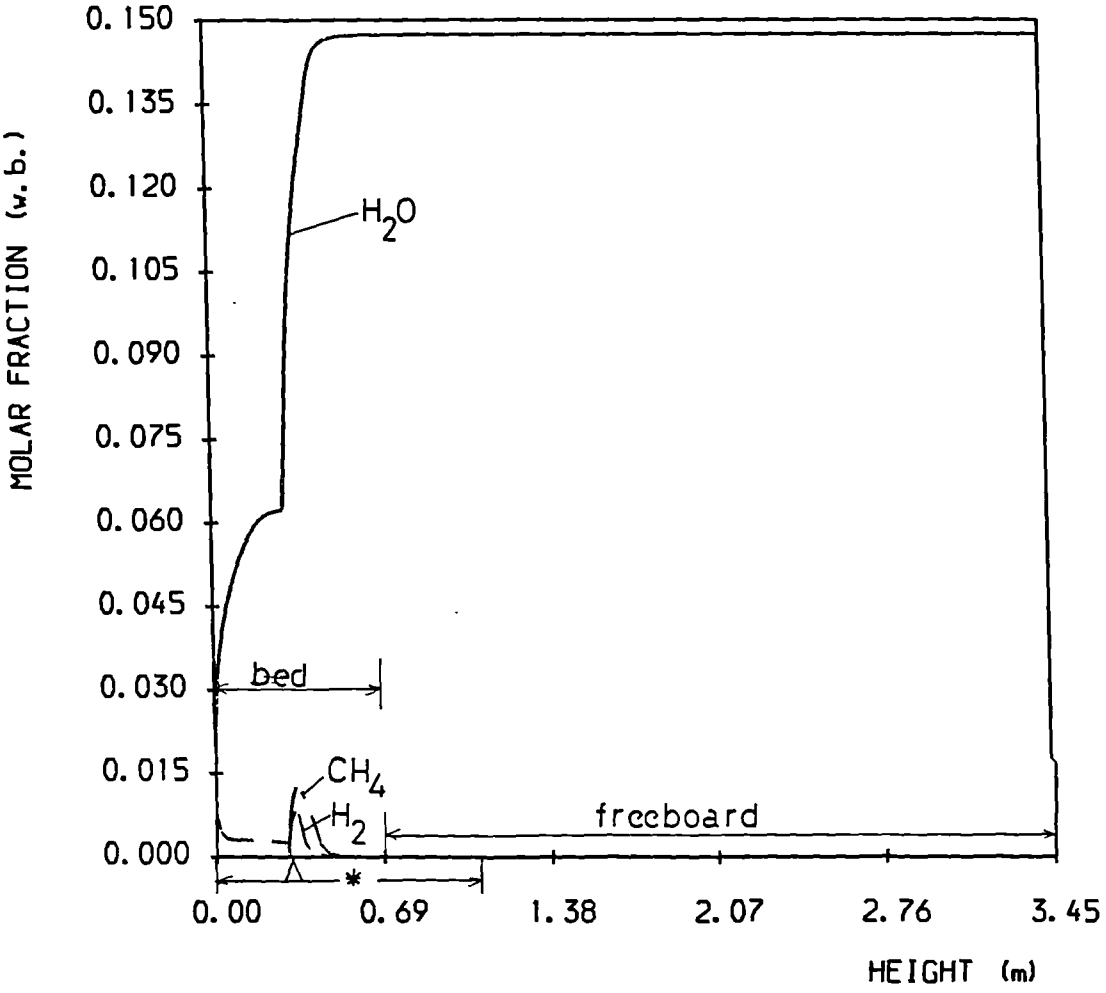

FIGURE 5.5. CONCENTRATION PROFILES IN THE SYSTEM-B&W, TEST 26 (H2O, H2, CH4, ^ =COAL FEEDING POINT, * =TUBE BANK REGION).

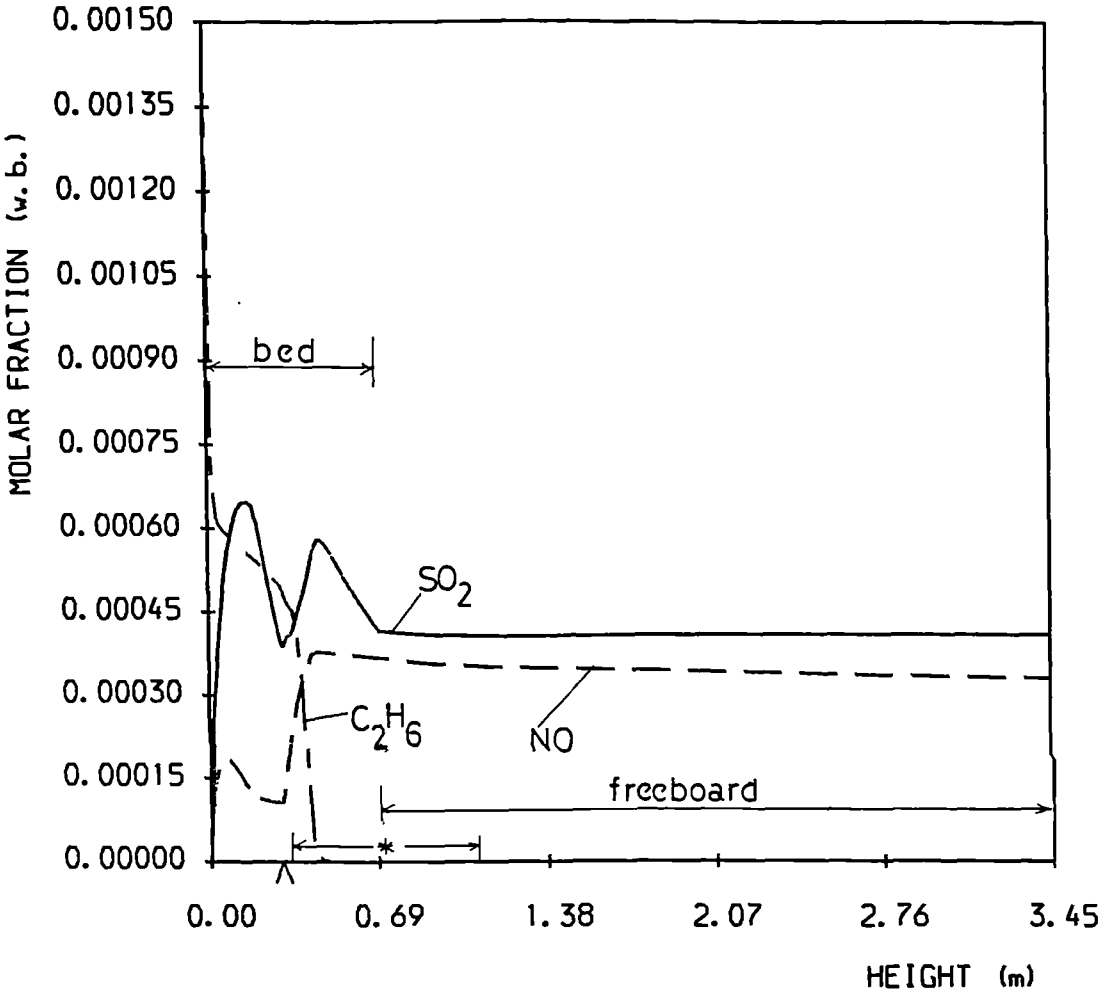

FIGURE 5.6. CONCENTRATION PROFILES IN THE SYSTEM-B&W, TEST 26 (SO2, NO, C2H6), ^ =COAL FEEDING POINT, * =TUBE BANK REGION).

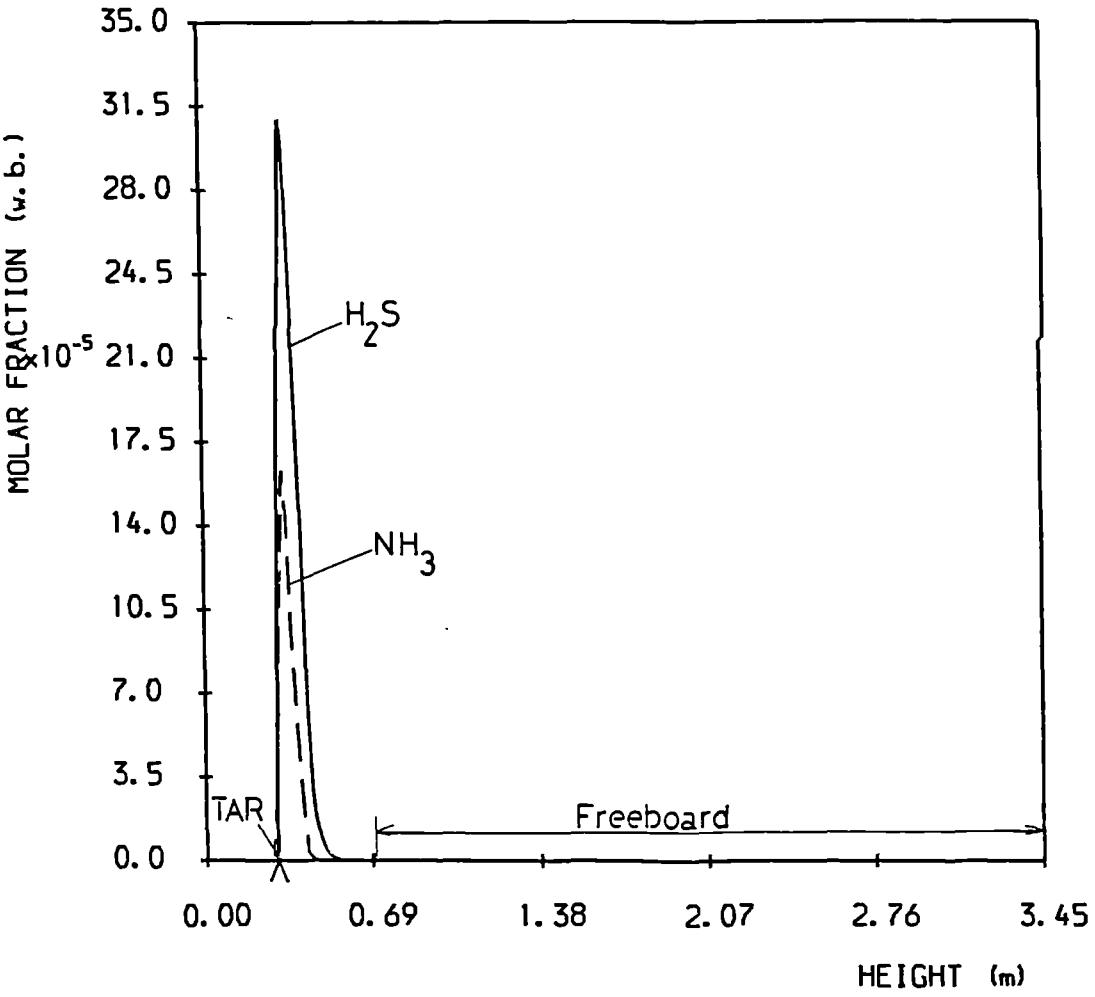

FIGURE 5.7. CONCENTRATION PROFILES IN THE SYSTEM-B&W, TEST 26 (H2S, NH3, TAR, ^ =COAL FEEDING POINT).

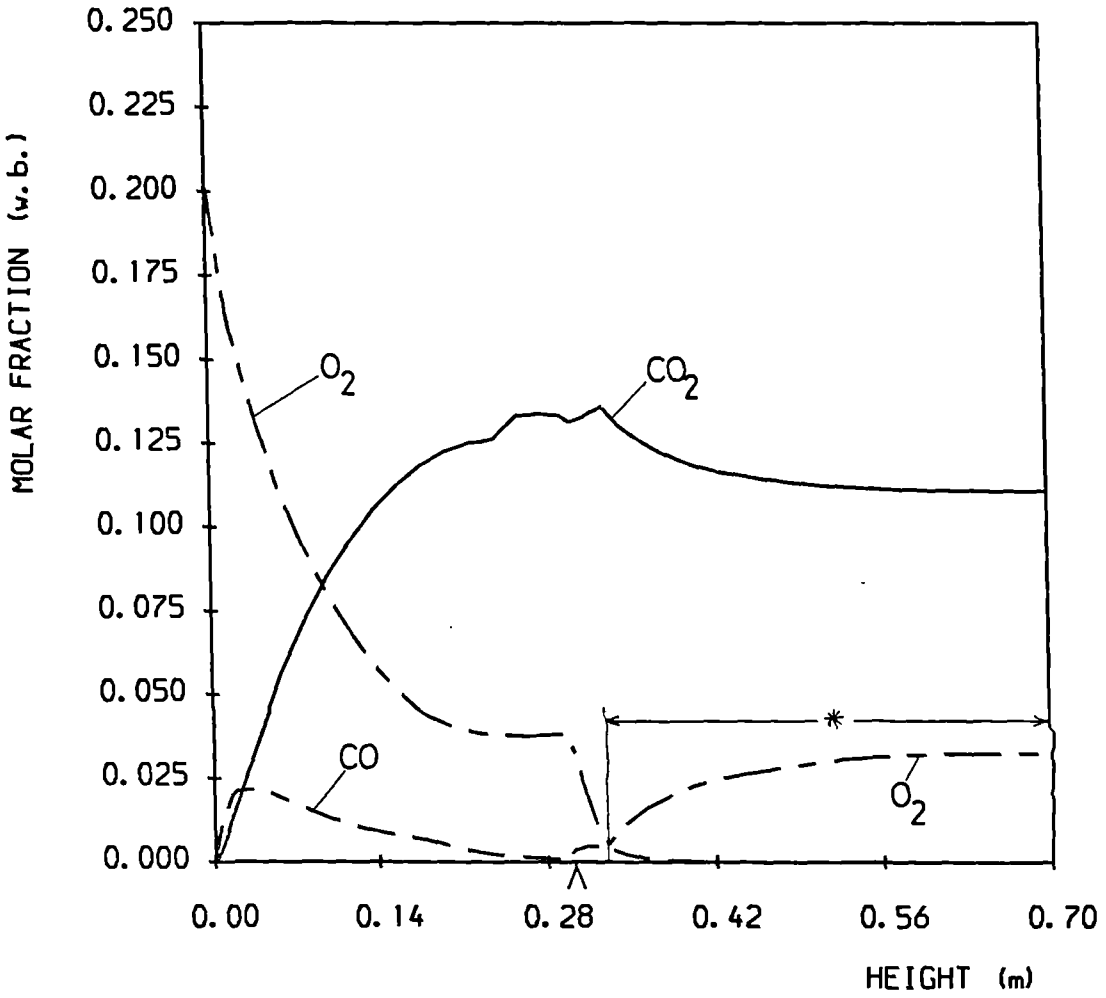

FIGURE 5.8. CONCENTRATION PROFILES IN THE EMULSION PHASE-B&W, TEST 26 (CO2, CO, O2, ^ =COAL FEEDING POINT, * =TUBE BANK REGION)

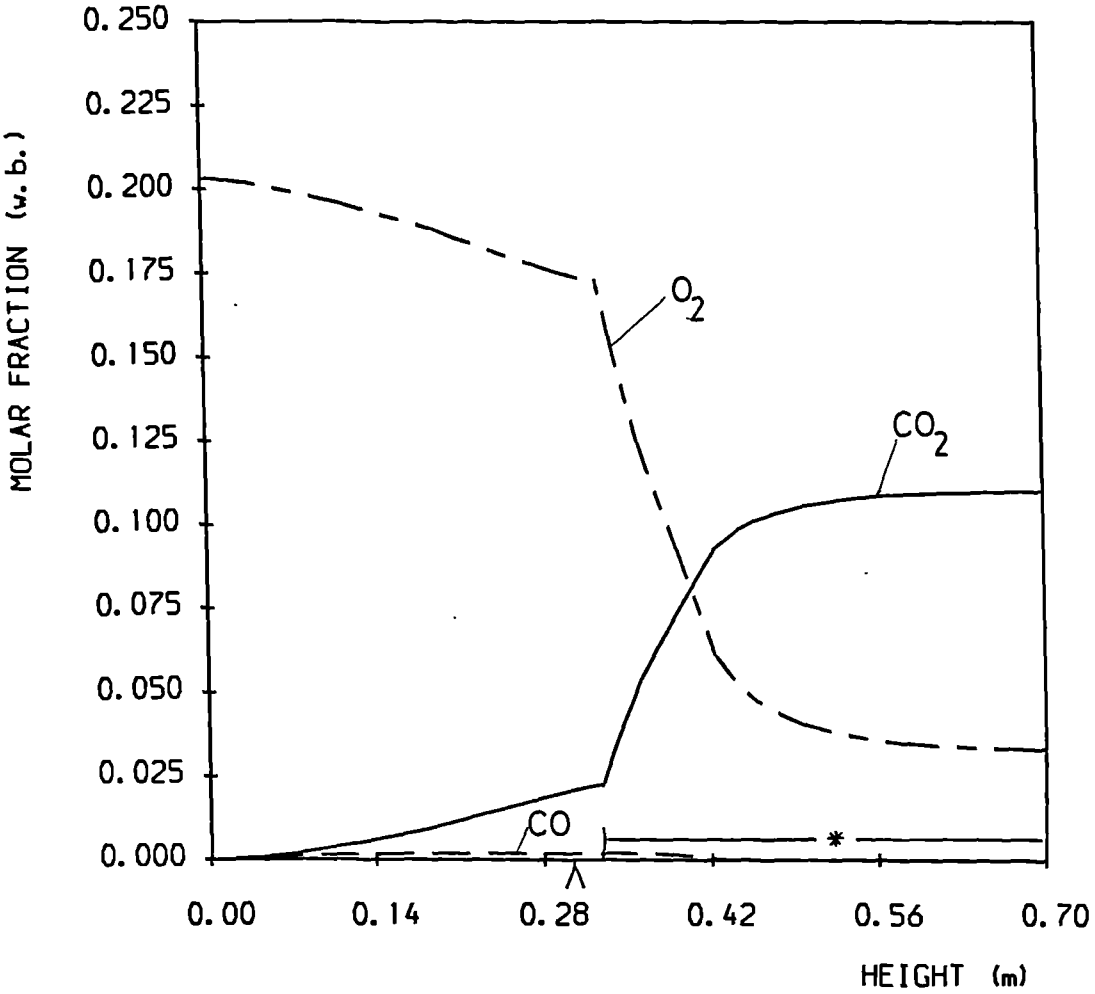

FIGURE 5.9. CONCENTRATION PROFILES IN THE BUBBLE PHASE-B&W, TEST 26 (CO2, CO, O2, ^ =COAL FEEDING POINT, * =TUBE BANK REGION).

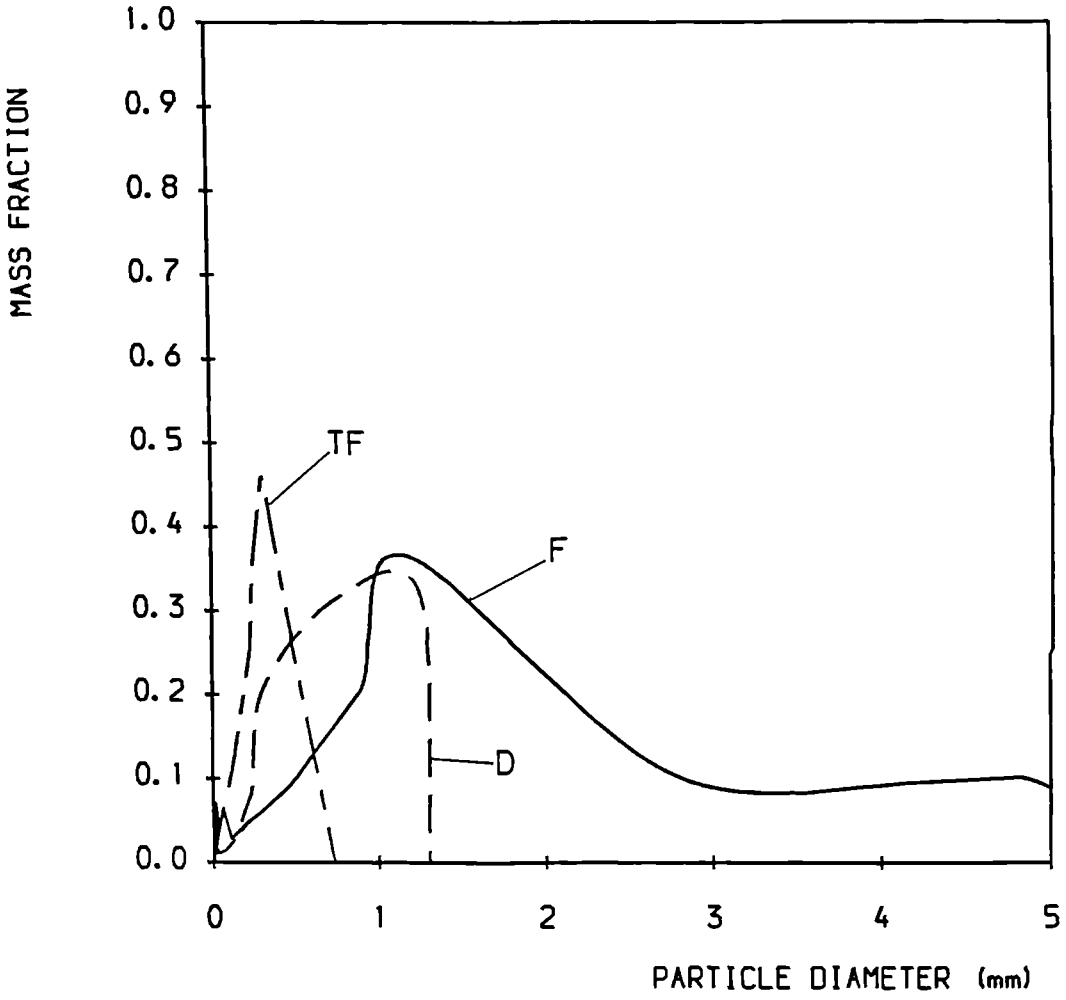

FIGURE 5.10. COAL PARTICLE SIZE DISTRIBUTION-B&W, TEST 26 (F=AS FED TO THE BED, D=IN THE BED, TF=AT THE TOP OF FREEBOARD)

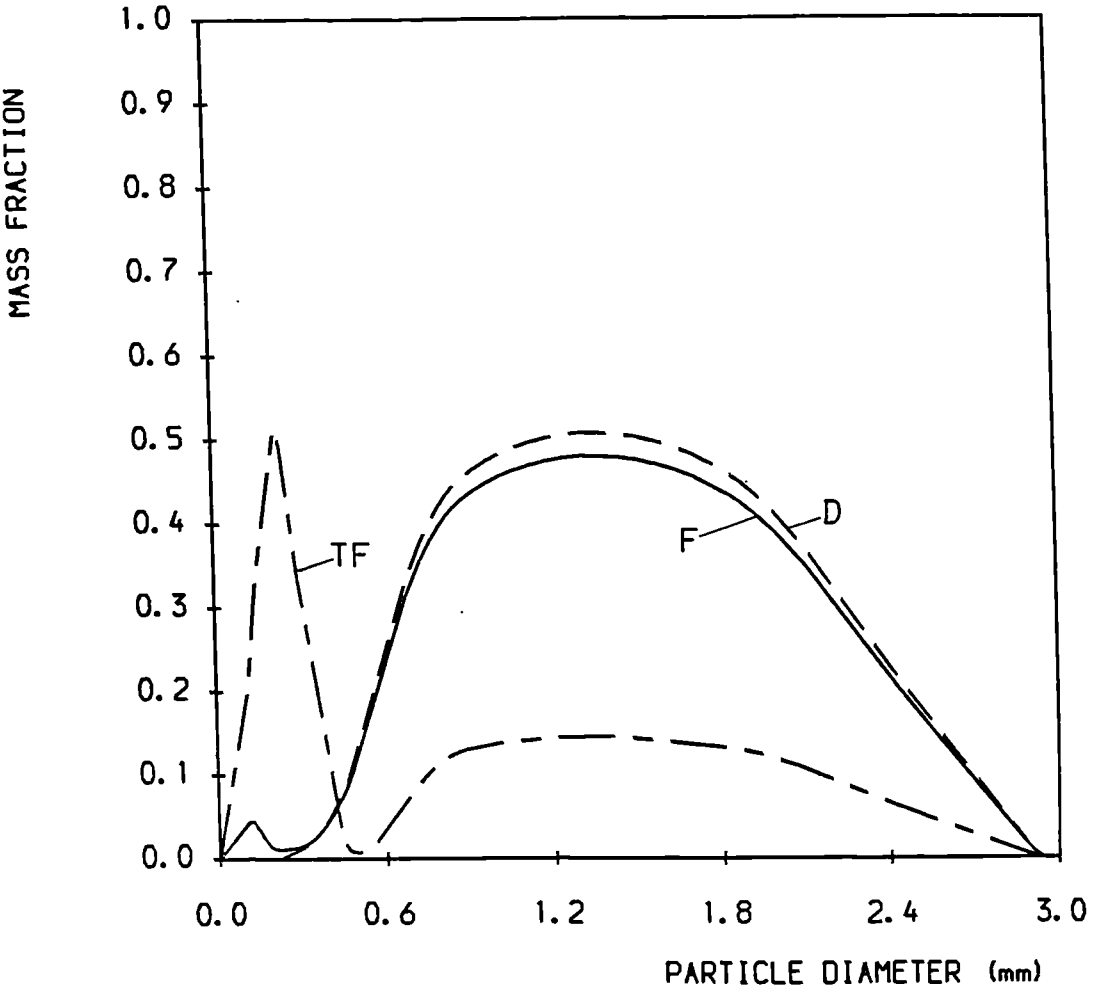

FIGURE 5.11. LIMESTONE PARTICLE SIZE DISTRIBUTION-B&W, TEST 26 (F=AS FED, D=BED, TF=AT THE TOP OF THE FREEBOARD)

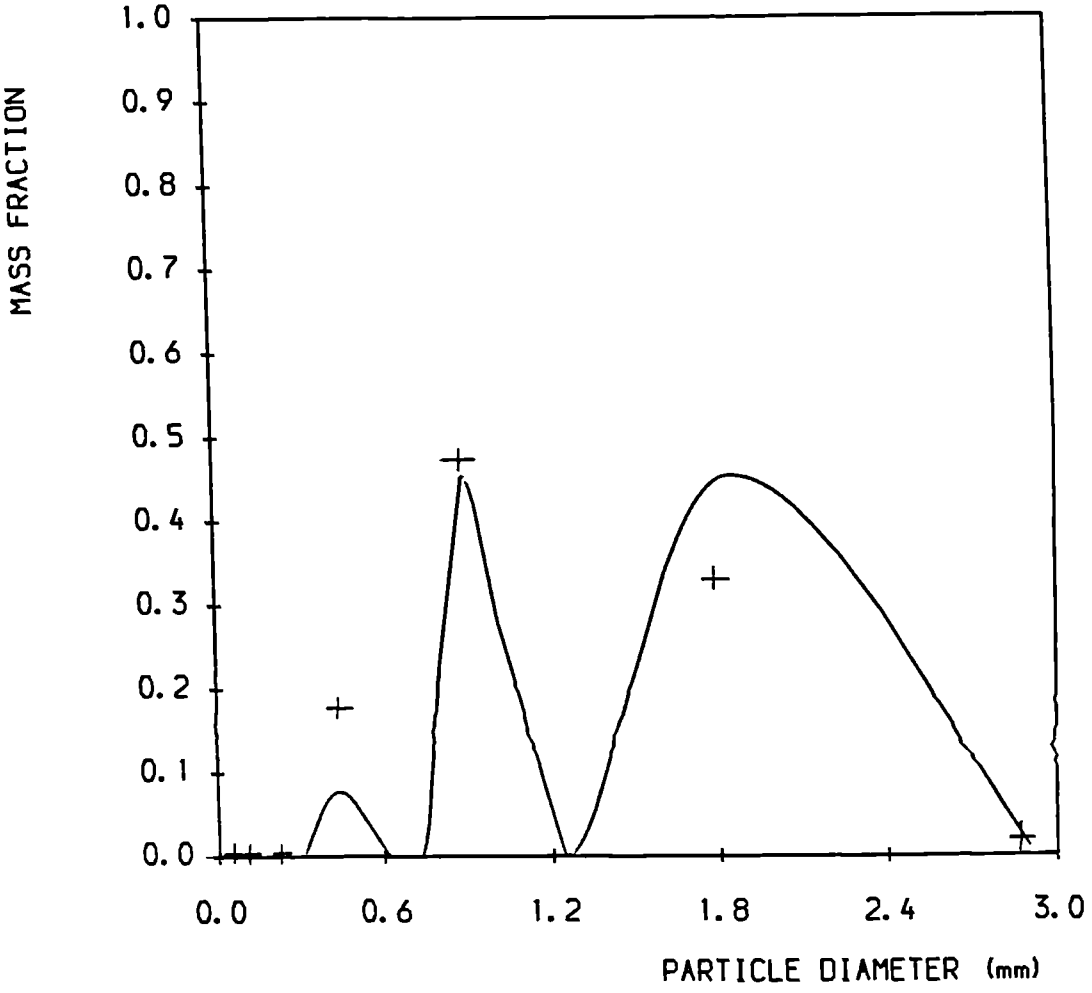

FIGURE 5.12. TOTAL PARTICLE SIZE DISTRIBUTION-B&W, TEST 26 (AVERAGE IN THE BED)
(+ =EXPERIMENTAL DETERMINATIONS)

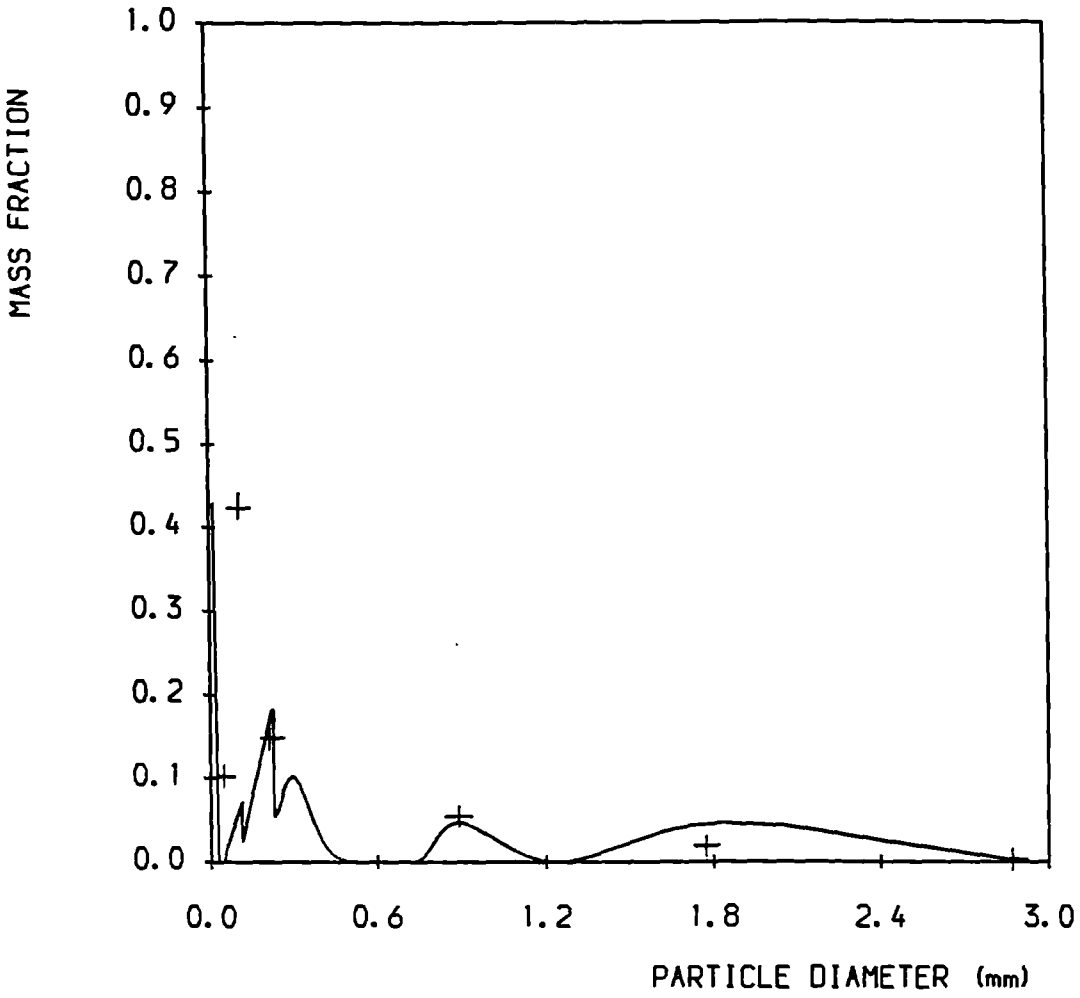

FIGURE 5.13. TOTAL PARTICLE SIZE DISTRIBUTION-B&W, TEST 26 (AT THE TOP OF THE FREEBOARD).
(+ =EXPERIMENTAL DETERMINATIONS)

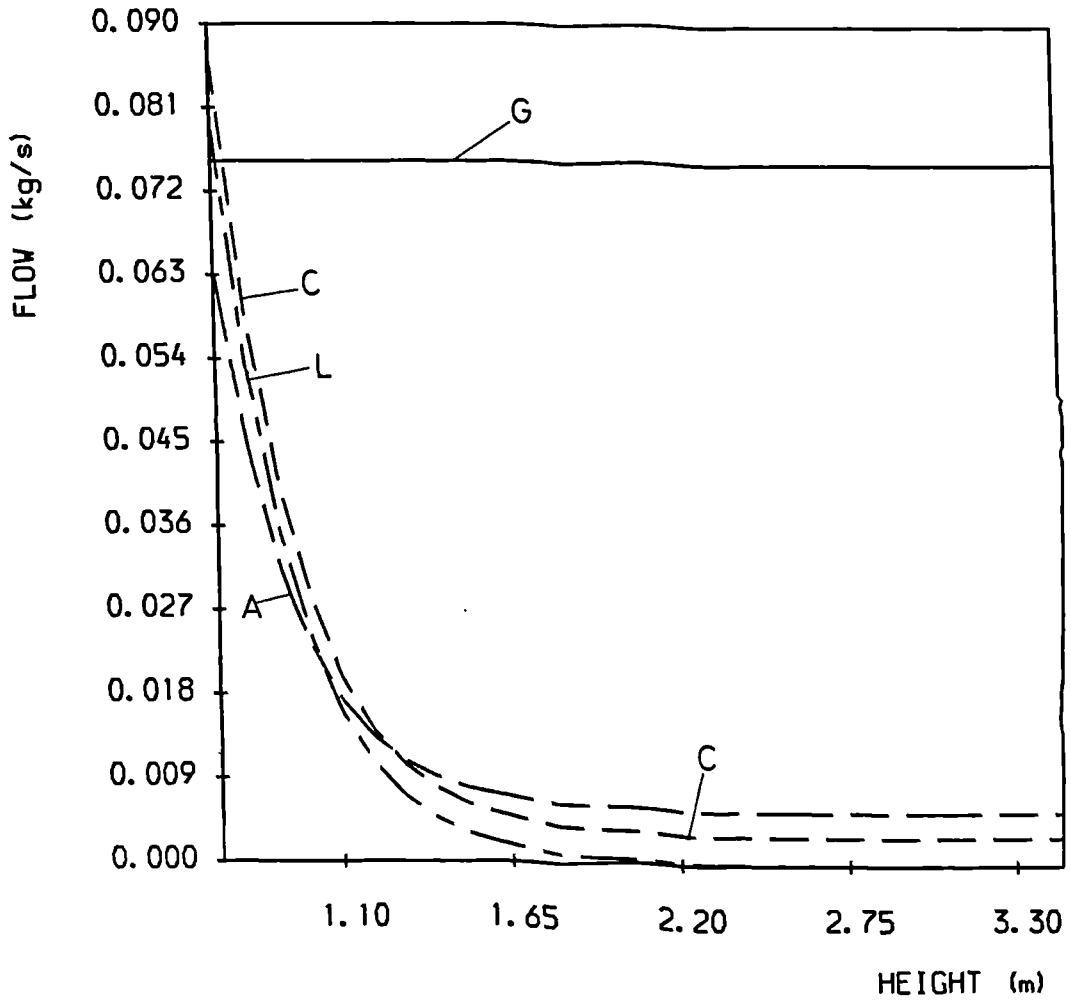

FIGURE 5.14. GAS AND SOLID FLOWS IN THE FREEBOARD-B&W, TEST 26 (G=GAS (sc: 0.1), C=COAL, L=LIMEST. (sc: 0.001), A=FREE ASH).

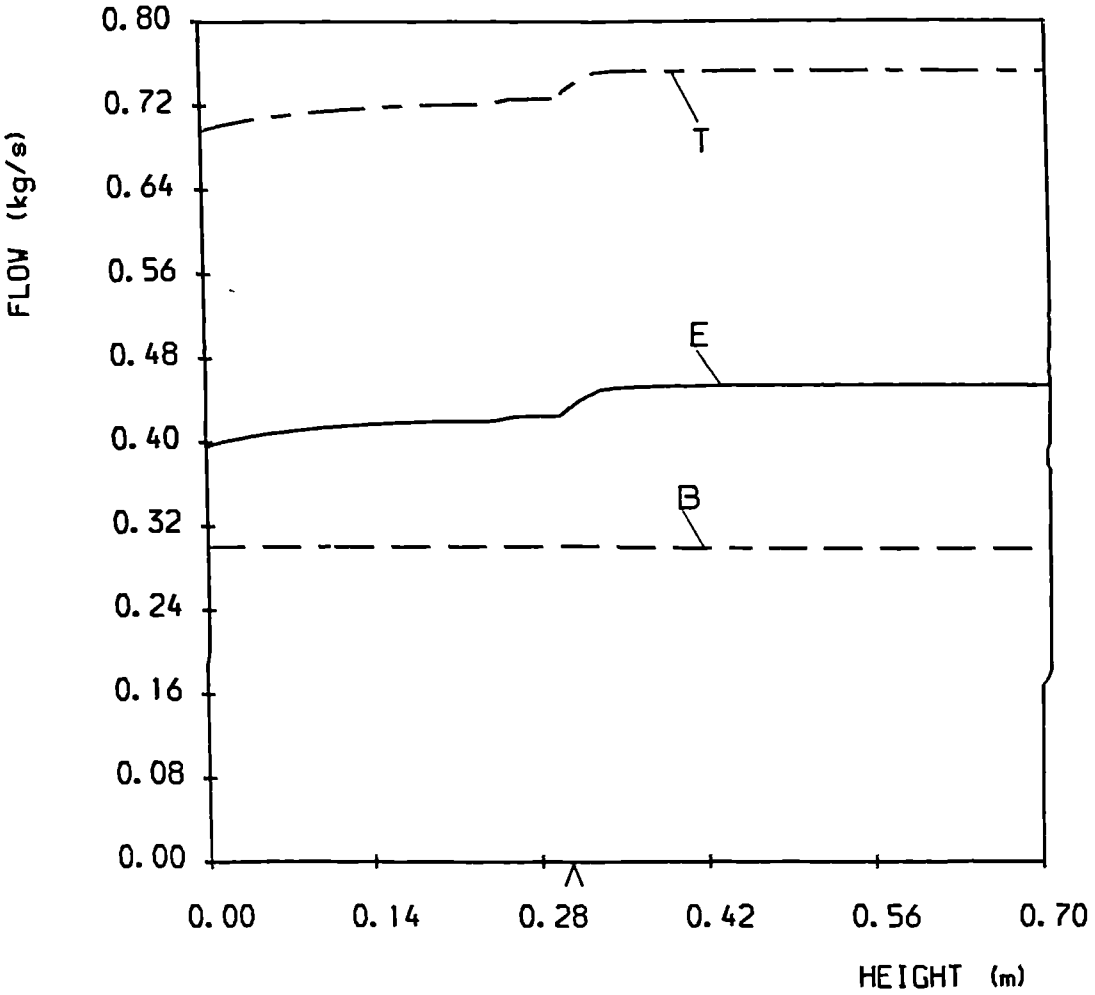

FIGURE 5.15. GAS FLOWS IN THE BED-B&W, TEST 26
(E=EMULSION PHASE, B=BUBBLE PHASE, T=TOTAL,
^ =COAL FEEDING POINT).

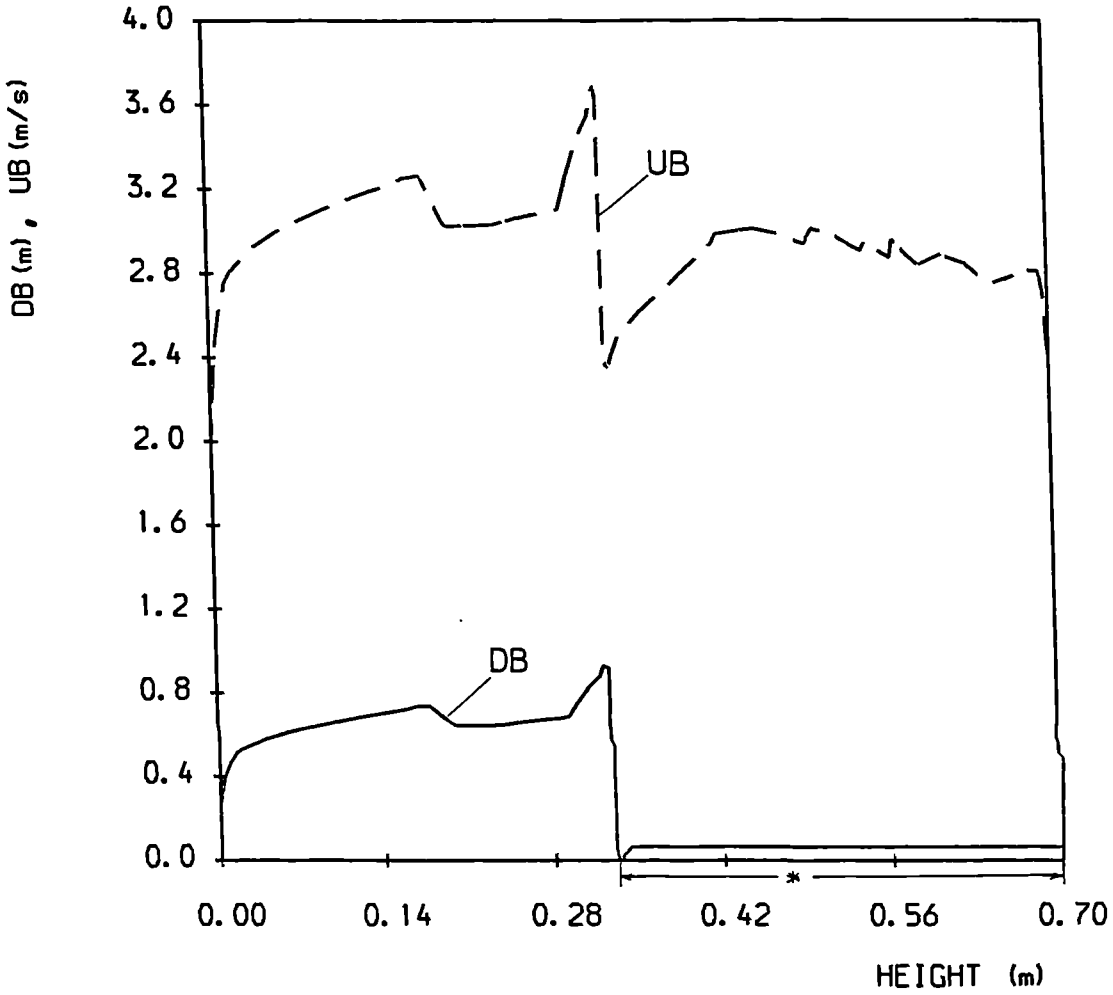

FIGURE 5.16. BUBBLE DIAMETER AND VELOCITY IN THE BED-B&W, TEST 26 (DB=DIAMETER, UB=VELOCITY, * =TUBE BANK REGION).

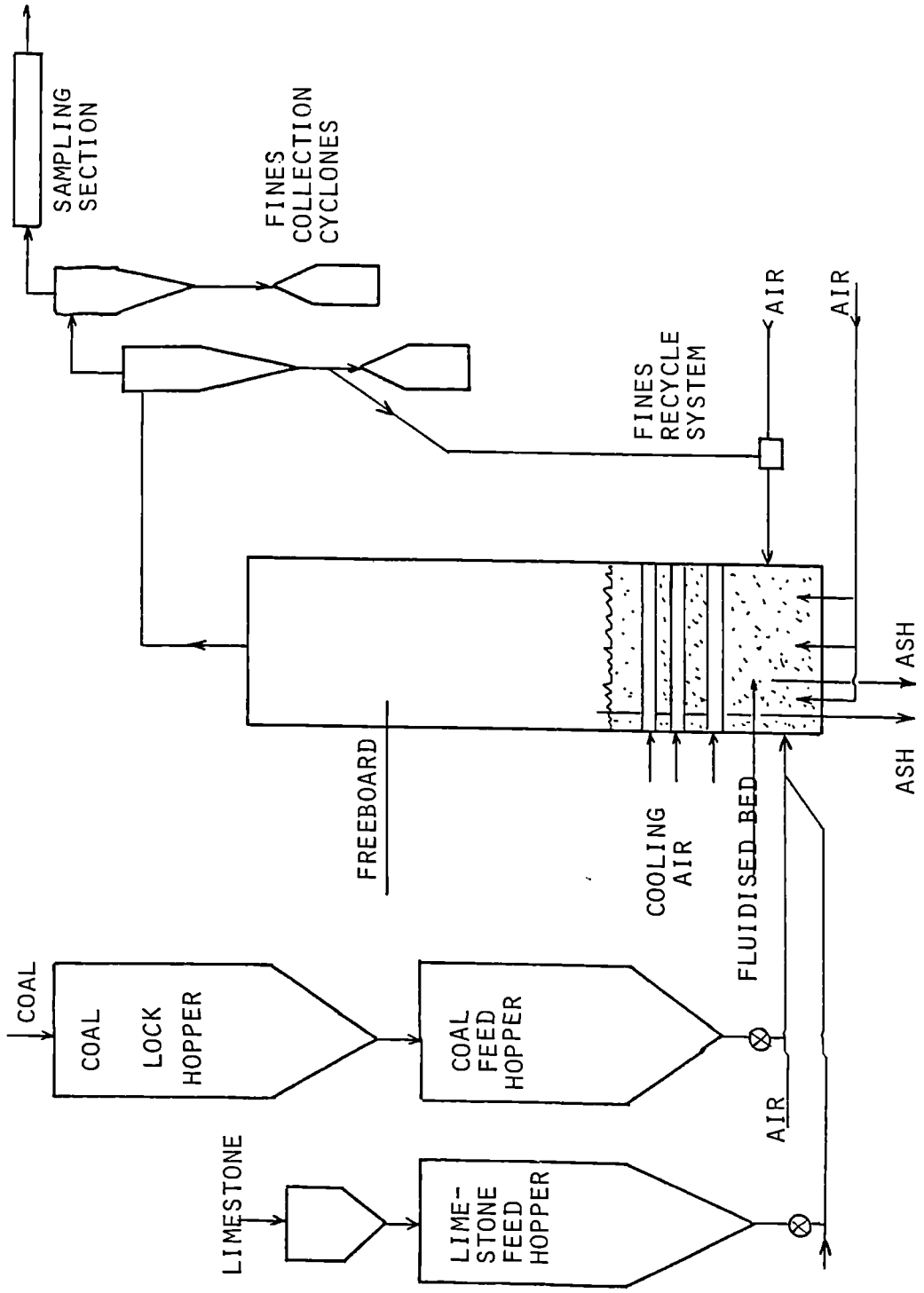

FIGURE 5.17. SCHEMATIC VIEW OF THE NATIONAL COAL BOARD TEST RIG.

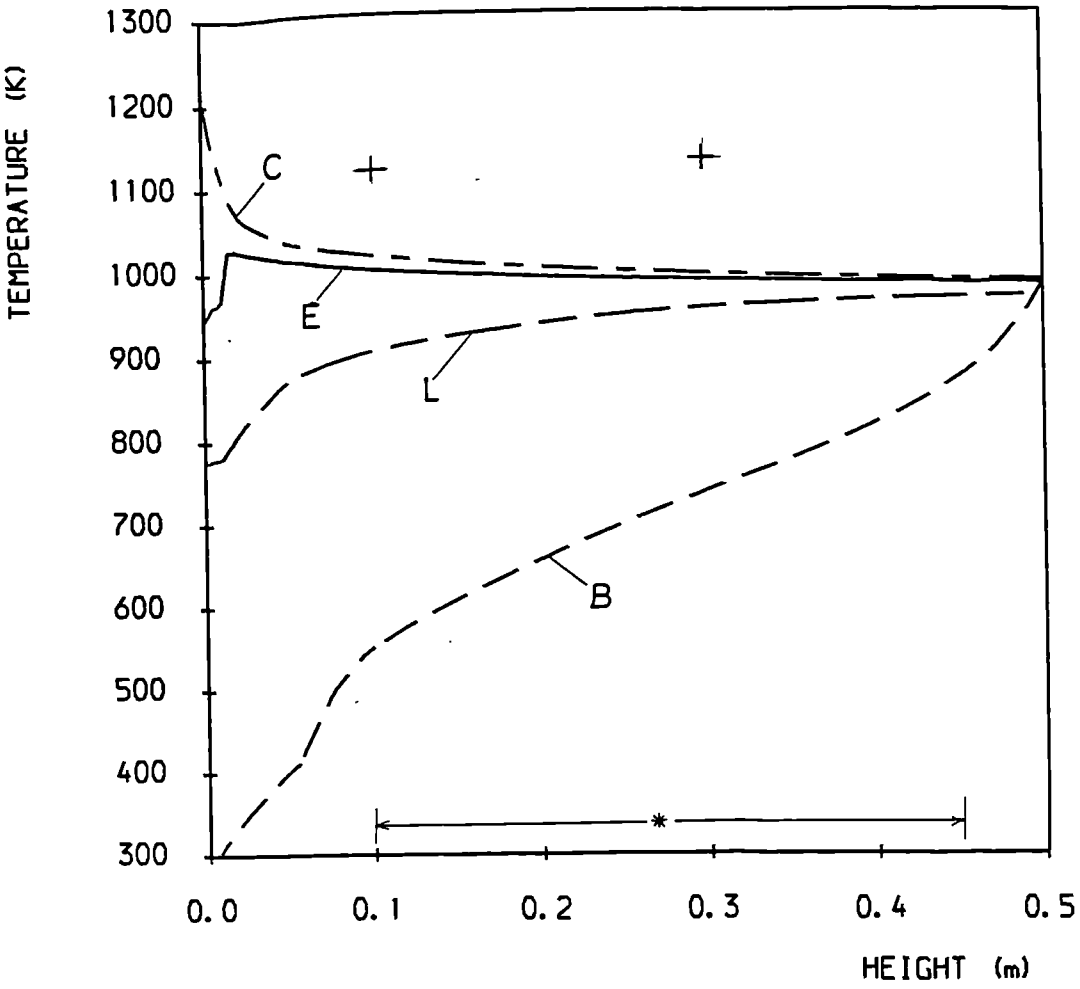

FIGURE 5.18. BED TEMPERATURE PROFILES-NCB, TEST 3
(E=EMULSION GAS, B=BUBBLE GAS, C=COAL, L=LIMESTONE,
+ =MEASURED AVERAGE, * =TUBE BANK REGION)

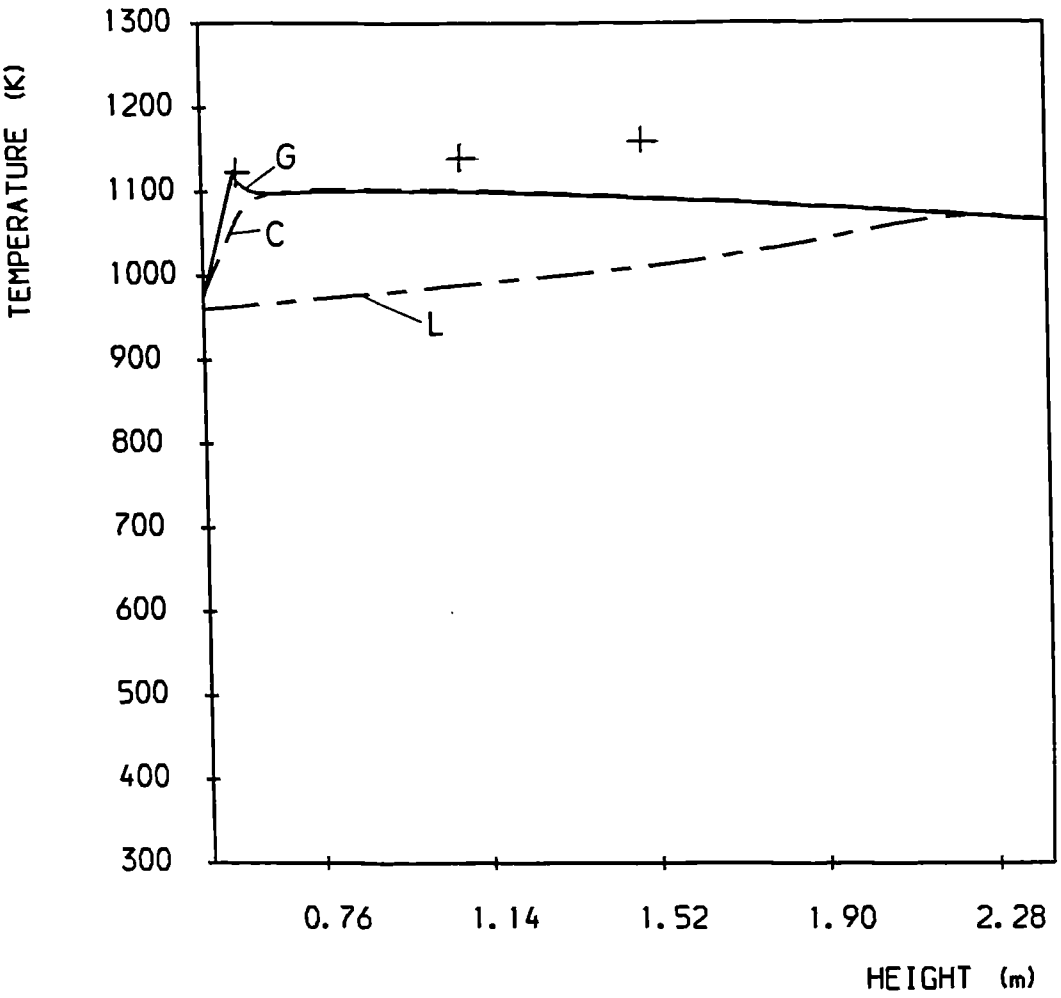

FIGURE 5.19. FREEBOARD TEMPERATURE PROFILES-NCB, TEST 3 (G=GAS, C=COAL, L=LIMESTONE, + =MEASURED AVERAGE)

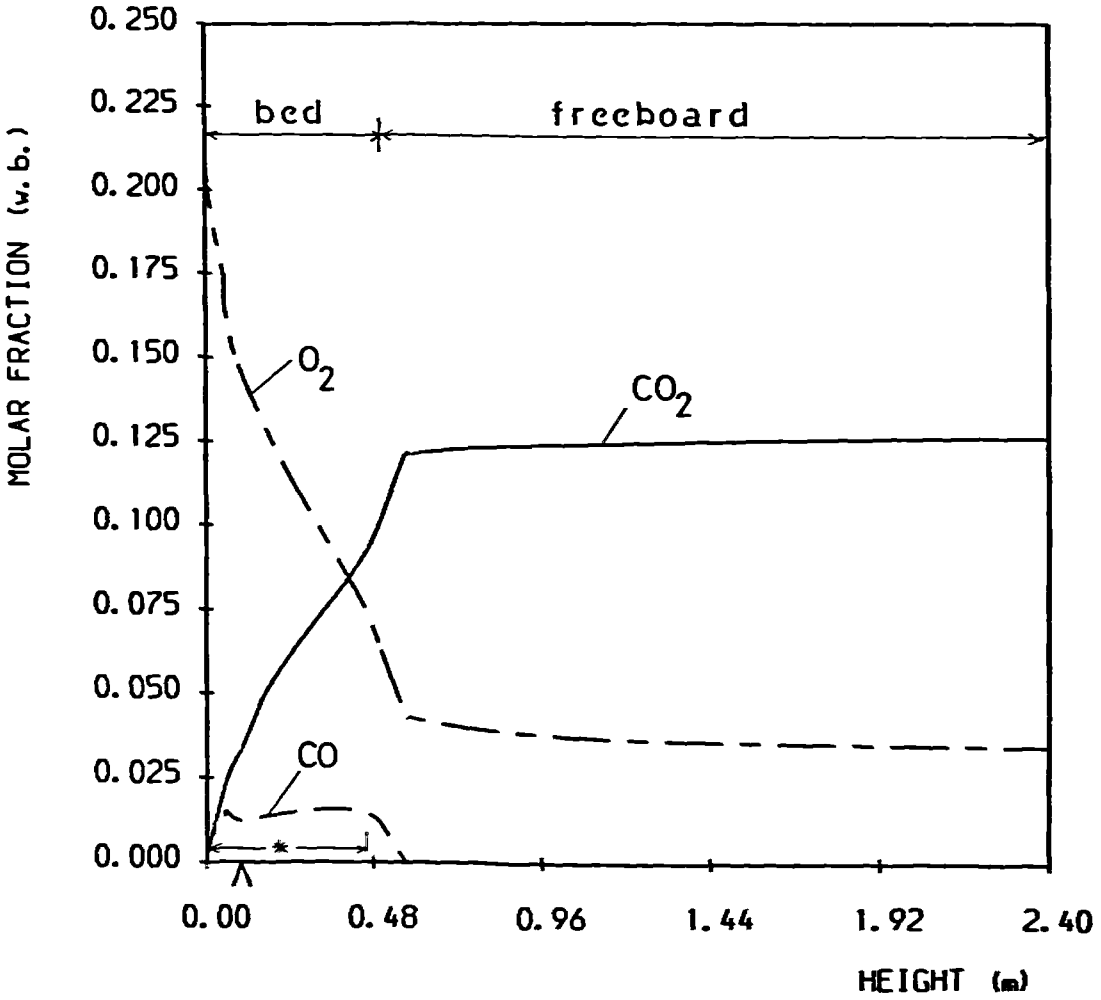

FIGURE 5.20. CONCENTRATION PROFILES IN THE SYSTEM-NCB, TEST 3 (CO2, CO, O2, ^ =COAL FEEDING POINT, * =TUBE BANK REGION).

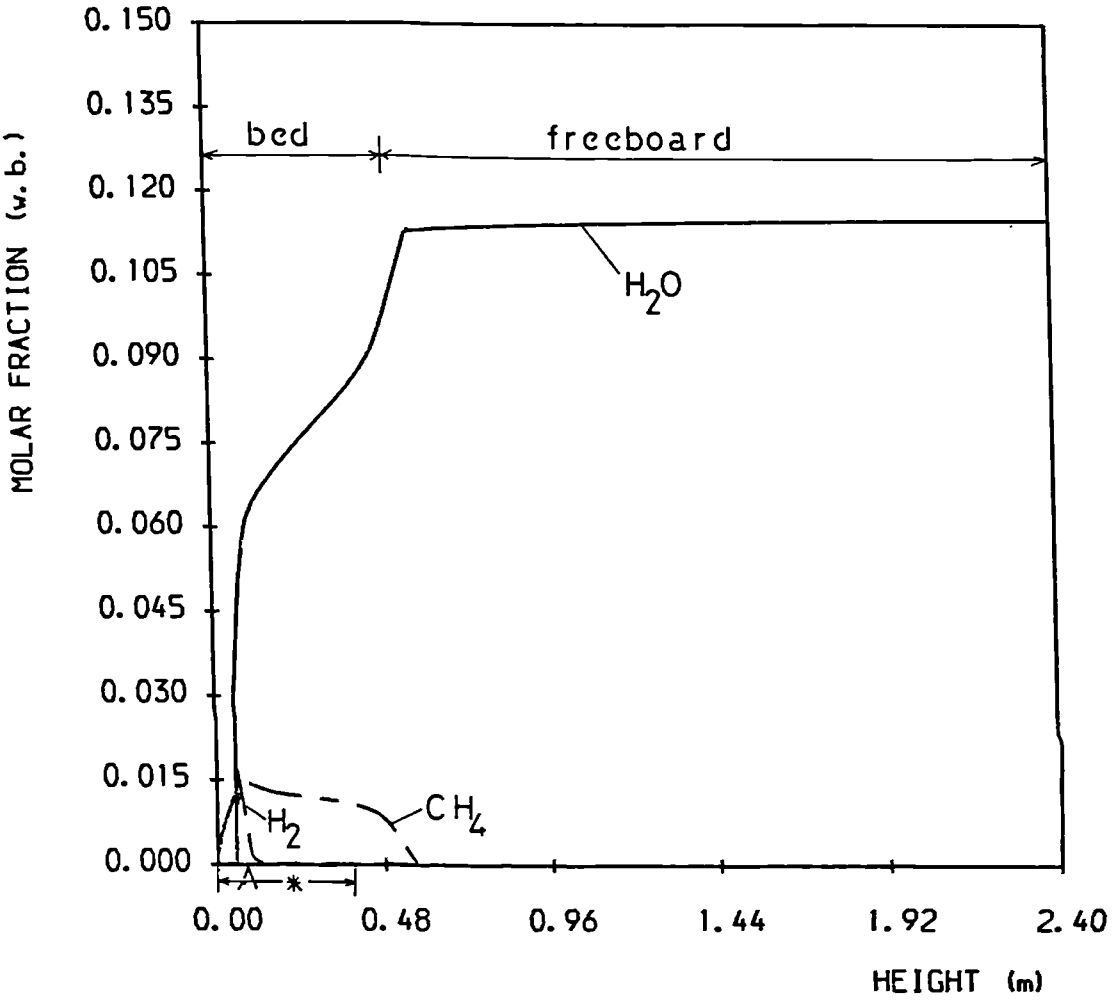

FIGURE 5.21. CONCENTRATION PROFILES IN THE SYSTEM-NCB, TEST 3 (H2O, H2, CH4, ^ =COAL FEEDING POINT, * =TUBE BANK REGION).

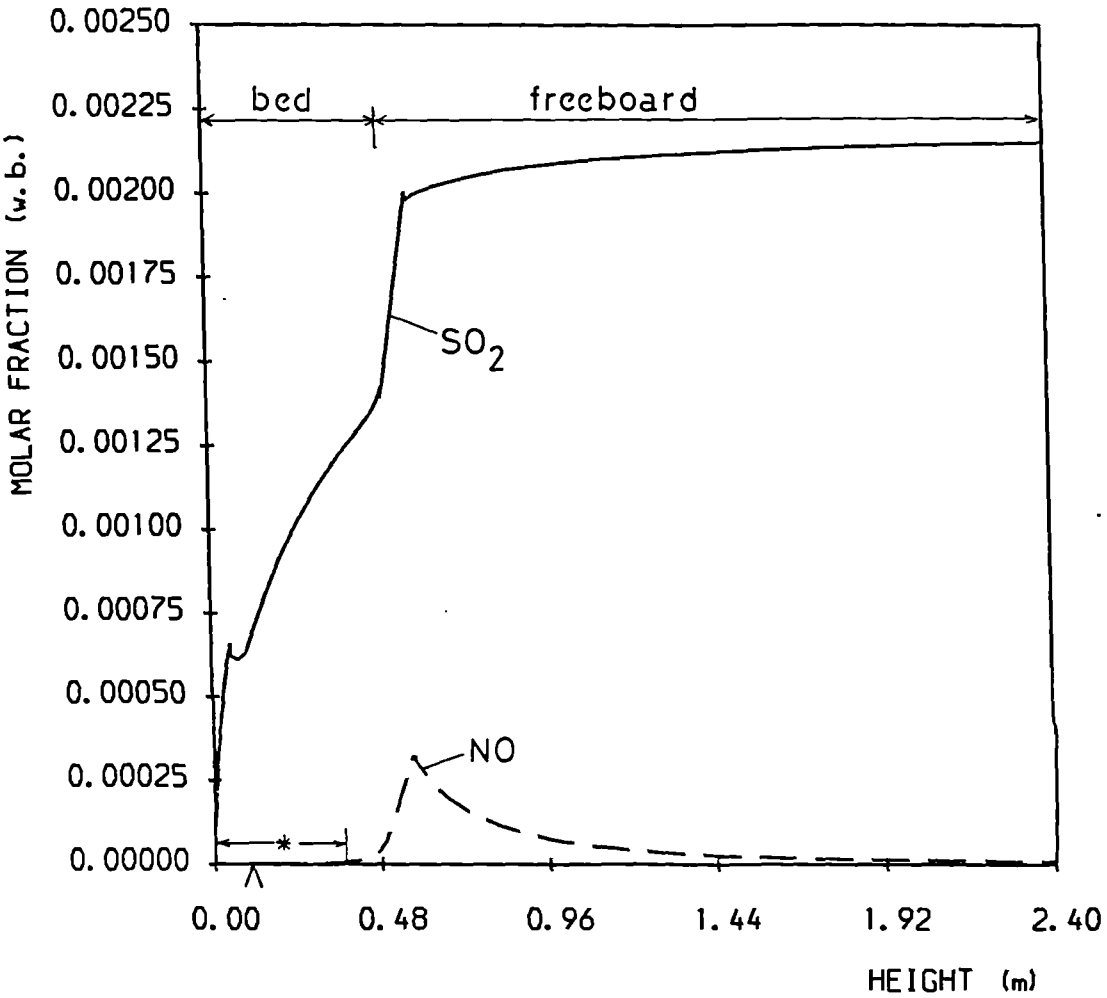

FIGURE 5.22. CONCENTRATION PROFILES IN THE SYSTEM-NCB, TEST 3 (SO2, NO, C2H6), ^ =COAL FEEDING POINT, * =TUBE BANK REGION).

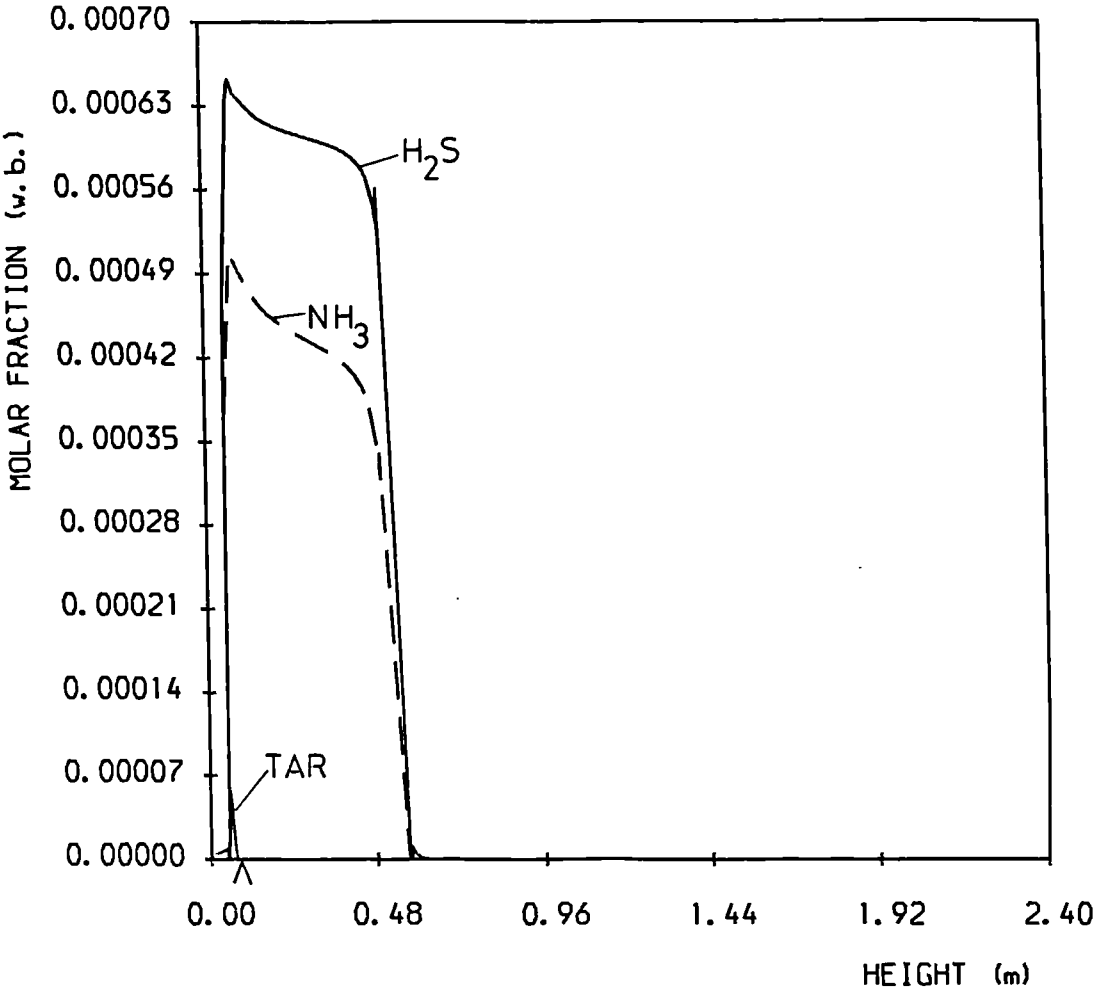

FIGURE 5.23. CONCENTRATION PROFILES IN THE SYSTEM-NCB, TEST 3 (H2S, NH3, TAR, ^ =COAL FEEDING POINT).

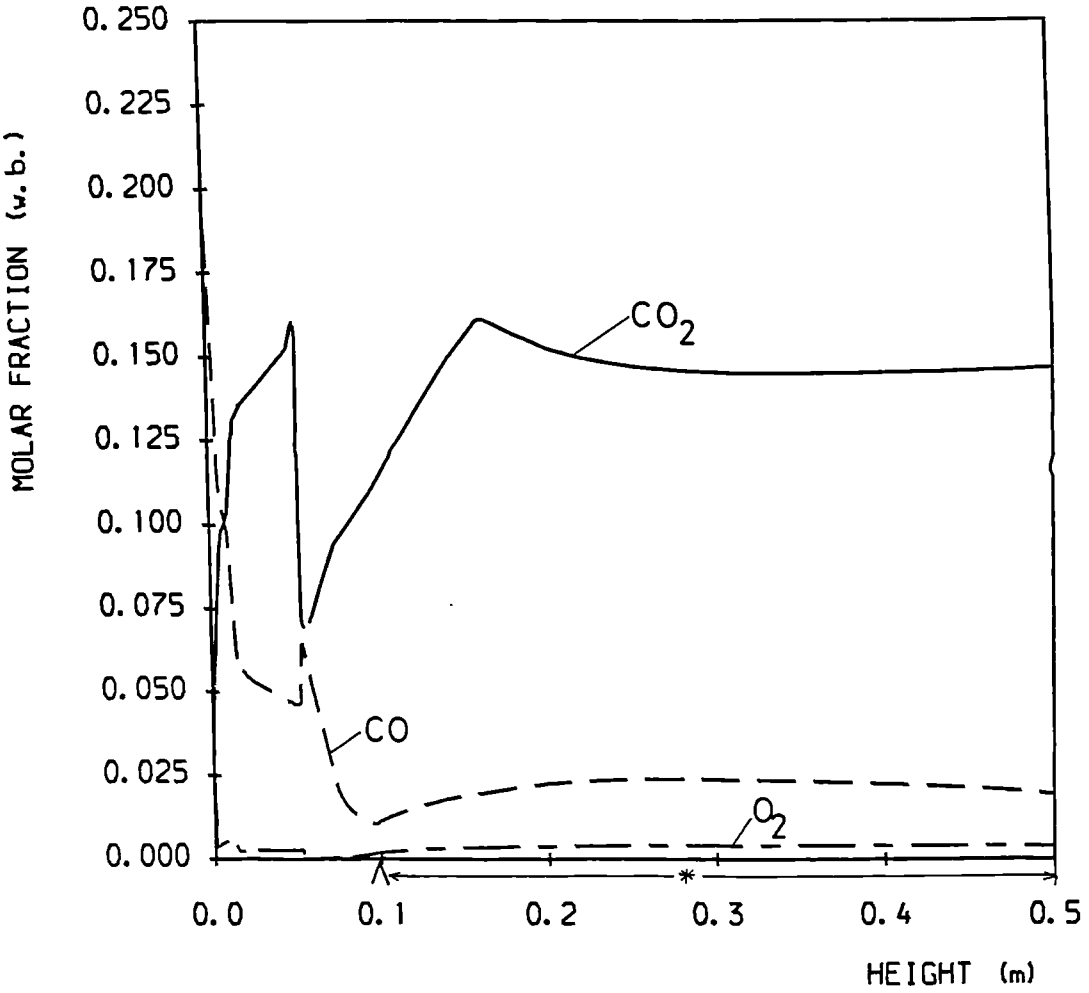

FIGURE 5.24. CONCENTRATION PROFILES IN THE EMULSION PHASE-NCB, TEST 3 (CO2, CO, O2, ^ =COAL FEEDING POINT, * =TUBE BANK REGION)

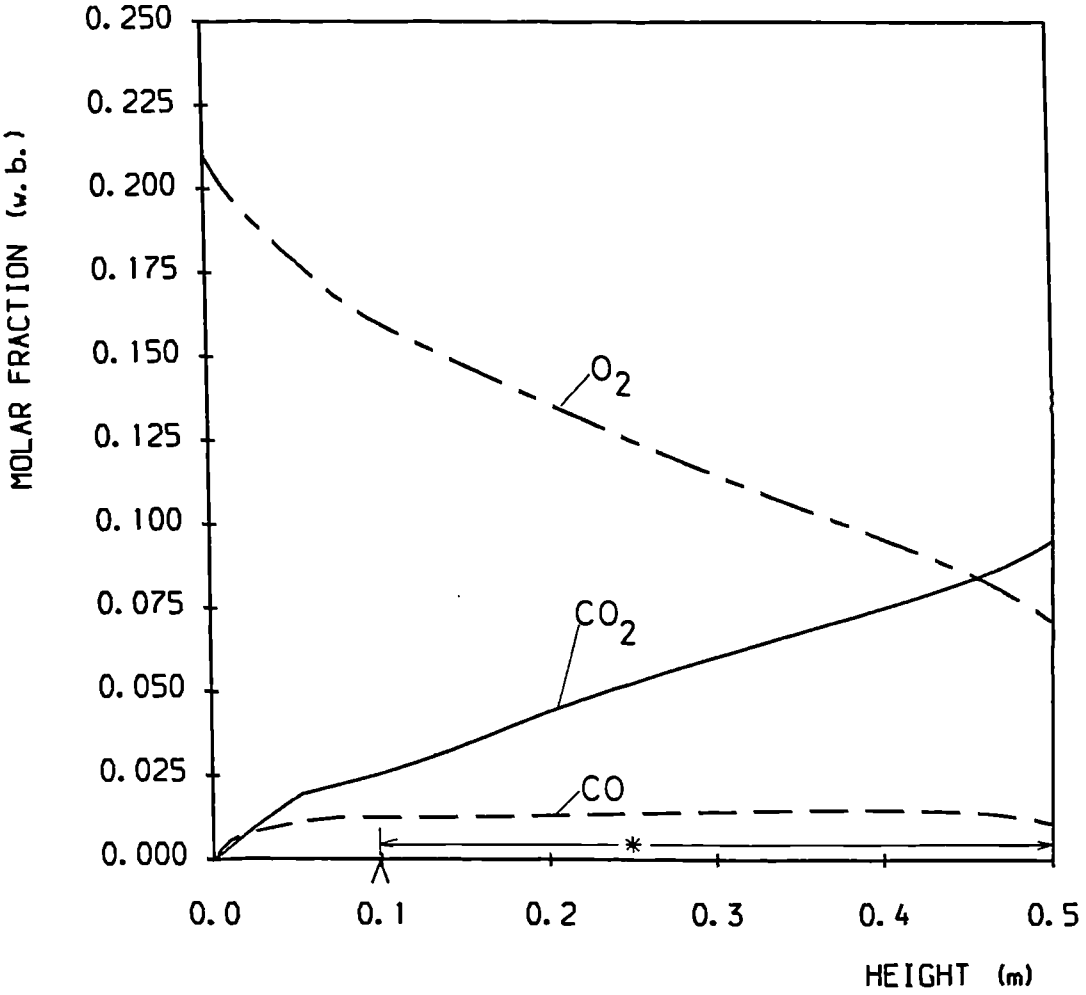

FIGURE 5.25. CONCENTRATION PROFILES IN THE BUBBLE PHASE-NCB, TEST 3 (CO2, CO, O2, ^ =COAL FEEDING POINT, * =TUBE BANK REGION).

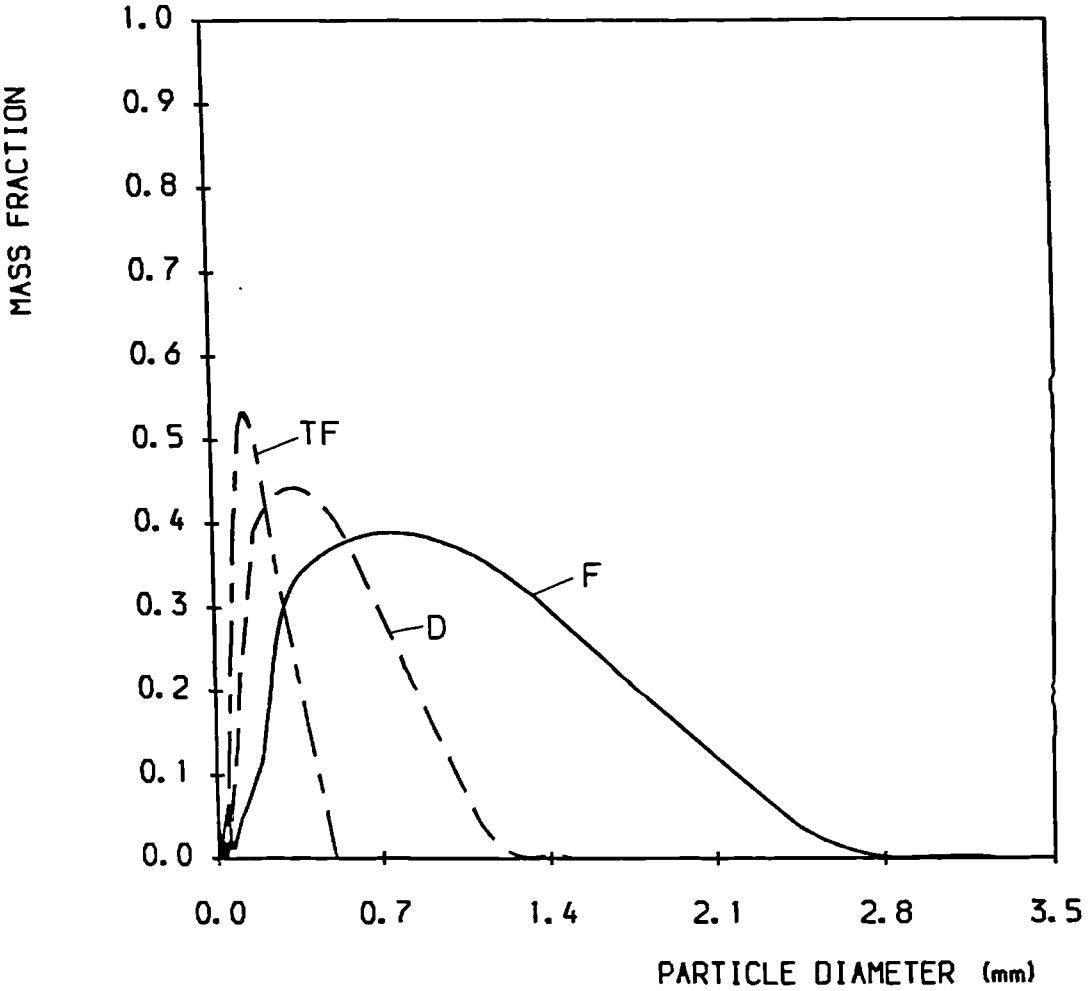

FIGURE 5.26. COAL PARTICLE SIZE DISTRIBUTION-NCB, TEST 3 (F=AS FED TO THE BED, D=IN THE BED, TF=AT THE TOP OF THE FREEBOARD)

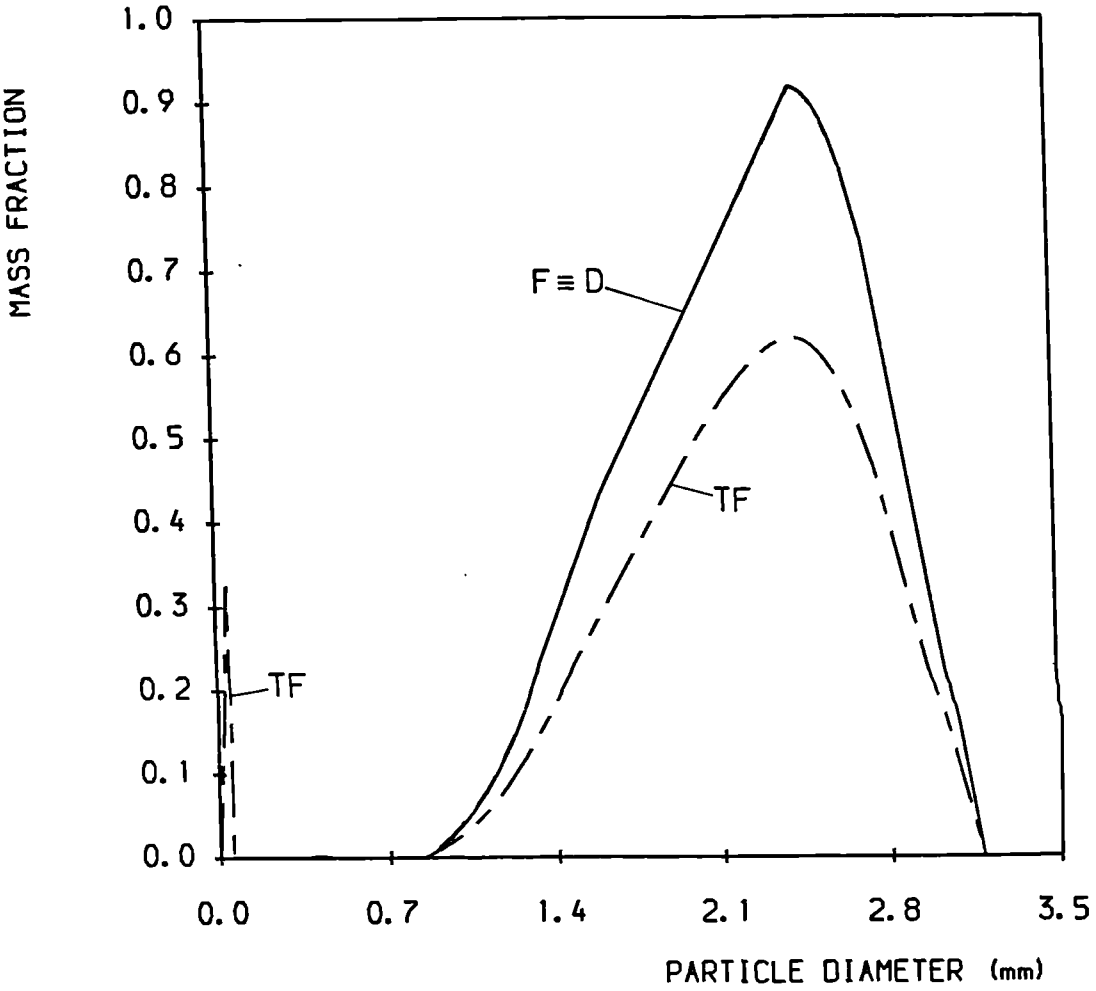

FIGURE 5.27. LIMESTONE PARTICLE SIZE DISTRIBUTION-NCB, TEST 3 (F=AS FED, D=BED, TF=AT THE TOP OF THE FREEBOARD)

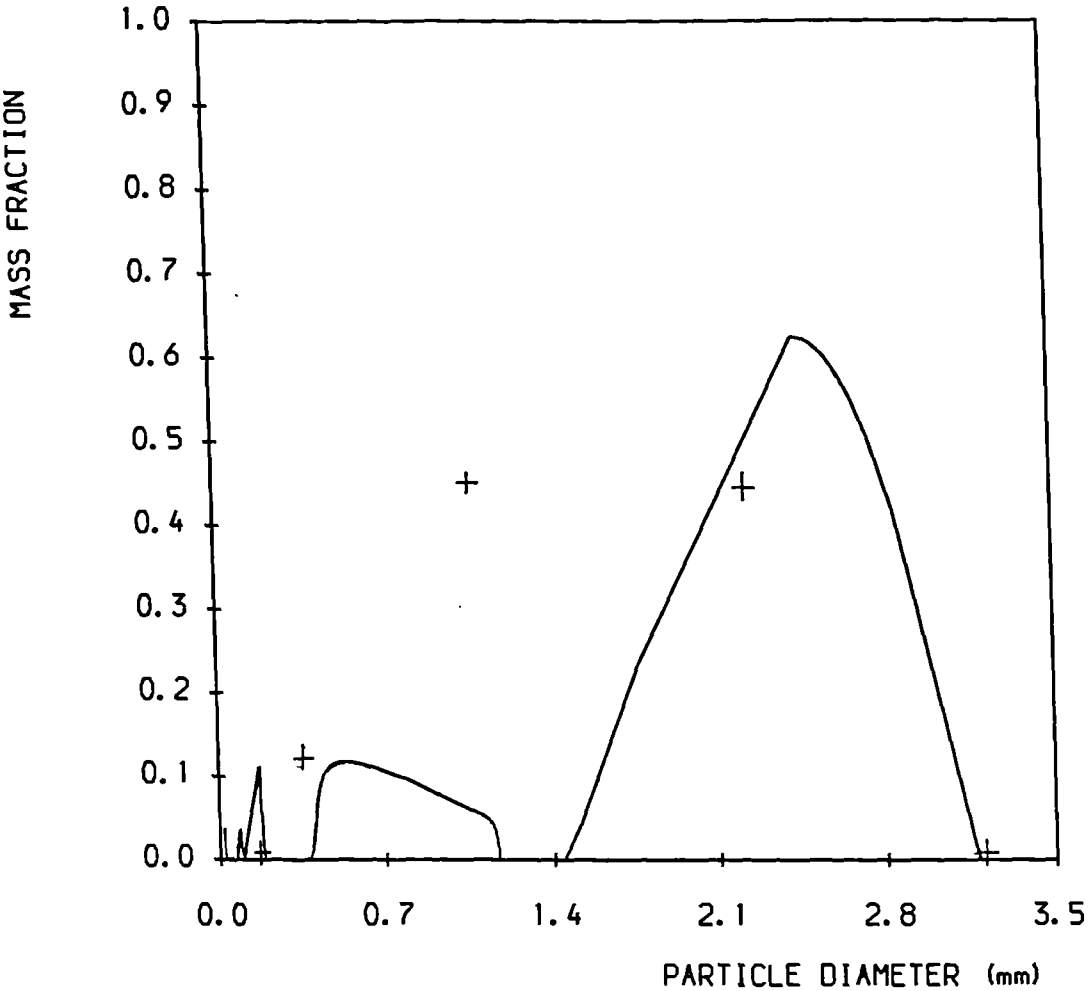

FIGURE 5.28. TOTAL PARTICLE SIZE DISTRIBUTION-NCB, TEST 3 (AVERAGE IN THE BED)
(+ =EXPERIMENTAL DETERMINATIONS)

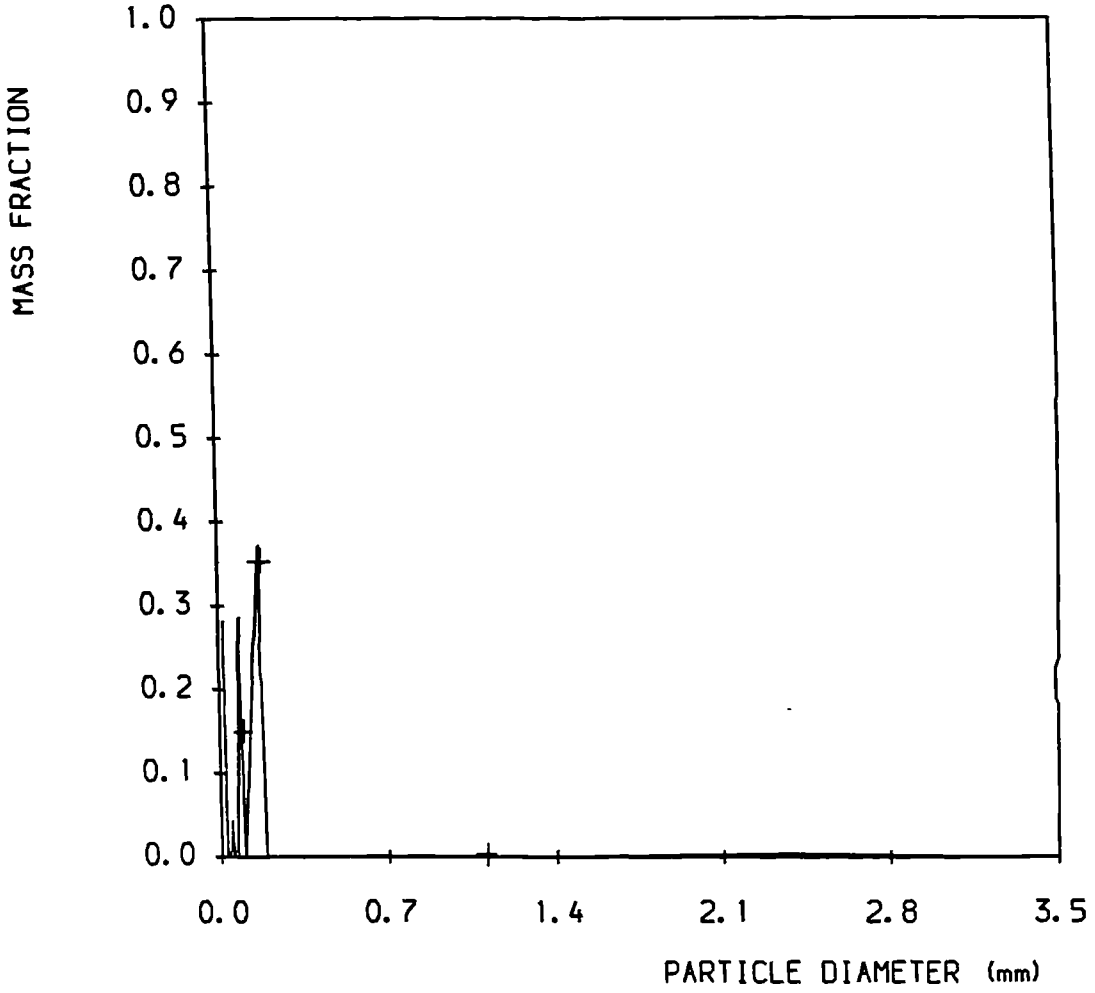

FIGURE 5.29. TOTAL PARTICLE SIZE DISTRIBUTION-NCB, TEST 3 (AT THE TOP OF THE FREEBOARD).
(+ =EXPERIMENTAL DETERMINATIONS)

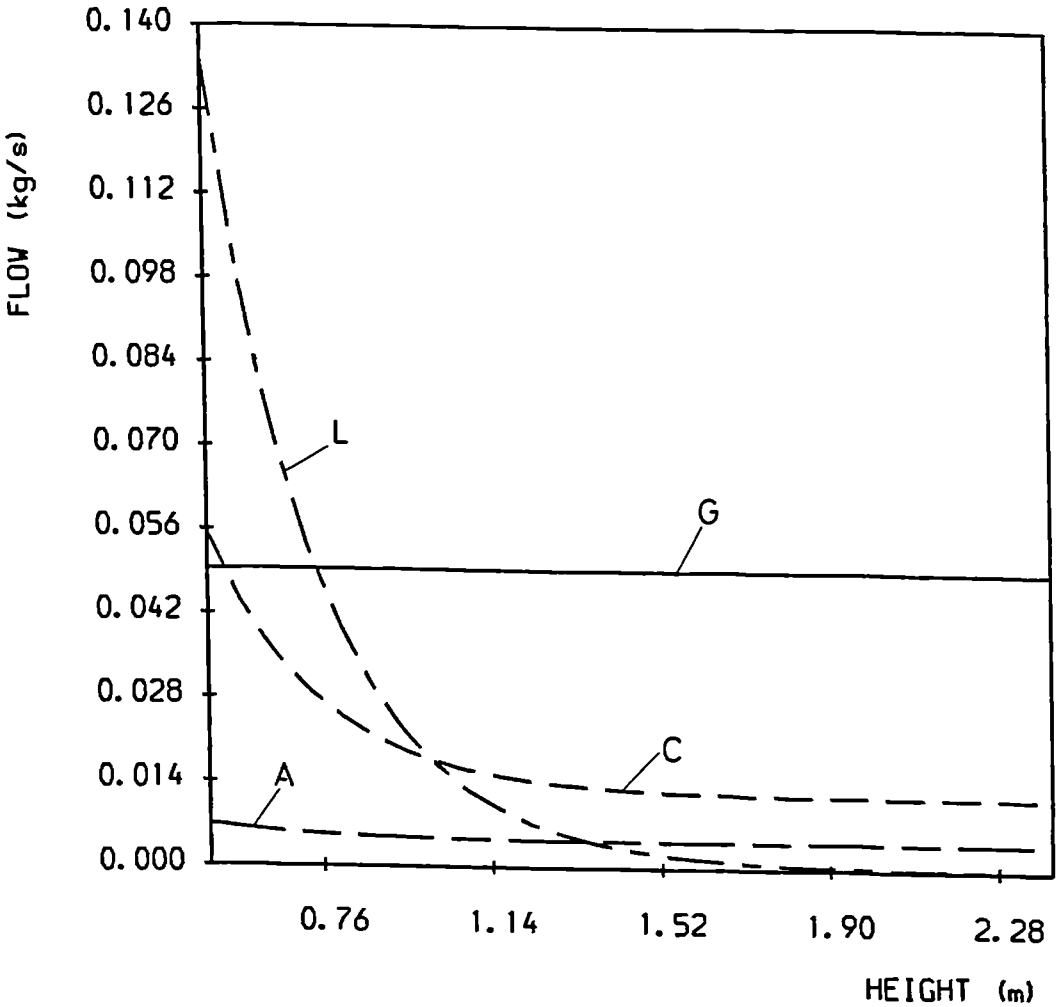

FIGURE 5.30. GAS AND SOLID FLOWS IN THE FREEBOARD-NCB, TEST 3 (G=GAS, C=COAL, L=LIMEST., A=FREE ASH).

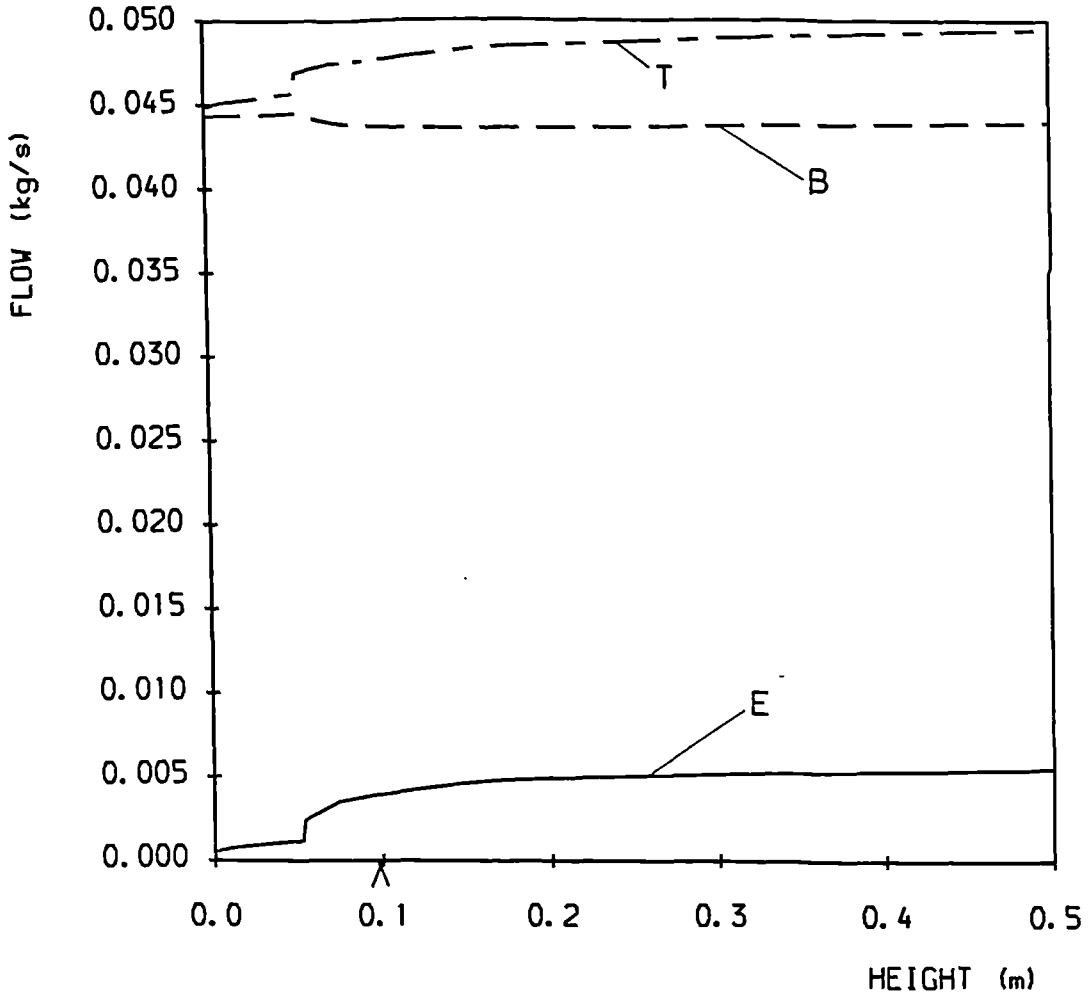

FIGURE 5.31. GAS FLOWS IN THE BED-NCB, TEST 3
(E=EMULSION PHASE, B=BUBBLE PHASE, T=TOTAL,
^ =COAL FEEDING POINT).

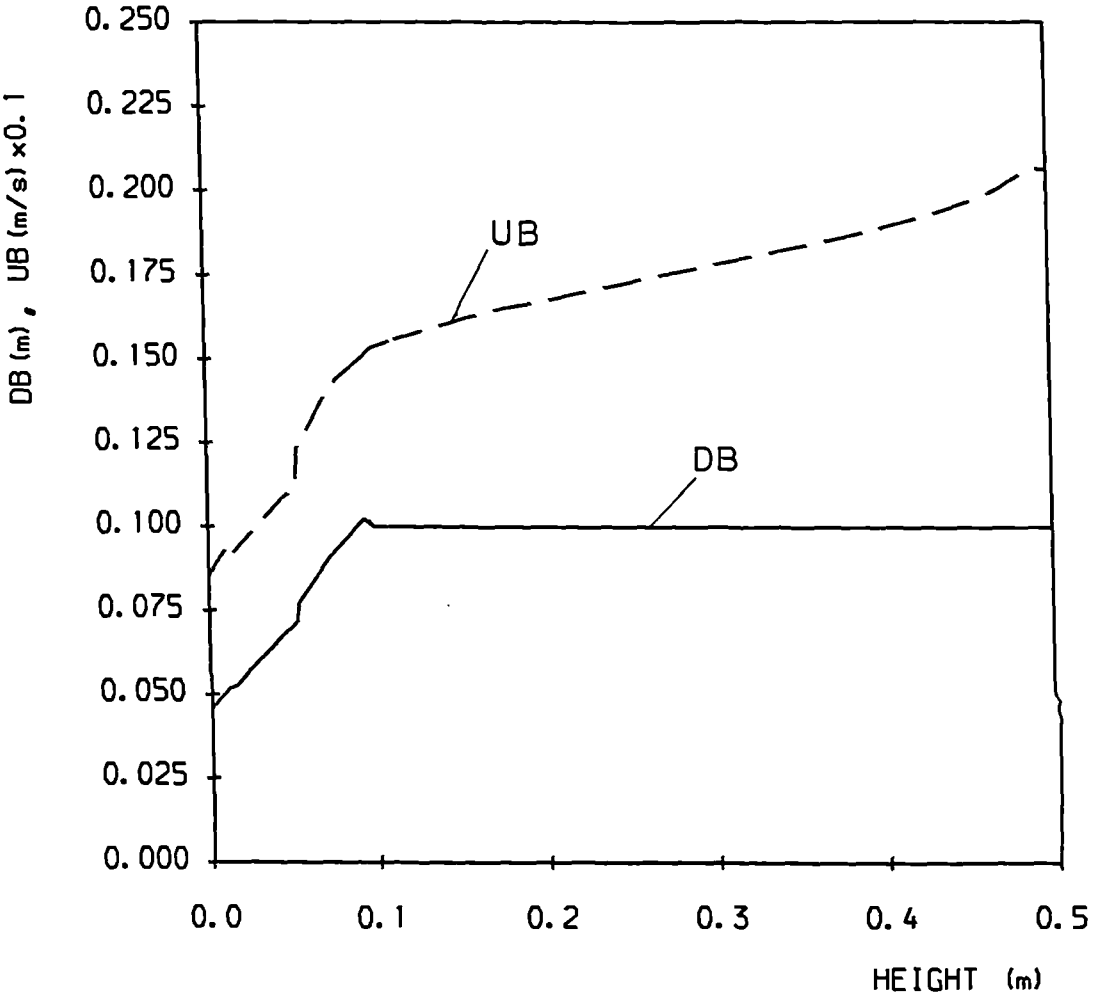

FIGURE 5.32. BUBBLE DIAMETER AND VELOCITY IN THE BED-NCB, TEST 3 (DB=DIAMETER, UB=VELOCITY (sc:0.1), * =TUBE BANK REGION).

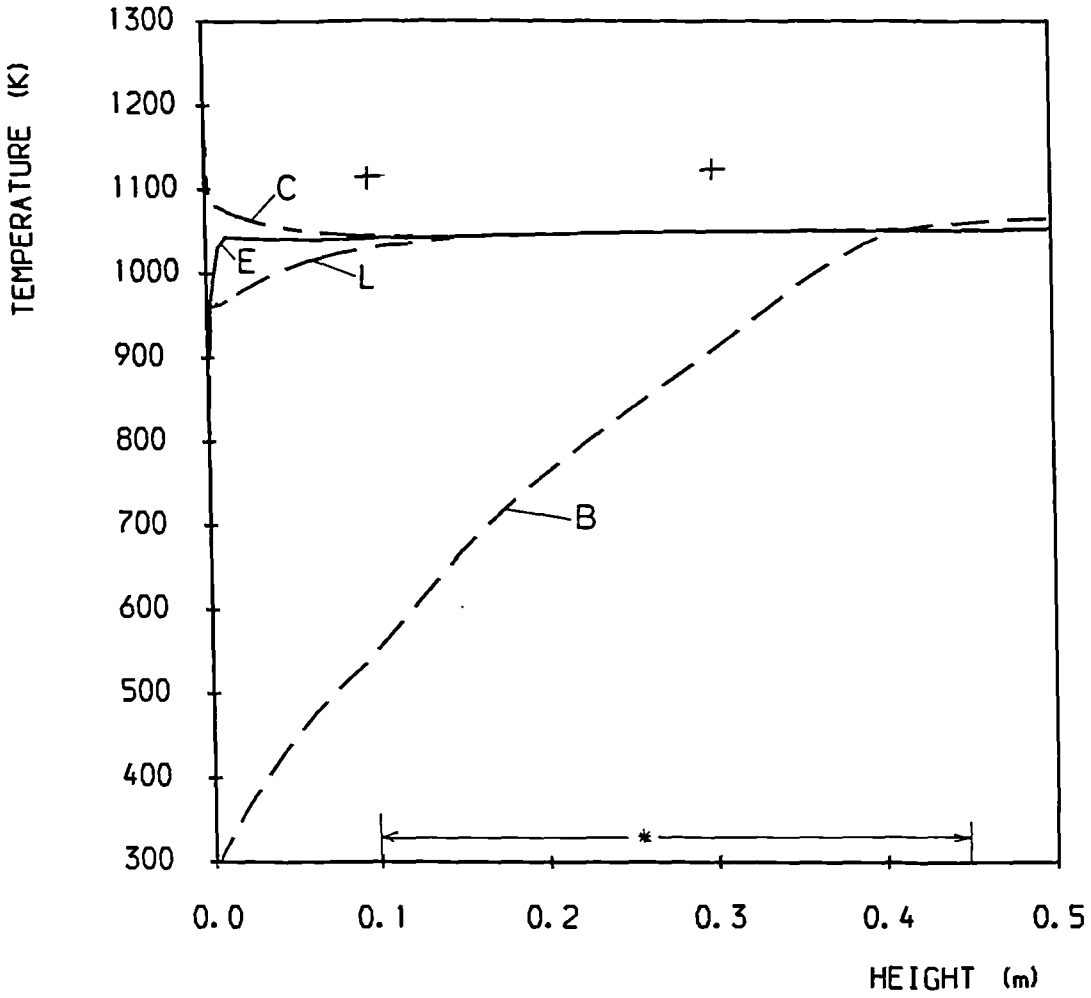

FIGURE 5.33. BED TEMPERATURE PROFILES-NCB, TEST 6
(E=EMULSION GAS, B=BUBBLE GAS, C=COAL, L=LIMESTONE,
+ =MEASURED AVERAGE, * =TUBE BANK REGION)

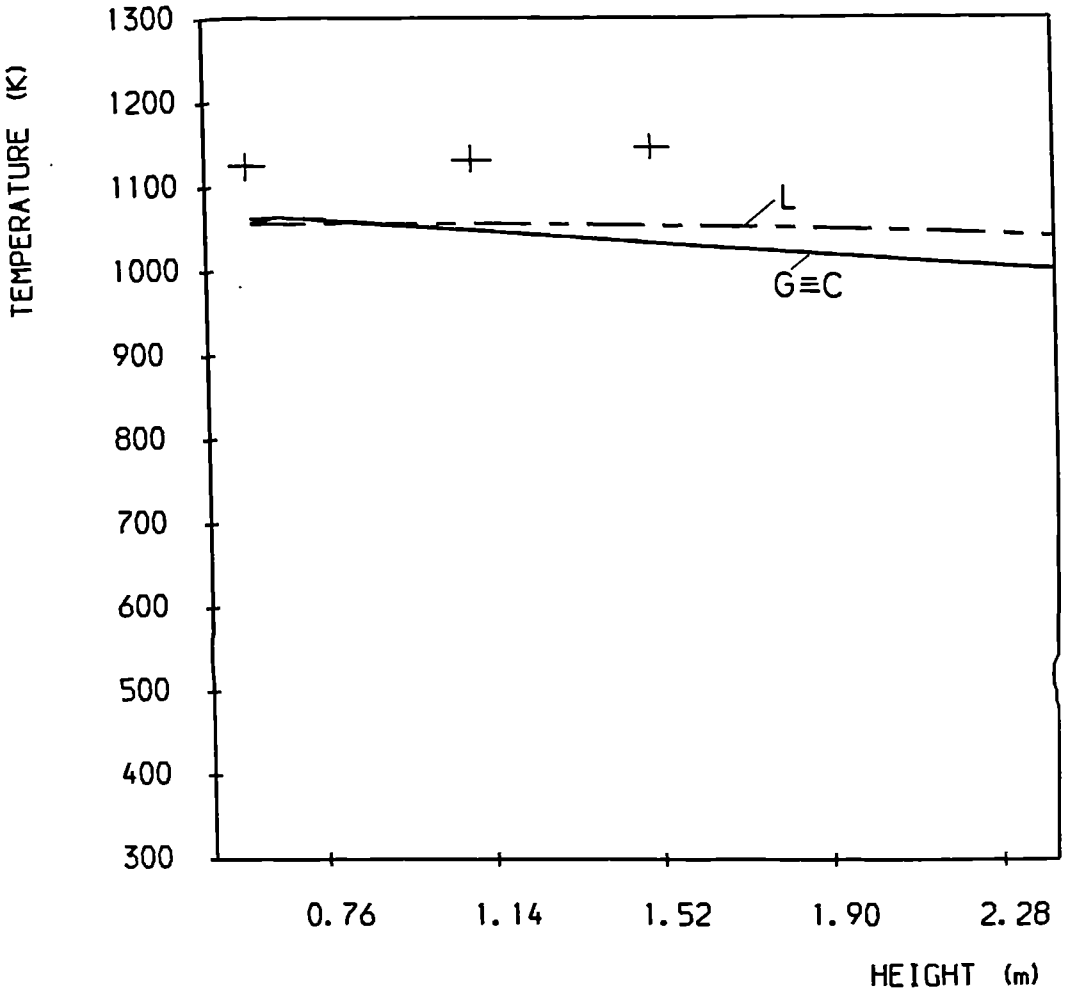

FIGURE 5.34. FREEBOARD TEMPERATURE PROFILES-NCB, TEST 6 (G=GAS, C=COAL, L=LIMESTONE, + =MEASURED AVERAGE)

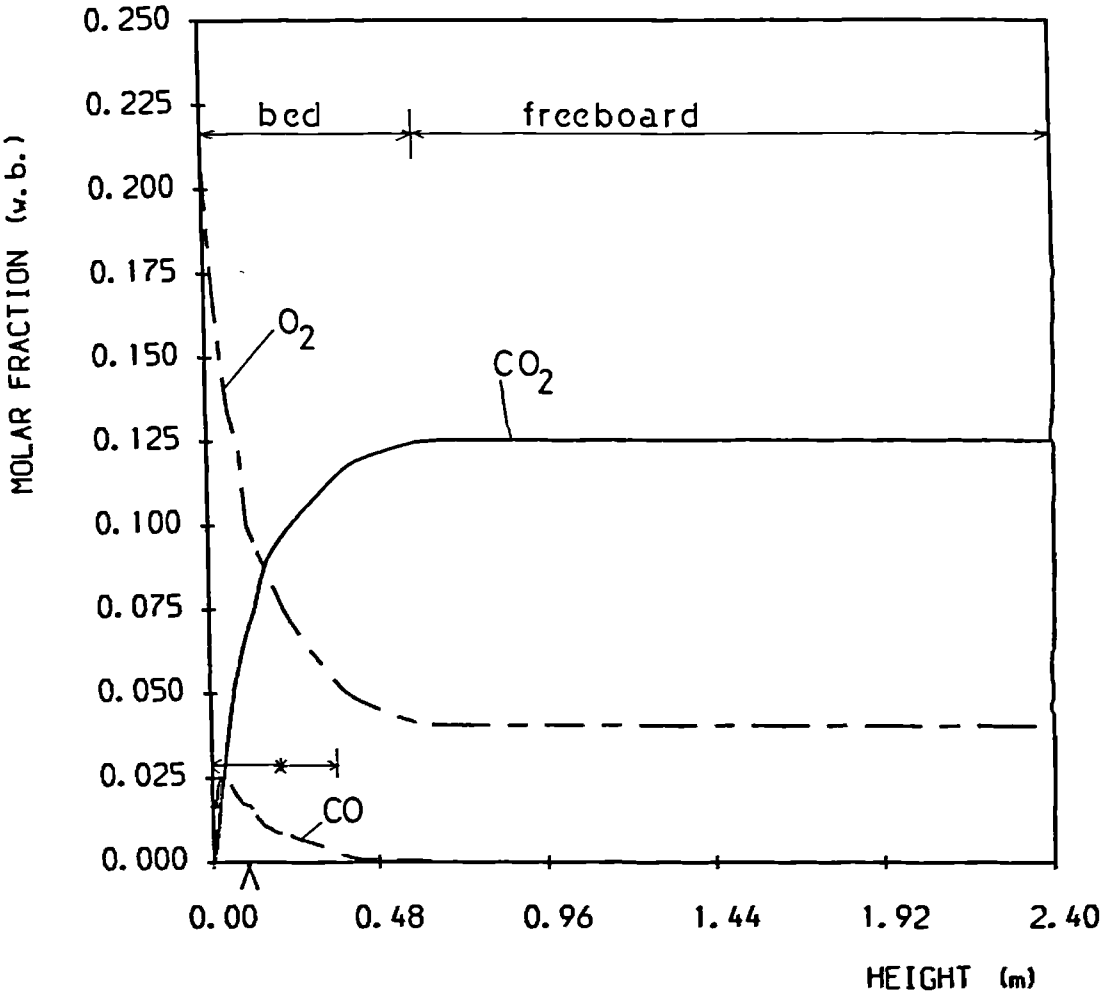

FIGURE 5.35. CONCENTRATION PROFILES IN THE SYSTEM-NCB, TEST 6 (CO2, CO, O2, ^ =COAL FEEDING POINT, * =TUBE BANK REGION).

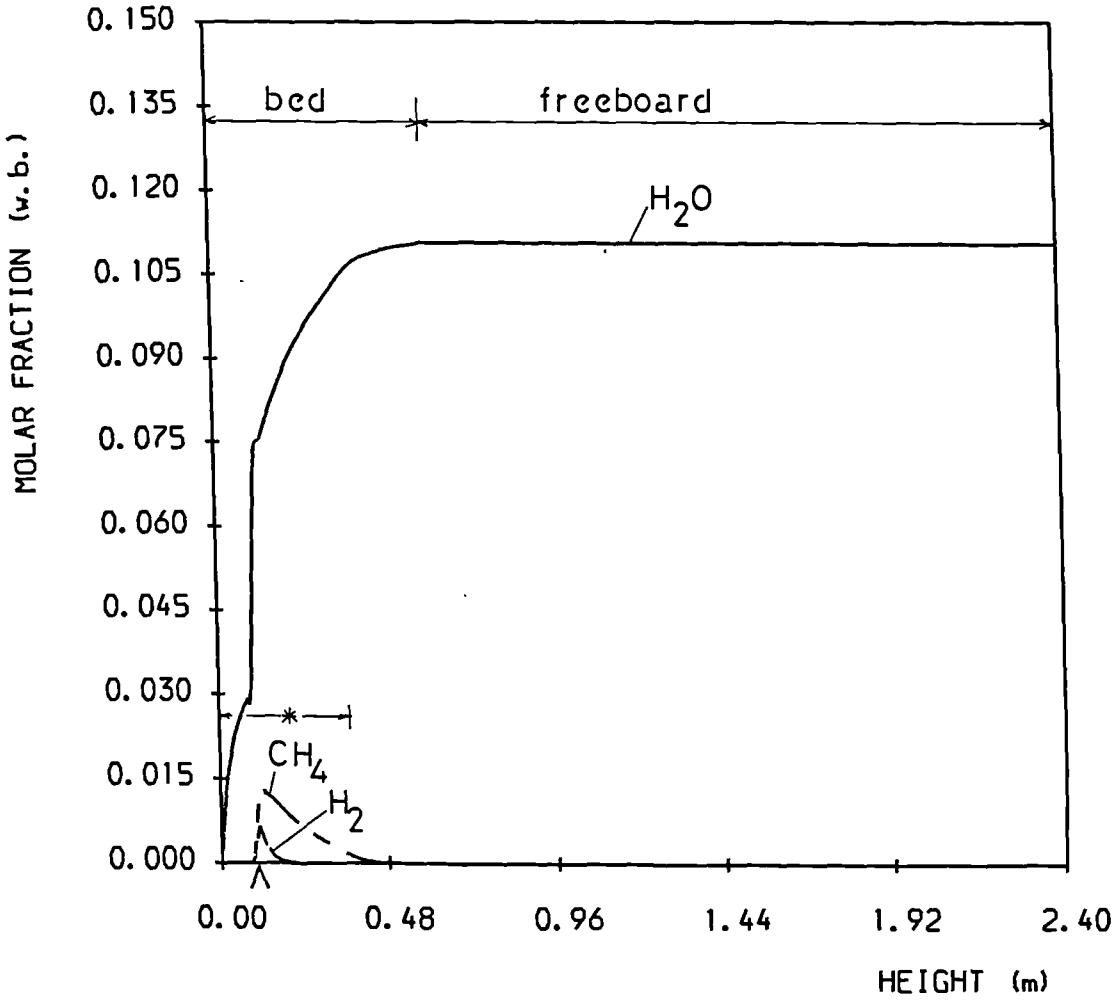

FIGURE 5.36. CONCENTRATION PROFILES IN THE SYSTEM-NCB, TEST 6 (H2O, H2, CH4, ^ =COAL FEEDING POINT, * =TUBE BANK REGION).

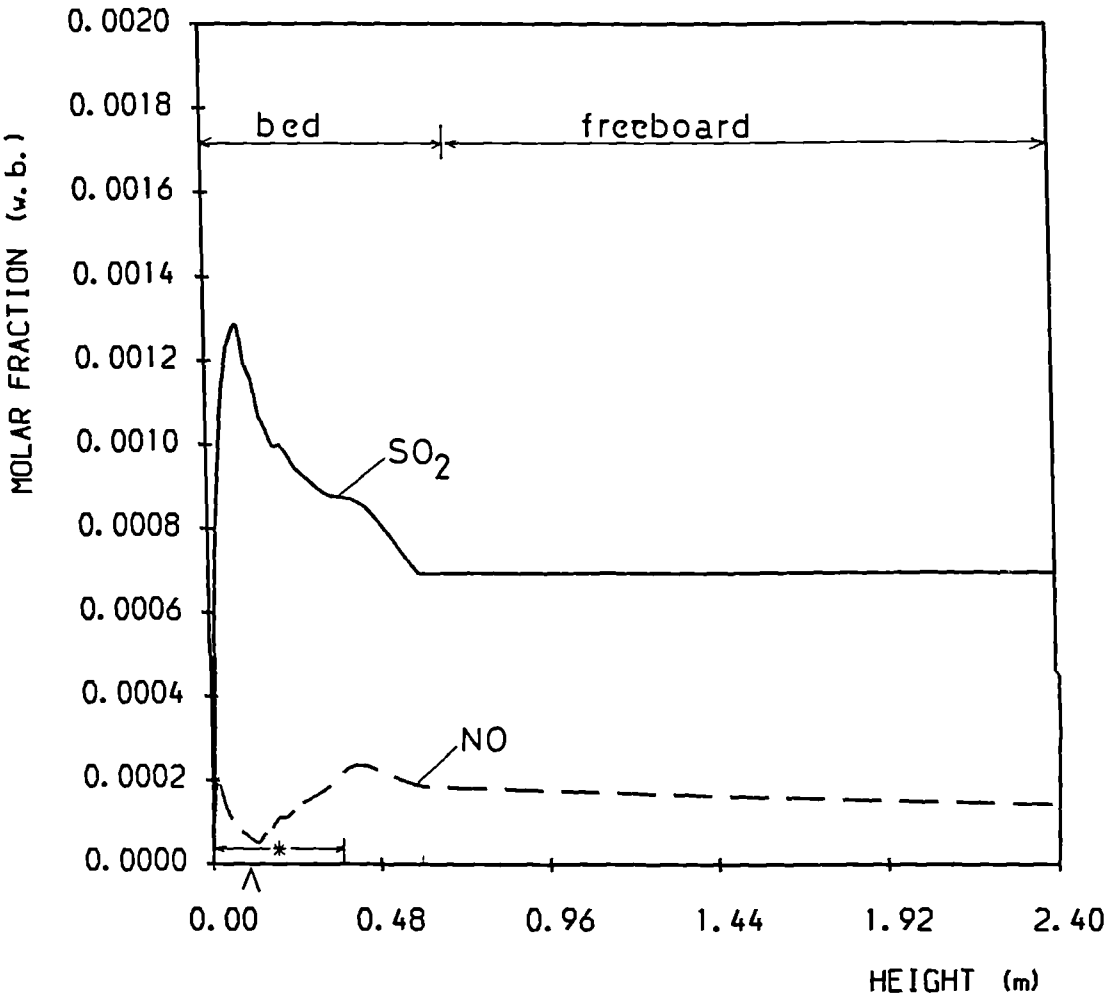

FIGURE 5.37. CONCENTRATION PROFILES IN THE SYSTEM-NCB, TEST 6 (SO2, NO, C2H6), ^ =COAL FEEDING POINT, * =TUBE BANK REGION).

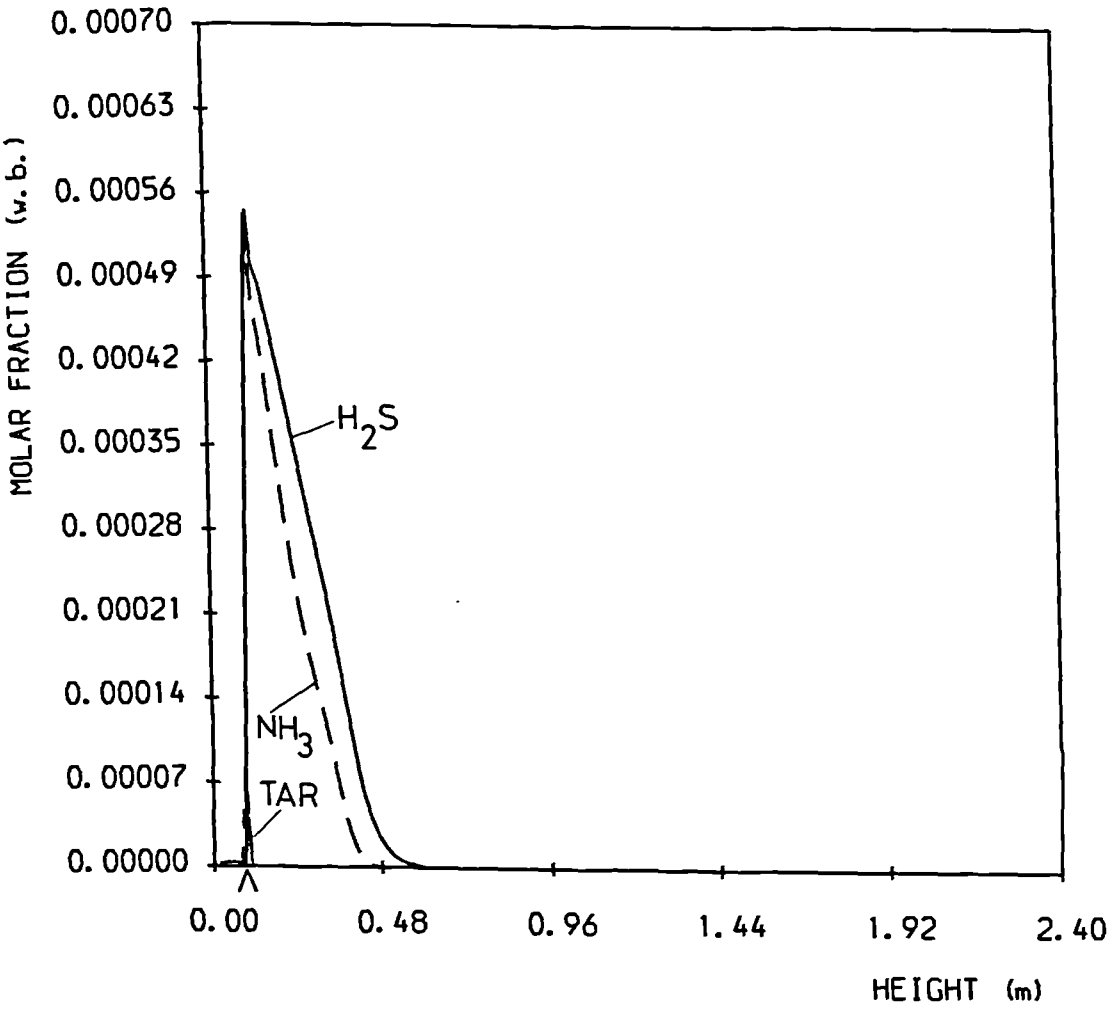

FIGURE 5.38. CONCENTRATION PROFILES IN THE SYSTEM-NCB, TEST 6 (H2S, NH3, TAR, ^ =COAL FEEDING POINT).

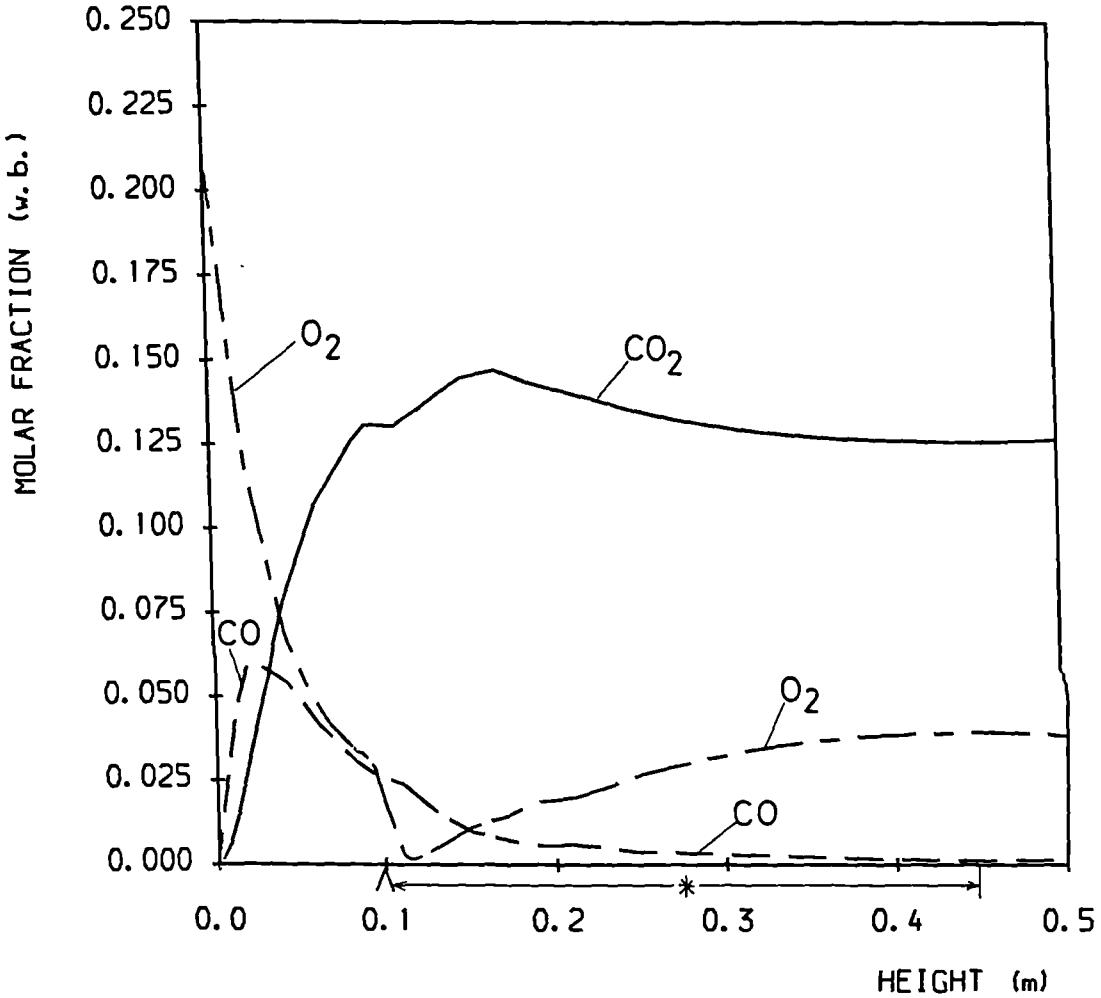

FIGURE 5.39. CONCENTRATION PROFILES IN THE EMULSION PHASE-NCB, TEST 6 (CO2, CO, O2, ^ =COAL FEEDING POINT, * =TUBE BANK REGION)

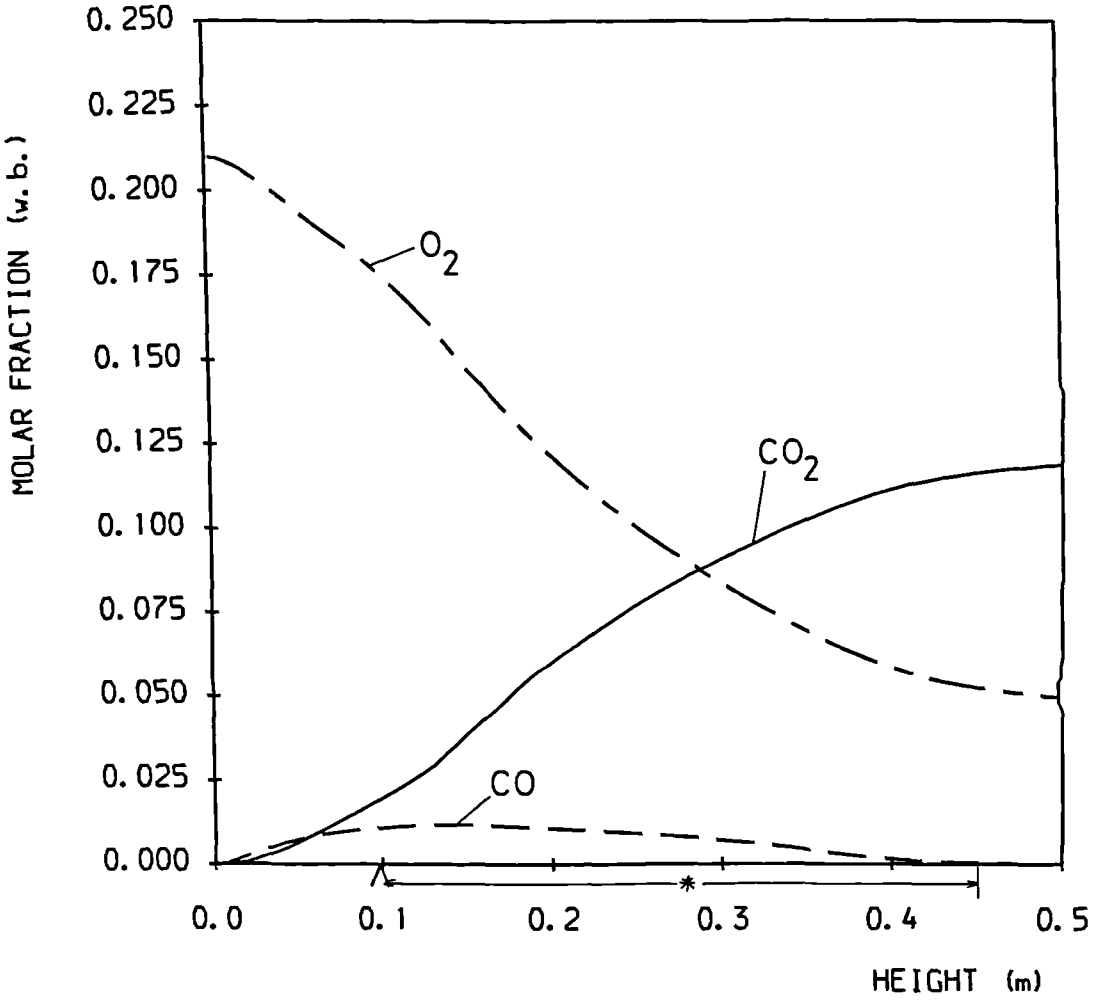

FIGURE 5.40. CONCENTRATION PROFILES IN THE BUBBLE PHASE-NCB, TEST 6 (CO2, CO, O2, ^ =COAL FEEDING POINT, * =TUBE BANK REGION).

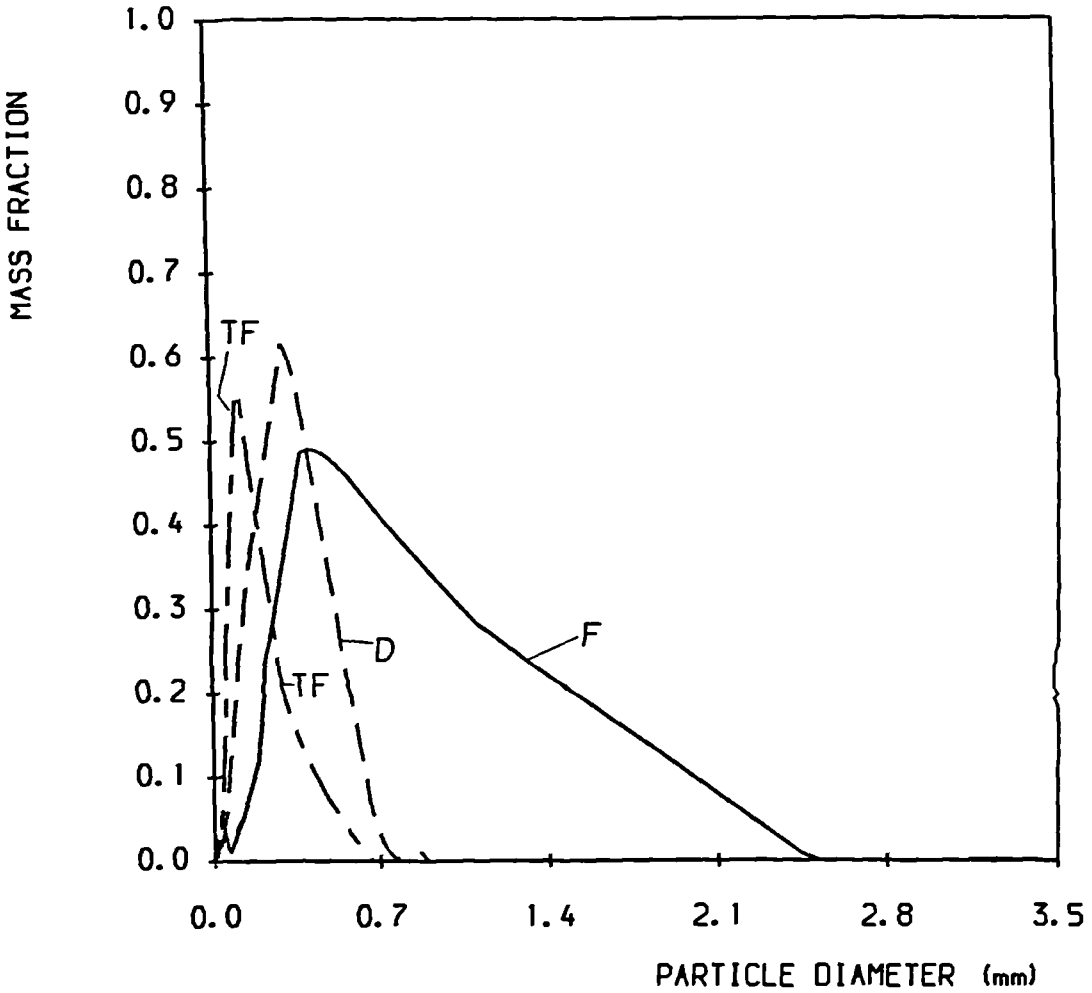

FIGURE 5.41. COAL PARTICLE SIZE DISTRIBUTION-NCB, TEST 6 (F=AS FED TO THE BED, D=IN THE BED, TF=AT THE TOP OF THE FREEBOARD)

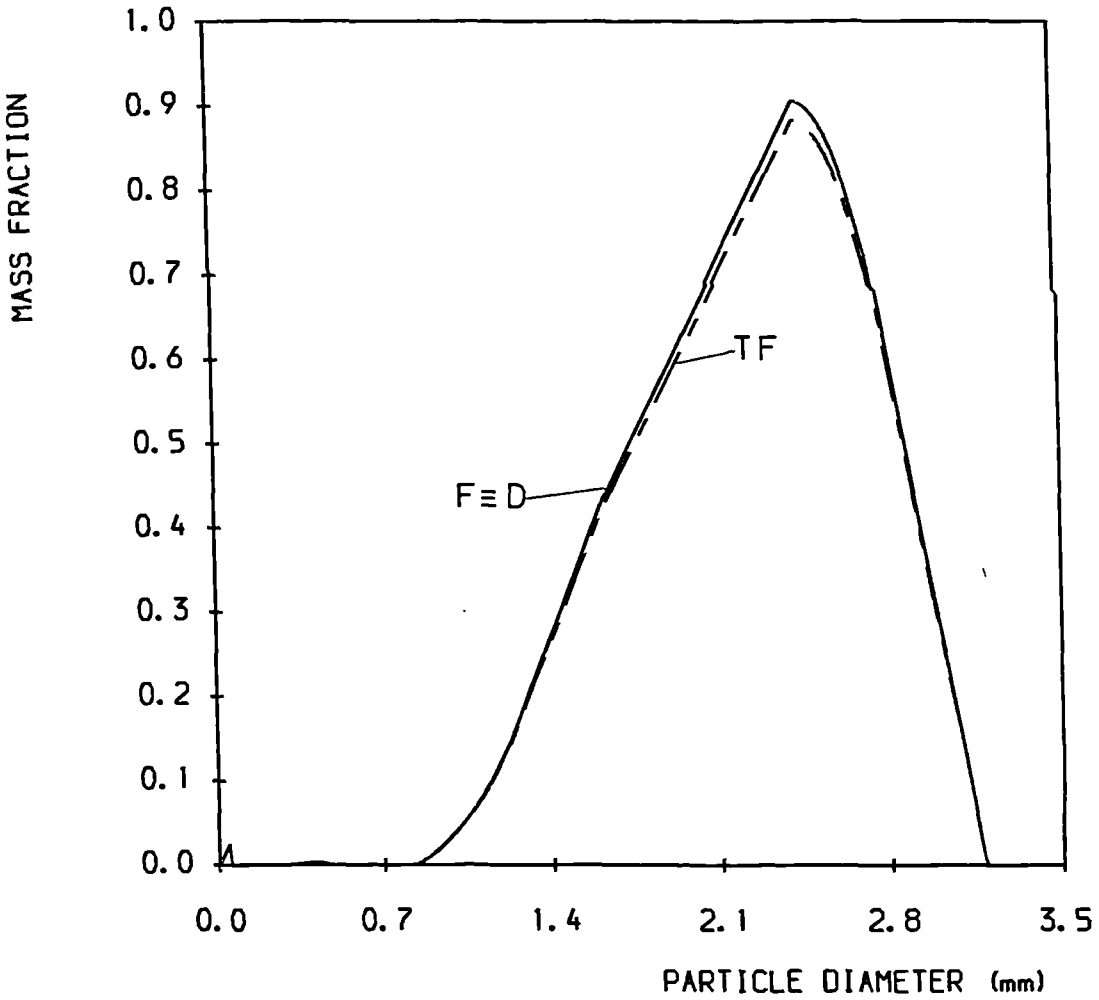

FIGURE 5.42. LIMESTONE PARTICLE SIZE DISTRIBUTION-NCB, TEST 6 (F=AS FED, D=BED, TF=AT THE TOP OF THE FREEBOARD)

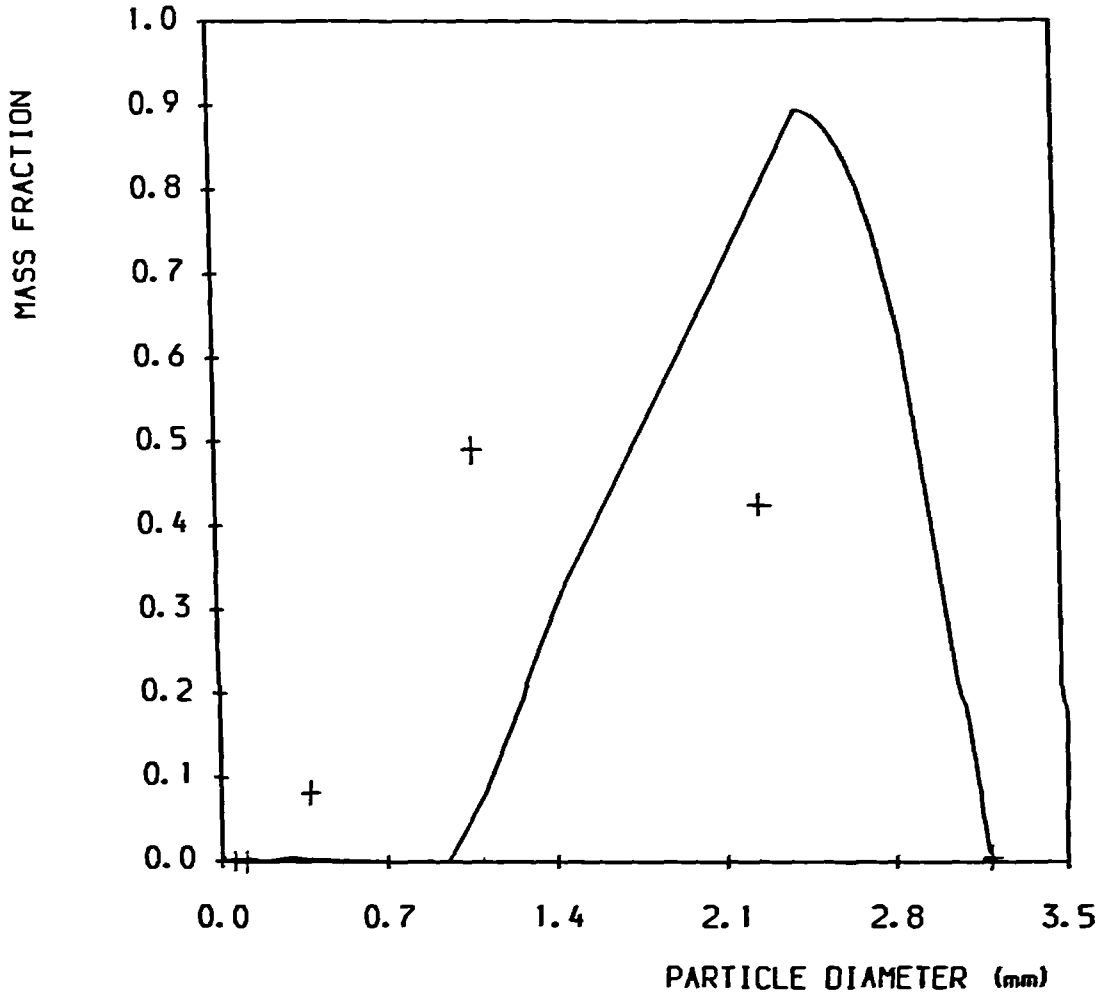

FIGURE 5.43. TOTAL PARTICLE SIZE DISTRIBUTION-NCB, TEST 6 (AVERAGE IN THE BED)
(+ =EXPERIMENTAL DETERMINATIONS)

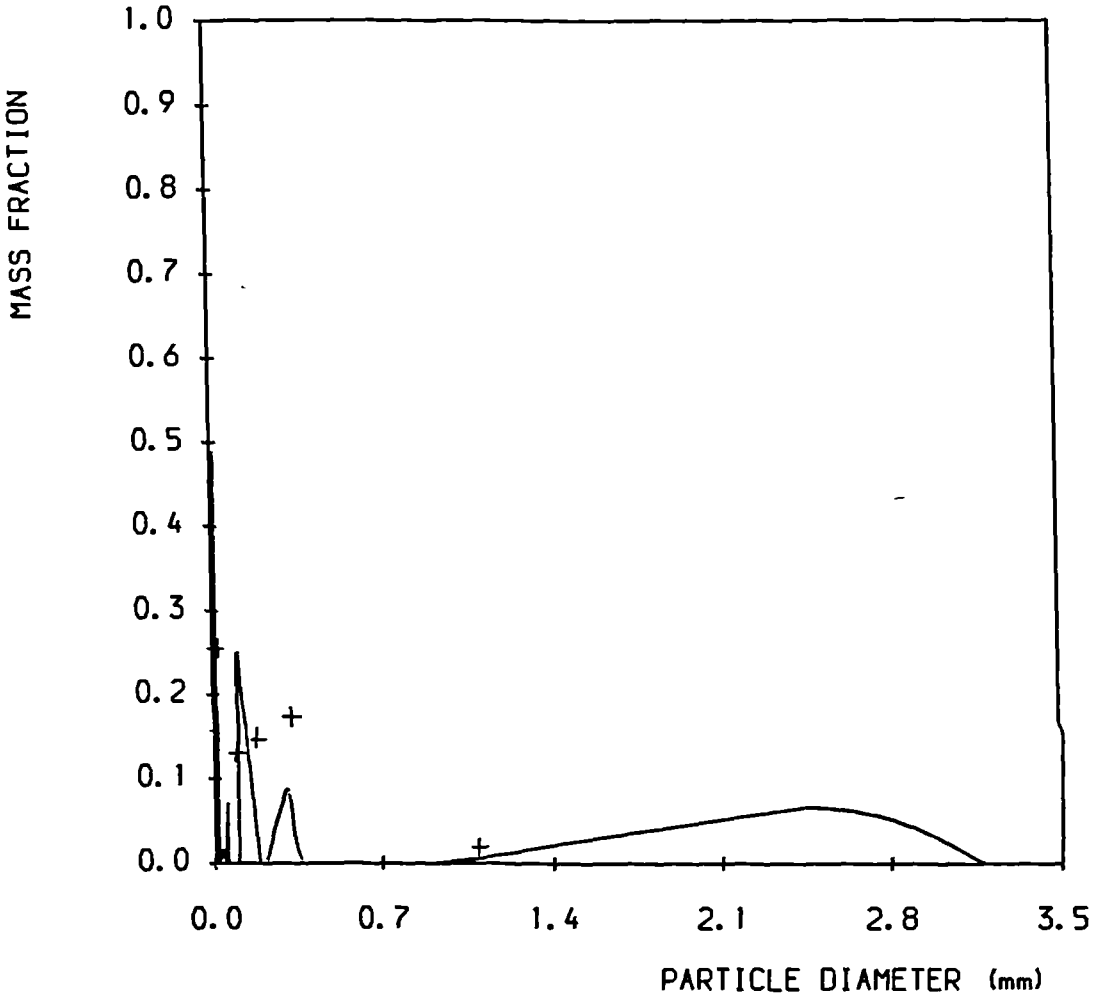

FIGURE 5.44. TOTAL PARTICLE SIZE DISTRIBUTION-NCB, TEST 6 (AT THE TOP OF THE FREEBOARD).
(+ =EXPERIMENTAL DETERMINATIONS)

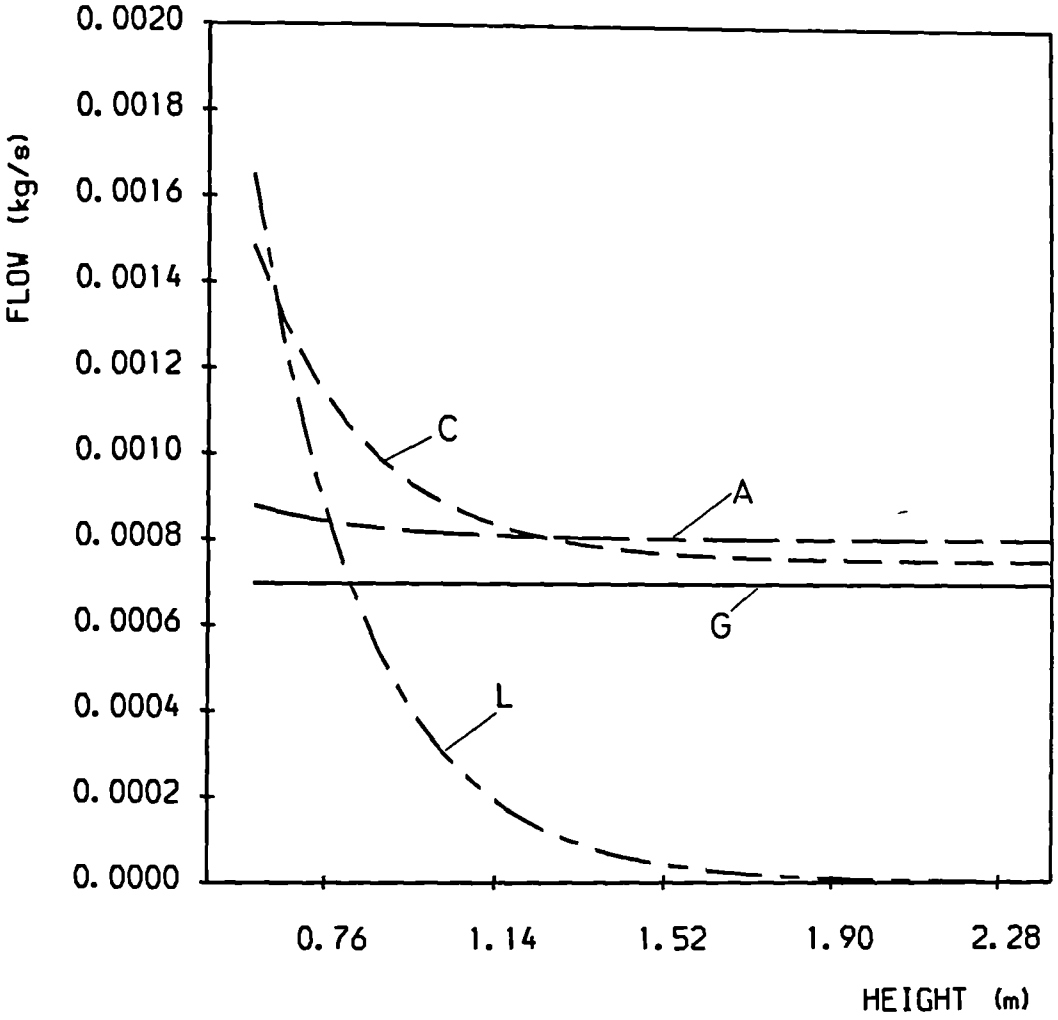

FIGURE 5.45. GAS AND SOLID FLOWS IN THE FREEBOARD-NCB, TEST 6 (G=GAS (sc:0.01), C=COAL, L=LIMEST. (sc:0.01), A=FREE ASH).

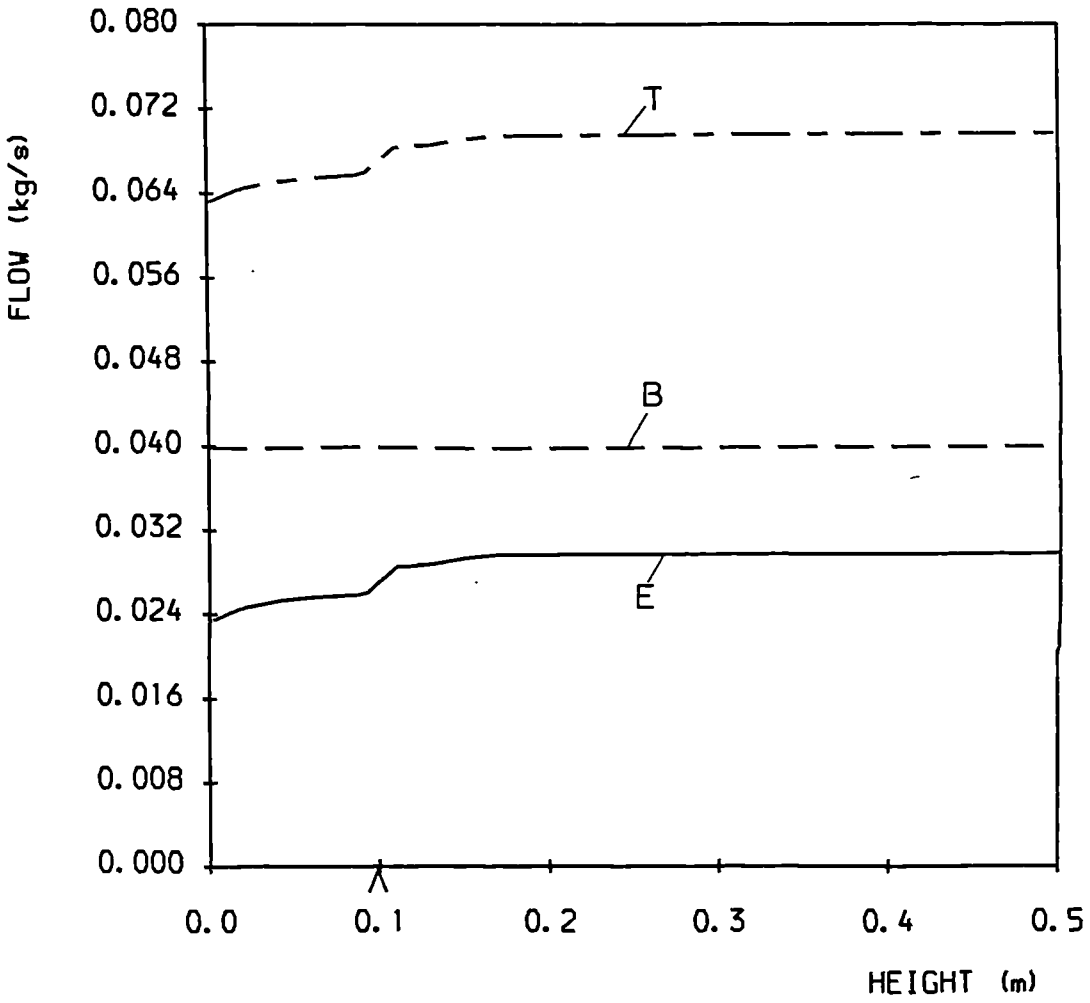

FIGURE 5.46. GAS FLOWS IN THE BED-NCB, TEST 6
(E=EMULSION PHASE, B=BUBBLE PHASE, T=TOTAL,
^ =COAL FEEDING POINT).

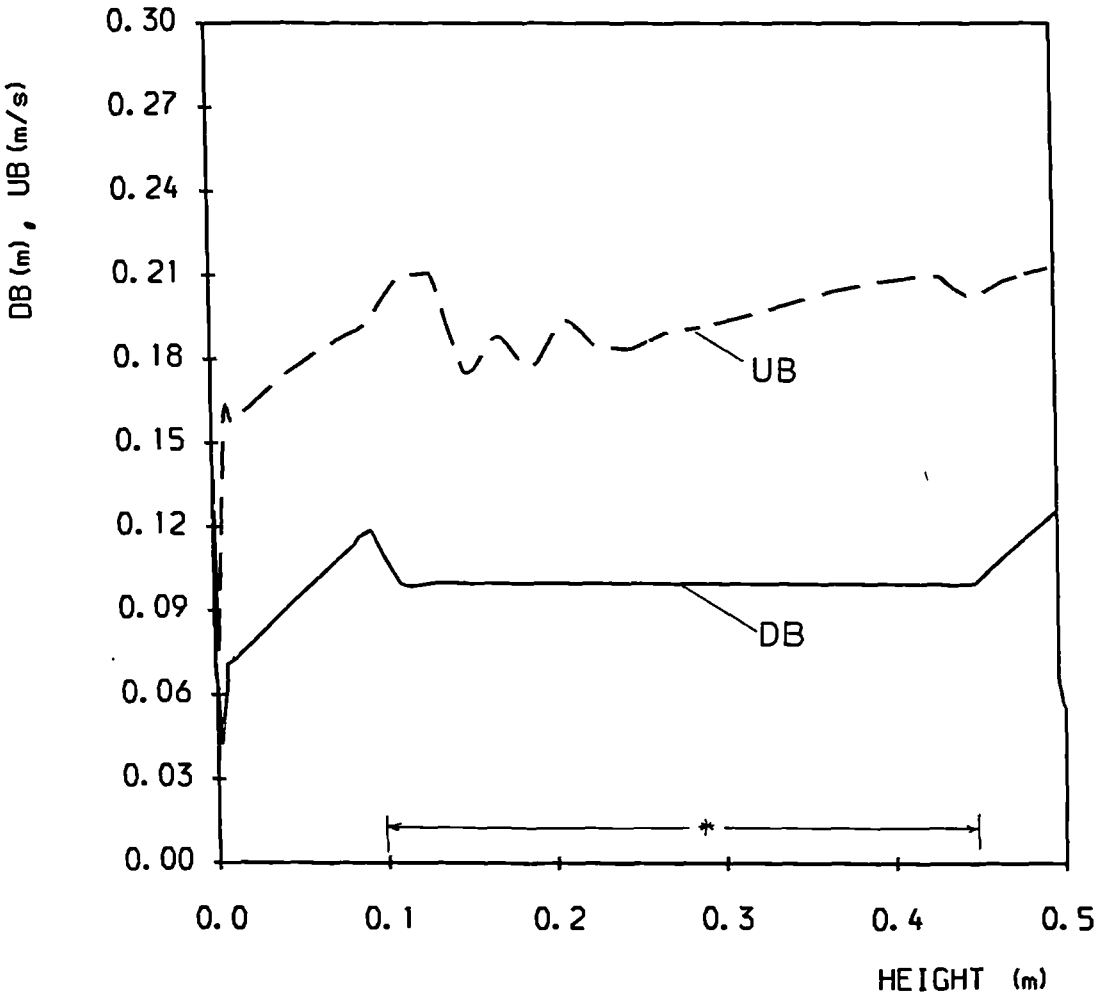

FIGURE 5.47. BUBBLE DIAMETER AND VELOCITY IN THE BED-NCB, TEST 6 (DB=DIAMETER, UB=VELOCITY (sc: 0.1) * =TUBE BANK REGION).

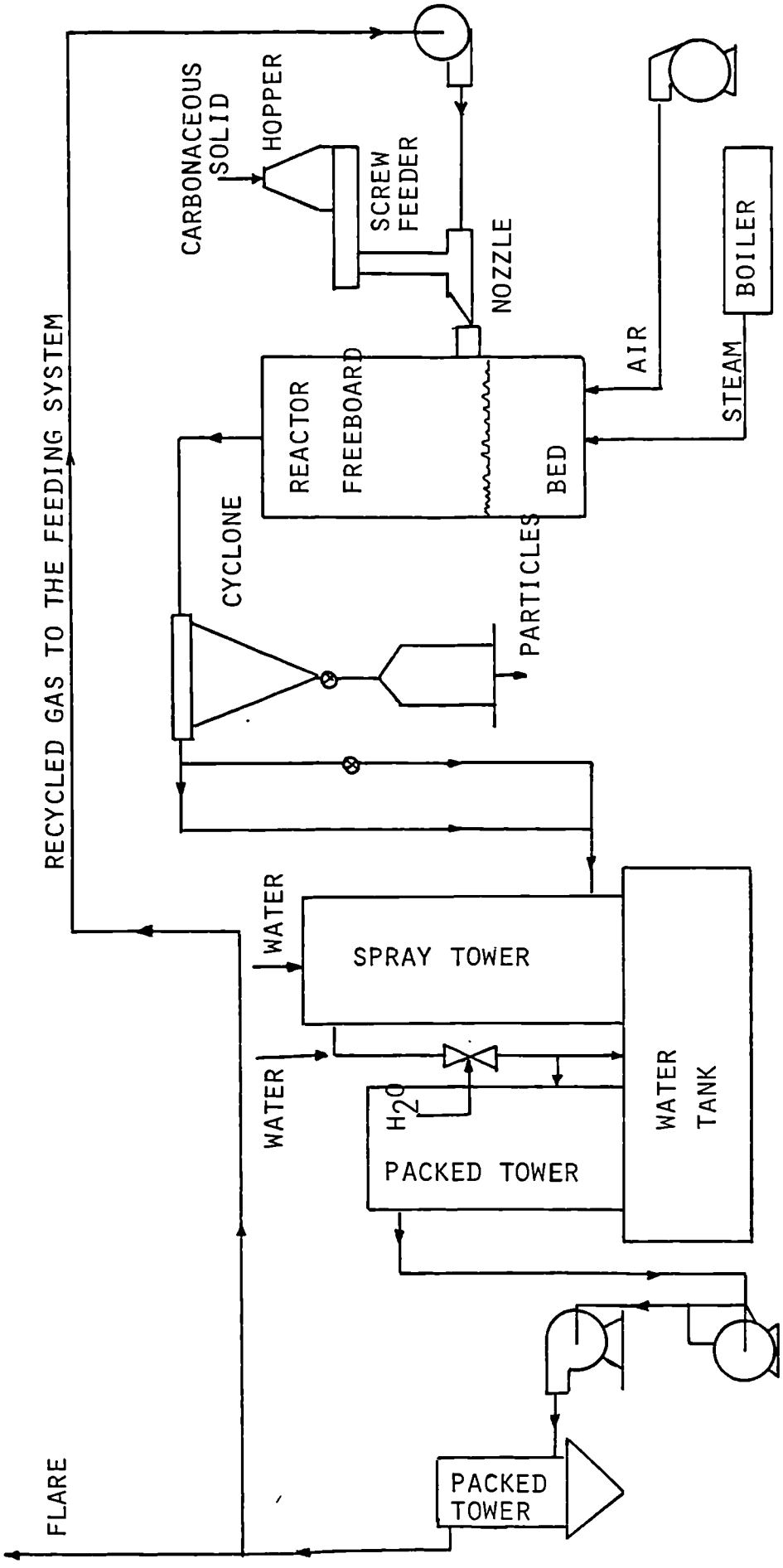

FIGURE 5.48. SCHEMATIC VIEW OF THE IPT GASIFICATION UNIT.

CHAPTER VI

6. DISCUSSION OF THE RESULTS

Before drawing attention to specific aspects of the results generated by the simulation program it is important to stress the following points:

a) As shown in Chapter III, the present mathematical model is based on:

1) The basic principles of mass and energy balances as defined by the differential equations as stated;

2) When it was not possible to use basic equations, then empirical and semi-empirical correlations for several phenomena involved in the processes occuring inside a fluidized bed boiler or gasifier were used. These correlations were taken from the published literature;

b) The program was tested for completely different equipment concepts, different fuel and other solid compositions and characteristics, and different operational conditions leading to the same degree of deviations;

c) Under no circumstance was the use of "adjusting factors" contemplated or employed either in the mathematical model or in the simulation program, in order to give improved correlation of predicted results with the data obtained from industrial operational results. This is an important point of this work, as it was not the intention of the model to give a best fit explanation or algorithm based on experimental data.

6.1. Temperatures

As it has been seen, the simulation can predict the temperature profiles of all phases throughout the entire system. This is illustrated by Figures 5.2, 5.3, 5.18, 5.19, 5.33 and 5.34. Tables 5.4 and 5.20 show some comparisons with observed values during some real operations.

These comparisons can be made only against the average temperatures due the simple reason that, in practice, it is impossible to measure temperature of independent phases due to the high mixing rate inside the bed and freeboard. Even between the emulsion and bubble phases an independent measurement is almost impossible. The thermocouple probes measure only local averages. On the other hand, differences of temperature between different phases are very important in the process due to the effects they have on the rate of the various chemical reactions. This can be achieved only by simulation.

Another aspect is the definition of averages. No publication could be found on this aspect and it is very difficult to verify which kind of average is measured by a probe inside a fluidized bed. During the present work, it has been assumed averages based on the enthalpy-flow, as shown in Appendix C. This choice is thought to be adequate to represent the energy flow through a given cross section of the bed or the freeboard.

Table 5.4 shows a very reasonable agreement between simulation and measurements of temperatures at

various positions for the case of a Babcock and Wilcox unit. Deviations around 5% have been verified. The same situation is shown by Table 5.20 in the case of a NCB unit, which has a completely different design from the Babcock and Wilcox unit. The same level of deviation was obtained for different operational conditions of the NCB plant. This is a good indication in favour of the validity of the present mathematical model due to the strong coupling among all physical and chemical phenomena in the process of fluidized bed combustion.

6.1.1. Temperature profiles

As an important feature of the present modelling, the various phase temperatures can be individually determined throughout the bed and freeboard. The model can show maxima and minima of temperatures which are fundamental, not only to achieve a more realistic computation of all parameters, as for instance local rates of chemical reactions, but also for practical design. As an example, it is possible to determine the maximum temperature achieved by the carbonaceous solid material. It normally occurs near the distributor (Fig.5.2, 5.18 and 5.33) and the program can predict a possible problem if the ash softening point is eventually surpassed, which can cause solid agglomeration and bed collapsing.

It is interesting to observe the completely different behaviour for the gas temperature in the emulsion and bubble phases. The former increasing much faster above the distributor due the extremely close contact with the

burning carbonaceous solid and the latter increasing much slower. The bubble phase can experience a drastic change in the temperature derivative in the region of the tubes bundle if, in a particular operation, the space between the tubes is smaller than the bubble diameter at the lower point of the tube bundle. The bubbles are forced to break leading to a substantial increase in the available surface area for heat and mass transfer.

The graphs also show that, in a typical fluidized bed combustor, the temperature of the gas phases are usually below the carbonaceous solid temperature but deviations from this general behaviour are possible, as shown by Fig.5.18. This can be explained by the following reasoning:

The entering part of the oxygen flow that goes to the emulsion is rapidly consumed near the distributor due the presence of the carbonaceous solid in this phase (Fig.5.24). This provokes a poor oxygen concentration in the sections above because the oxygen to the emulsion comes now from the bubble phase by a slow process of diffusion. Therefore a build up of CO and other combustible gases can be achieved in the emulsion. As the temperature in the bubble phase increases from the distributor to the top of the bed, there are also increases in the mass transfer and the rate of combustion reactions. Therefore the transfered CO from the emulsion phase reacts faster with the available oxygen in the bubble phase leading to the sharp increase in the temperature in the region near the surface of the bed.

The mixing of the two streams of gases in the freeboard, just after the bed surface, also causes a local increase of the temperature, as shown more clearly by Fig.5.19.

Although all chemical reactions have been computed in the freeboard, it has been noted that, after a few centimetres from the top of the bed, the temperatures for all phases remain almost constant throughout that region (Fig.5.3, 5.19, 5.34). This basically indicates that:

a) Due to the sharp decrease in the solid concentration with the freeboard height (Fig.5.14, 5.30, 5.45), the available particle surface area is not enough to maintain an important rate of solid-gas reactions in the freeboard (Fig.5.4, 5.5, 5.20, 5.21, 5.35, 5.36);

b) The gas-gas reactions reach the chemical equilibrium condition in a relatively short distance from the top of the bed (the same figures as before).

These facts show that significant alterations of temperature in the freeboard after a small distance from the bed surface are mainly due to heat losses to walls or tubes in this region.

With respect to the influence of fluidization dynamics in the temperature profiles, it has been observed that the rate of circulation is one of the most important. This is readily noticed by the equations 3.17. The calculation of the rate of circulation for individual species as given by eq.(3.151a). This equation is an attempt to model individual rate of circulation, since the

work of Talmor and Benenati (1963) refers only to the total rate based on the average diameter of particles in the bed. As pointed out by Kunii and Levenspiel (1969), these equations can be useful as a first approximation. More experimental work is expected in this area, which can improve the results for temperature profiles calculated in the model.

Finally, the fluctuations observed in the plotting of the emulsion gas temperature (Fig.5.2, for example) are due to the choice of tolerance for the solution of the differential system of mass and energy balances. This choice is dictated by the desired precision versus computer processing time and therefore the mentioned fluctuations can be made smaller but at the cost of a dramatic increase in the CPU time.

6.2.Concentrations

As it could be seen, the model can predict the gas and solid compositions throughout the entire system. They were used as a test for the validity of the model by comparisons with experimental data during the course of the program development. After this, they are a very important parameter, generated by the computation, to predict favourable operations of the equipment and therefore as an optimization tool.

6.2.1. Gas compositions

Several gaseous flows are present in the process, e.g., emulsion gas, bubble gas, gaseous mixture through the freeboard. The composition of the gas flows in the emulsion and in the bubble changes dramatically in the bed, as shown, for instance, by Fig.5.8, 5.9, 5.24, 5.25, 5.39, 5.40. Therefore the same is true for the average in each section as shown by Fig.5.4 to 5.7, 5.20 to 5.23 and 5.35 to 5.38.

It is almost impossible to measure individual phase compositions in a fluidized bed and therefore make an independent verification of these actual profiles against those generated by the simulation. Even average compositions throughout the bed are not very easy to measure and are rarely reported. This is the case of the Babcock and Wilcox and National Coal Board reports used as sources of experimental data.

On the other hand, the composition of the gaseous mixture leaving the freeboard, which is a direct consequence of the process, is easily determined and can be used as a strong indication of the model validity. Also this composition is an important parameter to study the process performance. For instance, the concentration of oxygen is an indication of air excess in the case of combustors. The CO and H_2 concentrations are the most important values in calculations of gasifier efficiencies. Therefore the quality of a simulation program for such equipment can be judge, in a broad sense, by observing the

deviations against the values obtained during the real operations.

The Tables 5.3 and 5.19 show the results obtained from simulation compared to those verified during the operations with the Babcock & Wilcox and NCB units for the gas leaving the freeboard.

The average deviations are below 5% which are not very far from the fluctuations obtained on measurements during the operations.

Greater deviations have been found for the predicted SO_2 concentrations and the possible reasons for this are:

a) The reactivity of the limestone (factor "ι" , used in the calculations of reaction (R-12) rate coefficient) probably do not depend only on the calcium conversion and particle diameter as described by Rajan et al.(1978,1979). The influence of the limestone chemical composition is not correlated in this parameter.

b) The rate of SO_2 absorption by CaO is strongly influenced by the temperature, as pointed out by Borgwardt (1970). It was observed on running the present program, that variations of even 5% in the limestone temperature profile can cause a substantial change in the concentration of sulphur dioxide in the gas flow. Therefore, improvements on the calculation of these profiles would lead to better prediction of SO_2 concentrations.

This does not invalidate the present approach but it would require better kinetic rate data from

experimental investigations and then a relatively easy modification in the computational frame for the calculation of the rate of reaction R-12.

6.2.1.1.Gas composition profiles

As can be seen the simulation program calculates the gas composition in each phase (emulsion and bubbles) and average composition throughout the bed height as well as for the gas flow throughout the freeboard. Some of these profiles are shown by Figures: 5.4 to 5.9 and 5.20 to 5.25 and 5.35 to 5.40.

It is interesting to note some typical trends of these profiles (some of the following points are valid only for fluidized bed combustors):

a) As expected there is a much sharper decrease of O_2 concentration and increase of CO_2 concentration in the emulsion phase than in the bubble phase (for example Fig.5.8 and 5.9);

b) There is a greater peak of CO concentration in the emulsion than the bubble phase. At higher points in the bed, the concentration of CO even in the emulsion tends to vanish due to the diffusion of O_2 from the bubble phase;

c) CH_4, H_2, H_2S, NH_3, Tar and C_2H_6 (in the test of B&W ethane was fed continuously with the fluidizing air) are produced mainly by the devolatilization. This is shown by the sharp increase in their concentrations near the feed point in the bed (Fig.5.5, 5.7, 5.21, 5.23, 5.36 and 5.38). Their concentrations drop to almost nil at a few centimetres from the feeding point and therefore no

appreciable concentrations are detected in the freeboard. It must be stressed that this behaviour is characteristic of combustors with the feeding port inside the bed. For the case of a feeding point above the bed surface it is possible that some noticeable concentration of these gases could be detected at the top of the freeboard. The present simulation, in fact, can deal with this case also;

d) SO_2 and NO are produced mainly by the combustion of the carbonaceous solid rather than by the devolatilization (Fig.5.6, 5.22 and 5.37);

e) For the cases tested, no appreciable change in the gas composition has been detected in the freeboard. It should be noticed that the B&W and NCB units have relatively deep beds. This probably provides space to achieve most of the chemical transformations inside the bed.

6.2.2. Solid compositions

The compositions of the various solids, i.e., carbonaceous, limestone and/or inert (sand and ash), in the bed and carried into the freeboard, are another point that serves as an indicator for the verification of the performance of a FBC or FBG. Mainly the degree of carbon conversion is seen as a good parameter to measure the efficiency of any combustor.

As explained, the present simulation model provides all this information at any point of the system, both in the bed and freeboard. Some of this information is more critical to an examination of the behaviour of the

equipment, and thus has been chosen to be specially printed during the computations.

Tables 5.5, 5 6, 5.7 present the various solid compositions for the Babcock and Wilcox boiler operation while Tables 5.21 and 5.22 for the NCB operations. From this it is interesting to observe:

a) The various elements in the carbonaceous particles apart from ash, decrease more or less proportionally with the carbon during the processing (Tab. 5.5 and 5.21);

b) The almost complete consumption of volatiles from the solid carbonaceous in all cases;

c) Almost no moisture survives in the average processed solid;

d) Table 5.21 shows that in some operations (NCB Test No.3, for example) the carbon in the volatiles is the major contribution to the maintenance of the combustion in the bed. It is possible therefore that, in some cases, the elutriated carbonaceous particles will have their carbon all in the form of "fixed-carbon" being consumed mainly in the freeboard;

e) Tables 5.6 and 5.7 show a reasonable agreement between the experimental and simulation values for the composition of the solids in the bed;

f) Some higher concentrations of unreacted carbon in the elutriated particles have been observed in the experimental results than that expected by the results of the present simulation. A possible cause for this is the

higher concentration of fine particles in the bubble wakes which are thrown into the freeboard and therefore elutriated. These particles have, in this way, a residence time inside the bed smaller than the average leading to the mentioned effect.

Finally. it must be remembered that the best results have been obtained with the adoption of the exposed-core (or ash free) model for the carbonaceous solid-gas reactions (R-1 to R-6) and with the unreacted-core model for all the other solid reactions or decompositions.

6.3.Particle distributions

One of the most important points in the present model is the prediction of the particle size distributions to be found in the bed and at any point of the freeboard.

It must be remembered that the estimation of particle size distributions is intrinsically correlated with almost all important parameters of the process, as commented in section 3.10. Therefore the prediction of these distributions is complex but fundamental to achieve a coherent mathematical model. In addition the precision obtained on the prediction of particle flows throughout the freeboard and consequently the entrainment at the top of the freeboard plays a very important role on the design of FBC or FBG equipment.

As can be observed, in tables 5.8 to 5.12 and 5.23 to 5.28, agreements as high as 96% have been obtained

between predicted and measured particle flow at the top of the freeboard. In particular the Table 5.11 and 5.26 which show the quality of predictions for the flow of particles at the top of the freeboard, if compared with previous works, for example Rajan et al., 1979,1980 (with no need of adjusting factors) and Overturf and Reklaitis (1983) whose prediction for the mass flow of particles is 8.3g/s.

Although the simulation can compute the various particle flows throughout the freeboard, the various comparisons with operational data have only been possible with the total flow at the top of the freeboard. This is probably due to difficulties in the experimental determinations which could neither distinguish the various solid species nor allow measurements of flows at various points within the freeboard.

It must be noticed, as well, that the present model achieved a very good prediction for the flow of recycled particles, as shown in table 5.27 for the NCB unit.

During the computations, some graphs have been generated which could help to illustrate various aspects of the particle size distributions in the process (Fig. 5.10 to 5.14, 5.26 to 5.30 and 5.41 to 5.45).

The following comments on the solid distributions have been thought to be interesting and worthy of mention:

a) The average particle diameter in the bed can become either greater or smaller than the respective feed stream (Tab. 5.12 and 5.28). This is due to the competing

effects: chemical reactions, attrition and recycling of particles for the decrease on one hand, and entrainment of fines to the freeboard, leaving the bigger particles in the bed, on the other hand (see also Fig.5.10, 5.11, 5.26, 5.27, 5.41 and 5.42). Also, it is interesting to observe the effect of the entrainment process on the size distribution curves for the mixture of particles which can be verified by comparing, for example, the Fig.5.12 with the Fig.5.13 (as well as 5.28 with 5.29 and 5.43 with 5.44) [Observation: the sum of the mass fractions, and therefore the area under each curve of particle size distribution are always numerically equal to one, as shown by all respective tables. Unfortunately, some graphs failed to represent the unit area correctly due to the computer plotting routine which passes a smooth curve through the points. As the number of points available on these distributions were small (one for each range of particle diameter) the graphs suffered some deformation].

b) Reduction due to chemical reactions plays a major part on the variation of the size distribution of particles in the bed. This can be verified, for instance, using the Fig.5.10 and 5.11. They show that the size distribution of limestone particles in the bed almost coincides with the respective feed particles while in the case of carbonaceous particles greater variations are observed due to the influence of chemical reactions to reduce particle sizes. It is convenient to remember that the exposed core (or ash free) model has proved to be the

best representation for the carbonaceous solid-gas reactions while the unreacted core was best used for the limestone decomposition and reactions.

c) The dramatic influence of the recycling of particles in the average diameter in the bed and on the entrainment of particles to the freeboard. As only for the test No.6 the recycling was not used during the tests of NCB unit, tables 5.26 and 5.28 can show these effects.

d) As explained before, it was not possible to verify the simulation computations against experimental determinations for the flow of solids at various sections in the freeboard. On the other hand the adoption of exponential decay of particles in that region (Fig.5.14, 5.30 and 5.45) led to very good predictions for the entrainment at the top of the freeboard. Therefore it seems that this model is the more appropriate to describe such processes.

6.4. Other process parameters

The present simulation is based on the solution of a set of differential mass and energy balances that define the temperature and concentration profiles throughout the entire system. Therefore the quality of the simulation can be verified by how well these profiles are calculated against available experimental data, as has been seen above. All other calculated parameters, as for instance carbon conversion, boiler efficiency, etc., are functions of the basic solution of that set of differential

equations. Nevertheless, various of these parameters have a practical usage because they provide an easy reference for the engineering design of such an equipment.

In this section some of the values generated by the simulation related to various parameters of the process are discussed and whenever possible compared with the reported experimental value. Tables 5.13, 5.14 and 5.29 to 5.34 list several of these values.

6.4.1. Carbon conversion

Probably this is the most commonly mentioned parameter for equipment consuming solid carbonaceous material because it is related to the efficiency of the operation. This relationship is more clear in the cases of combustors but it loses some meaning in the case of gasifiers. This is because in the former case the quality of the produced gas flow (basically CO_2 and N_2) is of secondary importance while in the latter case the produced gas composition is the first concern.

The present simulation calculates the carbon conversion, as well as all other solid conversions, in the bed and at any point of the freeboard, as described in Chapter V.

As can be seen in the tables 5.13, 5.29, 5.31 and 5.33 the average deviations between simulation and experimental values were around 3%. It can not be forgotten that these practical measurements depend on the analysis of solid residuals in the bed, which can include a series of uncertainties.

Other consequences from the solution of the mass balances equations for the carbonaceous solid components (shown in the same tables as above) are for instance:

a) Mass flow of flue gas, with deviations around 5% against the experimental data;

b) Rate of energy output, with the same level of deviations.

6.4.2. Calcium conversion and correlated parameters

The calcium conversion in the bed as well Ca/S ratio and sulphur retention are commonly referred to in the engineering design and operation reports of FBC boilers.

Due to the already commented problems in the estimation of limestone reactivity, the precision achieved for the concentration of SO_2 in the flue gas was poor. Consequently this is reflected in the predictions of the parameters mentioned above, as can be verified in the tables 5.13, 5.29, 5.31 and 5.33. In spite of this, the program could predict with some precision the Ca/S ratio and the solid composition in the bed, this last shown in Tab.5.6 against the experimental values.

6.4.3. Heat transfer to tubes and walls

Good agreement between simulation and real data have been found with the prediction of the total heat transfer to tubes in the system, as shown in Tab.5.14 in the case of the Babcock and Wilcox unit. Unfortunately no data on these values was reproduced in the NCB report.

It must be noticed that some data generated by

the simulation can serve as an important guide for the design of the tubes bundle as well as the insulation of the system. For instance the heat transfer coefficients, temperature of tubes and external wall, and heat flow to the external ambience, can be predicted.

6.4.4. Pressure losses

The pressure drop in the system is mainly concentrated in the distributor. The pressure drop in the bed is relatively small and does not represent a measurable influence in the process. The total pressure assumed during the solution of the mass and energy balances is the average between the values at the bottom of the bed and the top of the freeboard.

The predicted values are within the expected deviations for this kind of calculation, as shown in tables 5.29, 5.31 and 5.33. Some greater deviations are probably due to fact that the correlation described in section 3.12.1, does not include enough information about the mechanical design of the distributor. Therefore this must constitute a point for improvements as soon as a more reliable and complete correlation is available in the literature.

6.5. Comparisons with other simulation results

The task to compare the present simulation program with existing programs is very difficult due to:

a) The published papers on mathematical modelling do not present the complete computer program and therefore

the computation for various cases can not be tested;

b) The cases reproduced in these papers do not present the complete list of input data that generated the computed results.

Despite these difficulties, some comparisons could be made for special cases where the authors referred to published reports of real unit operations. This is the case of Overturf and Reklaitis (1983b) who tested their model using the data published in Babcock and Wilcox (1978) (test No.26) which was also used in the present work.

On the other hand the comparisons could be made only for very few aspects due to the small number of results published in Overturf and Reklaitis (1983b). They present tables to show the effects of adjusting factors of their model on the predicted flue gas composition, as already commented in Chapter II. The table below reproduces some of these results with the measured values and the values predicted by the present model which does not use any adjusting factor. It should be noticed that the model of Overturf and Reklaitis does not allow one to predict gas concentrations other than CO_2, CO, and O_2. and therefore only the molar fractions for these gases have been reproduced from the Table 5.3 for these comparisons.

Component	Molar composition (%), dry basis				
	Real operation	Present Simulat.	Overturf and Reklaitis (1983) "Grid Factor"		
			10	50	150
CO_2	13.8	13.00962	7.19	12.10	12.55
CO	0 to 0.9	0.00002	0.49	0.32	0.25
O_2	3.9	3.83248	9.23	4.41	3.93

TABLE 6.1.Comparisons between the Overturf and Reklaitis (1983) and the present model concerning the flue gas composition during the operation of the Babcock and Wilcox unit, test No.26.

As can be seen the results of Overturf and Reklaitis (1983) depend too much on the chosen value for the enhancement "Grid Factor" that adjust the mass transfer coefficient between emulsion and bubble phases, as already explained in the section 2.7.2.

Also, in the paper referred to above, the authors showed the influence of the "Emulsion Phase Temperature" on the flue gas composition. This was necessary because they assume a "CSTR" model for the emulsion phase with an adjustable temperature, the value of which must be set for the computations. As in the present model the emulsion gas and particle temperatures are computed, such adjustments are not necessary.

Overturf and Reklaitis (1983b) also contains several other tables showing the influences of various "Multipliers" for:

1) Bubble size which vary from 0.03 to 0.183 m;

2) Gas-gas diffusion rate for which the

multiplier may vary from 0.01 to 100.0;

3) Homogeneous reaction rate (because they consider only the CO combustion in the gas-gas set of reactions) for which the multiplier may vary from 0.1 to 0.67;

4) Char emissivity which may vary from 0.01 to 1.0.

In all cases the variations observed in the flue gas composition are in the same range shown in Table 6.1.

For the rate of particle elutriation their result is 8.3 g/s while the measured value and the prediction by the present work is shown in Table 5.11.

Finally, Overturf and Reklaitis (1983b) presented the temperature and composition profiles for the bubble and emulsion phases throughout the bed. These profiles are shown in Fig.5 of their work, and can be compared with the Fig.5.2, 5.8 and 5.9 of the present. The effect of their hypothesis of "CSTR" reactor for the emulsion with a uniform temperature and composition assumed in their model can be noticed. It led to steeper variations in the bubble gas temperature and in the bubble gas compositions. Unfortunately these profiles could not be compared with the real situation. The only evidence is the average values of temperature in the bed obtained in the present work which reproduces the observed ones, as shown in Table 5.4 and the flue gas composition shown in Tab.5.3 and 6.1.

CHAPTER VII

7.CONCLUSIONS AND SUGGESTIONS FOR FUTURE WORK

A comprehensive mathematical model and computer program that simulates the operation of a fluidized bed boilers and gasifiers consuming carbonaceous solids has been developed.

The computer program based on the mathematical model has been tested for some commercial and pilot plants. Comparisons between simulation generated results and real operational data have shown low deviations for almost all parameters. In addition it is clear that no mathematical model previously published so far could either provide the same amount of details of the behaviour of process parameters or give the same precision in the prediction of their values, as the one developed in this thesis.

Some specific comments on the simulation model and indications for future developments are listed below.

7.1.On the basic hypothesis and mathematical approach

a) The modification on the two-phase model, which includes the cloud region in the emulsion and allowing this phase to depart from the minimum fluidization condition, has shown to be a good representation for the fluidization dynamics. The conceptual separation of the cloud region seems to be unnecessary but some future work can be concentrated on this aspect;

b) The highly coupled mass and energy transfer

processes, combined with the various chemical process and particle flows and size variations, are the very nature of the fluidized carbonaceous solid combustion or gasification. Also, the so-called gasification reactions cannot be excluded even for a combustion model because they contribute not only to the generation of important final and intermediary products, but they also play a fundamental part in the energy balances. Another example of the strong coupling between all the effects, is that small variations in the temperature profile can cause significant variations in the bed fluid dynamics, carbon conversion, gas compositions. particle size distributions in the bed and freeboard, entrainment, etc. The reverse is also true, i.e . imprecise determinations of, for instance, emulsion-bubble flow partition, bubble size and bubble growth or particle size distributions can lead to great deviations in all the other parameters mentioned. In addition, the conditions vary tremendously from point to point of in the fluidized bed and therefore only comprehensive models that solve the combined set of differential mass and energy balances are able to achieve a more realistic simulation of a FB boiler or gasifier. Therefore the simple fact that the present simulation program is capable of being processed to generate information that describes, within reasonable degree of deviations, the behaviour of a real operation, is by itself a strong indication of the coherence of the mathematical structure. It also shows that the use of apparently independent correlations taken from the

literature (the semi-empirical previously published data mentioned earlier) which describe various phenomena of the processes, can actually be put together in a logic building exercise that uses basic differential mass and energy balances as a linkage between them, leading at the end, to an important tool which can allow the prediction of real equipment operation;

c) The vertical one-dimensional differential mass and energy treatment, for the bed and freeboard section, proved to be a reasonable mathematical approach to the simulation.

7.2. On the temperature profiles

a) The model allows the computation of individual temperature profiles for the gas in the emulsion, gas in the bubbles, carbonaceous, limestone and inert solids throughout the bed and freeboard;

b) Although great variations in temperature for each phase have been verified, the average value does not vary too much throughout the entire system;

c) The temperature of the carbonaceous solid reaches its maximum at points near the distributor where these particles meet layers of high O_2 concentrations;

d) Due to close contact, the temperature of the gas and solids in the emulsion tend to be almost the same in regions just above the distributor;

e) For the case of FBC boilers, the simulation shows that the bubble phase temperature tends to increase

slowly towards the emulsion gas and particle temperatures from the bottom to the top of the bed. This behaviour is typical, but the eventual surpassing of the bubble over the emulsion average temperature becomes possible mainly in regions near the top of the bed, and is probably more likely in the case of gasification processes;

f) Sharper increases in the bubble phase temperature can be achieved in the region of the tube bundle if the space between the tubes is smaller than the bubble diameter at the lower part of that bundle. This is mainly due to the increase in the bubble phase area for heat and mass transfer;

g) The temperature of the gaseous phase tends to increase just above the bed surface due to the fast combustion of CO and other gases previously stored in the lean O_2 emulsion phase which now come into contact with the rich O_2 bursting bubble phase;

h) No appreciable variations of temperature have been computed in the freeboard above the region near the bed surface;

i) The temperature profiles in the bed are especially sensitive to the rate of solid circulation. The eq.(3.151a) is useful as a first attempt to calculate individual solid circulation but more improvement can be achieved with future experimental work in this area;

j) Comparisons with experimental data, of average temperatures at various points and for different process units, only showed small deviations, always around 5%;

7.3.On the concentration profile of gases

a) The simulation is capable of predicting the concentration profiles of thirteen different gases (CO_2, CO, O_2, N_2, H_2O, H_2, CH_4, SO_2, NO, C_2H_6, H_2S, NH_3 and Tar) throughout the bed and freeboard. In the bed the profiles for the two gaseous phases (emulsion and bubbles) are also computed;

b) As expected, the simulations predicted a much sharper decrease of O_2 concentration and increase of CO_2 concentration in the emulsion phase than in the bubble phase;

c) Greater peaks of CO concentration are shown in the emulsion than the bubble phase. At higher points in the bed, the concentration of CO even in the emulsion tends to vanish due to the diffusion of O_2 from the bubble phase;

d) CH_4. H_2, H_2S, NH_3, Tar and C_2H_6 (in the test of B&W ethane was fed continuously with the fluidizing air) are produced mainly by the devolatilization process. This is shown by the sharp increase in their concentrations near the feeding point in the bed. Their concentrations drop to almost nil at a few centimetres from the feeding point and therefore no appreciable concentrations are detected in the freeboard. It must be stressed that this behaviour is characteristic of combustors with the feeding port inside the bed. For the case of a feeding point above the bed surface it is possible that some noticeable concentration could be detected at the top of the freeboard. The present simulation can deal with this case;

e) In the tested cases, in which bituminous and semi-bituminous coal were used, it was verified that SO_2 and NO were produced mainly by the combustion of the carbonaceous solid rather than by the devolatilization;

f) For the cases tested, no appreciable changes in the gas composition have been detected in the freeboard. It should be noticed that the B&W and NCB units have relatively deep beds which provide space to achieve most of the chemical transformations before the gas currents reach the top of the bed;

g) The predicted composition of the gas leaving the freeboard agrees with the real operational data within a 5% average deviation.

h) Greater deviations have been obtained for the SO_2 concentrations however. As the deviations do not follow a consistent pattern, it is suggested that future work should concentrate on the study of the SO_2 absorption by limestone and limestone reactivity. Also, as the rate of SO_2 absorption by CaO is strongly influenced by the limestone temperature, improvements in the calculation of the solid temperature profiles would lead to better predictions of SO_2 concentrations. This is linked with better correlations for the solid circulation in the bed, as commented above.

7.4. On the composition of solids

a) The model is capable of predicting the composition of the carbonaceous solid (C, H, O, N, S, Ash, Volatiles and Moisture), limestone ($CaCO_3$, CaO, $CaSO_4$, Moisture) and inert solids (SiO_2 and Moisture) in the bed and throughout the freeboard;

b) The various elements in the carbonaceous particles, apart from ash, decrease more or less proportionally with the carbon during the processing;

c) The almost complete consumption of volatiles from the solid carbonaceous was verified in all cases;

d) No moisture survives in the average processed solid;

e) In some operations, the carbon in the volatiles can constitute the major contribution to the maintenance of the combustion in the bed. It is possible therefore, in some cases, that the elutriated carbonaceous particles can have their carbon in the "fixed-carbon" consumed mainly in the freeboard;

f) A good agreement between the experimental and simulation values for the composition of the solids in the bed have been obtained;

g) The best results have been obtained with the adoption of the exposed-core (or ash free) model for the carbonaceous solid-gas reactions (R-1 to R-6) and with the unreacted-core model for the all other solid reactions or decompositions.

7.5. On the particle size distributions

a) The mathematical model is capable of predicting the particle size distributions for all solids in the bed and through the freeboard. These distributions are calculated for each individual solid and for the mixture;

b) The program is also able to predict the flow of entrainment for each kind of particle at any point of the freeboard and therefore the flow leaving the system. The flow of recycling, if used, is also computed;

c) Very good agreement has been obtained between simulation and experimental results for all points mentioned above. Deviations lower than 5% have been obtained for different equipment and situations;

d) The average particle diameter in the bed can be either greater or smaller than the respective fed stream. This is due to the competing effects: chemical reactions, attrition and recycling of particles for the decrease in one side and entrainment of fines to the freeboard, leaving the bigger ones in the bed, on the other side;

e) In the case of fluidized bed combustion of coal, reduction due to chemical reactions plays a major part in the variation of the size distribution of carbonaceous particles in the bed;

f) A dramatic influence of the recycling of particles on the average diameter in the bed and on the entrainment of particles to the freeboard has been

verified;

g) Exponential decay for the flow of particles in the freeboard has proved to be the best representation found so far.

7.6. Suggestions for future work

Here a summary of the possible points for improvement in the modelling of fluidized bed boilers and gasifiers are presented.

The various aspects are listed below in an order that the author imagine to be of decreasing importance but in several points it is almost impossible to set an order of priority:

1) Tests of sensitivity. Although the values fed into the program for the computations shown, have been taken from the mentioned sources exactly as they were reported (Babcock and Wilcox, and National Coal Board), this verification is interesting in order to establish the influence of possible errors of input information on the computed results. Some of these parameters which seem to be a possible source for the deviation between simulation results and operational data are:

a) Particle densities (apparent and real) of the various solids;

b) Particle size distributions;

c) Flow of gases injected through the distributor;

d) Expanded bed height, if in the case of shallow

beds.

2) A more detailed model to include the limestone reactivity for SO_2 absorption. This reactivity should include not only the effects of porosity decay but also the very likely influence of chemical composition of the fed limestone.

3) Verify the possibility of improvements if the second derivatives in the differential mass and energy balances, which describe diffusional effects in the vertical direction, are included. Although these second derivatives can increase the complexity of the mathematical problem, it is suspected that the computing time could possibly diminish because of the effect of "softening" the sharp variations of concentrations and temperatures. Also the inclusion of the horizontal coordinate could be interesting in order to improve the study of the effects of the solid feeding. On the other hand, no reliable empirical or semi-empirical correlations describing the diffusional parameters in a fluidized bed have been published so far and therefore this next step is limited by the experimental research in this area.

4) The inclusion of a third phase that can be called "bubble wake" separated from the emulsion. This phase can be treated as a plug flow regime and possibly lead to a model which would explain the higher concentration of unreacted carbon in the elutriated particles.

5) The inclusion of time as another independent

variable to transform the present steady-state model into a dynamic model that would allow the simulation of batch operations and start-up or shut-down phases of FB boilers or gasifiers;

6) The inclusion of two other directions to allow a complete three-dimensional simulation which would compute the patterns of individual particles inside the bed. Apart from the computer processing time required for such solutions, which will take much longer than the present program, that kind of approach depends strongly on further experimental research in the fluidization dynamics.

APPENDIX A - GAS-SOLID REACTION RATE PARAMETERS

The auxiliary parameters used for the calculations of various resistances in the gas-solid reactions are presented below.

From Yoon et al.(1978) the effectiveness factor is given by:

$$\eta_i = \frac{1}{\phi_i}\left[\frac{1}{\tanh(3\,\phi_i)} - \frac{1}{\phi_i}\right] \quad , \quad 1 \leq i <= 14 \qquad (A.1)$$

while the Thiele is given by:

$$\phi_i = \frac{d^o_{P,m}}{6}\left[\frac{k_i\ c^o_{S_i}\ R\ T_G}{\gamma_i\ D_{core_i}}\right]^{1/2} \qquad (A.2)$$

where: $1 \leq i <= 14$ and $1 \leq m \leq 3$. The parameters "γ_i" are the stoichiometric coefficient of the solid representating unreacted solid component in the reaction "i" (shown in Tab.3.2). They are:

$\gamma_i = 1$ for $i < 7$ and $9 \leq i \leq 12$;

$\gamma_i = \dot{b}_{i,}$ for $7 \leq i \leq 8$.

Obviously the drying processes do not involve reactions and therefore the effectiveness factor is not calculated.

The fraction of the particle radius that is occupied by the unreacted core has been taken as:

$$\tau_i = (1 - \Lambda_j^{1/3}) \qquad (A.3)$$

Here the representative unreacted solid "j" for each reaction "i" is given in the last column of Tab.3.2.

The intrinsic reaction rate is given by the Arrhenius formula:

$$k_i = k_{o_i} \exp\left(-\frac{\tilde{E}_i}{R\ T_{P,m}}\right) \qquad (A.4)$$

here: $1 \leq i \leq 12$, $1 \leq m \leq 2$ and $i \neq 10$. The Arrhenius constant, k_{o_i}, and the activation energy, $\tilde{E}_i$ are described in the main text for each individual reaction (see Tab.3.2 for the relation between "i" and "m").

The initial concentrations of the solid reactive agents for each set of reactions are given by:

- Reactions between gases and carbonaceous material:

$$c_{SI,i} = \frac{w_{fix,I}\ \rho_{PI,m=1}}{M_{1,}} \quad , \ 1 \leq i \leq 5 \qquad (A.5)$$

- Devolatilization of carbonaceous material (reactions from i=7 to i=9):

$$c_{SI,i} = \frac{w_{vol,I}\ \rho_{PI,m=1}}{M_{2,}} \quad , \ 7 \leq i \leq 9 \qquad (A.6)$$

- Drying of solid particles ("reactions" i=10,13 and 14):

$$c_{SI,i} = \frac{w_{mst,I,m}\ \rho_{PI,m}}{M_{5}} \qquad (A.7)$$

Here m=1 for i=10, m=2 for i=13, and m=3 for i=14.

- Limestone calcination (reaction i=11):

$$c_{SI,11} = \frac{w_{j=22,I,m=2}\ \rho_{PI,m=2}}{M_{22}} \qquad (A.8)$$

- Sulfur absorption (reaction i=12):

$$c_{SI,12} = c_{SI,11}\ \Lambda_{22} \qquad (A.9)$$

The effective diffusivity in the outer shell and in the particle core are estimated by the following formula proposed by Walker et al.(1959):

$$D_{shell,i} = D_G\ \theta^2_{shell,m} \qquad (A.10)$$

and

$$D_{core,i} = D_G\ \theta^2_{core,m} \qquad (A.11)$$

see Tab.3.2 for relations between "m" and "i". The void fractions "θ" are calculated by:

$$\theta_{core,m} = \rho_{PI,m}\ v_{PI,m} \quad , \ 1 \leq m \leq 3 \qquad (A.12)$$

and

$$\theta_{shell,m} = \rho_{shell,m}\ v_{shell,m} \quad , \ 1 \leq m \leq 3 \qquad (A.13)$$

The specific volume of pores are given by:

$$v_{P,m} = \frac{1}{\rho_{PI,m}} - \frac{1}{\rho_{PU,m}} \quad , \ 1 \leq m \leq 3 \qquad (A.14)$$

and

$$v_{shell,m} = \frac{1}{\rho_{shell,m}} - \frac{1}{\rho_{PI,m}} \qquad (A.15)$$

with the apparent shell densities formed for the reacted solids "rs"- ash for $1 \leq i \leq 5$, devolatilized solid for $6 \leq i \leq 9$, dried material for i=10, 13 and 14, $CaO+CaSO_4$ for i=11 and $CaCO_3+CaSO_4$ for i=12- are given by:

$$\rho_{shell,m} = \rho_{rs} = \rho_{P,m}\, w_{rs,m} \qquad 1 \leq m \leq 3 \qquad (A.16)$$

The bulk gas diffusivity, D_G, is given by Field et al.(1967) as:

$$D_G = \frac{8.677 \times 10^{-5}\, T_{film}^{1.75}}{P} \qquad (A.17)$$

here the film temperature has been approximated by:

$$T_{film} = \frac{T_{P,m} + T_G}{2} \qquad (A.18)$$

in which the particle temperature, "T_P", must be referred to the particle "m" involved in the reaction "i".

APPENDIX B - TUBES AND BED HEAT TRANSFER PARAMETERS

The parameters used for the calculation of the heat transfer by convection between tubes and bed are described below.

$$\lambda_{mf} = \lambda_{GA} \frac{(1 - \varepsilon_{mf})}{0.04 + \frac{\lambda_{GA}}{\lambda_S}} + 0.1 \, \rho_{GA} \, C_{GA} \, d_P \, U_{mf} \qquad (B.1)$$

$$\rho_{mf} = \rho_P \, (1 - \varepsilon_{mf}) \qquad (B.2)$$

$$C_{mf} = C_S \qquad (B.3)$$

APPENDIX C - AVERAGE TEMPERATURE AND DERIVATIVE

The average temperature at a given point "z" of the reactor is given by:

$$T_A = T^* \frac{\sum_{k=1}^{5} C_k F_k (T_k - T^*)}{\sum_{k=1}^{5} C_k F_k} \qquad (C.1)$$

here k=1 to 5 represents: 1=carbonaceous solid, 2=limestone, 3=inert, 4=gas in the emulsion and 5=gas in the bubble phase (in the freeboard section 4=5=gas phase). The specific heat C_k must be calculated at the respective temperature T_k. The enthalpy reference temperature is T^*=298.15K.

- The average temperature derivative at any point is given by:

$$\frac{dT_A}{dz} = \frac{\sum_{k=1}^{5} C_k F_k \frac{dT_k}{dz}}{\sum_{k=1}^{5} C_k F_k} \qquad (C.2)$$

the same relationship between index "k" is valid. This average is justified by the basic energy balances shown in the section "Basic equations" and each factor $C_k F_k \frac{dT_k}{dz}$ represents the rate of energy consumption or production per unit of bed length.

APPENDIX D - INTERNAL TUBE HEAT TRANSFER PARAMETERS

The heat transfer coefficient between the internal surface of the tubes and the flowing fluid (liquid or vapour) is determined by the Nusselt number or:

$$\alpha_{JT} = \frac{N_{Nu,JT}\ \lambda_{fluid}}{L_T} \tag{D.1}$$

The various situations would depend on the tube internal surface temperature and the fluid physical - state. The respective Nusselt numbers are given by correlations well reported in the classical literature and here they have been taken from Isachenko et al.(1977) as:

- Pure convection (Sub-cooled liquid, saturated or super-heated vapour):

For $N_{Re,JT} < 5.0x10^5$,

$$N_{Nu,JT} = 0.33\ N_{Re,JT}^{0.5} N_{Pr,JT}^{0.43} \left[\frac{N_{Pr,fluid}}{N_{Pr,JWT}}\right]^{0.25} Z_T^{0.1} \tag{D.2}$$

where

$$Z_T = \frac{L_T}{d_T} \tag{D.3}$$

and for $N_{Re,JT} \geq 5.0x10^5$,

$$N_{Nu,JT} = 0.022\ N_{Re,JT}^{0.8}\ N_{Pr,fluid}^{0.43}\ \varepsilon_T \tag{D.4}$$

where

$$\varepsilon_T = 1 \quad \text{if} \quad Z_T \geq 15 \tag{D.5}$$

or

$$\varepsilon_T = \frac{1.38}{Z_T^{0.12}} \quad \text{if} \quad Z_T < 15 \tag{D.6}$$

here

$$N_{Re,T} = G_{M,liq}\, d_{JT}/\mu_{liq} \tag{D.7}$$

- Saturated boiling liquid:

$$\alpha_{JT} = 0.122\, (T_{JWT} - T_{liq})^{2.33}\, P_{JT}^{0.5} \tag{D.8}$$

For the situations were the boiling process is initiating (nucleate boiling combined with one phase fluid convection) Isachenko et al. suggests an average heat transfer coefficient given by:

$$\alpha_{boil-conv} = \alpha_{conv}\, \frac{4\,\alpha_{conv} + \alpha_{boil}}{5\,\alpha_{conv} - \alpha_{boil}} \tag{D.9}$$

that must be applied for $0.5 < (\alpha_{boil}/\alpha_{conv}) < 2$.

The possibility of internal condensation is too remote to be considered.

APPENDIX E - HEAT TRANSFER BETWEEN TUBES AND THE FREEBOARD

For the convective heat transfer between the tubes and the gas flow in the freeboard, these calculations assume the classical correlation given by:

$$E_{CGFTF} = \alpha_{GOTF} (T_{GF} - T_{WOTF}) \frac{dA_{OTF}}{dz} \qquad (E.1)$$

where in the case of vertical tubes:

$$\alpha_{GOTF} = 0.330 \, N_{Re,Td}^{0.6} \, N_{Pr,GF}^{1/3} \qquad (E.2)$$

and in the case of horizontal tubes:

$$\alpha_{GOTF} = 0.648 \, N_{Re,Tl}^{0.5} \, N_{Pr,GF}^{1/3} \qquad (E.3)$$

Here the Reynolds number "$N_{Re,Td}$" is based on the tube diameter and "$N_{Re,Tl}$" on the tube length (one pass).

The procedure to determine the external wall temperature "T_{WOTF}" is similar to the one adopted in the calculations for the bed section (see eq.3.144). The internal coefficient "α_{JTF}" is computed as described in the Appendix D.

In the case of inclined tubes an average between the vertical and the horizontal coefficients, based on the angle of the inclination, is assumed to compute the value of "α_{GOTF}".

For the radiative heat transfer between particles and the tubes in the freeboard the calculations use a similar approach of the one employed in the computations between tubes and particles in the bed (sec.3.8.4.1).

REFERENCES

1) Adánez,J.; Miranda,J.L.; Gavilán,J.M., 1985, Fuel, 64, 801-804.

2) Amitin, A.V.; Martyushin,I.G.; Gurevich,D.A., 1968, "Dusting in the Space Above the Bed in Converters with a Fluidized Catalyst Bed", Chem. Technol. Fuels Oils, 3-4, 181.

3) Aris,R.; Amundson,N.R., 1973, "Mathematical Methods in Chemical Engineering", Vol.2, 316-328, Prentice Hall, Englewood Cliffs, N.J., U.S.A..

4) Arthur,J.A., 1951, Trans. Faraday Soc., 47: 164-178.

5) Asai,M.; Kiyoshi,A.; Tsuji,S., 1984, "Particle Behavior in the Vicinities of Tubes in Fluidized Bed Boiler", The Inst. of Energy, London, 3rd International Fluidized Conference, DISC/1/1.

6) Asaki,Z.; Fukunaka,Y.; Nagase,T.; Kondo,Y., 1974 "Thermal Decomposition of Limestone in a Fluidized Bed", Metallurgical Transactions, Vol.5, 381-390.

7) Avedesian,M.M.; Davidson,J.F., 1973, Transactions of the Institute of Chemical Engineers, 51, 121-131.

8) Babcock and Wilcox, 1976, "Summary Evaluation of Atmospheric Pressure Fluidized Bed Combustion Applied to Electric Utility Large Steam Generators", EPRI FP-308, Vol.II: Appendices.

9) Babcock and Wilcox, 1978, "SO_2 Absorption in Fluidized Bed Combustion of Coal- Effect of Limestone Particle Size", EPRI FP-667, Project 719-1, Final Report.

10) Babu,S.P.; Shah,B.; Talwalkar,A., 1978, "Fluidization

Correlations for Coal Gasification Materials - Minimum Fluidization Velocity and Fluidized Bed Expansion Ratio", AIChE Symposium Series, No.176, Vol.74, 176-186.

11) Biba,V.; Macak,J.; Klose,E.; Malecha,J., 1978, "Mathematical Model for the Gasification of Coal under Pressure", Ind. Eng. Chem. Process Des. Dev., Vol.17, No.1, 92-98.

12) Baron,R.E.; Hodges,J.L.; Sarofim,A.F., 1977, AIChE 70th Annual Meeting, New York, NY.

13) Batchelder,H.R.; Busche,R.M.; Armstrong,W.P., 1953, "Kinetics of Coal Gasification", Ind. Eng. Chemistry, Vol.45, No.9, 1856-78.

14) Behie,L.A.; Kohoe,P., 1973, "The Grid Region in a Fluidized Bed Reactor", AIChE J., 19, 1070.

15) Borghi,G.; Sarofim,A.F.; Beer,J.M., 1977, AIChE 70th Annual Meeting, New York.

16) Borgwardt,R.H., 1970, "Kinetics of the Reaction of SO_2 with Calcinated Limestone", Environmental Science and Technology, vol.4, No.1, 59-63.

17) Borgwardt,R.H.; Drehmel,D.C.; Kittleman,T.A.; Mayfield,D.R.; Owen,J.S., 1971, "Selected Studies on Alkaline Additives for Sulfur Dioxide Control", EPA-RTP.

18) Borgwardt,R.H., 1985, "Calcination Kinetics and Surface Area of Dispersed Limestone Particles", AIChE Journal, vol.31, No.1, 103-111.

19) Botteril, 1983, "Fluidized Beds,Combustion and Applications", ed. by J.R.Howard, Applied Science Publishers.

20) Branch,M.C.; Sawyer,R.F., 1972, "Ammonia Oxidation in an Arc-Heated Flow Reactor", Fourteenth Symposium (International) on Combustion, The Combustion Institute, Pittsburgh, Pennsylvania, U.S.A., 967-974.

21) Brikci-Nigassa,M., 1982, "A Pilot Scale Study of Monosized Coal Combustion in a Fluidized Bed Combustor", PhD Theses, Department of Chemical Engineering and Fuel Technology, University of Sheffield.

22) Campbell,E.K.; Davidson,J.F., 1975, Paper A-2, Institute of Fuel Symposium Series No.1.

23) Catipovic,N.M.; Jovanovic,G.N.; Fitzgerald,T.J., 1978, AIChE Journal, 24, 3, 543.

24) Chang,C.C.; Fan,L.T.; Walawender,W.P., 1984, "Dynamic Modeling of Biomass Gasification in a Fluidized Bed", AIChE, Symposium Series, No.234, Vol.80, 80-90.

25) Chen,T.P.; Saxena,S., 1977, "Mathematical Modelling of Coal Combustion in Fluidized Beds with Sulphur Emission Control by Limestone or Dolomite", FUEL, Vol.56, October, 401-413.

26) Chen,T.P.; Saxena,S.C., 1978, "A Mechanistic Model Applicable to Coal Combustion in Fluidized Beds", AIChE Symposium Series, No.176, Vol.74, 149-161.

27) Chirone,R.; D'Amore,M.; Massimilla,L., 1984, "Carbon Attrition in Fluidized Combustion of Petroleum Coke", Presented at the 20th Symp. (Int.) on Combustion, The Combustion Institute, Ann Arbor.

28) Davidson,J.F.; Harrison,D., 1963, "Fluidized Particles", Cambridge University Press.

29) Delvosalle, C.; Vanderschuren, J., 1985, "Gas-to-particle and Particle-to-particle Heat Transfer in Fluidized beds of Large Particles", Chem. Eng. Science, Vol.40, 5, 769-779.

30) DeSai,P.R.; Wen,C.Y., 1978, Morgantown, W.V. Tech. Information Center, U.S. Dept. of Energy, MERC/CR-78/3.

31) De Soete,G., 1973, "Le Mechanism de Formation de NO à Partir d'ammoniac et d'amines dans les Flammes d'hydrocarbures", International Flame Research Foundation, Doc. No. G19/a/3.

32) Dryer,F.L.; Glassman,I., 1972, "High-Temperature Oxidation of CO and CH_4", 14th Symposium (International) on Combustion, Pittsburgh, Pennsylvania, August 20-25, 987-1003.

33) Edelman,R.B.; Fortune,O.F., 1969, "A Quasi-Global Chemical Kinetic Model for the Finite Rate Combustion of Hydrocarbon Fuel with Application to Turbulent Burning and Mixing in Hypersonic Engines and Nozzles", AIAA paper No 69-86.

34) Field,M.A.; Gill,D.W.; Morgan,B.B.; Hawksley,P.G.W., 1967, "Combustion of Pulverized Fuel", Brit. Coal Utiliz. Res. Assoc. Mon. Bull., 31, 6, 285-345 (cited from De Sai and Wen, 1968).

36) Fine,D.H.; Slater,S.M.; Sarofim,A.F.; Williams,G.C., 1974, "Nitrogen in Coal as a Source of Nitrogen Oxide Emission from Furnaces", Fuel, Vol.53, 120-125.

36) Franks,R.G.E., 1967, "Mathematical Modelling in Chemical Engineering", Willey, N.Y..

37) Fredersdorff,C.G. von; Elliot,M.A., 1963, "Chemistry of Coal Utilization", Supplementary Volume (H.H.Lowry,ed.) J.Wiley and Sons, N.Y..

38) Gallo,J.G.; Quassim,R.Y.; Saddy,M., 1981,"Heat Transfer in Fluidized Beds with Horizontal Immersed Tubes", Fluidized Combustion Conference, 28th-30th Jan., Energy Research Inst., Univ.of Cape Town.

39) Gelperin,N.I.; Einstein,V.G.; Kwasha,V.B., 1967, "Fluidization Technique Fundamentals", Izd., "Khimia", Moscow, USSR.

40) Gibbs,B.M., 1978, "A Mechanistic Model for Predicting the Performance of a Fluidized Combustion", Institute of Fuel, Symposium Series,No.1, Vol.I, A5.1-A5.10

41) Gibson,M.A.; Euker,C.A., 1975, "Mathematical Modeling of Fluidized Bed Coal Gasification", Paper presented at AIChE meeting, Los Angeles, Calif..

42) Gordon,A.L.; Amundson,N.R., 1976, "Modelling of Fluidized Bed Reactors-IV: Combustion of Carbon Particles", Chemical Engineering Science, 31, (12), 1163-1178.

43) Gordon,A.L.; Caram,H.S.; Amundson.N.R., 1978, "Modelling of Fluidized Bed Reactors- V: Combustion of Carbon Particles- An Extension", Chemical Engineering Science, 32, (6), 713-722.

44) Gregory,D.R.; Littlejohn,R.F., 1965, The BCURA Monthly Bulletin, 29, (6), 173.

45) Haslan,R.T.; Russel,R.P., 1926, "Fuel and Their Combustion", N.Y., Mc Graw Hill.

46) Ho,Tho-Ching; Chen,T.K.; Hopper,J.R., 1984, "Pressure

Drop Across the Distributor in a Fluidized Bed with Regular and Irregular Distributor Design", AIChE, Symposium Series, 241, Vol.80, 34-40.

47) Horio,M.; Wen,C.Y., 1977, "An Assessment of Fluidized-Bed Modelling", AIChE Symp. Series, Vol.73, No.161, 9-21.

48) Horio,M.; Mori,S.; Muchi,I., 1977(a), "A Model Study for Development of Low NO_x Fluidized-bed Coal Combustion", Proceedings of 5th International Conference of Fluidized Bed Combustion, Washington DC, Conf-771272-p2, Vol.II, 605-624 (1978).

49) Horio,M.; Rengarajan,P.; Krishnan,R.; Wen,C.Y., 1977(b), "Fluidized Bed Combustor Modelling", West Virginia University, Morgantown, USA, NASA Report No. NAS3-19725.

50) Horio,M.; Wen,C.Y., 1978, "Simulation of Fluidized Bed Combustors", AIChE Symposium Series, 74, 176.

51) Hottel,H.C.; Howard,J.B., 1971, "New Energy Technology", MIT Press, Cambridge, Mass., USA.

52) Hottel,H.C.; Williams,G.C.; Nerheim,N.M.; Shneider,G.R., 1965, 10th International Symposium on Combustion.

53) Howard,J.B.; Williams,G.C.; Fine,D.H., 1972, "Kinetics of Carbon Monoxide Oxidation in Postflame Gases", 14th Symposium (International) on Combustion, Pittsburgh, Pennsylvania, Aug. 20-25, 975-986.

54) Hughes,R.; Deumaga,V., 1974, "Insulation Saves Energy", Chem. Eng., 27, 95-100.

55) Ingraham, T.R.; Marier,P., 1963, "Kinetic Studies on the Thermal Decomposition of Calcium Carbonate", Canad. J.

of Chem. Eng., Vol.41, 170-73.

56) IGT-Institute of Gas Technology, 1976, "Preparation of a Coal Conversion System Technical Data Book, Final Report, October 31, 1974-April 30,1976", U.S. Energy Res. Develop., Adimin. Report No FE-1730-21. National Technical Information Service, Springfield,Va..

57) IPT-Instituto de Pesquisas Tecnológicas do Estado de São Paulo (São Paulo, S.P., CEP 05508, Cx.Postal 7141, Brazil), 1979, "Apoio Técnico,Pesquisa e Desenvolvimento para Produção de Gás de Síntese a Partir de Eucalyptus SPP-Fase 1A", Relatório No. 12.723.

58) Isachenko,V.P.; Osipova,V.A.; Sukomel,A.S., 1977, "Heat Transfer", Mir, Moscow, USSR.

59) Ishida,M.; Wen,C.Y., 1973, Environ. Sci. Technol., 1, 103.

60) Johnson,J.L., 1979, "Kinetics of Coal Gasification", N.Y. J.Wiley and Sons.

61) Johnstone,H.F.; Batchelor,J.D.; Shen,W.Y., 1955, AIChE J., 1, 318 (cited from Horio and Wen, 1977).

62) Kanury,A.M., 1975, "Introduction to Combustion Phenomena", Gordon and Breach Science, London, U.K..

63) Karapetyants,M.Kh., 1978, "Chemical Thermodynamics", Mir, Moscow, USSR.

64) Kasaoka,S.; Sakata,Y.; Tong,C., 1985, "Kinetic evaluation of reactivity of various coal char for gasification with carbon dioxide in comparison with steam", International Chemical Engineering, Vol.25, No.1, 160-175.

65) Kato,K.; Wen.C.Y., 1969, Chem. Eng. Sci., 24, 1351

(cited from Horio and Wen, 1977).

66) Kim,M.; Joseph,B., 1983, "Dynamic of Moving-Bed Gasifiers", Ind. Eng. Chem. Process Des. Dev., 22, 212-217.

67) Kobayashi,H.; Arai,F., 1965, Chem. Eng. Tokyo, 29, 885 (cited from Horio and Wen, 1977).

68) Kobayashi,H.; Arai,F., 1967, "Determination of a Gas Cross-Flow Coefficient between the Bubble and Emulsion Phases by Measuring the Residence Time Distribution of a Fluid in a Fluidized Bed", Kagaku Kogaku, 31, 239.

69) Kobayashi,H.; Arai,F.; Chiba,T.; Tanaka,Y., 1969, Chem. Eng. Tokyo, 33,675 (cited from Horio and Wen, 1977).

70) Kothari,A.K., 1967, M.S. Thesis, Illinois Institute of Technology, Chicago.

71) Kubashewski,O; Evans,E.L.; Alcock,C.B., 1967, "Metallurgical Thermochemistry", 4th. ed., Pergamon Press, London, p422.

72) Kunii,D.; Yoshida,K.; Hiraki,I., 1967, Proc. Intern. Symp. on Fluidization, Netherlands Univ. Press, Amsterdam (cited from Kunii and Levenspiel, 1969).

73) Kunii,D.; Levenspiel,O., 1968, Ind. Eng. Chem. Fundamentals, 7, 446.

74) Kunii,D.; Levenspiel,O., 1969, "Fluidization Engineering", J.Wiley, N.Y..

75) La Nauze,R.D.; Jung,K.; Kastl,J., 1984, "Mass Transfer to Large Particles in Fluidized Beds of Small Particles", Chem.Eng. Sci., 39, 11, 1623-1633.

76) Leith,D.; Mehta,D., 1973, "Cyclone Performance and Design", Atmospheric Environment, Pergamon Press, Vol.7,

527-549.

77) Lewis,W.K.; Gilliland,E.R.; Lang,P.M., 1962, Chem. Eng. Progr. Symp. Series, 58, 38, 65.

78) Loison,R.; Chauvin,R., 1964, "Pyrolyse Rapide du Charbon", Chimie et Industrie, Vol.91, 3.

79) Maloney,D.J.; Jenkins,R.G., 1985, "Influence of coal preoxidation and the relation between char structure and gasification potential", FUEL, Vol.64, 1415-1422.

80) Mamuro,T.; Muchi,I., 1965, J. Ind. Chem. Tokyo, 68, 126 (cited from Horio and Wen, 1977).

81) May,W.G., 1959, Chem. Eng. Progr., 55, (12), 49 (cited from Horio and Wen, 1977).

82) Merrick,D.; Highley,J., 1974, "Particle Size Reduction and Elutriation in a Fluidized Bed Process", AIChE Symp. Series, 70, 137, 366.

83) MIT, Energy Laboratory, 1978, "Modeling of Fluidized Bed Combustion of Coal, Final Report,A "First Order" System Model of Fluidized Bed Combustor", Vol.I, Massachusetts Institute of Technology, Report to US Dept. of Energy, contract No.E(49-18)-2295.

84) Mori,S.; Muchi,I., 1972, J. Chem. Eng. Japan, 5, 251 (cited from Horio and Wen, 1977).

85) Mori,S; Wen,C.Y., 1975, AIChE J., 21, 109 (cited from Horio and Wen, 1977).

86) Muchi, I., 1965, Memories of the Faculty of Engineering, Nayoga Univ., 17, 79 (cited from Horio and Wen, 1977).

87) Murray,J.D., 1966, Chem. Eng. Progr. Symp. Series, 62,

(62), 71 (cited from Kunii and Levenspiel, 1969)

88) Nunn,T.R.; Howard,J.B.; Longwell,J.P.; Peters,W.A., 1985, "Product Compositions and Kinetics in the Rapid Pyrolysis of Sweet Gum Hardwood", Ind. Eng. Chem. Process Des. Dev., Vol.24, 3, 836-844.

89) Oguma,A.; Yamada,N.; Furusawa,T.; Kunii,D., 1977, Preprint for 11th Fall Meeting of Soc. of Chem.Eng. Japan,121.

90) Olofsson J., 1980, "Mathematical Modelling of Fluidized Bed Combustors", IEA Coal Research, London and National Swedish Board fo Energy Source Development, Spanga, Report No. ICTIS/TR14, 100p.

91) Orcutt,J.C.; Davidson,J.F.; Pigford,R.L., 1962, Chem. Eng. Progr. Symp. Ser., No.38, 58, 1 (cited from Horio and Wen, 1977).

92) Overturf,B.W.; Reklaitis,G.V., 1983a, "Fluidized-Bed Reactor Model with Generalized Particle Balances-Part I: Formulation and Solution", AIChE Journal, Vol.29, No.5, 813-820.

93) Overturf,B.W.; Reklaitis,G.V., 1983b, "Fluidized-Bed Reactor Model with Generalized Particle Balances-Part II: Coal Combustion Application", AIChE Journal, Vol.29, No.5, 820-829.

94) Parent,J.D.; Katz,S., 1948, "Equilibrium Compositions and Enthalpy Changes for the Reaction of Carbon, Oxygen and Steam", IGT Research Bulletin,2.

95) Park,D.; Levenspiel,O.; Fitzgerald,T.J., 1981, "A Model for Scale Atmospheric Fluidized Bed Combustors", AIChE

Symposium Series, No.277, Vol.77, 116-126.

96) Partridge,B.A.; Rowe,P.N., 1966, Trans. Inst. Chem. Engrs., 44, T349 (cited from Horio and Wen, 1977).

97) Perry,R.H.; Chilton,C.H., 1973, "Chemical Engineer's Handbook", 5th ed., McGraw Hill.

98) Quan,V.; Marble,F.E.; Kliegel,J.R., 1972, "Nitric Oxide Formation in Turbulent Diffusion Flames", 14th Symposium (International) on Combustion, Pittsburgh, Pennsylvania, Aug. 20-25, 851-860.

99) Rajan,R.; Krishnan,R.; Wen,C.Y., 1978, "Simulation of Fluidized Bed Combustors; Part II: Coal Devolatilization and Sulfur Oxides Retention", AIChE Symposium Series, No.176, Vol.74, 112-119.

100) Rajan,R.; Krishnan,R.; Wen,C.Y., 1979, "Simulation of Fluidized Bed Coal Combustors", West Virginia Univ., Morgantown, W.Virginia, NASA CR-159529.

101) Rajan,R.; Wen,C.Y., 1980, "A Comprehensive Model for Fluidized Bed Coal Combustors", AIChE Journal, Vol.26, No.4, 642-655.

102) Raman,P.; Walawender,W.P.; Fan,L.T.; Chang,C.C., 1981, "Mathematical Model for the Fluid-Bed Gasification of Biomass Materials. Application to Feedlot Manure", Ind. Eng. Chem. Process Des. Dev., Vol.20, No.4,686-692.

103) Reid,R.C.; Prausnitz,J.M.; Sherwood,T.K., 1977, "The properties of Gases and Liquids", 3rd ed., McGraw Hill, N.Y..

104) Rossberg,M., 1956, Z.Elecktrochem., 60: 952-956.

105) Rowe,P.N., 1978, Chemical Reaction Engineering,

Houston, Am. Chem. Soc., Symp. Ser., 63, 436.

106) Rowe,P.N.; Partridge,B.A., 1962, Proc. Symp. on Interaction between Fluids and Particles, Inst. Chem. Engrs., 135, June 1962 (cited from Kunii and Levenspiel, 1969).

107) Salatino,P.; Massimilla,L., 1985, "A Descriptive Model of Carbon Attrition in the Fluidized Combustion of Coal Char", Chem. Eng. Science, Vol.40, No. 10, 1905-1916.

108) Saxena,S.C.; Grewal,N.S.; Venhatoramana,M. 1978, "Modeling of a Fluidized Bed Combustor with Immersed Tubes", University of Illinois at Chicago Circle, Report to US Dept. of Energy, Report No.FE-1787-10.

109) Sergeant,G.D.; Smith,I.W., 1973, Fuel, 52, 52-57.

110) Siminski,V.J.; Wright,F.J.; Edelman,R.B.; Economos,C.; Fortune,O.F., 1972, "Research on Methods of Improving the Combustion Characteristics of Liquid Hydrocarbon Fuels", AFAPLTR 72-74, Vols. I and II, Air Force Aeropropulsion Lab., Wright Patterson Air Force Base, Ohio.

111) Shen,C.Y.; Johnstone,H.F., 1955, AIChE J.,1, 349 (cited from Horio and Wen, 1977).

112) Sit,S.P.; Grace,J.R., 1981, "Effect of Bubble Interaction on the Interphase Mass Transfer in Gas Fluidized Beds", Chem. Engng. Sci., Vol.36, 327-335.

113) Souza-Santos,M.L., 1985, "Desenvolvimento de Modelo de Simulação de Gaseificadores com Diversos Tipos de Combustíveis", Report No 20689, DEM/AET, IPT-Instituto de Pesquisas Tecnológicas do Estado de São Paulo, São Paulo, S.P., C.Postal 7141, Brasil.

114) Stubington,J.F.; Barrett,D.; Lowry,G., 1984, "Bubble Size Measurements and Correlation in a Fluidized Bed at High Temperatures", Chem. Eng. Res. and Design, vol. 62, 173-178

115) Talmor,E.; Benenati,R.F., 1963, AIChE Journal, 9, 536.

116) Thompson,D.; Brown,T.D.; Beer,J.M., 1972, "Formation of NO in a Methane-Air Flame", 14th Symposium (International) on Combustion, Pittsburgh, Pennsylvania, Aug. 20-25, 787-799.

117) Thurner,F.; Mann,U., 1981, Ind. Eng. Chem. Progress Des. Dev., 20, 482-448.

118) Tojo,K.; Chang,C.C.; Fan,L.T., 1981, "Modeling of Dynamic and Steady-State Shallow Fluidized Bed Coal Combustors. Effects of Feeder Distribution", Ind. Eng. Chem. Process Des. Dev., Vol.20, No.3, 411-416.

119) Toomey,R.D.; Johnstone, H.F., 1952, "Gaseous Fluidization of Solids Particles", Chemical Engineering Progress, 48(5), 220-226.

120) Toor,F.D.; Calderbank,P.H., 1967, Proc. Intern. Symp. on Fluidization, Netherland Univ. Press, p.373 (cited from Horio and Wen, 1977).

121) van Deemter,J.J., 1961, Chem. Eng. Sci., Vol.13, 143 (cited from Horio and Wen, 1977).

122) van Heek,K.H.; Muhlen,H.J., 1985, "Aspects of coal properties and constitution important for gasification", FUEL, Vol.64, 1405-1414.

123) Vaux,W.G.; Schruben,J.S., 1983, "Kinetics of Attrition in the Bubbling Zone of a Fluidized Bed", AIChE Symposium

Series, No.222, Vol.79.

124) Vilienskii,T.V.; Hezmalian,D.M., 1978, "Dynamics of the Combustion of Pulverized Fuel (Dinamika Gorenia Prilevidnovo Tolpliva)", Energia, Moscow, 246p.

125) Walker,P.L.,Jr.; Rusinko,F.,Jr.; Austin,L.G., 1959, "Gas Reactions of Carbon", Advan. Catalysis, 2, 134.

126) Walsh,P.M.; Mayo,J.E.; Beer,J.M., 1984, "Refluxing Particles in the Freeboard of a Fluidized Bed", AIChE Symposium Series, No.234, Vol.80.

127) Weimer,A.W.; Clough,D.E., 1981, "Modeling a Low Pressure Steam-Oxygen Fluidized Bed Coal Gasification Reactor", Chemical Engineering Science, Vol.36, 549-567.

128) Wen,C.Y.; Chen,L.H., 1982, "Fluidized Bed Freeboard Phenomena: Entrainment and Elutriation", AIChE J., 28, 117.

129) Wen,C.Y.; Chen,L.H., 1983,"A Model for Coal Pyrolysis in an Inert Atmosphere", Journal of The Chinese Inst. of Chem. Engineers, Vol.14, 173-189.

130) Wen,C.Y.; Lee,E., 1979, "Coal Conversion Technology", (in "Energy Science and Technology", Addison-Wesley).

131) Wen,C.Y.; Yu,Y.H., 1966, AIChE Journal, 12, 610-612.

132) Williamson,I.M., 1972, "Computing Properties of Saturated Steam", Chem. Eng., 15, 128, May.

133) Xavier,A.M.; Davidson,J.F., 1978, in "Fluidization", Eds.Davidson,J.F. and Keairns,D.L., 333, Cambridge University Press.

134) Yates,J.G.; Rowe,P.N., 1977, Trans. Inst. Chem. Engrs., 55, 137.

135) Yaws,C.L.; Borrenson,R.W.; Gorin,C.E.; Hood,L.D.;

Miller,J.W.; Schorr,G.R.; Thakore,S.B., 1976(a), "Correlation Constants for Chemical Compounds (22)", Chem. Eng., 16, 79-87, Aug..

136) Yaws,C.L.; Miller,J.W.; Schorr,G.R.; Shah,P.N.; Mc Ginley,J.J.; 1976(b), "Correlation Constants for Liquids (23)", Chem. Eng., 25, 127-135, Oct.

137) Yaws,C.L.; Miller,J.M.; Shah,P.N.; Schorr,G.R.; Patel,P.M., 1976(c), "Correlation Constants for Chemical Compounds (24)", Chem. Eng., 22, 153-162, Nov.

138) Yoon,H.; Wei,J.; Denn,M.M., 1978, AIChE J., 24(5): 885-903.

139) Zhang,G-T.; Ouyang,F., 1985, "Heat Transfer Between the Fluidized Bed and the Distributor Plate", Ind. Eng. Chem. Process Des. Dev., Vol.24, No. 2, 430-433.